International Agreement Report

Assessment of RELAP5/MOD3.3 and TRACE V5.0 Computer Codes against LOCA Test Data from PSB-VVER Test Facility

Prepared by:
M. Kynčl, R. Pernica

Research Centre Řež,TSO
Hlavní 130
250 68 Husinec-Řež, Czech Republic

K. Tien, NRC Project Manager

Division of Systems Analysis
Office of Nuclear Regulatory Research
U.S. Nuclear Regulatory Commission
Washington, DC 20555-0001

Manuscript Completed: July 2013
Date Published: December 2013

AVAILABILITY OF REFERENCE MATERIALS
IN NRC PUBLICATIONS

International Agreement Report

Assessment of RELAP5/MOD3.3 and TRACE V5.0 Computer Codes against LOCA Test Data from PSB-VVER Test Facility

Prepared by:
M. Kynčl, R. Pernica

Research Centre Řež,TSO
Hlavní 130
250 68 Husinec-Řež, Czech Republic

K. Tien, NRC Project Manager

Division of Systems Analysis
Office of Nuclear Regulatory Research
U.S. Nuclear Regulatory Commission
Washington, DC 20555-0001

ABSTRACT

This report documents the USNRC system thermal-hydraulic codes assessment performed at Research Centre Rez. RELAP5/MOD3.3 and TRACE V5.0 computer codes were assessed against the experimental data from two LOCA tests carried out at PSB-VVER test facility built and operated at Electrogorsk Research and Engineering Center on NPPs Safety in Russia. Experimental data and all necessary information for developing the facility database and facility model notebook were available through the OECD/NEA/CSNI/WGAMA PSB Project.

In the RELAP5/MOD3.3 case, in addition to the best estimate post test analysis of LB LOCA experiment denoted as CL-2x100-01 by EREC and as Test-5a as part of the OECD PSB project, the uncertainty and sensitivity analysis was performed, and the results are presented here. Double ended cold leg guillotine break with initial power scaled further down to 15% was simulated in Test-5a.

In the TRACE V5.0 case, the best estimate post test analysis of SB LOCA experiment denoted as CL-4.1-03 by EREC and as Test-3 as part of the OECD PSB project was carried out, and the results are presented here. A 4.1% cold leg break was simulated in Test-3. The test scenario applied was very close to the scenario realized in LOBI test BL-34.

The RELAP5/MOD3.3 thermal-hydraulic model of PSB-VVER test facility was developed without using the SNAP Model Editor. The development of the TRACE V5.0 thermal-hydraulic model of the PSB-VVER test facility started from RELAP5/MOD3.3 model in SNAP environment. Firstly, the reference case input deck from RELAP5/MOD3.3 study was imported to SNAP and secondly, the thermal-hydraulic model was converted to TRACE V5.0. The resulting TRACE V5.0 thermal-hydraulic model was systematically verified using the Test-5a experimental data. After that, only few computer runs were needed to properly define the initial and boundary conditions of Test-3 in order to validate the TRACE V5.0 thermal-hydraulic model of the PSB-VVER test facility for analysis of SB LOCA.

CONTENTS

FIGURES

TABLES

EXECUTIVE SUMMARY

The purpose of this work is to contribute to the USNRC thermal-hydraulic codes assessment as agreed in the CAMP agreement. RELAP5/MOD3.3/Release and TRACE V5.0 Patch 3 computer codes are assessed against LOCA test data from the PSB-VVER test facility.

ACKNOWLEDGMENTS

ABBREVIATIONS

AA_{tot}	average amplitude (total)
ACC	accumulator
ACL	accumulator level
ADS	atmospheric dump system; steam dump to atmosphere
BE	best estimate
BP	(core) bypass
CAMP	Code Application and Maintenance Program
CCFL	counter current flow limitation
CCVM	CSNI code validation matrix
CHF	critical heat flux
CL	cold leg
D	discrete statistical distribution
DAS	data acquisition system
DP	differential pressure
ECCS	emergency core cooling system
EREC	Electrogorsk Research and Engineering Center on NPPs Safety
FFTBM	fast Fourier transform based method
FRSB	fuel rod simulator bundle
gspf	grid spacer factor
HPIS	high pressure safety injection system
IBF	integrated break flow
LN	lognormal statistical distribution
LOCA	loss of coolant accident
LPIS	low pressure safety injection system
maxT	maximum cladding temperature
N	power of FRSB or normal statistical distribution
n	number of calculations
NPP	nuclear power plant
P	pressure
PCM	primary coolant mass
PCS	primary coolant system
pdf	probability distribution function

PRZ	pressurizer
PSB	integral experimental equipment
PWR	pressurized water reactor
R5/M3.3	RELAP/MOD3.3/Release
SG	steam generator
T	temperature
t_1 (s)	time of beginning of first FRSB cladding heatup
t_2 (s)	time of core quenching
t_3 (s)	time of beginning of last FRSB cladding heatup
t_{acc1}	time of start of accumulator injection
t_{hpis}	time of start of high pressure injection
t_{max}	time of maximum cladding temperature maxT reached during first FRSB cladding heatup
U	uniform statistical distribution
UP	upper plenum
UPP	upper plenum pressure
USNRC	United States Nuclear Regulatory Commission
VVER	water cooled water moderated energetical reactor (WWER)
μ	mean
σ	standard deviation

1. INTRODUCTION

The report documents an assessment performed for RELAP5/MOD3.3/Release and TRACE V5.0 Patch 3 thermal hydraulic system codes at Research Centre Rez, Czech Republic. The computer codes were assessed against the experimental data from two LOCA tests carried out at PSB-VVER test facility built and operated at Electrogorsk Research and Engineering Center on NPPs Safety in Russia [1]. The system code assessment process is structured in [2] as follows:

1. Formulate assessment matrices for each class of transient studied, e.g., large-break LOCA, small-break LOCA.
2. Select key parameters for these classes.
3. Perform assessment calculations. Compare the test data with the results of calculations for the key parameters.
4. Perform uncertainty analyses for the capability of the codes to predict test data and plant transients.

Another step can be identified based on [3]:

5. Perform sensitivity analyses to select important variables, for which the uncertainty distribution has to be determined with good accuracy.

In case of RELAP5/MOD3.3 code assessment, all five steps are addressed below. The transient studied is the large-break LOCA experiment, double ended cold leg guillotine break with initial power scaled further down to 15% of prototypical [4].

In the case of TRACE V5.0 code assessment, the first three steps are addressed below. The transient studied is the small-break LOCA experiment, 4.1% cold leg break with initial power scaled further down to 15% of prototypical [5].

The methodology applied in step 3 is outlined in [6]. Specifically, the test data are compared with the results of calculations on the steady state level and on the transient level. In the first substep, the code results are checked for whether they are within the measurement uncertainty intervals; in the second substep, the methodology based on Fast Fourier Transform [7] is applied.

In the case of RELAP5/MOD3.3 code assessment, the PSB-VVER test facility model had been developed, verified, and validated against LOCA test data within the domestic project JC_2/2006.

In the case of TRACE V5.0 code assessment, the PSB-VVER test facility model development started with conversion of final reference case RELAP5/MOD3.3 PSB-VVER test facility model in SNAP software [8] environment. Further steps in TRACE V5.0 PSB-VVER test facility model development, verification, and validation are outlined below.

The report is organized so that the PSB-VVER test facility description with details addressing the measurement system is presented in Chapter 2. RELAP5/MOD3.3 code assessment is presented in details in Chapter 3, while TRACE V5.0 code assessment case is presented in Chapter 4.

2. PSB-VVER FACILITY DESCRIPTION

The PSB-VVER integral test facility [1] was built in the Elektrogorsk Research and Engineering Center on NPPs Safety (EREC) to model the primary system of a PWR NPP unit with VVER-1000 reactor. The facility was designed to preserve a facility to plant volumetric ratio 1:300 and elevation ratio 1:1. In the series of tests conducted within the OECD/NEA/CSNI/WGAMA PSB-VVER project, the maximum power of fuel rod simulator bundle (FRSB) was 1.5MWt, i.e. the power was further scaled down to 15% of prototypical.

The PSB-VVER test facility is a model of a primary coolant system (PCS) and emergency core cooling system (ECCS) of a VVER-1000 NPP with all main components. In addition, the secondary system components are included as practical. The facility is also equipped with systems for LOCA simulations.

Figure 1 shows that 4 components are used to simulate RPV in the facility, i.e. the downcomer model, the core model, the core model bypass and the upper plenum model. In the core model, a bundle of 168 fuel rod simulators is located in a hexagonal channel. Full height fuel rod simulators are arranged in a triangular lattice. In addition to lower and upper spacer grids, there are 15 spacer grids over the heated length. In the radial direction there are three material zones, central nichrome heater rod, periclase insulator, and stainless steel cladding. In the case of instrumented fuel rod simulators, two cladding layers are used and the thermocouples are located between the external and internal claddings. The core model is separated from the upper plenum model by the core upper plate simulator. A VVER-1000 NPP unit is a four loop plant. In the facility, each loop is simulated separately with hot leg pipe model, SG model, loop seal pipe model, RCP model, loop isolation valve and cold leg pipe model. The pressurizer surgeline is divided in two by a T-joint so that the pressurizer model can be connected either to the hot leg in loop No. 2 or to the hot leg in loop No. 4. Although the SG model is a vertical vessel, the primary side arrangement of the vertical hot header interconnected by nearly horizontal coiled tubes to the vertical cold header is representative of a horizontal steam generator. There are 34 coiled tubes along the height per one SG. The length and the diameter of one tube is the same as of the reference plant. The low inertia RCP model is used to provide forced coolant circulation in the primary circuit. The programmable electromotor frequency is used to achieve the desired initial steady state coolant flow and to model a RCP coastdown if requested in case of a transient/accident being simulated. The pressurizer model is a full height vessel with corresponding subsystem models of pressurizer heaters, pressurizer spray, pressurizer relieve valve, and coolant fill and drain.

In addition to primary system components, Figure 2 shows the ECCS components diagram, and secondary system components diagram. Two accumulators (ACC) are connected to the upper plenum and other two ACCs are connected to the downcomer. The active safety injection system is designed so that various actions of HPIS and LPIS can be simulated including the hot leg injection, cold leg injection, upper plenum and downcomer injection. The actual configuration of HPIS/LPIS is test dependent.
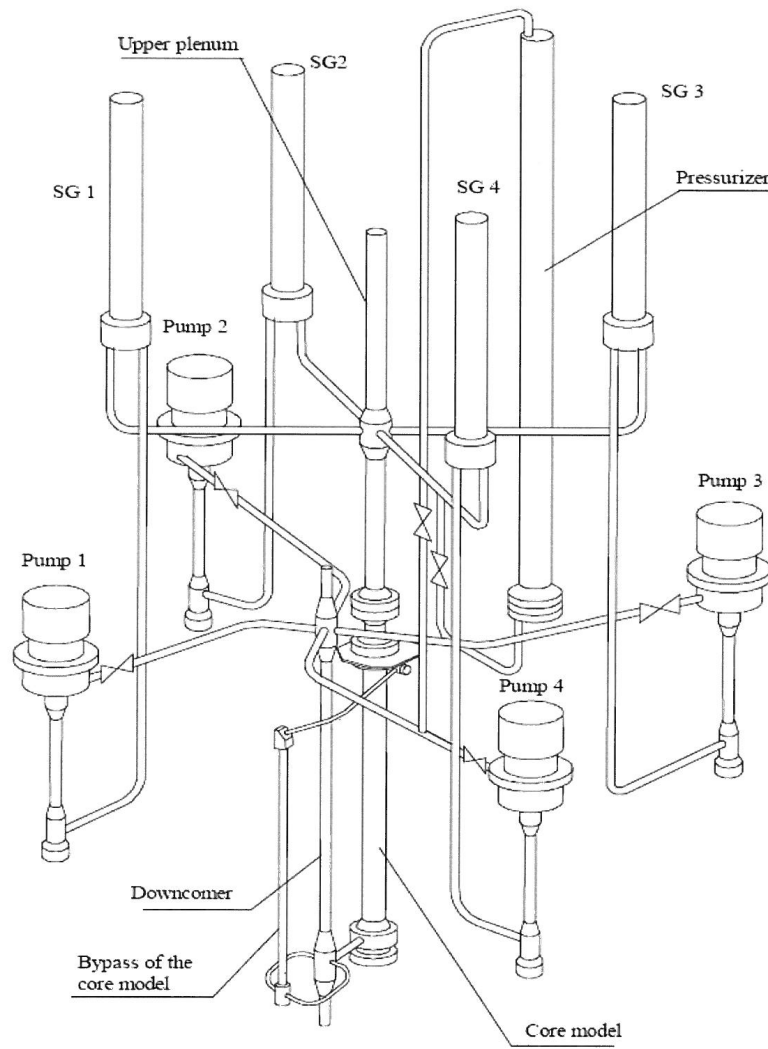
Figure 1 PSB-VVER test facility
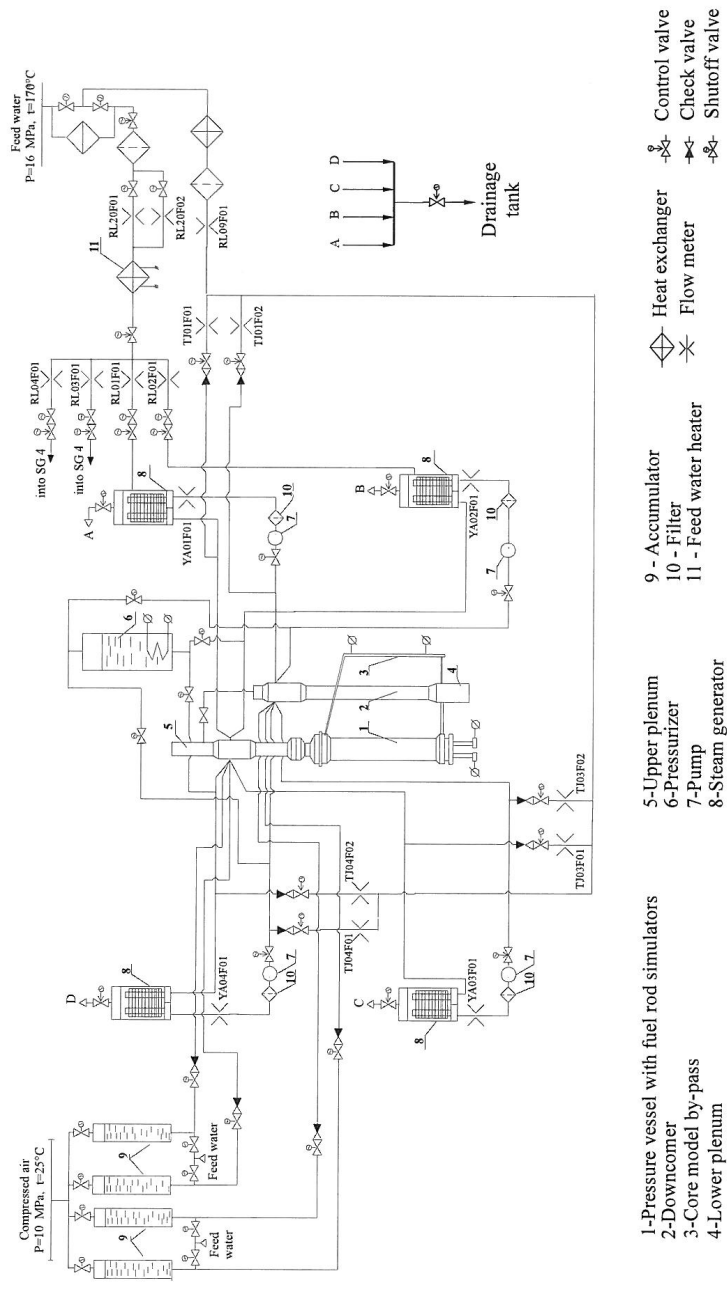
Figure 2 Thermal-hydraulic diagram of PSB-VVER test facility

1-Pressure vessel with fuel rod simulators
2-Downcomer
3-Core model by-pass
4-Lower plenum

5-Upper plenum
6-Pressurizer
7-Pump
8-Steam generator

9 - Accumulator
10 - Filter
11 - Feed water heater

Heat exchanger
Flow meter

Control valve
Check valve
Shutoff valve

The PSB-VVER measurement system designated as Data Acquisition System (DAS) includes more than 1000 measuring channels. The number of active measurement channels and the data record frequency is test specific. The measurement channels, e.g. YC01DP01 or YP01P01, are identified according to the following rules. The first two capital letters designate the test facility functional subsystem. The two digit numbers that follow identify the subsystem number, e.g. the primary coolant loops. Next, one or two capital letters identify the measured parameter, and finally, two or three digit numbers specify the actual measurement channel. The test facility functional subsystem identifiers are presented in Table 1. The measured parameters identifiers are presented in Table 2. In both cases, only the subsystems and their corresponding measurements which are later used for the code assessments are listed.

Table 1 PSB-VVER test facility subsystems identification

Test facility technological subsystem	Identifier
Primary coolant system loops	YA
Steam generator	YB
Reactor pressure vessel simulator	YC
Reactor coolant pumps	YD
Pressurizer	YP
Accumulators	TH

Table 2 PSB-VVER test facility measurement identification

Measured parameter	Identifier
Pressure	P
Differential pressure	DP
Fluid temperature	T or TF
Wall temperature	T or TH
Mass flow rate	F
Liquid level	L
Power	N

Actual measurement locations are identified on following Figures 3 to 14. All figures presented in this section are adopted from [1].
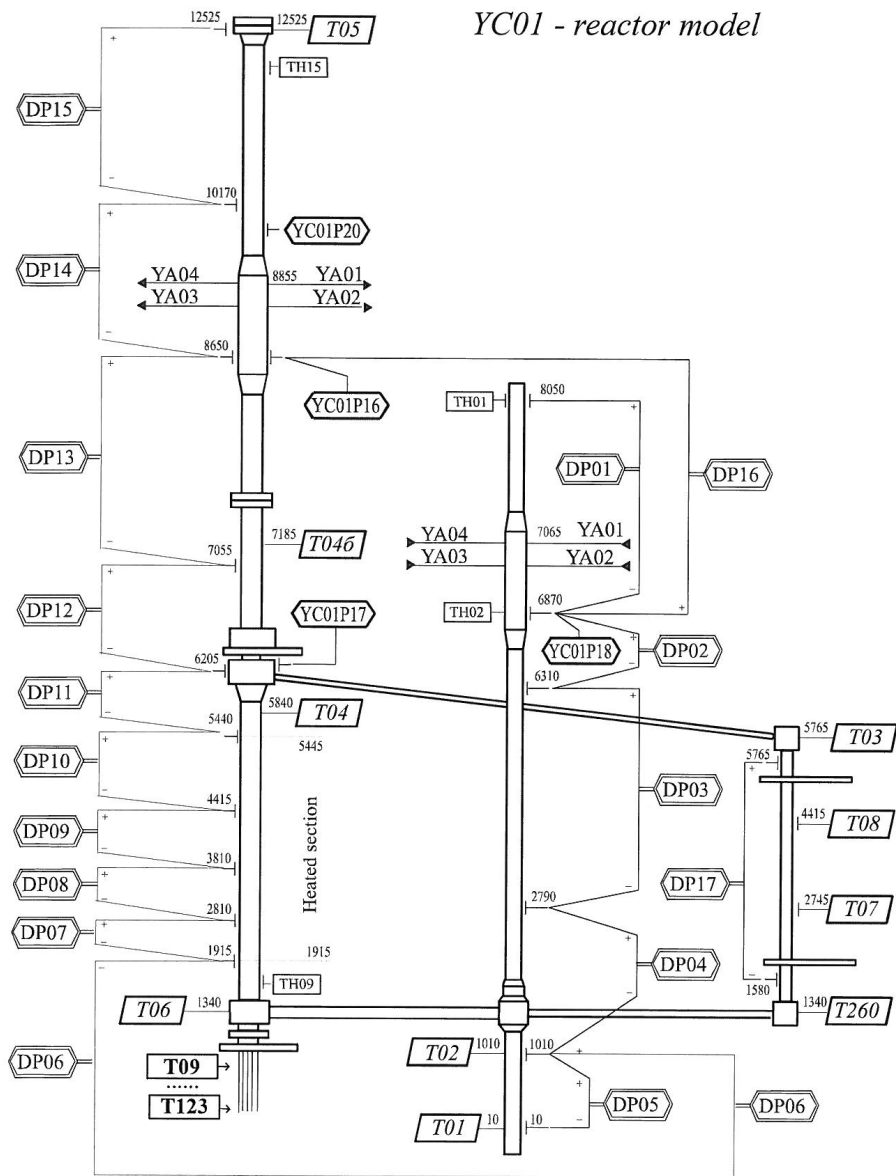
Figure 3 Reactor model measurements
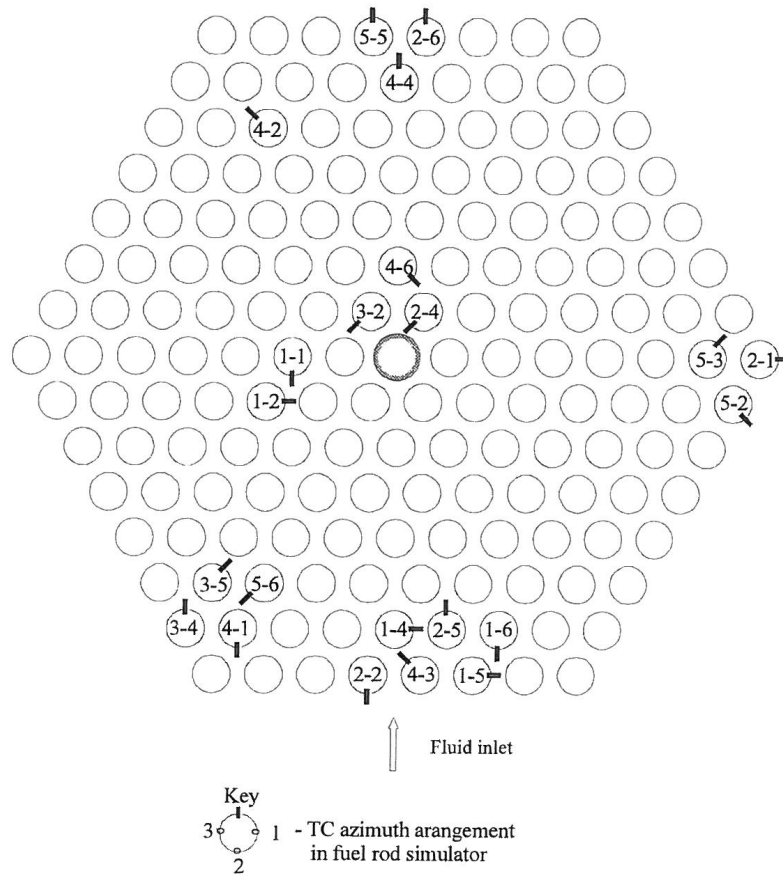
Figure 4 Fuel rod simulator bundle cross section
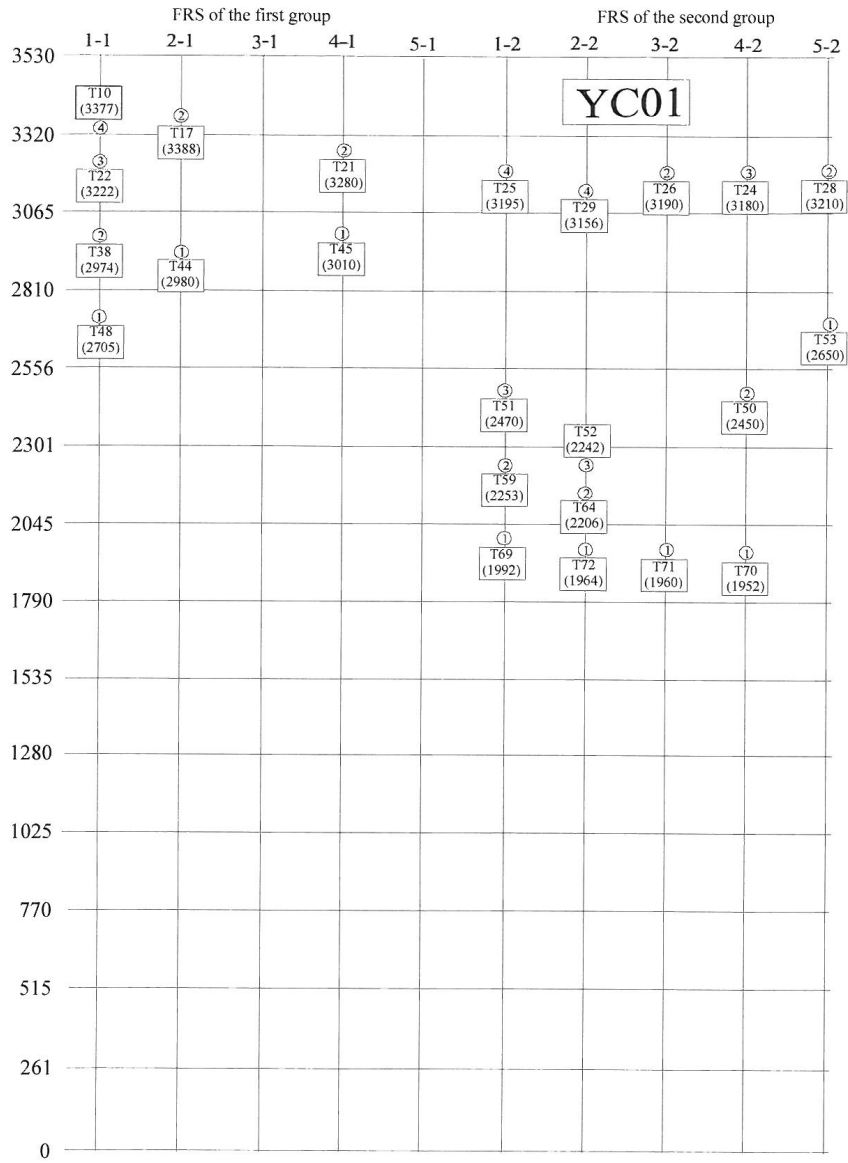
Figure 5 Axial positions of thermocouples (Groups No. 1 and No. 2)
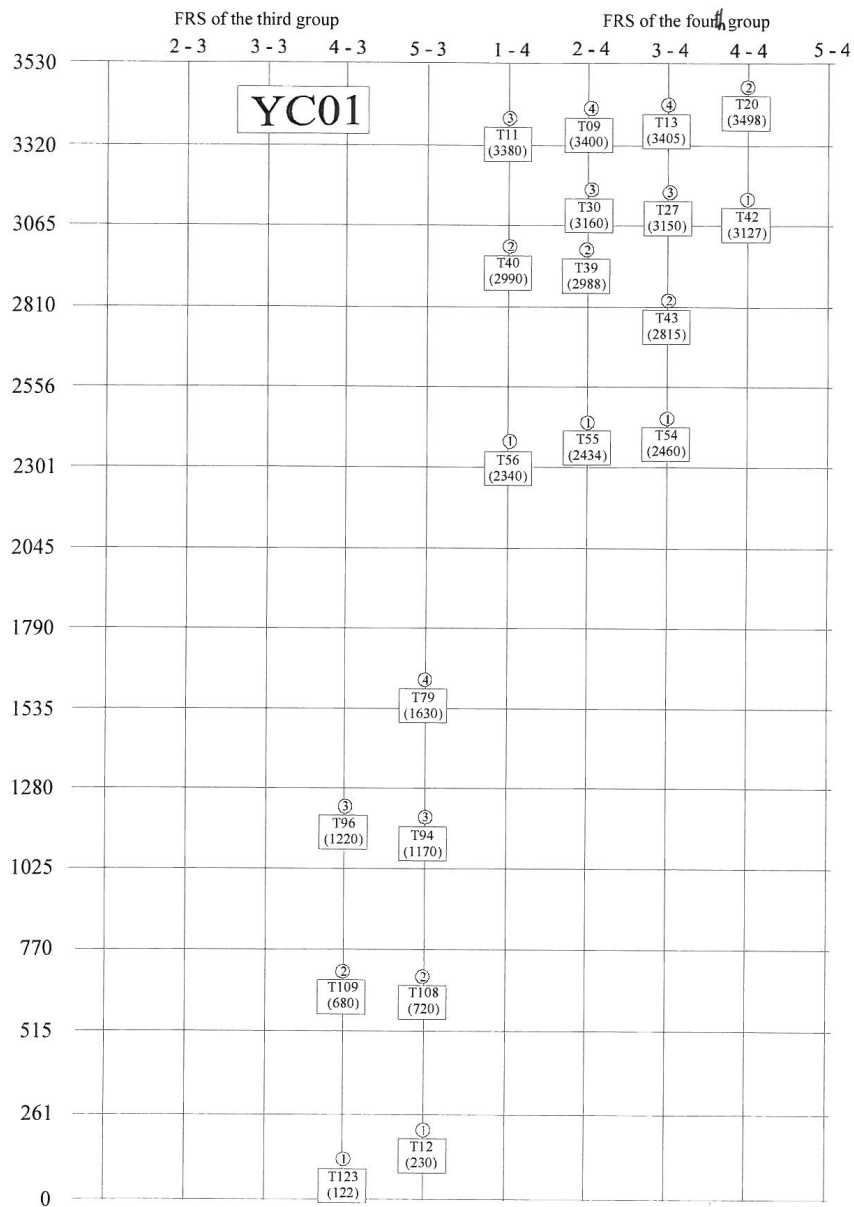
Figure 6 Axial positions of thermocouples (Groups No. 3 and No. 4)
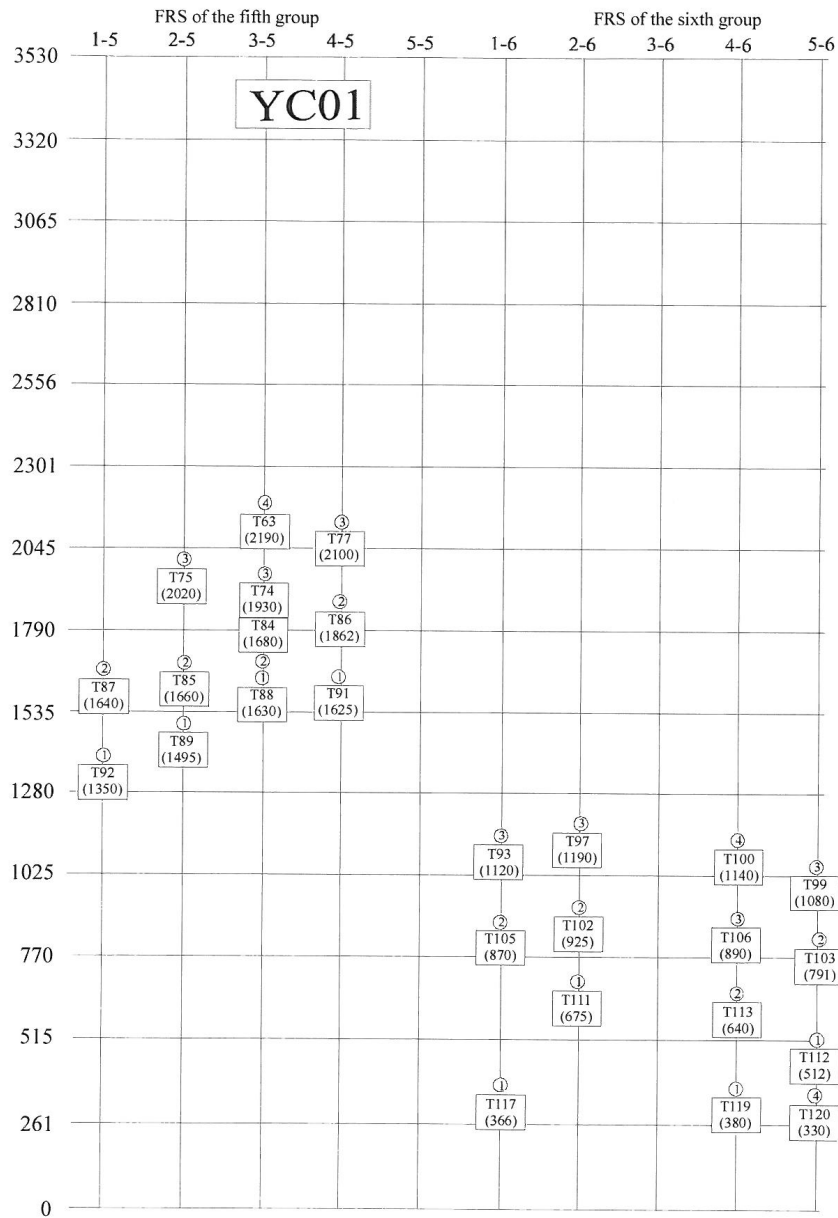
Figure 7 Axial positions of thermocouples (Groups No. 5 and No. 6)
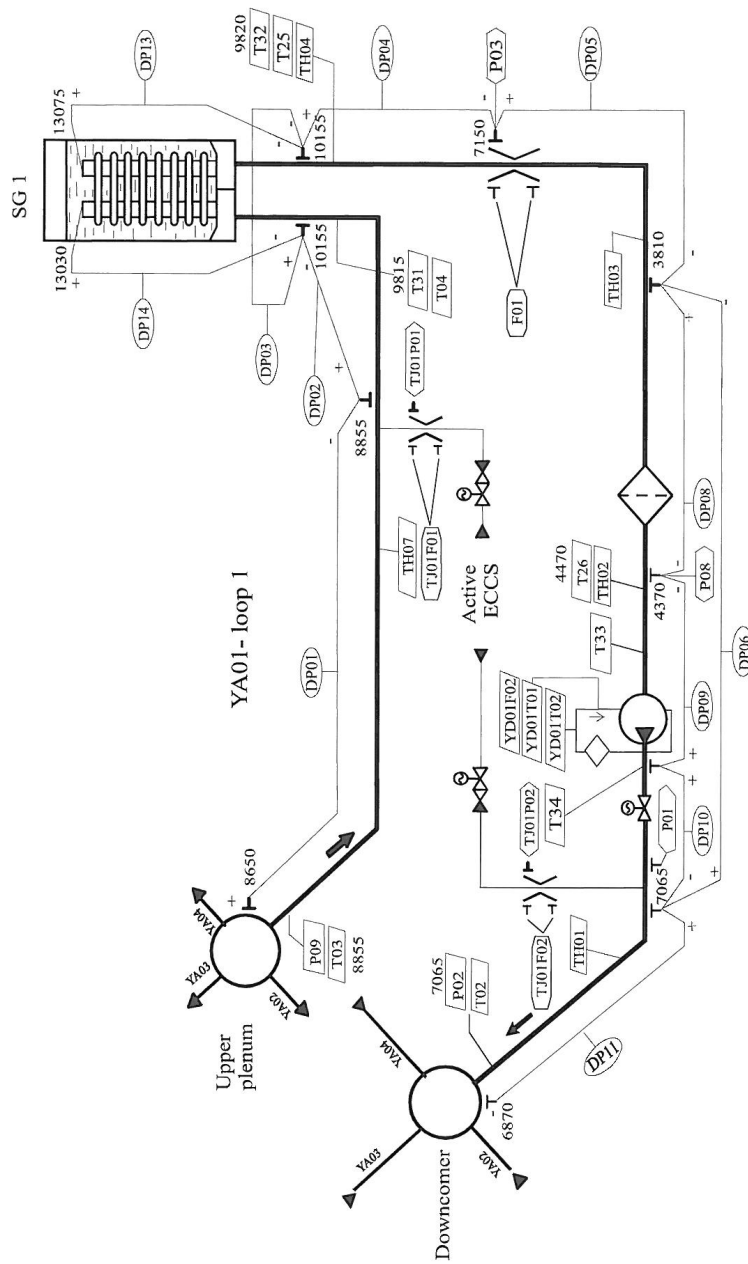
Figure 8 Primary coolant loop model measurements (Loop No. 1)

12
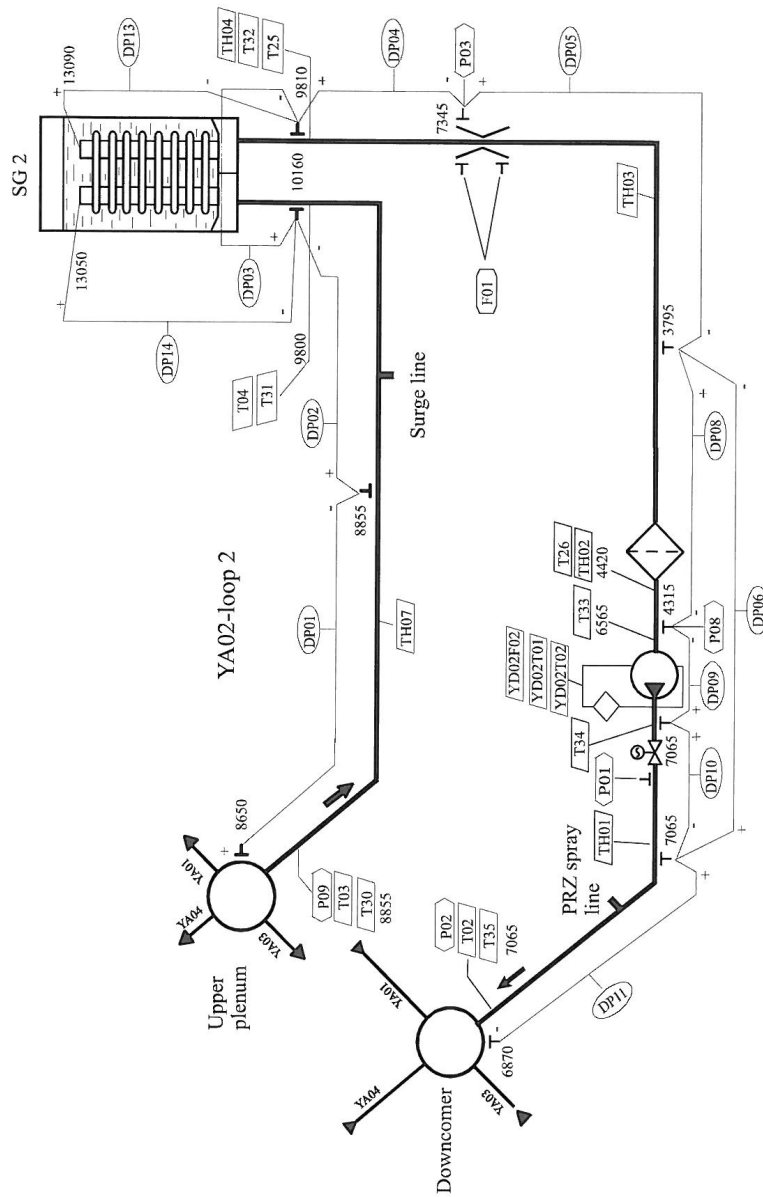
Figure 9 Primary coolant loop model measurements (Loop No. 2)
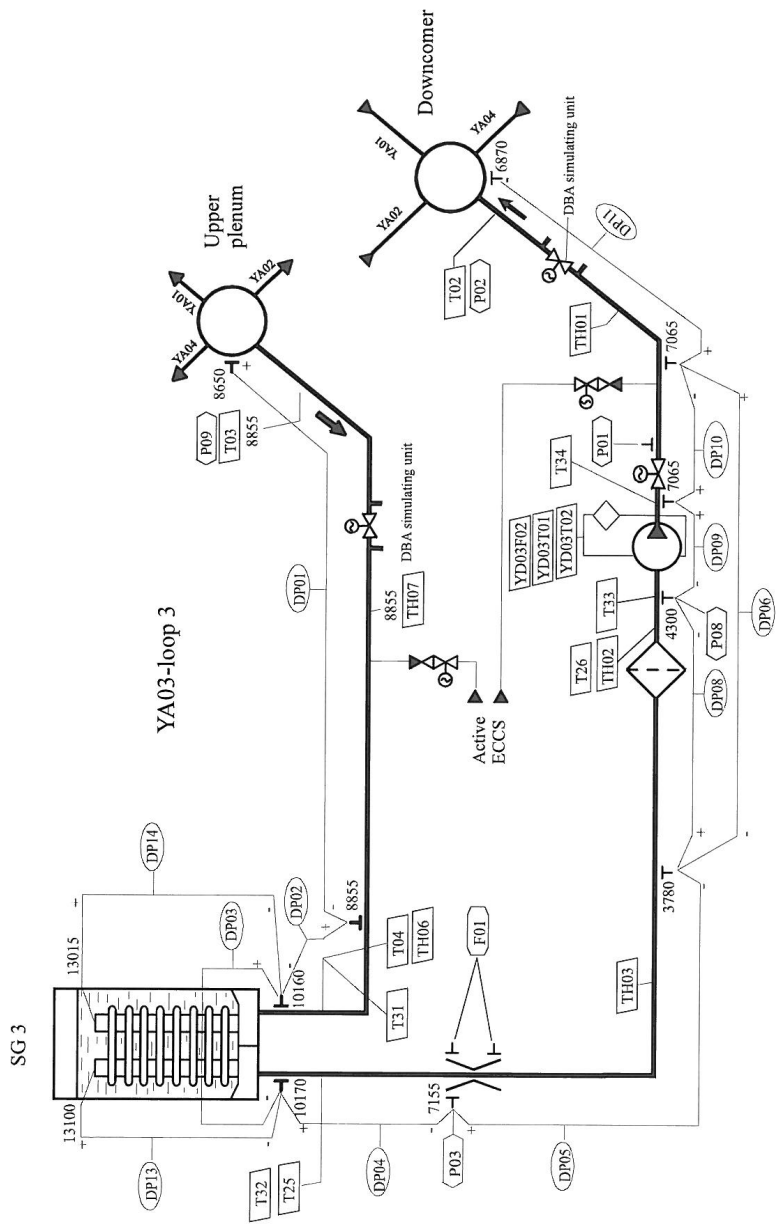
Figure 10 Primary coolant loop model measurements (Loop No. 3)
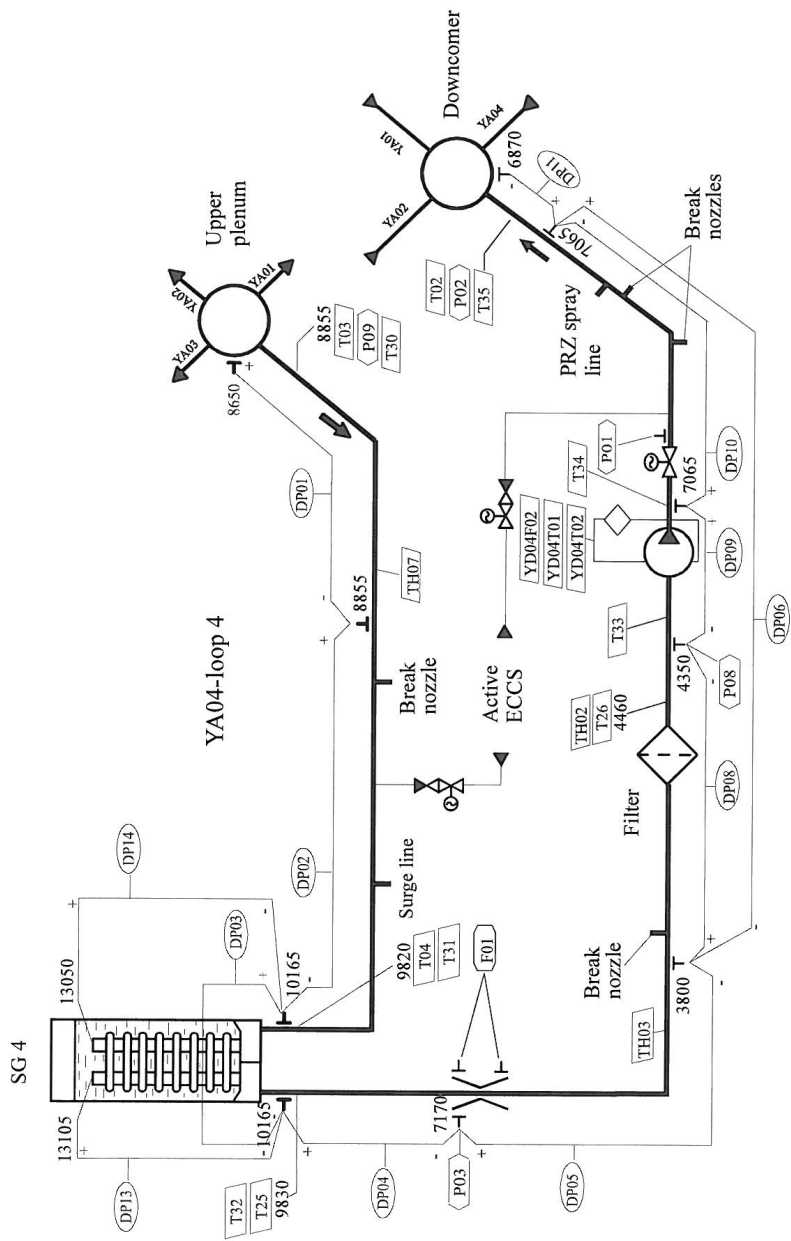
Figure 11 Primary coolant loop model measurements (Loop No. 4)
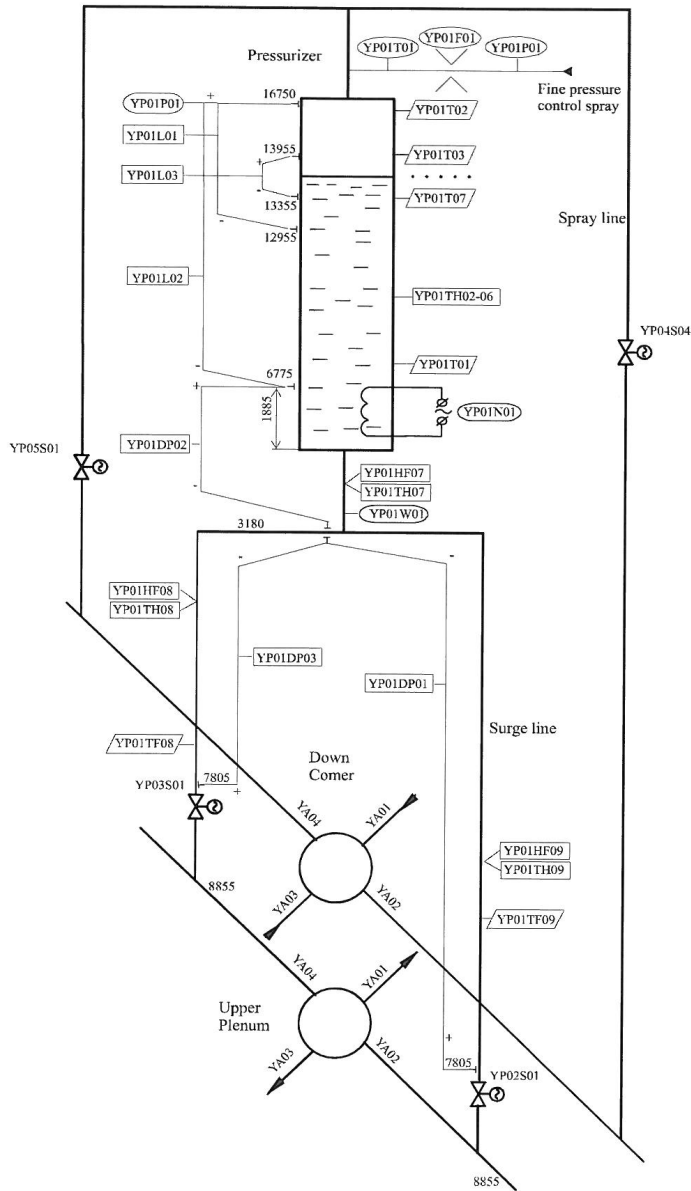
Figure 12 Pressurizer model measurements

10 MW steam
discharge line

RA01-04F01
RA01-04F02

RA01-04P01

RA01-04T01

RA01-04F01
RA01-04F02

14225

YB01-04P01

14230

1.5 MW steam
discharge line

RA01-04T01

RL01-04F02

water level

12960

feed water

13025   YB01-04TF01

RL01-04P02

RL01-04T02

YB01-04L01

14230

towards
primary-to-secondary
break line

11105

YB01-04L02

SG tube
bundle botton

10595

10525

10105

drainage
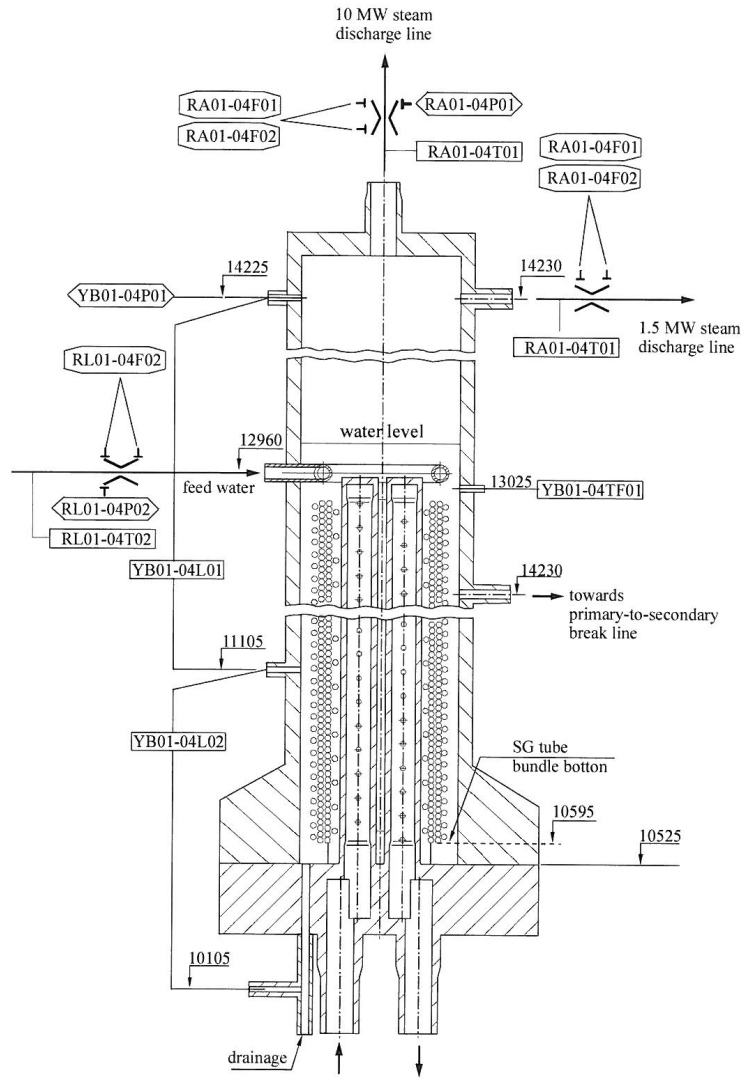
Figure 13 Steam generator models measurements

17
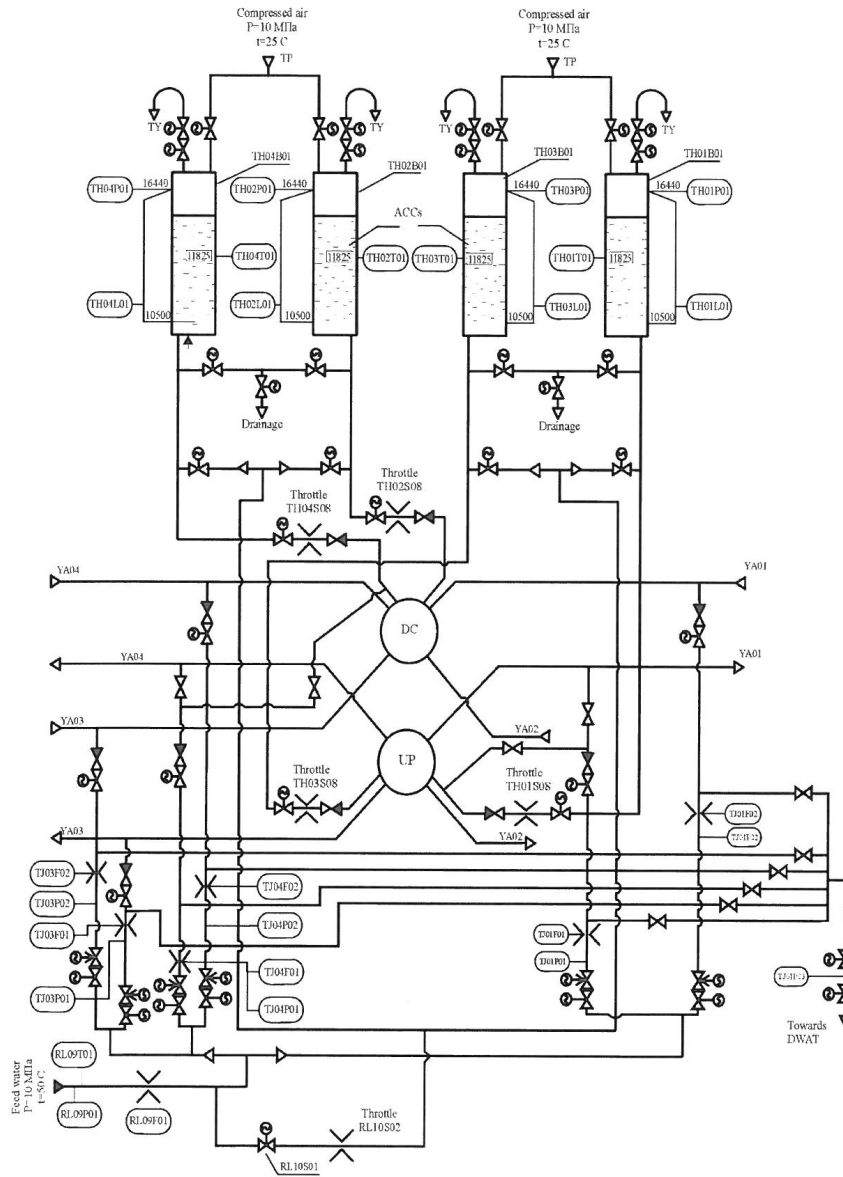
Figure 14 Emergency core cooling system model measurements

3. RELAP5/MOD3.3 CODE ASSESSMENT

As for as large-break LOCA analyses, the RELAP5/MOD3.3 code developmental assessment [9] is based on LOFT large-break LOCA test L2-5 [10-12]. Recently, the L2-5 test was reanalyzed [13] within the frame of larger international program BEMUSE [3]. Four out of total 14 participants used RELAP5/MOD3.3 code in [13] and contributed to the independent RELAP5/MOD3.3 code assessment for large-break LOCA analyses. The authors of this report had participated in the BEMUSE project also with RELAP5/MOD3.3 code as NRI-1 group. Since the results of the BEMUSE project were already published [3], the contribution of NRI-1 group is not repeated here. However, the methodology applied for BEMUSE Phases II and III is used here to present another RELAP5/MOD3.3 code independent assessment for large-break LOCA analyses. The results of the independent RELAP5/MOD3.3 code assessment against large-break LOCA test performed at PSB-VVER test facility [4] are reported below.

The first two steps in the thermal-hydraulic system code assessment process are defined in [2] as:

- Formulate assessment matrices for each class of transient studied, e.g., large-break LOCA, small-break LOCA.
- Select key parameters for these classes.

When addressing these steps the authors ask the reader to refer to [14]: "The construction of VVER Thermal Hydraulic Code Validation Matrix follows the logic of the CSNI Code Validation Matrices (CCVM) [12]. Similar to the CCVM it is an attempt to collect together in a systematic way the best sets of available test data for VVER specific code validation, assessment and improvement, including quantitative assessment of uncertainties in the modelling of phenomena by the codes." Since the PSB-VVER test facility was not in operation at the time the report [14] was compiled, the phenomena vs. system test large-break LOCA matrix refers PSB-VVER as "expected to be suitable". Test facility vs. phenomena, specifically the suitability of test data for the code assessment, is further discussed in [4]. The selection of key parameters to be compared is based on [13] and [15].

3.1 PSB-VVER Test-5a Description

The general objectives of PSB-VVER large-break LOCA experiment are listed in [4]:

- Investigate the thermal-hydraulic response of the VVER-1000 primary system to the cold leg double ended guillotine break.
- Evaluate the capability of the PSB-VVER test facility to simulate the LB LOCA in VVER-1000.
- Obtain experimental data for validation of thermal-hydraulic codes applied to LB LOCA analysis of VVER-1000 NPP.

Internally at EREC, the test is denoted as CL-2x100-01. In the context of PSB-VVER OECD Project, the test is denoted as Test-5a.

Test-5a specific PSB-VVER facility configuration is discussed in Table 3.

Table 3 Test-5a specific PSB-VVER test facility configuration

Subsystem	Description
Pressurizer	Surgeline was connected to the hot leg loop No. 4.
Core bypass	Two orifices with a diameter of 7 mm were installed at the inlet/outlet of the core bypass.
Steam generators	Under initial steady state operation all SGs were connected to each other by the steam header. The steady state pressure was adjusted by steam dump valve RA06S01 located at common steam line.
Feedwater	Under initial steady state operation the SG secondary side coolant levels were adjusted by RL01S06, RL02S06, RL03S06, and RL04S06 valves. The feedwater temperature was close to 214 °C.
Accumulators	ACC No. 1 and ACC No. 3 surgelines were connected to the upper plenum simulator. ACC No. 4 surgeline was connected to the downcomer simulator. ACC No. 2 was isolated throughout the test.
HPIS	Two lines of HPIS were connected to cold legs of PCS loops No. 1 and No. 3.
LPIS	One line of LPIS was connected to PCS loop No. 3 with injection points at the hot leg and at the cold leg. One line of LPIS was connected to the RPV simulator with injection points at the upper plenum simulator and at the downcomer simulator.
Break unit	The break unit was located in the horizontal section of PCS loop No. 3 cold leg between the downcomer simulator inlet nozzle and RCP. Break nozzles were smooth edged channels with a diameter of 50 mm and a length of 350 mm.
Upper plenum	Under steady state operation the upper plenum simulator warm-up line was opened. The line was closed 2 minutes prior to the initiation of the transient.

The PSB-VVER DAS recorded the measured parameters with a frequency of 20 Hz throughout the test. Data from 14 pressure gauges were recorded with a frequency of 200 Hz.

Test-5a specific PSB-VVER facility initial conditions are presented in Table 4.

Table 4 Test-5a specific PSB-VVER test facility initial conditions

Parameter	Measurement	Value	Measurement accuracy
Primary coolant system			
Upper plenum pressure, MPa	YC01P16	15.71	± 0.06
Hot leg inlet coolant temperature, °C	YA01T03	321	± 3
	YA02T03	321	± 3
	YA03T03	320	± 3
	YA04T03	323	± 3
Cold leg outlet coolant temperature, °C	YA01T02	292	± 3
	YA02T02	292	± 3
	YA03T02	290	± 3
	YA04T02	290	± 3
FRSP power, kW	YC01N01	1512	± 15
BP power, kW	YC01N02	16.1	± 0.7
Pressurizer level, m	YP01L02	6.5	± 0.3
Secondary coolant system			
SG pressure, MPa	YB01P01	7.78	± 0.05
	YB02P01	7.81	± 0.05
	YB03P01	7.84	± 0.05
	YB04P01	7.77	± 0.05
SG level, m	YB01L01	1.68	± 0.08
	YB02L01	1.70	± 0.08
	YB03L01	1.67	± 0.08
	YB04L01	1.71	± 0.08
Accumulators			
ACC pressure, MPa	TH01P01	5.93	± 0.03
	TH03P01	5.91	± 0.03
	TH04P01	6.06	± 0.03
ACC level, m	TH01L01	5.65	± 0.07
	TH03L01	5.65	± 0.07
	TH04L01	5.69	± 0.07

Test-5a specific PSB-VVER facility boundary conditions are presented in Table 5.

Table 5 Test-5a specific PSB-VVER test facility boundary conditions

Time, s	Event
0	Break simulation
0	Start of RCPs coastdown simulation
0	Steam line isolation signal, start of RA06S01 valve closing
0.4	SCRAM, FRSB and BP power controlled to simulate decay heat
4.1	SG feedwater isolation, start of RL02S06 valve closing
4.7	SG feedwater isolation, start of RL01S06 valve closing
4.7	SG feedwater isolation, start of RL04S06 valve closing
5.9	SG feedwater isolation, RL01S06 valve closed
6.5	SG feedwater isolation, RL04S06 valve closed
8.7	SG feedwater isolation, start of RL03S06 valve closing
9.9	SG feedwater isolation, RL02S06 valve closed
10.2	Start of ACC-4 injection
10.7	Start of ACC-1 and ACC-3 injection
10.8	SG feedwater isolation, RL03S06 valve closed
11.0	Pressurizer emptied
15.5	Steam line isolation signal, valve RA06S01 closed
40.3	Start of HPIS injection
40.3	Start of LPIS injection
89.0	Stop of ACC-1 injection
92.0	Stop of ACC-4 injection
107.0	Stop of ACC-3 injection
159.0	Start of 1st FRSB cladding heatup
231.3	Stop of RCPs coastdown simulation
556.0	Stop of 1st FRSB cladding heatup (cladding quenched)
921.8	Stop of HPIS injection
921.8	Stop of LPIS injection
1187.0	Start of 2nd FRSB cladding heatup
1477	FRSB power switched off – end of the experiment

In PSB-VVER Test-5a the large-break LOCA accident, double ended guillotine cold leg No. 3 break was simulated with boundary conditions simulating coincident loss of offsite power. The FRSB and core bypass power levels were controlled to simulate decay heat power. The frequencies of RCP electro motors were programmed to simulate the RCPs coastdown. The ECCS actions were simulated. Two periods of FRSB cladding heatup were observed based on thermocouple measurements. The first one occurred just after the end of accumulator injection and was terminated by the continuing HPIS/LPIS injection. The second FRSB cladding heatup occurred after the stop of HPIS/LPIS injection. This heatup was terminated by operators after the cladding temperature reached the prescribed level.

3.2 RELAP5/MOD3.3 Thermal-Hydraulic Model of PSB-VVER Test Facility

The facility database was compiled in an MS-ACCESS environment. Facility design data and thermal-hydraulic characteristics as reported as part of OECD/NEA PSB-VVER Project were organized in two tables with a total of 600 records. The facility model notebook was compiled in an MS-EXCEL environment developing RELAP5/MOD3.3 T-H model of the PSB-VVER facility in several steps up to the code input deck. The input deck for steady state runs consists of 31170 lines.

In the verification step, the initial and boundary conditions for the RELAP5/MOD3.3 PSB-VVER facility model were set up to simulate Test-3 of OECD/NEA PSB-VVER project, i.e. the small-break LOCA experiment, 4.1% cold leg break with initial power scaled further down to 15% of prototypical [5]. In the verification step, the "null transient" method was applied to reproduce the test specific initial conditions. As the acceptance criterion, the code calculated data were requested to be within the corresponding channel measurement accuracy interval. The small-break LOCA transient was analyzed in code restart mode with specification of test specific trips in order to simulate the boundary conditions of the experiment. As the acceptance criterion, the calculated data were requested to reproduce the measured data qualitatively (phenomena and trends), with only key parameters (e.g. primary system pressure) being compared quantitatively.

In the validation step, the initial and boundary conditions of the reference case calculations (steady state run and transient run) were set up for the facility model in question to simulate Test-5a of OECD/NEA PSB-VVER project, i.e. the large-break LOCA experiment, double ended guillotine cold leg break with initial power scaled further down to 15% of prototypical [4]. This case is described in detail in Chapter 3.3 below.

In order to facilitate the description of RELAP5/MOD3.3 T-H model of PSB-VVER test facility, the reference case steady state R5/M3.3 code input deck was imported to SNAP [8] and thermal-hydraulic views were reorganized as shown in Figures 15 to 26.

The hydraulic part of PSB-VVER facility T-H model consists of 1580 control volumes and 1841 junctions. Its thermal part consists of 849 heat structures with a total of 6296 mesh points. Resulting R5/M3.3 PSB-VVER test facility T-H model is rather detailed. The basic idea was to have control volume centers at the actual locations of measurement gauges. This approach had to be compromised only if higher order nodalization criteria had been applied, e.g. at core model, the node boundaries were placed at grid spacer locations, control volume centers at ascending legs were placed at the same elevation as control volumes in descending legs, etc.

The nodalization of reactor pressure vessel model is illustrated in Figure 15. Downcomer inlet annulus is represented by a total of 12 annulus components in three axial levels and 4 azimuthal sectors. Single junction components (cn49; n=1, 4) are used to model primary coolant cold leg outlets. Multiple junction components (not shown in this view) are used to simulate axial and azimuthal flows between the downcomer inlet annular sectors. Multiple junction components are also used to connect the downcomer inlet annulus with main downcomer that is modelled with pipe component (c030) having 36 axial control volumes. In order to represent the actual design of the downcomer lower part, branch component (c031) and annulus component (c035) are used. A combination of single junction components (c036, c040, c045), pipe components (c037, c051), and annulus component (c041) is used to model the lower plenum simulator. The hydraulic part of the core simulator is modelled with 5 pipe components each having 16 control volumes. Four pipes (c061, c062, c063, and c064) represent the azimuthal sector of the corresponding PCS loop. Pipe (065) is used to model the central part of the FRSB. Multiple junction components (not shown in this view) are used to simulate radial and azimuthal cross flows in FRSB. Two fuel rod heat structures per each sector (central and azimuthal) are used to distinguish between uninstrumented and instrumented fuel rods in the bundle. The design of instrumented fuel rods differs slightly in that internal and external claddings are used along the heated section (thermocouples are located in between). The surface factors are defined to account for the actual number of fuel rod simulators in each sector. Other heat structures are used to model unheated parts of FRSB. Multiple junction component (c076), two pipe components (c077, c078), and single junction component (c079) are used to model the core bypass simulator. A part of pipe (c078) vertical section is heated. Pipe component (c070) with 33 control volumes models the combined simulator of the upper plenum and upper head. Upper plenum outlet annulus is represented by a total of 12 annulus components in three axial levels and 4 azimuthal sectors. Multiple junction components (not shown in this view) are used to simulate axial and azimuthal flows between the upper plenum outlet annular sectors. Single junction components (cn04; n=1, 4) are used to model the primary coolant hot leg inlets.

PSB-VVER Reactor Pressure Vessel Model

Upper Head

Upper Plenum Outlet Annulus   Upper Plenum Outlet Annulus

Upper Plenum

Downcomer Inlet Annulus   Downcomer Inlet Annulus

Core Bypass

Downcomer   Core

Lower Plenum

Downcomer Outlet Annulus
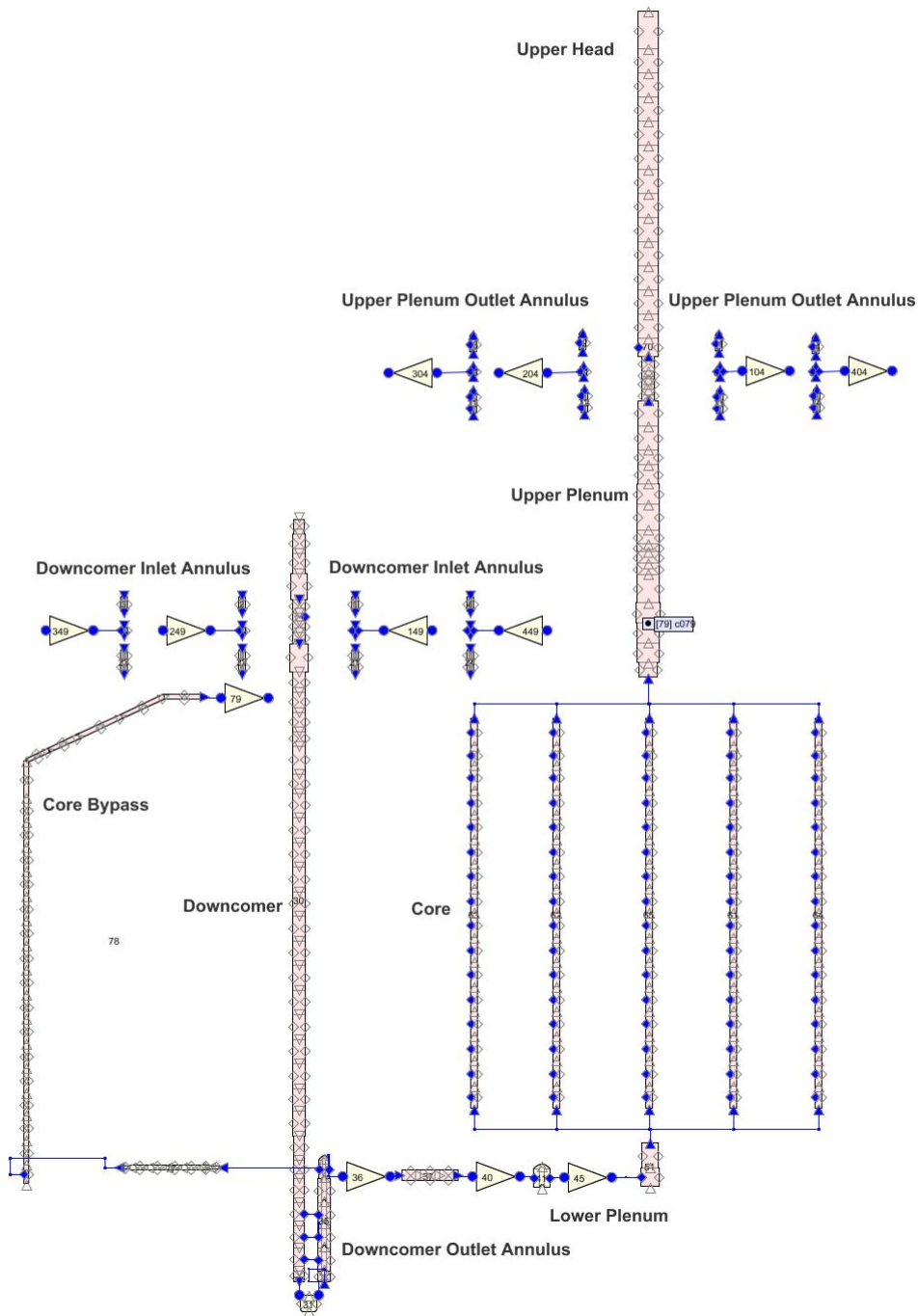
Figure 15 R5/M33 reactor pressure vessel model

The nodalization of PCS loops is illustrated in Figures 16 to 19. Pipe components (cn05; n=1, 4) each with 22 control volumes are used to model the hot legs. Two single junction components (cn09, cn14; n=1, 4) and the single volume component (cn10; n=1, 4) per loop are used to model the steam generator inlets. Steam generator primary side models consist of a hot header model, pipe components (cn15; n=1, 4), horizontal tube bundle simulator, pipe components (cn2r; n=1, 4; r=1, 9), and cold header model, pipe components (cn31; n=1, 4). Multiple junction components are used to model flow paths between the tube bundle and the headers. In the PSB-VVER test facility, the steam generator simulator consists of 34 nearly horizontal coiled tubes. In R5/M3.3 facility T-H model, the individual tubes are grouped to have nine tube rows along the height of steam generator vessel. Two single junction components (cn32, cn34; n=1, 4) and the single volume component (cn33; n=1, 4) per loop are used to model steam generator outlets.

PSB-VVER Primary Coolant System Model - Loop No. 1

Steam Generator

114

132

134

109

105

Hot Leg

Cold Leg

Reactor Coolant Pump

141

136

HPIS/LPIS

661

135

660

Loop Seal
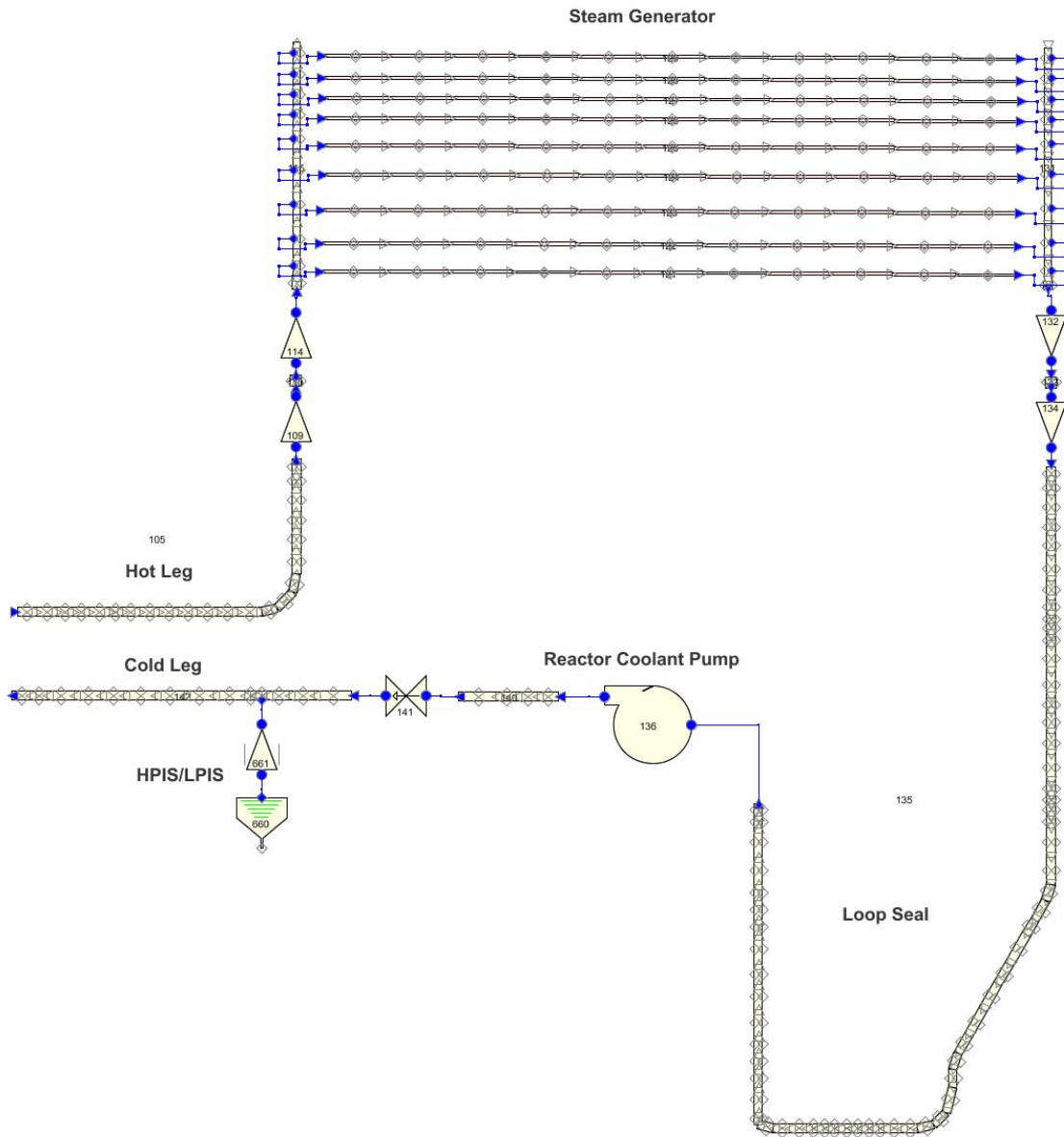
Figure 16 R5/M33 primary coolant system model – Loop No. 1

PSB-VVER Primary Coolant System Model - Loop No. 2

Steam Generator

214

209

205

Hot Leg

232

234

235

Cold Leg

Reactor Coolant Pump

241

236

Loop Seal
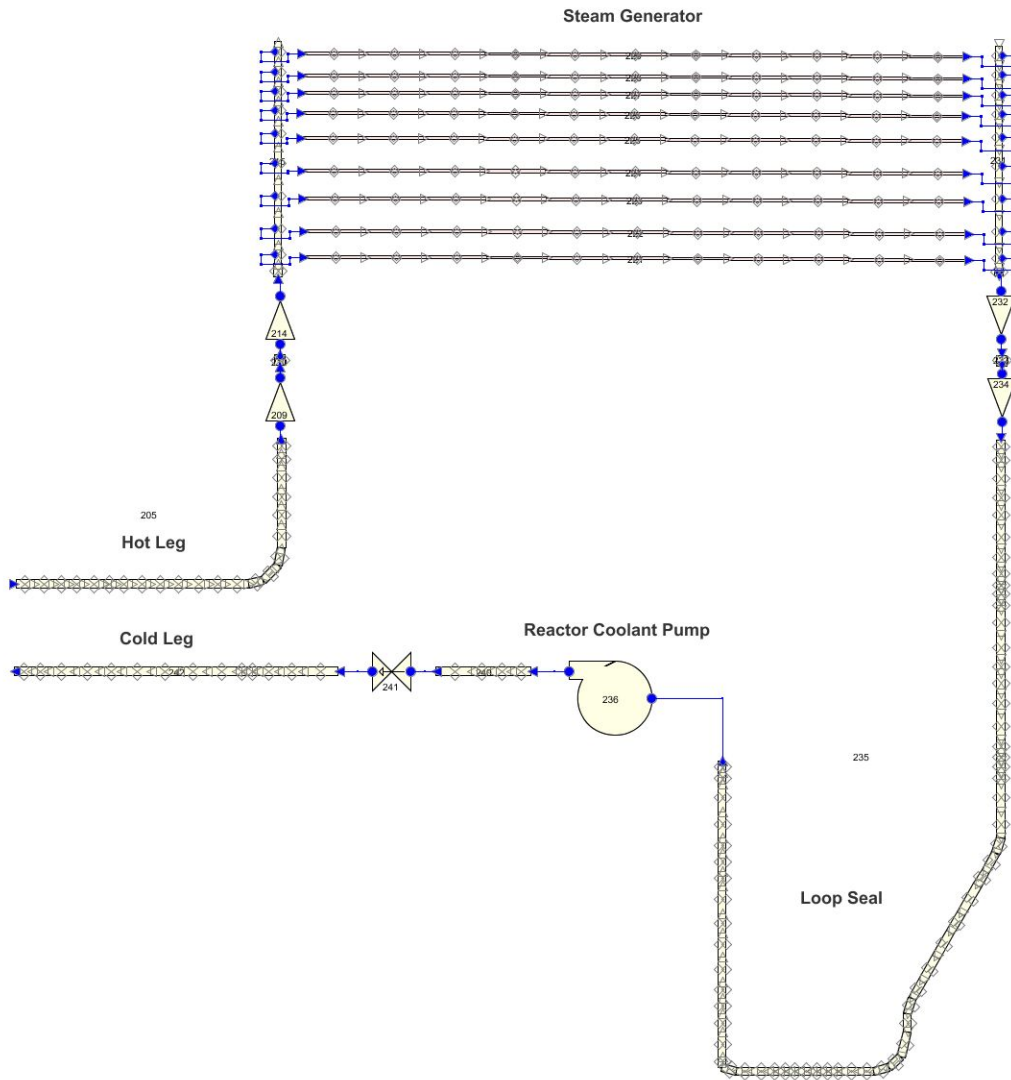
Figure 17 R5/M33 primary coolant system model – Loop No. 2

PSB-VVER Primary Coolant System Model - Loop No. 3

Steam Generator

HPIS/LPIS

670

305

671

Hot Leg

314

309

Cold Leg

Reactor Coolant Pump

343

342

341

336

666

HPIS/LPIS

665

332

334

335

Loop Seal

710

712

713

Break

720

722

723
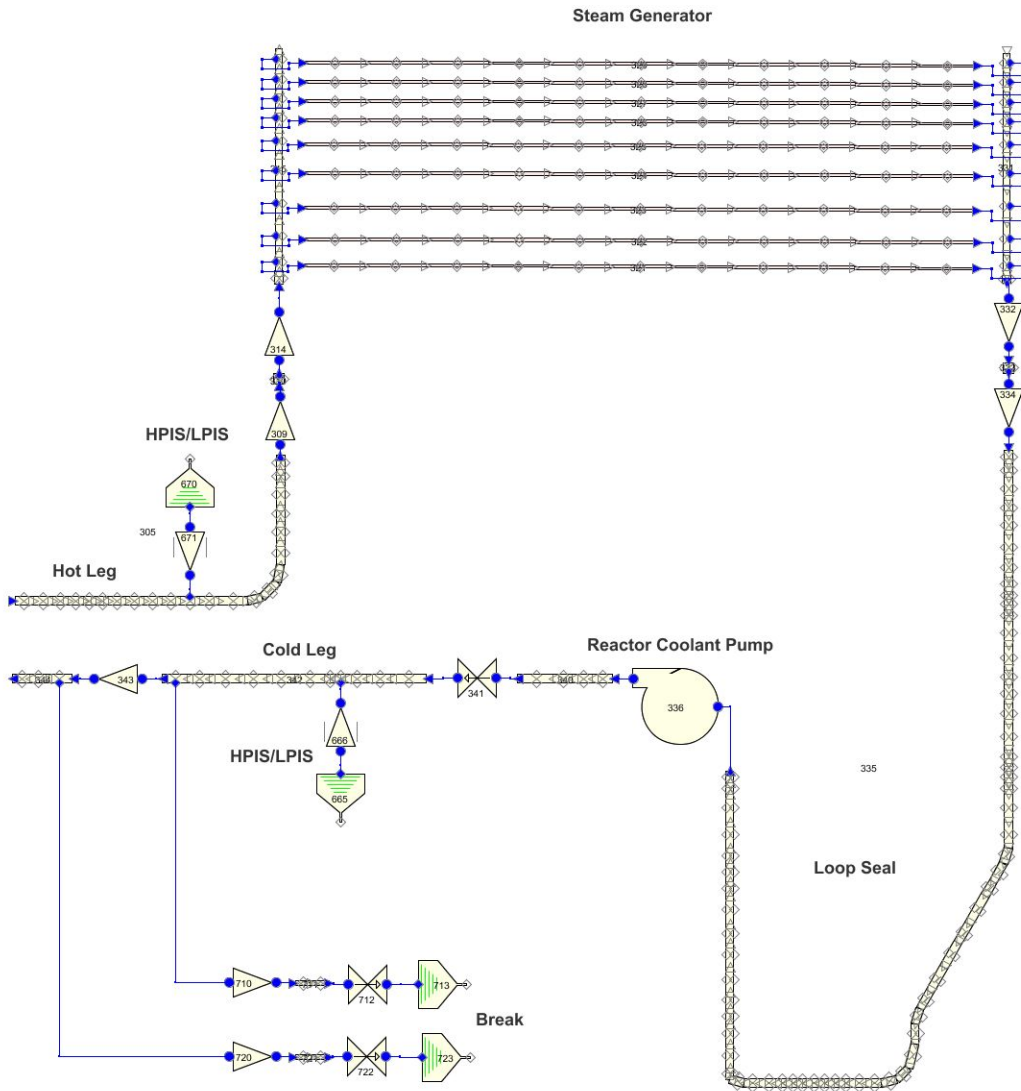
Figure 18 R5/M33 primary coolant system model – Loop No. 3

PSB-VVER Primary Coolant System Model - Loop No. 4
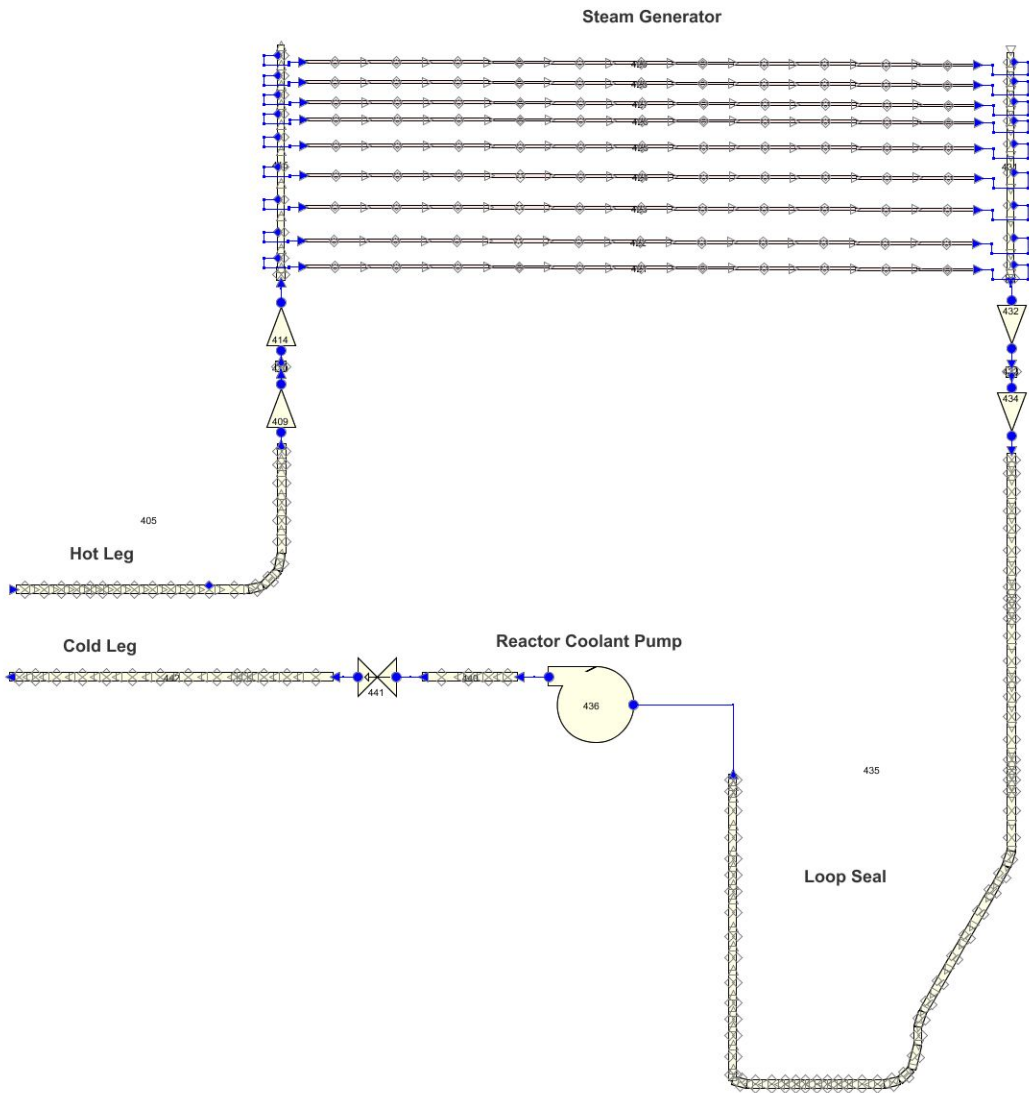
Figure 19 R5/M33 primary coolant system model – Loop No. 4

Pipe components (cn35, n=1, 4) each with 64 control volumes are used to represent the loop seals. Reactor coolant pumps are modelled with pump components (cn36, n=1, 4). The intact loop cold legs are modelled using pipe components (cn40, n=1, 2, 4) with 3 control volumes, valve components (cn41, n=1, 2, 4), and pipe components (cn42, n=1, 2, 4) with 14 control volumes. In Test-5a, the break was simulated to occur at cold leg No. 3, so the nodalization of the broken loop cold leg is different and follows standard guidelines to model the double ended cold leg break. The actions of HPIS/LPIS are modelled using time dependent volume and time dependent junction components. The injection points are Test-5a specific.

The nodalization of the pressurizer and the pressurizer surgeline models is illustrated in Figure 20. Only the loop No. 4 hot leg connected surgeline is modelled using single junction component (c506), pipe component (c507) with 5 control volumes, valve component (c508), and pipe component (c509) with 23 control volumes. An attempt was made to model the loop No. 2 hot leg connected surgeline as well. This concept had to be abandoned due to computational difficulties (long dead end pipe). The model of the common part of the pressurizer surgeline begins with the branch component (c510) and continues using the pipe component (c511) with 5 control volumes. The actual connection to the pressurizer is modelled by the single junction component (c514). The pipe component (c515) with 55 control volumes is used to model the pressurizer vessel. The single junction component (c519), connected to the top of the pressurizer, and the time dependent volume component (c520) are used to adjust the desired steady state pressurizer pressure. Similarly, the time dependent junction (c529) and the time dependent volume (c530) components are used to adjust the desired steady state pressurizer coolant level. Time dependent junction components (c541 and c549), and time dependent volume components (c540 and c550) are used to achieve the desired steady state surgeline coolant temperature. In transient runs, the steady state control components are removed from the model.

PSB-VVER Pressurizer Model

Steady State Pressure Control

Pressurizer

Steady State Level Control
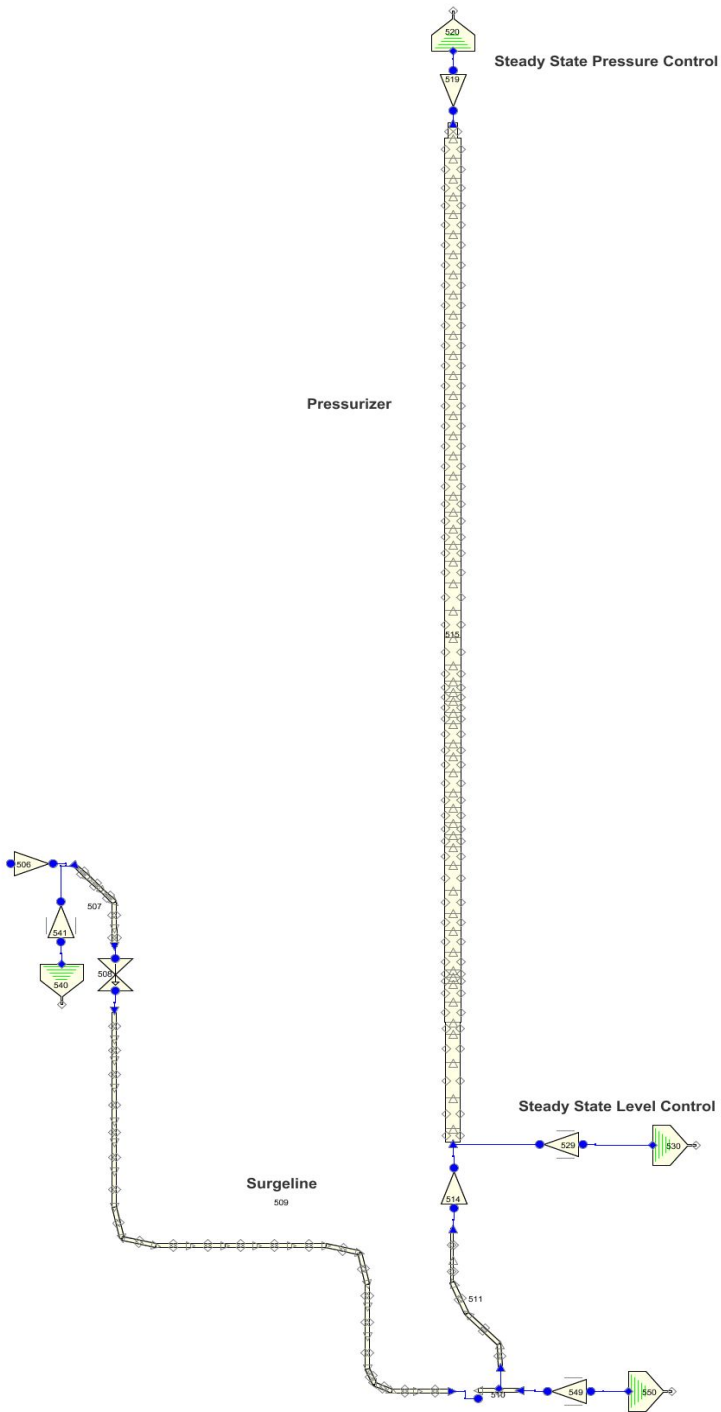
Surgeline

Figure 20 R5/M33 pressurizer model

The nodalization of the accumulators and accumulator surgelines is illustrated in Figure 21. Hydro-accumulator (TH20B01) was isolated during the Test-5a and therefore is not modelled here. Two hydro accumulators (c610 and c630) are connected to the upper plenum; one hydro-accumulator (c640) is connected to the downcomer. Only the check valves (c612, c632, and c642) are modelled explicitly. The respective surgelines isolation valves are not part of the model. The model also accounts for the actual locations of Test-5a specific HPIS/LPIS injection.
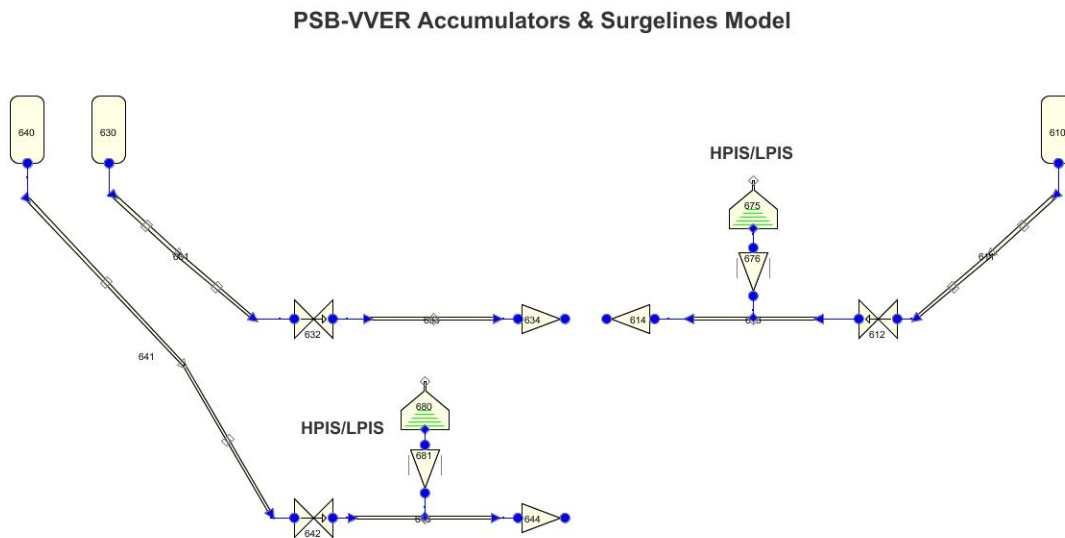
Figure 21   R5/M33 emergency core cooling system model

The nodalization of SG secondary side and associated steam and feedwater lines is illustrated in Figures 22 to 25. The combination of branch components is used to model the steam generator secondary side. Considering the top view, the central part of the vessel where the coiled tube bundle is located is treated as the "boiler" section, whereas the peripheral annular part is treated as the "downcomer" section. The lateral cross flow paths are modelled to simulate the internal recirculation of the secondary coolant. Nine rows of branch components correspond to nine rows of tube bundle simulated on the steam generator primary side. The branch components (cn71; n=1, 4) are used to account for the steam-water separation. The upper parts of steam generator vessels are modelled using the pipe components (cn75; n=1, 4), each with 3 control volumes. In PSB-VVER facility, there are two main steam lines per one steam generator. The 1.5 MWt steam line is designed to remove the heat generated by the 1.5 MWt FRSB power. If 10 MWt FRSB power (to follow 1:300 scale) were used for the particular test, the 10 MWt steam line would have been used. During the PSB-VVER experiments carried out within the frame of OECD/NEA PSB-VVER project only the 1.5 MWt FRSB power systems had been available. However, in order to account for unisolatable parts of 10 MWt steam lines and also for future use of the model, the 10 MWt steam lines are modelled and discussed here.

The 1.5 MWt steam line models consist of single junction components (cn83; n=1, 4), pipe components (cn84; n=1, 4), valve components (cn85; n=1, 4), pipe components (cn86; n=1, 4), single junction components (cn87; n=1, 4), and pipe components (cn88; n=1, 4). Actually, the later components are parts of 10 MWt steam lines.

The 10 MWt steam line models consist of single junction components (cn93; n=1, 4), pipe components (cn92; n=1, 4), valve components (cn91; n=1, 4), pipe components (cn90; n=1, 4), and valve components (cn89; n=1, 4). Valves in the 10 MWt steam lines were closed throughout the Test-5a.

The lengths and therefore the nodalization of individual steam lines vary accordingly to the loop specific design of the PSB-VVER test facility.

The combinations of time dependent volume components (cn95; n=1, 4), time dependent junction components (cn96; n=1, 4), pipe components (cn97; n=1, 4), and single junction components (cn98; n=1, 4) are used to model individual steam generator feedwater lines. In this, the facility steam generator feedwater system model is highly simplified.

The single junction components (cn94; n=1, 4) simulate the connections of individual steam lines to the main steam line.

Valve components (cn81; n=1, 4) are used to simulate actions of power operated relieve valves or safety valves. The test specific trip logic has to be set up to model steam dump to atmosphere. Time dependent volume components (cn82; n=1, 4) are used to model the boundary conditions.
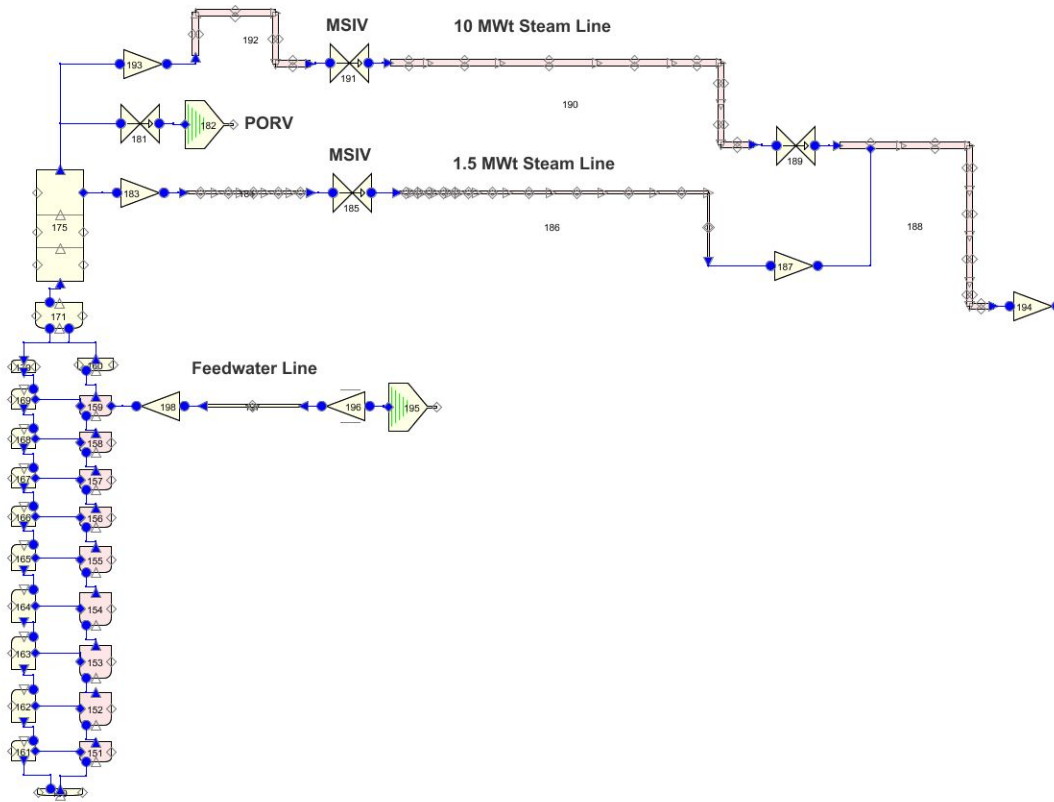
Figure 22 R5/M33 secondary coolant system model – Loop No. 1

PSB-VVER Secondary Coolant System Model - Loop No. 2
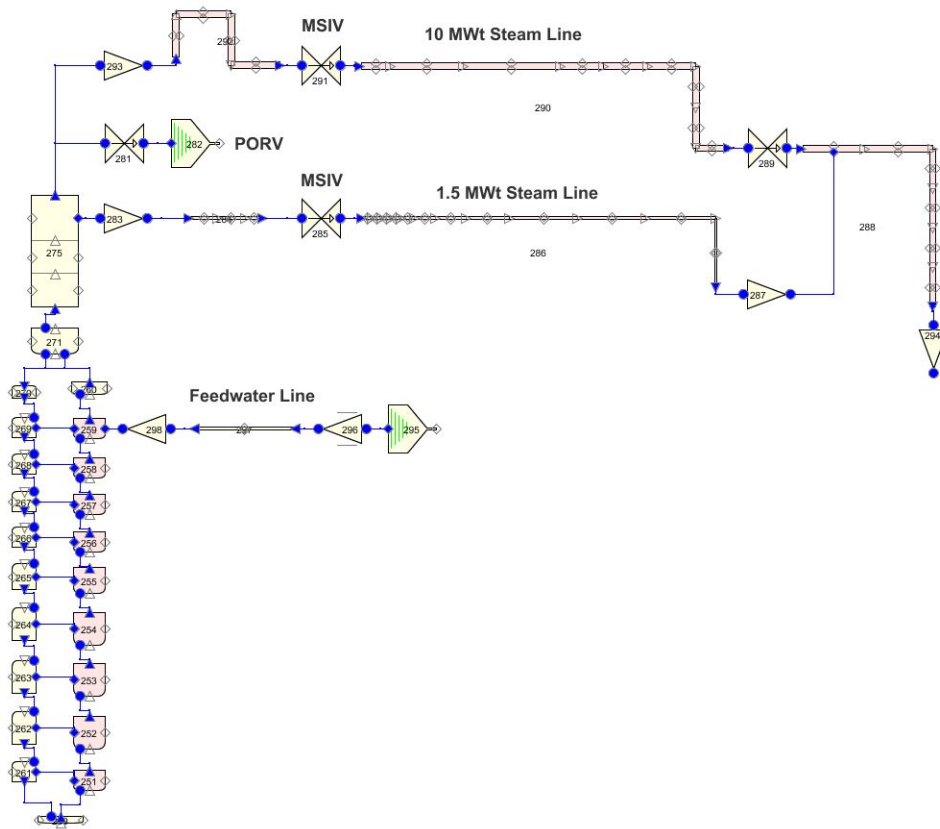
Figure 23 R5/M33 secondary coolant system model – Loop No. 2

PSB-VVER Secondary Coolant System Model - Loop No. 3
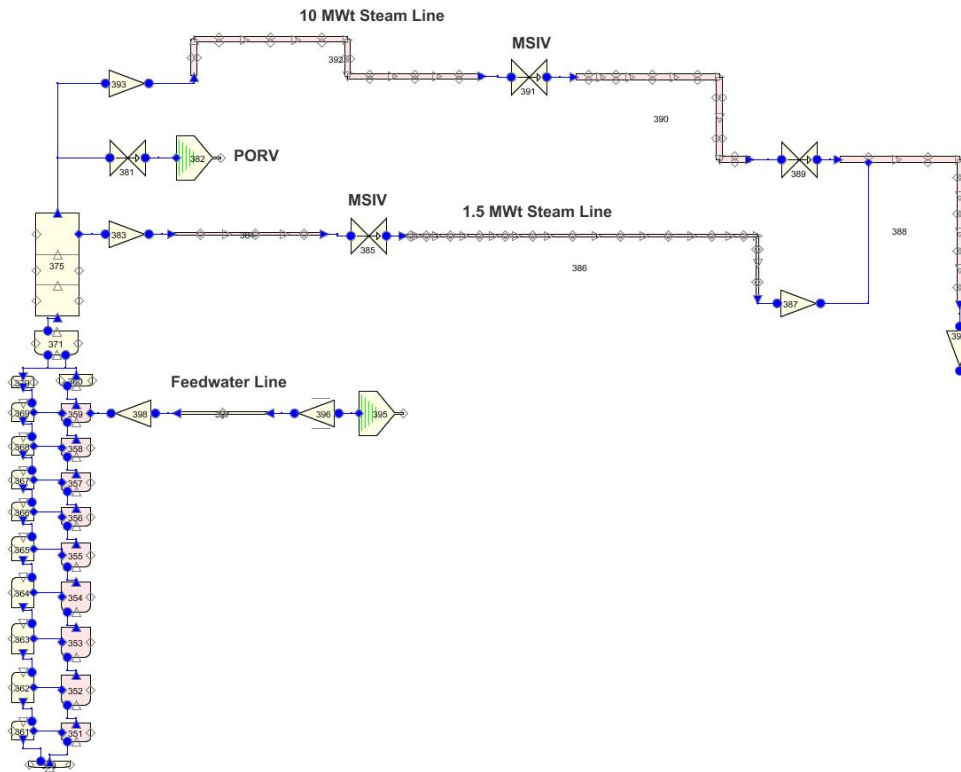
Figure 24 R5/M33 secondary coolant system model – Loop No. 3
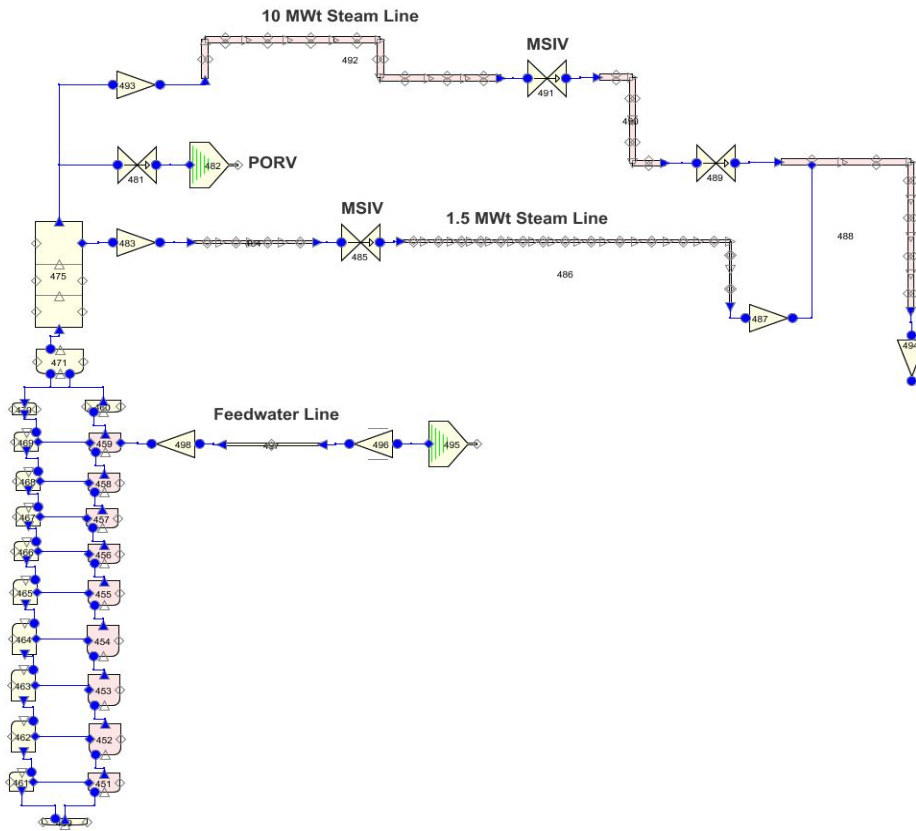
Figure 25 R5/M33 secondary coolant system model – Loop No. 4

The nodalization of the main steam line is illustrated in Figure 26. The main steam line is simulated using two pipe components connected with the single junction component. Valve component (c957) models the steam dump valve RA06S01.

PSB-VVER Main Steam Line Model
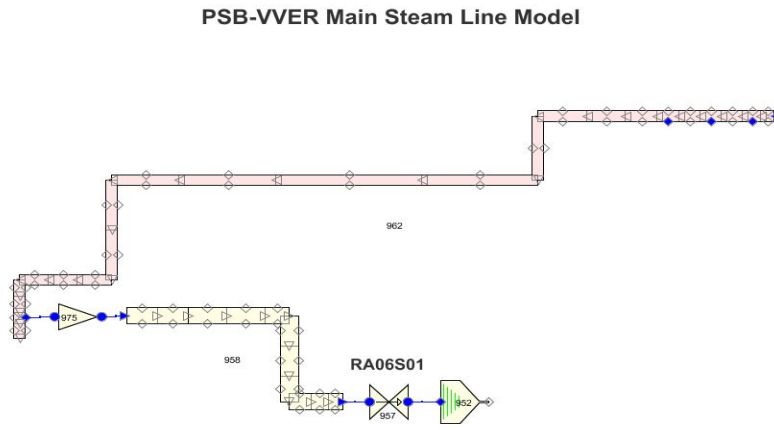
Figure 26 R5/M33 main steam line model

A number of heat structure components are used to simulate heat transfer in steam generators and heat losses from the pipe walls to the environment.

There are more than 2900 control systems used in the model. They are set up to simulate I&C actions, to drive the model to the desired steady state, to facilitate the comparison of calculated data with measured data (e.g. differential pressures), etc.

In this project, the developmental model control option 19 was activated, i.e. Bestion correlation was used for interphase friction in rod bundle geometry (pipe components c06n; n=1, 5).

As for as the flow process models, the counter current flow limitation models (Wallis and Kutateladze) are applied at selected junctions. Multiple junction component (c068) is used to model flow paths at the upper core plate simulator. Wallis CCFL model is selected. In order to account for CCFL phenomena at the upper plenum simulator, Kutateladze CCFL model is activated at junction No. 14 of the pipe component c070. Wallis CCFL model is activated at junction No. 9 of the pipe component c030 that simulates the downcomer. Kutateladze CCFL model is also invoked for SG inlet junctions (cn09; n=1, 4).

3.3 RELAP5/MOD3.3 PSB-VVER Test Facility Model Validation

The third step in the thermal-hydraulic system code assessment process is defined in [2] as:

- Perform assessment calculations. Compare the test data with the results of calculations for the key parameters.

This study follows the concept of the OECD/NEA BEMUSE Project, specifically Phase II [13]. In that, the reference case was run in two steps, i.e. the steady state run and the transient run to enable code data evaluation on the steady state level and on the transient level.

3.3.1 Reference Case

Similarly as in Phase II of the BEMUSE project, reference case in PSB-VVER Test 5a post test analysis was run and the test data were compared with the results of the calculation in two steps, on the steady state level, and on the transient level. A 500-second "null transient" code calculation was used to simulate the test specific initial conditions. Code control blocks were set up to force the code to reach predefined primary system coolant mass flows and secondary system steam line pressures. A series of preliminary code runs was needed to adjust energy loss coefficients at selected junctions. A total of 119 measured and calculated parameters characterizing facility initial conditions were compared. In close to 80% of cases, the calculated value at 500 seconds was within the measurement accuracy interval $<\mu-2\sigma; \mu+2\sigma>$, where μ is the measured value of the parameter and 2σ is the measurement accuracy of the parameter as reported in [4]. Table 6 illustrates this steady state data evaluation process in the case of primary system loop No. 1. Please refer to Table 2 and Figure 8 for the measurement channel identification. Please note that pressures (P) are in MPa, coolant temperatures (T) in °C, and differential pressures (DP) in kPa. The "FALSE" cases were further evaluated as follows:

- In the model, hydraulic characteristics of PCS loops are identical. For example, the differential pressure over steam generator (YA01DP03) is false in Table 6. However, the corresponding parameter evaluation for other loops is true. In the case of differential pressure over loop seal descending leg (YA0nDP05), loop # 3 and loop #4 parameter evaluations are true and loop #1 and loop #2 are false.
- A check is made for two other PSB-VVER tests modelled with RELAP5/MOD3.3. The "FALSE" cases are ignored in this study if two out of three cases available are true. Normally, the request for additional information would be necessary.

On the transient level, the test data were compared with the results of the calculation using FFTBM [7]. The selection of 23 parameters to be compared closely follows earlier studies [13] and [15]. For each parameter, the FFTBM algorithm is run in time window 0 – 1477 s (whole transient) to get average amplitudes (AA) and weighted frequencies (WF). These results are further combined using corresponding weighting factors to obtain total average amplitude (AA$_{tot}$) and total weighted frequency (WF$_{tot}$). In [7], the authors discuss the accuracy of code predictions as follows:

- AA$_{tot} \leq 0.3$ characterize very good code predictions
- $0.3 \leq$ AA$_{tot} \leq 0.5$ characterize good code predictions

- The acceptability factor K is then defined for total average amplitude K = 0.4, and for primary system pressure K = 0.1. The acceptable code predictions are those with $AA_{tot} \leq 0.4$, and $AA_{PSP} \leq 0.1$.

Table 6 R5/M33 Test-5a reference case steady state data evaluation – PCS #1

Experiment		Reference case (steady state)		Measurement accuracy (2σ)	Is cntrlvar value in the interval
Channel ID	Value (μ)	Cntrlvar	Value		<μ-2σ; μ+2σ>?
YA01P01	15.74	106	15.62	0.22	TRUE
YA01P03	15.81	104	15.61	0.23	TRUE
YA01P08	15.76	105	15.63	0.06	FALSE
YA01P09	15.67	103	15.60	0.06	FALSE
YA01T02	292	114	291.9	3	TRUE
YA01T03	321	108	321.8	3	TRUE
YA01T26	294	111	291.9	3.7	TRUE
YA01T32	293	110	291.9	2	TRUE
YA01T33	293	112	291.9	2	TRUE
YA01DP01	1.9	115	1.8	0.5	TRUE
YA01DP02	8.7	116	8.7	0.5	TRUE
YA01DP03b	4.2	117	3.5	0.5	FALSE
YA01DP04	-22.4	118	-21.8	1.5	TRUE
YA01DP05	-23.1	119	-24.1	0.7	FALSE
YA01DP08	4.5	121	4.5	0.3	TRUE
YA01DP09b	-5.9	122	-9.9	0.7	FALSE
YA01DP10	0.6	123	0.5	0.5	TRUE
YA01DP11	-0.9	124	-1.0	0.7	TRUE
YA01DP13	-20.5	125	-20.5	0.7	TRUE
YA01DP14	-19.6	126	-19.8	0.7	TRUE

The results of FFTBM application on the reference case are summarized in Table 7. Since $AA_{tot} < 0.4$ and $AA_1 = AA_2 = 0.1$, the reference case code predictions are acceptable and can be followed by the uncertainty and sensitivity studies.

Table 7 Test-5a R5/M33 reference case FFTBM results

N	Parameter	ID Exp	ID Cal	AA
1	Upper plenum pressure	YC01P16	cntrlvar-11	0.10
2	Pressurizer pressure	YP01P01	cntrlvar-7	0.10
3	Accumulator #1 pressure	TH01P01	cntrlvar-297	0.11
4	Accumulator #4 pressure	TH04P01	cntrlvar-300	0.12
5	Steam generator #1 secondary side pressure	YB01P01	cntrlvar-511	0.18
6	Steam generator #2 secondary side pressure	YB02P01	cntrlvar-521	0.18
7	Core inlet coolant temperature	YC01T06	tempf-04101	0.12
8	Core outlet coolant temperature	YC01T04b	tempf-07009	0.51
9	HPIS flow	TJ04F01	mflowj-681	0.40
10	Integrated break flow	MBr	cntrlvar-702	0.11
11	Primary coolant mass	M1k	cntrlvar-580	0.66
12	Accumulator #1 level	TH01L01	cntrlvar-197	0.03
13	Accumulator #4 level	TH04L01	cntrlvar-198	0.04
14	Differential pressure across downcomer	YC01DP03	cntrlvar-16	0.97
15	Differential pressure across downcomer	YC01DP04	cntrlvar-17	0.98
16	Differential pressure across the downcomer outlet and core simulator inlet	YC01DP06	cntrlvar-19	0.99
17	Differential pressure across the core	DP_CORE	cntrlvar-657	1.22
18	Differential pressure across the upper plenum	YC01DP13	cntrlvar-26	1.30
19	Differential pressure across the upper plenum outlet and downcomer inlet	YC01DP16	cntrlvar-29	0.77
20	Peak cladding temperature	max (YC01T09 - YC01T123)	cntrlvar-656	0.46
21	Cladding temperature – core bottom	YC01T113	httemp-65300320	0.70
22	Cladding temperature – core center	YC01T55	httemp-65301020	0.53
23	Cladding temperature – core top	YC01T39	httemp-65301220	0.51
	Total average amplitude - **AA$_{tot}$**	-	-	0.37

Appendix A contains the figures with graphical comparisons of measured and RELAP5/MOD3.3 calculated results.

Figure A.1 compares the data for integrated break mass flows. In the experiment, this parameter was not measured directly, but a specific algorithm for measured data evaluation was applied. The Henry-Fauske critical flow model was applied in calculations with Cd = 0.83 in the reference case.

Figure A.2 and Figure A.3 show good agreement between measured and calculated primary system pressures. Consequently, the timing of the accumulator injection is well predicted in the model (see Figures A.4 – A.7).

Actions of HPIS and LPIS were simulated during the experiment. Coolant was injected to the upper plenum simulator, to the downcomer simulator, to the intact loop (No. 1) hot leg, and to the broken loop (No. 3) hot and cold legs. As an example, Figure A.8 compares the data for one injection line. In the R5/M33 model, all five injection lines liquid mass flows were modelled as boundary conditions to match integrated HPIS/LPIS mass flow in the experiment.

Figure A.9 shows the comparison of the primary system coolant mass between evaluated in experiment and R5/M33 results. The experimental data is the product of the specific algorithm using data measured directly. According the experimenters the accuracy of this evaluation is ± 50 kg.

Figures A.10 – A.13 show the comparison of the secondary system pressure (at the steam generator steam dome) between measured and R5/M33 results. With reverse heat transfer across the tube bundle, the calculated data agrees well with the measurement up to approximately 600 s.

Figures A.14 – A.15 show the comparison of the core simulator inlet and outlet coolant temperatures between measured and R5/M33 results. Perhaps the most challenging phenomena to reproduce by the code are those related to the upper plenum ECCS injection (from two accumulators and one line of HPIS/LPIS). The measured data show that subcooled liquid reached the core simulator outlet region up to approximately 120 s. In the attempt to capture the phenomena, the CCFL models were activated at two axial levels of the RPV model. The Kutateladze CCFL model was activated at the junction just below the injection points. Wallis CCFL models were activated at the junctions representing the flow through the upper core plate simulator.

Figures A.16 – A.18 show the comparison of differential pressures across the downcomer and lower plenum simulators between measured and R5/M33 results. With a direct downcomer simulator ECCS injection it was difficult again to reproduce the measured values more correctly. The Wallis CCFL model was activated at the junction just below the injection point.

Figures A.19 – A.20 show the comparison of differential pressures across the core and upper plenum & upper head simulators between measured and R5/M33 results. Qualitatively, the liquid phase distribution is predicted correctly during the accumulator injection period only for the upper plenum & upper head simulator.

Figure A.21 compares the data for pressure drop across the downcomer and the upper plenum simulators.

Two periods of FRSB cladding heatup were observed during the experiment. First one begun approximately 50 s after the stop of accumulator injection when FRSB liquid level decreased. As

43

shown in Figure A.22, in contrast with experimental data, the code predicts the first heatup to occur also in the lower third region of FRSB. As shown in Figures A.23 – A.25, the timing of the first FRSB cladding heatup and quench is predicted quite correctly for the two other cladding temperatures selected for comparison. Please note that measurement channel selection was based on [15]. During the experiment, the first FRSB cladding heatup was terminated by the continuing HPIS/LPIS injections which gradually lead to the primary system coolant mass partial recovery. The second FRSB cladding heatup occurred after the stop of HPIS/LPIS injection (operator action) when primary coolant mass inventory substantially decreased again as a result of continuing boil-off. The transient was terminated by the facility operator when peak cladding temperature reached the predetermined value. During the experiment, the second heatup was not recorded in the bottom third FRSB region and, this is correctly predicted by the R5/M33 model. As for R5/M33 model predictions of FRSB cladding temperatures in mid and top FRSB regions, the start of the second heatup is delayed by approximately 80 s.

3.3.2 Uncertainty Study

In the performed uncertainty study, the fully probabilistic methods with propagation of uncertainties of code input parameters are applied.

For the probabilistic methods, two types of uncertainties can be distinguished:

- The uncertainties of the first type are directly modelled by uncertain input parameters (e.g. physical models).
- The uncertainties of the second type are not modelled via input parameters. They are uncertainties due to the nodalization, treatment of (relative) deficiencies of the code, scaling effect, and user effect.

Three different main steps are used to establish input uncertain parameters:

- Identification of the main phenomena.
- Identification of the sensitive parameters for these phenomena.
- Establishment of the list of the parameters taken into account.

This method is performed by expert judgment. The aim is to consider all the potentially influential parameters. As far as possible, the specificities of PSB-VVER are taken into account. Previous studies have been considered [17], [18].

3.3.2.1 Uncertain Input Parameters

The uncertainty of an input variable (geometrical data, physical model constant, etc.) can be modelled by a different method. The uncertainty of an input variable can be described directly by its pdf. Such an uncertain input variable can have dimensions. If the dimensionless uncertainty parameter of multiplicative form is used (the nominal value of the parameter being 1), that is the multiplier.

The following sources of uncertainties are considered:

- Physical models. These uncertainties belong to the used code (RELAP5/MOD3.3).

- Initial and boundary conditions. Uncertainties belong to the experimental equipment (PSB-VVER) and the modelled test Test-5a.
- Geometric modelling of experimental equipment by means of the RELAP5/MOD3.3 code. It is fixed to reference the case that respects the RELAP5/MOD3.3 user's guidelines in the nodalization of the PSB-VVER equipment and makes the best account of this kind of solved process. Nodalization is performed by respecting the rules of the user's guidelines manual code [19], [20].
- 3-D flow modelling is applied by means of pressure vessel modelling in input RELAP5/MOD3.3 dates.

Uncertainties of the scaling effect and user's effect are not considered. The scaling effect is not serious because the evaluated Test-5a was realized on the modelled experimental equipment (PSB-VVER).

3.3.2.1.1 Probability Distribution Function

The range of variation of an input uncertain parameter is specified by means of the probability distribution function (pdf). One of the following statistical distributions is used:

- Normal distribution   (N)
- Lognormal distribution   (LN)
- Uniform distribution   (U)
- Discrete distribution   (D)

the indicated ranges of variation for parameters with normal and lognormal distribution correspond to 2.5% and 97.5% percentiles, i.e. $\mu \pm 1.96\,\sigma$ and $e^{\mu \pm 1.96\sigma}$, respectively. These percentiles are given to specify the probability density functions.

Discrete distribution is the case of alternative physical models (choice among two, three or more correlations to describe the same physical phenomenon).

A list of 31 considered uncertain input parameters is introduced in Table 8.

Table 8 List and description of uncertain input parameters

phenomena or main physical laws	parameter number	parameter description	type of pdf	imposed range of variation; uncertainty	reference; comments; uncertain method
flow rates repartition in the circuit/pressure drops	1	form loss coefficient (active core)	LN	ξ_{cf}=0.1 (0.05; 0.2)	preliminary study; expert judgement
flow rate at the break	2 m	break discharge coefficient	U	Cd = 0.83 (0.664; 0.996)	preliminary study; expert judgement
	3 m	thermal nonequilibrium constant	D	discrete parameters: control weight 0.14 0.60; 0.0 0.40	[19] A9.17, p.209; preliminary study; expert judgement
	4 m	liquid entrainment alternative models	D	discrete parameters: control weight 0 0.25; 1 0.25; 2 0.25; 3 0.25	[19], A9.6, p.79; preliminary study; expert judgement
fuel thermal behaviour	5	initial core power	N	1512 ±15 kW (1497; 1527)	[4], Table B.1; YC01N01
	6	multiplier cladding thermal conductivity	N	c = 1.0 (0.9; 1.1)	[21], Table A.7
	7	multiplier cladding specific heat capacity	N	c = 1.0 (0.9; 1.1)	[21], Table A.8
	8	multiplier MgO thermal conductivity	N	c = 1.0 (0.9; 1.1)	[1], Fig. 2.3; preliminary study; expert judgement
	9	multiplier MgO specific heat capacity	N	c = 1.0 (0.9; 1.1)	[1], Table 2.3; preliminary study; expert judgement
pump behaviour	10 m	multiplier pump two-phase head difference multiplier	U	1 ± 0.2 (0.8; 1.2)	[9], Vol. III, 2.3.2, p. 118; expert judgement

phenomena or main physical laws	parameter number	parameter description	type of pdf	imposed range of variation; uncertainty	reference; comments; uncertain method
heat transfers in the rewetted zone	11 m	multiplier heat transfer fouling factor (± 18%)	N	1 ± 18% (0.82; 1.18)	[20], Vol. IV, 4.2.3.4.1, p. 133; expert judgement
critical heat flux	12 m	multiplier CHF correlation (PG-p)	N	gspf = 1.0 (0.72; 1.28)	[20], Vol. IV, 4.3, p. 192-202
primary circuit thermal losses	13	heat transfer coefficient on outside surfaces of piping	LN	α=3.5 $Wm^{-2}K^{-1}$ (1.75; 7)	preliminary study; expert judgement
counter current flow limitation (CCFL)	14 m	upper core plate: c of Wallis correlation (m = 1)	U	c=2.1 ± 0.1 (2.0; 2.2)	preliminary study; expert judgement
	15 m	upper plenum: c of Kutateladze correlation (m = 1)	U	c=0.8± 0.2 (0.6; 1)	preliminary study; expert judgement
	16 m	steam generator inlet: c of Kutateladze correlation (m = 1)	U	c=1.0 ± 0.2 (0.8; 1.2)	preliminary study; expert judgement
	17 m	downcomer: c of Wallis correlation (m = 1)	U	c=1.0 ± 0.2 (0.8; 1.2)	preliminary study; expert judgement
accumulator data	18	accumulator initial liquid level	N	0 ± 0.07 m (-0.07; 0.07)	[4], Table B.1 TH0nL01n=1,3,4
	19	friction form loss in the accumulator line ξ_{acc}	LN	ξ_{acc} = 30 (15; 60)	preliminary study; expert judgement
	20	accumulator initial liquid temperature	N	0 ± 3.4 °C (-3.4; 3.4)	[4], Table B.1 TH0nT01n=1,3,4
	21	accumulator initial liquid pressure	N	0 ± 0.03 MPa (-0.03; 0.03)	[4], Table B.1 TH0nP01n=1,3,4
pressurizer data	22	initial level	N	6.5 ± 0.5 m (6; 7)	[4], Table B.1 YP01L02
	23	initial pressure	N	15.58 ± 0.06 MPa (15.52; 15.64)	[4], Table B.1 YP01P01
	24	friction form loss in the surge line	LN	ξ_{press} = 3.9 (1.95; 7.8)	preliminary study; expert judgement
initial conditions in systems	25	initial intact loop mass flow rate	N	± 0.1 kg/s (-0.1; 0.1)	[4], Table B.1 YA0nF01b n=1,4

phenomena or main physical laws	parameter number	parameter description	type of pdf	imposed range of variation; uncertainty	reference; comments; uncertain method
	26	initial pressure on parogenerator secondary side	N	7.6 ± 0.2 MPa (7.4; 7.8)	[4], Table B.1 YB01P01 expert judgement
	27	initial upper-head mean temperature	N	304 ± 3 °C (301; 307)	[4], Table B.1 YC01T05
data related to injections (HPSI/LPSI)	28	liquid injection variation	N	± 0.004 kg/s	[4], Table B.1 TJ01F01
	29	liquid injections temperature	N	50 ± 5 °C (45; 55)	[4], Figure A.10 RL09T01
containment pressure	30	multiplier cold leg discharge pressure	N	c=1.0 ± 0.02 (0.98; 1.02)	[4], Table B.1; YE11P02
	31	multiplier hot leg discharge pressure	N	c=1.0 ± 0,02 (0.98; 1.02)	[4], Table B.1; YE12P02

3.3.2.1.2 Physical Model Uncertainties

Uncertainties of the RELAP5/MOD3.3 physical models are evaluated on the basis of the code documentation [19], [20] and comparison of code calculations results with experimental data [16], [17].

In Table 8 the number of parameter describing an uncertainty of the physical model is followed by the lower case letter m.

Physical model uncertainties are described by means of the probability distribution functions (pdf) for 10 uncertain parameters. Two of them, the thermal nonequilibrium constant and the liquid entrainment (parameter 2 and parameter 3, respectively), are described by alternative models, i.e. discrete distributions are used. Normal distributions are used for multipliers of the heat transfer fouling factor and the CHF correlation grid spacer factor (parameter 11 and parameter 12, respectively).

Uniform distributions are used for the break discharge coefficient and for the pump two-phase head multiplier (parameter 2 and parameter 10, respectively) and for constants used in 4 uncertain parameters of CCFL models (parameters 14 – 17).

3.3.2.1.3 Uncertainties of Initial and Boundary Conditions

These uncertainties are specified with help of PSB-VVER descriptions [1] and Test-5a experimental data report [4]. 21 uncertain parameters involve:

- local pressure drop of active core (parameter 1) and primary circuit thermal losses (parameter 13),
- fuel thermal behaviour (parameters 5-9),

- accumulator data (parameters 18-21),
- pressurizer data (parameters 22-24),
- initial conditions in systems (parameters 25-27),
- data related to active ECCS (HPSI/LPSI) (parameters 28, 29),
- containment pressure (parameters 30, 31).

3.3.2.2 PSB-VVER Test-5a Experimental Data

PSB-VVER Test-5a experiment [4] is briefly described in section 3.1 above. Key experimental data are compared with R5/M33 reference case results in section 3.3.1 above and in Appendix A. In the context of the uncertainty study, key experimental data are presented in integrated form in Figures B.1 and B.2. Experimental time dependent values of pressures in accumulator (ACC), pressurizer (PRZ), upper plenum (UPP), steam generator (SG), power of FRSB (N) and primary coolant mass (PCM) are shown in Figure B.1. Experimental time dependent values of the integrated break flow (IBF), the primary coolant mass (PCM) and the maximum cladding temperature (maxT) are shown in Figure B.2.

3.3.2.3 Uncertainty Method and Uncertainty Analysis Results

The propagation of uncertainties of code input parameters is evaluated as follows.

Uncertain code output parameters are statistically evaluated as α = 95% tolerance limit with a confidence level β of 95% on the basis of code results obtained in a propagation step. The propagation step involved: n code runs performed by varying simultaneously the values of all the uncertain input parameters according to their pdf. The number n of performed code runs in order to obtain (95%, 95%) tolerance limits is given by Wilks' formula [22]. The n values of the uncertain output parameter are ordered: $Y(1) < Y(2) \ldots< Y(n-1) < Y(n)$. For Wilks' formula at the first order is n = 59.

In such a case the minimal value Y(1) is the lower (95%, 95%) tolerance limit (lower uncertainty bound) and the majoring value Y(59) is the upper (95%, 95%) tolerance limit (upper uncertainty bound). An uncertainty band of the code output parameter is a difference $Y(59) - Y(1)$.

Two kinds of uncertain output parameters are evaluated: scalar and time trends output parameters.

3.3.2.3.1 Scalar Output Parameters

Uncertainty bounds are estimated for 7 scalar output parameters:

- Accumulator injection time t_{acc} (s)
- Cladding first overheating time t_1 (s)
- Maximum peak cladding temperature time t_{max} (s)
- Complete core quenching time t_2 (s)
- Cladding first overheating time interval $t_2 - t_1$ (s)
- Cladding last overheating time t_3 (s)
- Maximum peak cladding temperature maxT (°C)

Lower and upper uncertainty bounds for 7 single-valued parameters are in Table 9.

Statistical bounds envelope experimental values for 5 parameters, including the maximum peak cladding temperature that is safety important. Only the experimental maximum peak cladding temperature time t_{max} = 398.5 s is higher than the calculated value of an upper uncertainty bound 395 s and cladding last overheating time t_3 = 1265.3 s is lower than the calculated value of an lower uncertainty bound 1268.5 s.

Table 9 One-sided (0.95; 0.95) tolerance bounds for the single-valued parameters

output uncertain parameter	lower uncertainty bound	reference calculation value	experimental value	upper uncertainty bound
accumulator injection time t_{acc} (s)	10.3	11.1	10.7	12.6
cladding first overheating time[*] t_1 (s)	108.2	155.5	181	238.5
maximum peak cladding temperature time t_{max} (s)	236.5	280	398.5	395
complete core quenching time[*] t_2 (s)	332.7	521.5	556.7	673
cladding first overheating time interval $t_2 - t_1$ (s)	159.2	366	375.7	542.9
cladding last overheating time[*] t_3 (s)	1268.5	1310.2	1265.3	1385.6
maximum peak cladding temperature maxT (°C)	276.6	457.2	428.7	638.2

[*]   Cladding overheating t_1, t_3 and quenching t_2 times are specified in the moment when the maximum peak temperature of rods cladding crosses the value 200 °C.

3.3.2.3.2 Time Trends Output Parameters

Time dependent uncertainty bands are estimated for 4 time trends output parameters:

- the maximum cladding temperature (maxT)
- the upper plenum pressure (UPP)
- the primary coolant mass (PCM)
- the integrated break flow (IBF)

Time dependent uncertainty bands of 4 time trends output parameters are presented for the maximum cladding temperature (maxT) in Figure B.3, for the upper plenum pressure (UPP) in Figure B.4, for the primary coolant mass (PCM) in Figure B.5, and for the integrated break flow in Figure B.6.

From the physical point of view it is convenient to evaluate the results of uncertainty analysis in two time intervals.

Time interval up to circa 650 s:

Some typical aspects of LBLOCA process are observed. Uncertainty analysis results as follows:

- Time dependent band of the maximum cladding temperature (maxT) envelope experimental values (Figure B.3).
- Time dependent band of the upper plenum pressure (UPP) envelope experimental values with exception the first 6 s of process (Figure B.4).

Time interval over 650 s up to circa 1000 s:

Time dependent values of the upper plenum pressure (lower than 0.25 MPa) predetermine process running.

Uncertainty analysis results show that experimental values of the upper plenum pressure and the maximum cladding temperature exceed their upper uncertainty bounds.

The reason is lower calculated values of the primary coolant mass (PCM) against experimental values (Figure B.5) that are also connected with the higher calculated values of the integrated break flow (IBF) against experimental values (Figure B.6). For both parameters, such disagreements last during the whole process. The original cause is very probably overestimated calculated values of the critical discharge from cold leg in the process beginning (up to circa 36 s).

3.3.3 Sensitivity Study

The sensitivity analysis of calculated results is performed with help of the code STATISTICA [23].

In the analysis the Spearman's rank correlation coefficient is applied both for the single-values parameters and the time trends output parameters.

3.3.3.1 Single-value Output Parameters Sensitivity Results

The determined sensitivity measures for the single-value output parameters are introduced in Table 10 and are shown in Appendix B in Figures B.7 - B.12.

Values of the Spearman's rank correlation coefficients, which are significant and can be counted as reliable, and the corresponding input uncertain parameter numbers are written in bold in Table 10.

Table 10 Sensitivity analysis of the single valued output parameters – Spearman's correlation coefficients

Input uncertain parameter number	Output uncertain parameter					
	t_{acc} Accumulator injection time	t_1 Cladding first overheating time	$t_2 - t_1$ Cladding first overheating time interval	t_3 Cladding last overheating time	t_{max} Maximum peak cladding temperature time	maxT Maximum peak cladding temperature
1	0.081	0.188	-0.107	-0.008	0.010	-0.052
2	-0.965	-0.125	0.075	-0.245	-0.173	0.137
3	0.040	0.055	0.037	0.251	0.110	0.037
4	-0.262	-0.109	0.082	-0.083	0.050	0.105
5	0.228	-0.131	0.058	-0.071	-0.093	0.083
6	-0.116	-0.193	0.129	0.035	-0.095	-0.019
7	0.081	0.250	-0.260	0.148	0.111	-0.271
8	0.003	0.273	-0.175	0.107	-0.123	-0.143
9	0.208	0.014	-0.139	-0.032	-0.142	-0.122
10	0.072	0.032	0.002	-0.074	-0.025	-0.059
11	-0.034	-0.119	-0.008	0.281	-0.048	0.144
12	0.181	0.075	-0.161	-0.037	-0.067	-0.026
13	0.023	0.049	-0.208	0.124	0.054	-0.129
14	0.103	0.023	0.216	-0.126	0.142	0.217
15	-0.069	0.160	-0.482	0.011	-0.234	-0.494
16	0.223	-0.212	0.185	0.342	-0.063	0.145
17	-0.035	-0.114	0.145	-0.183	0.109	0.116
18	-0.027	-0.131	0.219	0.098	0.059	0.303
19	0.106	-0.006	0.200	-0.006	0.145	0.134
20	-0.047	-0.065	-0.109	0.066	-0.201	0.013
21	0.010	0.123	-0.060	-0.016	-0.152	-0.069
22	0.146	-0.022	-0.016	-0.206	0.141	-0.045
23	-0.170	0.016	-0.086	-0.026	-0.032	-0.020
24	-0.055	-0.099	0.073	-0.044	0.111	0.078
25	0.032	0.180	-0.169	-0.063	-0.054	-0.116
26	0.195	0.253	-0.238	0.172	-0.136	-0.165
27	-0.018	-0.051	0.072	-0.037	-0.081	0.041
28	-0.040	0.068	-0.008	0.057	-0.023	-0.061
29	0.093	0.071	-0.013	-0.103	0.162	0.015
30	-0.020	-0.155	-0.043	-0.035	-0.320	0.049
31	0.097	-0.007	-0.076	0.033	0.129	-0.054

3.3.3.2 Time Trends Output Parameters Sensitivity Results

The sensitivity analyses of calculated time trends of the output parameters are performed for 4 important measured or evaluated parameters during Test 5a. They are:

- the maximum cladding temperature (maxT),
- the upper plenum pressure (UPP),
- the primary coolant mass (PCM),
- the integrated break flow (IBF).

The sensitivity analyses of 4 time trends output parameters are carried out with time steps. Values of the Spearman's rank correlation coefficients considering all 31 uncertain input parameters are shown in figures of Appendix B:

- Figures B.13 – B.20 for the maximum cladding temperature (maxT),
- Figures B.21 – B.28 for the upper plenum pressure (UPP),
- Figures B.29 – B.36 for the primary coolant mass (PCM),
- Figures B.37 – B.44 for the integrated break flow (IBF).

3.3.3.3 Sensitivity Code Results for Uncertain Input Parameters

On the basis of the Spearman's rank correlation coefficients shown in Figures B.13 – B.44 the uncertainties of 17 input uncertain parameters are evaluated as significant at least for one from time trends output parameters maxT, UPP, PCM and IBF. Time trends of the Spearman's correlation coefficients of output parameters maxT, UPP, PCM and IBF for each from these 17 significant input parameters are shown in Figures B.45 – B.61. The list of 17 input uncertain parameters and corresponding figures numbers follows in Table 11.

Table 11 List of significant input uncertain parameters for the time trends output parameters maxT, UPP, PCM and IBF

Parameter number	Uncertain input parameter	Figure No.
2 m	break discharge coefficient	Figure B.45
3 m	thermal nonequilibrium constant	Figure B.46
5	initial core power	Figure B.47
7	cladding specific heat capacity	Figure B.48
10 m	pump two-phase head difference multiplier	Figure B.49
13	heat transfer coefficient on outside surfaces of piping	Figure B.50
14 m	upper core plate: c of Wallis correlation	Figure B.51
15 m	upper plenum: c of Kutateladze correlation	Figure B.52
16 m	steam generator inlet: c of Kutateladze correlation	Figure B.53
17 m	downcomer: c of Wallis correlation	Figure B.54
18	accumulator initial liquid level	Figure B.55
19	friction form loss in the accumulator line ξ_{acc}	Figure B.56
22	initial level in pressurizer	Figure B.57
26	initial pressure on steam generator secondary side	Figure B.58
28	liquid injection variation	Figure B.59
29	liquid injections temperature (HPSI/LPSI)	Figure B.60
30	cold leg discharge pressure	Figure B.61

3.4 Conclusions on RELAP5/MOD3.3 Code Assessment

Section 3 of this report contains results obtained in the assessment of RELAP5/MOD3.3 code against the PSB-VVER Test-5a experiment. In addition to the traditional structure of thermal-hydraulic code assessment reports, i.e. facility description, test description, thermal-hydraulic code facility model description, and the thermal-hydraulic code facility model verification and validation, this report also presents the results of the uncertainty and sensitivity study. Methodically, the authors repeated the contribution of NRI-1 team in recent BEMUSE project [3], [13], and [16].

As for as Test-5a LB LOCA experiment carried out at PSB-VVER test facility, it is important to note that Test-5a initial FRSB power was scaled down to 15% of prototypical. This was the reason that the measured cladding temperatures showed qualitatively different trends when compared to typical PWR LB LOCA.

In the RELAP5/MOD3.3 PSB-VVER model validation step, it is shown that in the reference case calculation the results meet the acceptance criteria when compared to data on the steady state level and on the transient level. In the latter case, the application of FFTBM [7] showed that total average amplitude for 23 parameters selected for quantitative comparison was AAtot = 0.37, with average amplitudes for primary system pressure equal to 0.1, which enabled the conclusion that the model reproduced the experimental data with good accuracy.

Non-parametric statistics with application of Wilks formula of first order was used in the uncertainty study. This method requires carrying out at least 59 code runs with random values of uncertain input parameters in order to evaluate one-sided lower and upper (0.95; 0.95) tolerance bounds for output parameters (peak cladding temperatures and other measured data). In the uncertainty study, 31 uncertainty input parameters were considered. Uncertainty bands were evaluated for selected scalar parameters as shown in Table 9 and for selected vector parameters (time trends) as shown in Figures B.3 – B.6. Uncertainty bounds envelop the experimental data for the start of accumulator injection; for the start of first FRSB cladding heatup, and for the duration of first FRSB cladding heatup. Uncertainty bounds do not envelop the experimental data for timing of peak cladding temperature during the first FRSB cladding heatup (upper uncertainty bound is by 3.5 s lower than in experiment), and for timing of final FRSB cladding heatup (lower uncertainty bound is by 3.2 s higher than in experiment).

Calculated lower and upper (0.95; 0.95) uncertainty bounds for peak cladding temperature during first FRSB cladding heatup envelop the measured value. This is the key finding when considering the licensing point of view.

From the time trends uncertainty results, the maximum cladding temperature uncertainty band as the most important result from the licensing point of view is discussed. Uncertainty band defined by one-sided lower and upper (0.95; 0.95) uncertainty bounds envelops experimental data up to approximately 700 s. After that, up to approximately 1000 s, with FRSB quenched, maximum cladding temperatures follow the saturation temperature and the uncertainty band lies slightly below the measured data. During that period, the calculated primary system pressure is lower than the measured one. In time interval approximately from 1200 s to 1300 s, the upper uncertainty bound is slightly lower than measured values of maximum cladding temperature due to calculated timing of final FRSB cladding heatup.

The sensitivity study was carried out on 60 code runs with random values of uncertain input parameters. Sensitivities of code output parameters on code physical models uncertainty

parameters and on uncertainties of initial and boundary conditions were evaluated. Based on Spearman's rank correlation coefficient, 17 out of 31 uncertain input parameters were evaluated as influential.

4. TRACE V5.0 CODE ASSESSMENT

As for small-break LOCA analyses, the TRACE V5.0 code developmental assessment [24] is based on LOFT, ROSA IV, Semiscale, and BETHSY small-break LOCA tests. The results of the independent TRACE V5.0 code assessment against small-break LOCA test performed at PSB-VVER test facility [5] are reported below.

First two steps in the thermal-hydraulic system code assessment process are defined in [2] as:

- Formulate assessment matrices for each class of transient studied, e.g., large-break LOCA, small-break LOCA.
- Select key parameters for these classes.

When addressing these steps the authors please the reader to refer to [14]: "The construction of VVER Thermal Hydraulic Code Validation Matrix follows the logic of the CSNI Code Validation Matrices (CCVM) [12]. Similar to the CCVM it is an attempt to collect together in a systematic way the best sets of available test data for VVER specific code validation, assessment and improvement, including quantitative assessment of uncertainties in the modelling of phenomena by the codes." Since the PSB-VVER test facility had not been in operation at the time the report [14] was compiled, the phenomena vs. system test large-break LOCA matrix refers PSB-VVER as "expected to be suitable". Test facility vs. phenomena, specifically the suitability of test data for the code assessment is further discussed in [5]. The selection of key parameters to be compared is based on [13] and [15].

4.1 PSB-VVER Test-3 Description

The general objectives of PSB-VVER small-break LOCA experiment are listed in [5]:

- Investigate the thermal-hydraulic response of the VVER-1000 primary system to the small break LOCA.
- Obtain experimental data for validation of thermal-hydraulic codes applied to SB LOCA analysis of VVER-1000 NPP.
- Comparison of the experimental data obtained on PSB-VVER with the data previously obtained on LOBI, BETHSY, SPES and LSTF facilities, for the purpose of determining the scaling effect on the accident behaviour. Hence, the test scenario closely followed that of BL-34 test performed on LOBI test facility [25].

Internally at EREC, the test is denoted as CL-4.1-03. In the context of PSB-VVER OECD Project the test is denoted as Test-3.

Test-3 specific PSB-VVER facility configuration is discussed in Table 12.

Table 12 Test-3 specific PSB-VVER test facility configuration

Subsystem	Description
Pressurizer	Surgeline was connected to the hot leg loop No. 4
Core bypass	Two orifices with a diameter of 7 mm were installed at the inlet/outlet of the core bypass
Steam generators	Under initial steady state operation all SGs were connected to each other by the steam header. The steady state pressure was adjusted by steam dump valve RA06S01 located at common steam line.
Feedwater	Under initial steady state operation the SG secondary side coolant levels were adjusted by RL01S06, RL02S06, RL03S06, and RL04S06 valves. The feedwater temperature was close to 170 °C.
Steam dump to atmosphere (ADS)	ADS line was connected to each steam generator. A throttle channel with l/d = 10; d = 12.1 mm was installed in each ADS line.
Accumulators	ACC No. 2 and ACC No. 4 surgelines were connected to the downcomer simulator.
HPIS	N/A.
LPIS	Three lines of LPIS were connected to cold legs of PCS loops No. 1, No. 3, and No. 4.
Break unit	Vertically upward oriented break unit was located in the horizontal section of PCS loop No. 4 cold leg between downcomer simulator inlet nozzle and RCP. Break nozzle was smooth edged channel (R = 6 mm) with a diameter of 10 mm and a length of 100 mm.
Upper plenum	Under steady state operation the upper plenum simulator warm-up line was opened. The line was closed 2 minutes prior the initiation of the transient.

The PSB-VVER DAS was recording the measured parameters with frequency of 5 Hz throughout the test.

Test-3 specific PSB-VVER facility initial conditions are presented in Table 13.

Table 13 Test-3 specific PSB-VVER test facility initial conditions

Parameter	Measurement	Value	Measurement accuracy
Primary coolant system			
Upper plenum pressure, MPa	YC01P17	15.71	± 0.06
Hot leg inlet coolant temperature, °C	YA01T03	310	± 3
	YA02T03	308	± 3
	YA03T03	311	± 3
	YA04T03	308	± 3
Cold leg outlet coolant temperature, °C	YA01T02	283	± 3
	YA02T02	283	± 3
	YA03T02	282	± 3
	YA04T02	282	± 3
FRSP power, kW	YC01N01	1129	± 15
BP power, kW	YC01N02	14.9	± 0.7
Pressurizer level, m	YP01L02	3.05	± 0.3
Secondary coolant system			
SG pressure, Mpa	YB01P01	6.88	± 0.05
	YB02P01	6.91	± 0.05
	YB03P01	6.93	± 0.05
	YB04P01	6.88	± 0.05
SG level, m	YB01L01	1.90	± 0.08
	YB02L01	1.91	± 0.08
	YB03L01	1.94	± 0.08
	YB04L01	1.90	± 0.08
Accumulators			
ACC pressure, MPa	TH02P01	4.08	± 0.03
	TH04P01	4.14	± 0.03
ACC level, m	TH02L01	4.58	± 0.07
	TH04L01	4.60	± 0.07

Test-3 specific PSB-VVER facility boundary conditions are presented in Table 14.

Table 14 Test-3 specific PSB-VVER test facility boundary conditions

Time, s	Event
0	Break simulation
4.1	Primary system pressure drops to 13 MPa: SCRAM
4.1	SCRAM, FRSB and BP power controlled to simulate decay heat
4.1	SG feedwater isolation, start of RL01-04S06 valve closing
4.1	Main stem line isolation, start of RA06S01 valve closing
4.1	RCPs trip, coastdown was not simulated
8.0	RCPs rotor speed drops to zero
9.9	SG feedwater isolation, RL04S06 valve closed
11.5	SG feedwater isolation, RL01S06 valve closed
13.4	SG feedwater isolation, RL02S06 valve closed
13.8	SG feedwater isolation, RL03S06 valve closed
17.5	Steam line isolation signal, valve RA06S01 closed
97	First core dryout
405	Second core dryout
406	Start of ACC-4 injection
414	Start of ACC-2 injection
1365	Stop of ACC-4 injection
1452	Stop of ACC-2 injection
2057	Final core dryout
2432	Start of LPIS injection (TJ01F02)
2432	Start of LPIS injection (TJ03F02)
2434	Start of LPIS injection (TJ04F02)
2593	FRSB power switched off – end of the experiment

In PSB-VVER Test-3 the small-break LOCA accident, vertically upward oriented cold leg No. 4 break was simulated with boundary conditions simulating a coincidental loss of offsite power. The FRSB and core bypass power levels were controlled to simulate decay heat power. The ECCS actions were simulated. Three periods of FRSB cladding heatup were observed based on thermocouple measurements. The first one, just a minor deviation from the saturation temperature, was monitored only at thermocouples located above the axial position of YC01T40 measurement (3.002 m above the FRSB bottom). The second, more distinctive FRSB heatup was also monitored only by thermocouples located 3.002 m above the FRSB bottom. This heatup was terminated by the accumulator injection. The third (final) heatup was monitored by the thermocouples located above 1.151 m above the FRSB bottom. This heatup was terminated by LPIS.

4.2 TRACE V5.0 Thermal-Hydraulic Model of PSB-VVER Test Facility

As already described in section 3.2, the facility database was compiled in an MS-ACCESS environment. Facility design data and thermal-hydraulic characteristics as reported in the frame of OECD/NEA PSB-VVER Project were organized in two tables with a total of 600 records.

In the case of the TRACE model of PSB-VVER test facility development, the Symbolic Nuclear Analysis Package (SNAP) [8] was applied. At the first step, the reference case steady state run input deck of R5/M33 T-H model of PSB-VVER test facility (see section 3.3.1 above) was imported to SNAP using File⇒Import⇒RELAP ASCII technique. At the second step, the R5/M33 model was converted to TRACE model of the facility using Tools⇒Convert to TRACE technique. This process ended up with revision 0 TRACE V5.0 model of PSB-VVER test facility. Tools⇒Check Model protocol summarized that there were 15 errors in the model, each of "elevation loop closure" type. All these errors were corrected in revision 1 of the model.

The model verification started with revision 2 of the model. As inherited from the R5/M33 model of the PSB-VVER test facility, the initial and boundary conditions were set up to simulate Test-5a of OECD/NEA PSB-VVER project, i.e. the large-break LOCA experiment, 2x100% cold leg break with initial power scaled further down to 15% of prototypical [4]. The "null transient" method was applied to reproduce the test specific initial conditions. As the acceptance criterion, the code calculated data were requested to be within corresponding channel measurement accuracy intervals. The large-break LOCA transient was analyzed in code restart mode with specification of test specific trips in order to simulate the boundary conditions of the experiment. As the acceptance criterion, the calculated data were requested to reproduce the measured data qualitatively (phenomena and trends), with only key parameters (e.g. primary system pressure) being compared quantitatively. The acceptance criteria were fulfilled in revision 55 of the TRACE model of PSB-VVER test facility. In each revision, typically, one change to the model was introduced and its effect was checked in the steady state and transient runs. Major changes related to the application of TRACE VESSEL component for the reactor pressure vessel simulator model started from revision 10.

The model validation started with revision 56 of the model. The initial and boundary conditions of the reference case calculations (steady state run and transient run) were set up for the facility model in question to simulate Test-3 of OECD/NEA PSB-VVER project, i.e. the small-break LOCA experiment, 4.1 % cold leg break with initial power scaled further down to 15% of prototypical [5]. This case is described in detail in Chapter 4.3 below. Please note that the validation case had been completed with revision 60 of the TRACE model of PSB-VVER test facility.

In SNAP model editor, the thermal-hydraulic views of the TRACE V5.0 PSB-VVER model were reorganized as shown in Figures 27 to 32.

As summarized in SNAP model editor navigator, TRACE V5.0 model of PSB-VVER facility consists of 338 hydraulic components, 1163 control systems, 156 thermal components, and 1730 connections.

The nodalization of reactor pressure vessel model is illustrated in Figure 27. VESSEL component (c010) with 4 axial levels, 2 radial rings, and 4 azimuthal sectors is used to model the upper part of the downcomer. Single junction components (c01n; n=1, 4) are used to model vessel (c010) to vessel (c015) connections for each azimuthal sector. VESSEL component (c015) with 10 axial levels, 1 radial ring, and 4 azimuthal sectors is used to model the middle part of the downcomer. Single junction components (c02n; n=1, 4) are used to model vessel

(c015) to vessel (c020) connections for each azimuthal sector. VESSEL component (c020) with 3 axial levels, 2 radial rings, and 4 azimuthal sectors is used to model the lower part of the downcomer. PIPE component (c037) with 3 cells is used to model a tube connecting the downcomer simulator and the lower plenum simulator. Multiple junction components (not shown in this view) are used to simulate axial and azimuthal flows between the downcomer inlet annular sectors. VESSEL component (c025) with 2 axial levels, 2 radial rings, and 4 azimuthal sectors is used to model the lower plenum simulator. Single junction components (c03n; n=1, 4) are used to model vessel (c025) to vessel (c030) connections for each azimuthal sector. VESSEL component (c030) with 21 axial levels, 1 radial ring, and 4 azimuthal sectors is used to model the core and upper plenum simulator. Single junction components (c04n; n=1, 4) are used to model vessel (c030) to vessel (c035) connections for each azimuthal sector in inner radial ring. Similarly, single junction components (c04n; n=6, 9) are used to model vessel (c030) to vessel (c035) connections for each azimuthal sector in outer radial ring. VESSEL component (c035) with 2 axial levels, 2 radial rings, and 4 azimuthal sectors is used to model the zone with nozzles. Single junction components (c05n; n=1, 4) are used to model vessel (c035) to vessel (c040) connections for each azimuthal sector in c035 inner radial ring. Similarly, single junction components (c05n; n=6, 9) are used to model vessel (c035) to vessel (c040) connections for each azimuthal sector in c035 outer radial ring. VESSEL component (c040) with 6 axial levels, 1 radial ring, and 4 azimuthal sectors is used to model the upper head simulator. Two identical PIPE components (c076, c077) with 7 cells and one PIPE component (c078) with 22 cells are used to model the core bypass simulator. A part of pipe (c078) vertical section is heated. Heat structures (106n2; n=1, 4) each with 14 axial cells and 13 radial nodes are used to model the fuel rod simulator bundle. During Test-3 FRSB was heated uniformly along the radial and axial directions. Each of four fuel rod simulator heat structure represents 42 actual fuel rod simulators that communicate the energy with the corresponding azimuthal sectors of VESSEL (c030), from axial level 2 to axial level 15. Axial conduction flag was activated. A number of heat structures are used to model downcomer simulator, core simulator, upper plenum and upper head simulators piping walls in order to account for stored heat and eventually for heat losses to environment. Wallis CCFL model is set up and activated at axial edges 16 of VESSEL (c030) component. This is to account for CCFL effects at the upper core plate.

RPV Model
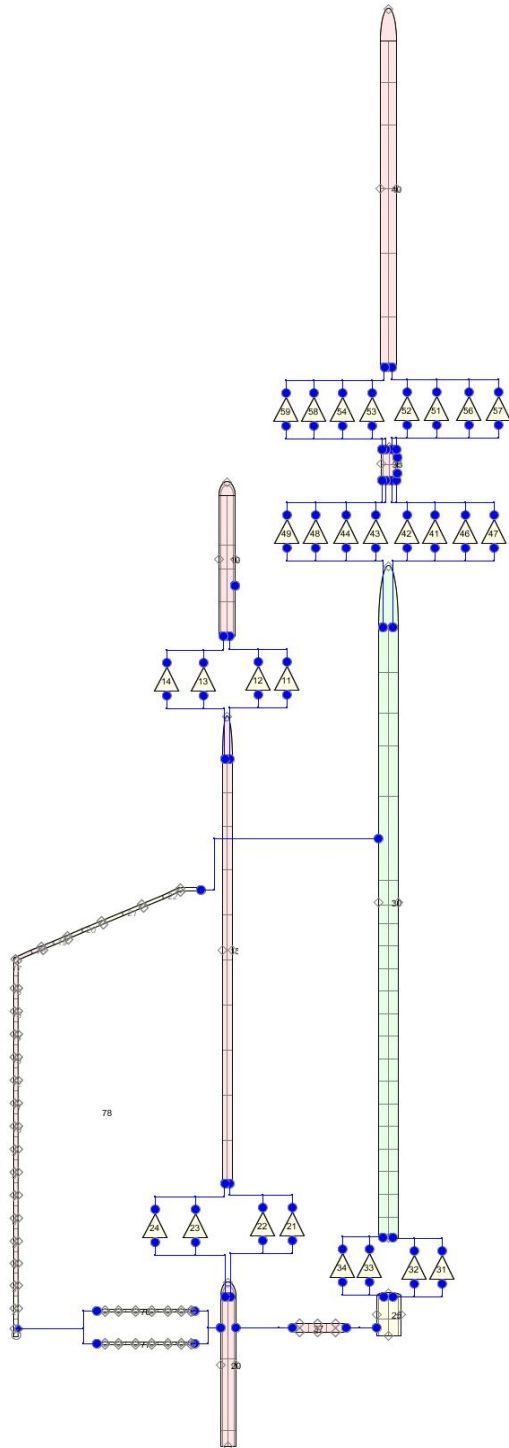
Figure 27 TRACE V5.0 reactor pressure vessel model

The nodalization of PCS loops is illustrated in Figure 28. PIPE components (cn05; n=1, 4) each with 14 cells are used to model the hot legs. PIPE components (cn10; n=1, 4) each with 1 cell are used to model steam generator inlets. Steam generator primary side models consist of hot header model, PIPE components (cn15; n=1, 4) each with 10 cells, horizontal tube bundle simulator, PIPE components (cn2r; n=1, 4; r=1, 9) each with 11 cells, and cold header model, PIPE components (cn31; n=1, 4) each with 10 cells. In the PSB-VVER test facility, the steam generator simulator consists of 34 nearly horizontal coiled tubes. In TRACE model, the individual tubes are grouped to have nine tube rows along the height of the steam generator vessel. PIPE component (cn33; n=1, 4) each with 1 cell are used to model steam generator outlets.
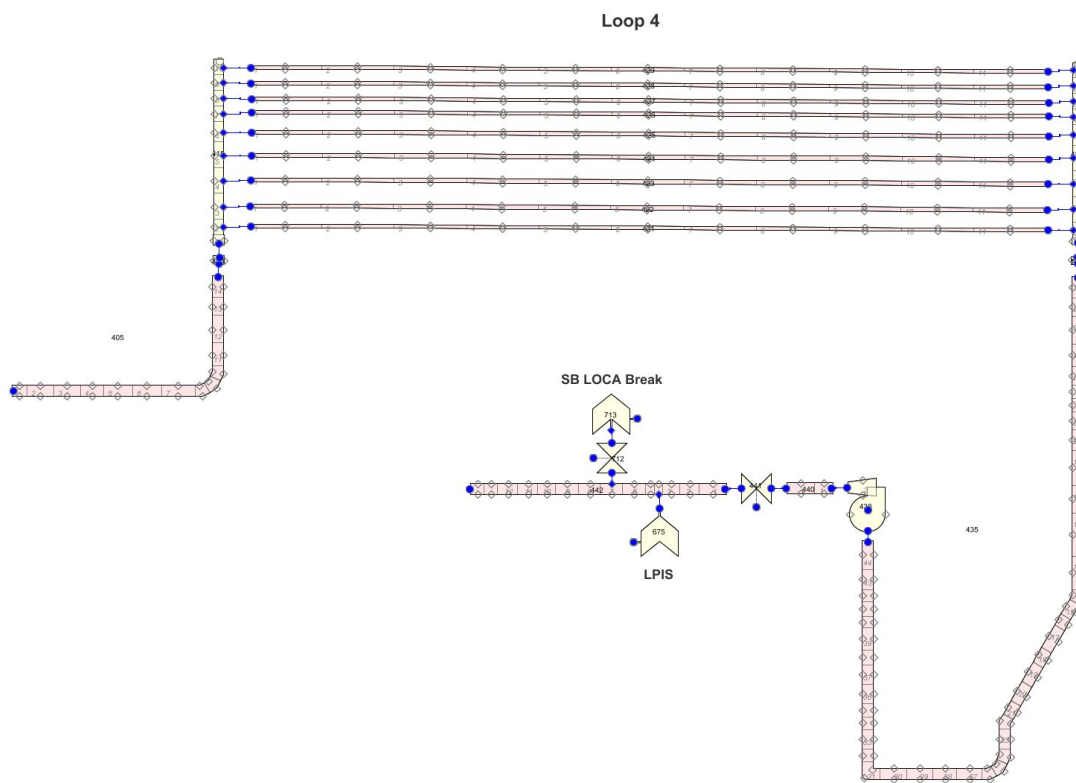
Figure 28 TRACE V5.0 primary coolant system model – Loop No. 4

PIPE components (cn35, n=1, 4) each with 44 cells are used to represent the loop seals. Reactor coolant pumps are modelled with PUMP components (cn36, n=1, 4) each with 2 cells. The intact loop cold legs are modelled using PIPE components (cn40, n=1, 4) each with 2 cells, valve components (cn41, n=1, 4), and pipe components (cn42, n=1, 4) with 14 control volumes. In Test-3, the break was simulated to occur at cold leg No. 4, so the nodalization of the broken loop cold leg follows standard guidelines to model the single ended cold leg break. The actions of LPIS are modelled using FILL components. The injection points are Test-3 specific.

66

Heat structures associated with those hydraulic components model piping walls.

The nodalization of the pressurizer and the pressurizer surgeline models is illustrated in Figure 29. Only the loop No. 4 hot leg connected surgeline is modelled using PIPE component (c507) with 4 cells, VALVE component (c508), and PIPE component (c509) with 23 cells. The model of the common part of the pressurizer surgeline begins with the PIPE component (c510) with 1 cell and continues using the PIPE component (c511) with 4 cells. The PIPE component (c515) with 24 cells is used to model the pressurizer vessel. VALVE component (c519), connected to the top of the pressurizer, and the BREAK component (c520) are used to adjust the desired steady state pressurizer pressure. Similarly, the mass flow controlled single junction component (c529), and the BREAK (c530) component are used to adjust the desired steady state pressurizer coolant level. Mass flow controlled single junction components (c541 and c549), and BREAK components (c540 and c550) are used to achieve the desired steady state surgeline coolant temperature. In transient runs, the steady state control component gains are set to zero.

The nodalization of the accumulators and accumulator surgelines is illustrated in Figure 30. Hydro-accumulators (TH10B01 and TH30B01) were isolated during the Test-3. Two active hydro accumulators (TH20B01 and TH40B01) were connected to the downcomer. The check valves (c6n2; n=1, 4) are modelled explicitly. The model also accounts for the actual locations of Test-3 specific LPIS injection.

Pressurizer & Surgeline
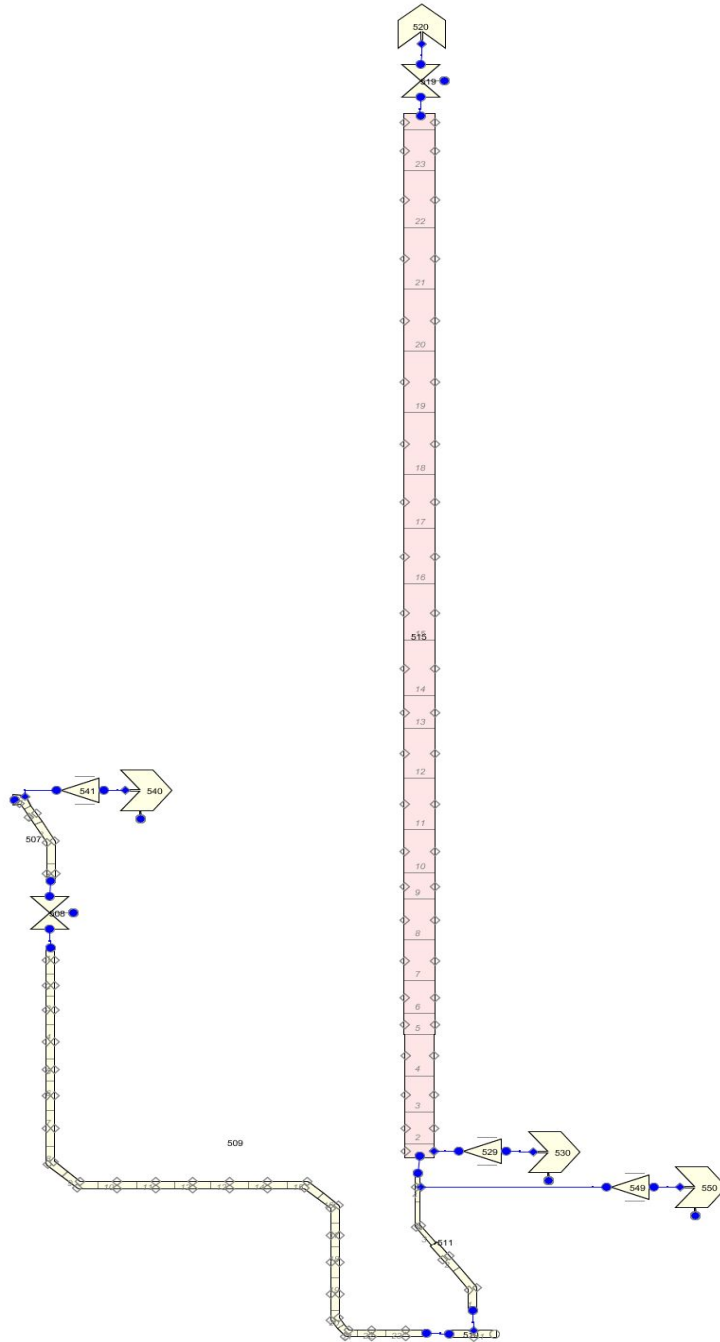
Figure 29 TRACE V5.0 pressurizer model
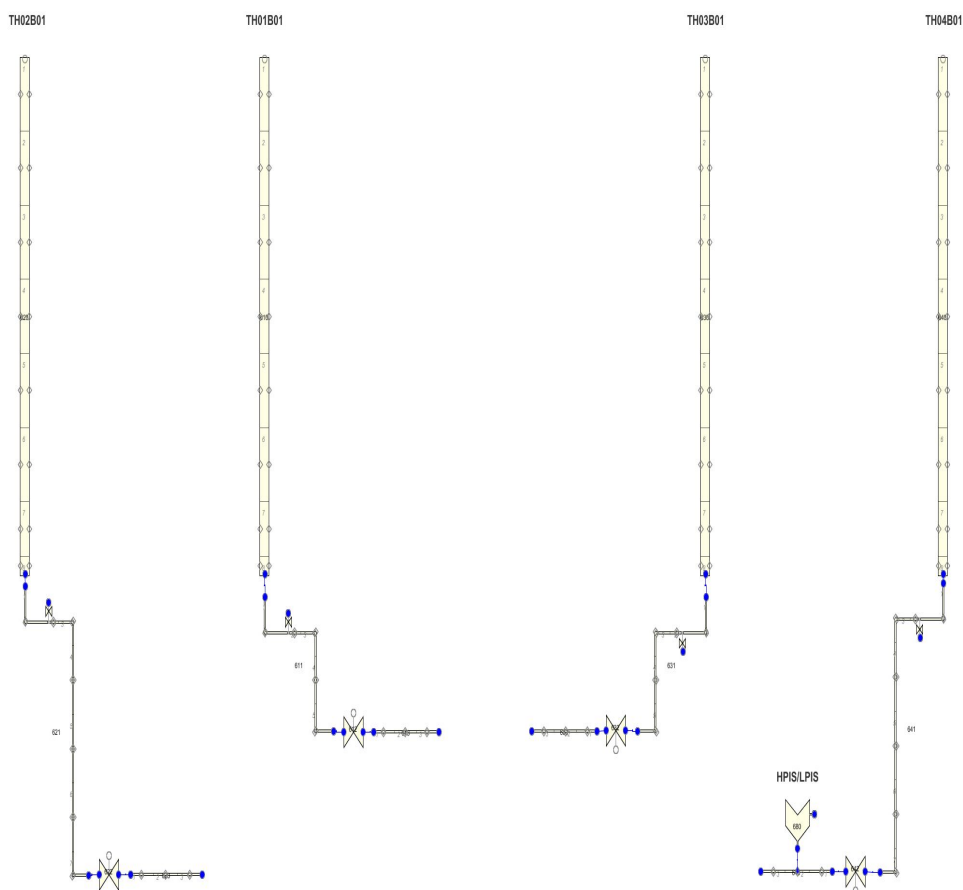
Figure 30 TRACE V5.0 emergency core cooling system model

The nodalization of SG secondary side and associated steam and feedwater lines is illustrated in Figure 31. The combination of single cell PIPE components is used to model the steam generator secondary side. Considering the top view, the central part of the vessel where the coiled tube bundle is located is treated as the "boiler" section, whereas the peripheral annular part is treated as the "downcomer" section. The lateral cross flow paths are modelled to simulate the internal recirculation of the secondary coolant. Nine rows of PIPE components correspond to the nine row tube bundle simulated on the steam generator primary side. The combination of three single PIPE components (e.g. c460, c470, and c471) is used to account for the steam-water separation. The upper parts of steam generator vessels are modelled using the pipe components (cn75; n=1, 4) each with 3 cells. In PSB-VVER facility, there are two main steam lines per one steam generator. The 1.5 MWt steam line is designed to remove the heat generated by the 1.5 MWt FRSB power. If 10 MWt FRSB power (to follow 1:300 scale) were used for the particular test, the 10 MWt steam line would have been used. During the PSB-VVER experiments carried out within the frame of OECD/NEA PSB-VVER project only the

1.5 MWt FRSB power systems were available. However, in order to account for unisolatable parts of 10 MWt steam lines and also for future use of the model, the 10 MWt steam lines are modelled and discussed here.
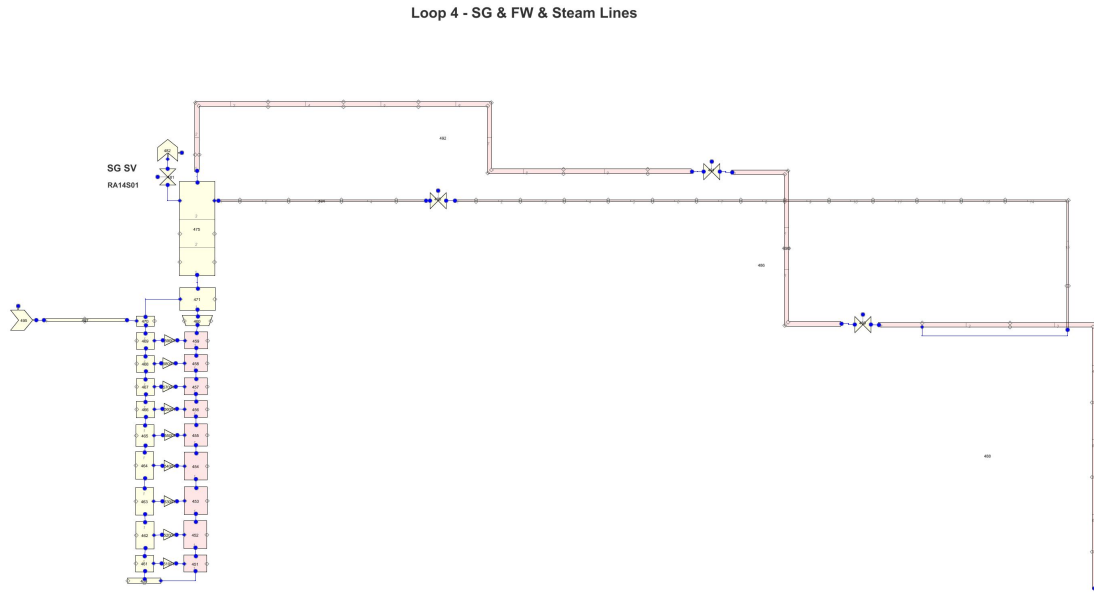
Figure 31 TRACE V5.0 secondary coolant system model – Loop No. 4

The 1.5 MWt steam line models consist of PIPE components (cn84; n=1, 4), VALVE components (cn85; n=1, 4), PIPE components (cn86; n=1, 4), and PIPE components (cn88; n=1, 4). Actually, the later components are parts of 10 MWt steam lines.

The 10 MWt steam line models consist of PIPE components (cn92; n=1, 4), VALVE components (cn91; n=1, 4), PIPE components (cn90; n=1, 4), and VALVE components (cn89; n=1, 4). Valves in the 10 MWt steam lines were closed throughout the Test-3.

The lengths and therefore the nodalization of individual steam lines vary accordingly to the loop specific design of the PSB-VVER test facility.

The combinations of FILL components (cn95; n=1, 4), and pipe components (cn97; n=1, 4) are used to model individual steam generator feedwater lines. In this, the facility steam generator feedwater system model is highly simplified.

70

VALVE components (cn81; n=1, 4) are used to simulate actions of power operated relief valves or safety valves. The test specific trip logic has to be set up to model the steam dump to atmosphere. BREAK components (cn82; n=1, 4) are used to model the boundary conditions.

The nodalization of the main steam line is illustrated in Figure 32. Main steam line is simulated using two PIPE components. VALVE component (c957) models the steam dump valve RA06S01.

A number of heat structure components are used to simulate heat transfer in steam generators and heat losses from the pipe walls to the environment.

There are 380 control blocks used in the model. They are set up to simulate I&C actions, to drive the model to the desired steady state, to facilitate the comparison of calculated data with measured data (e.g. differential pressures), etc.
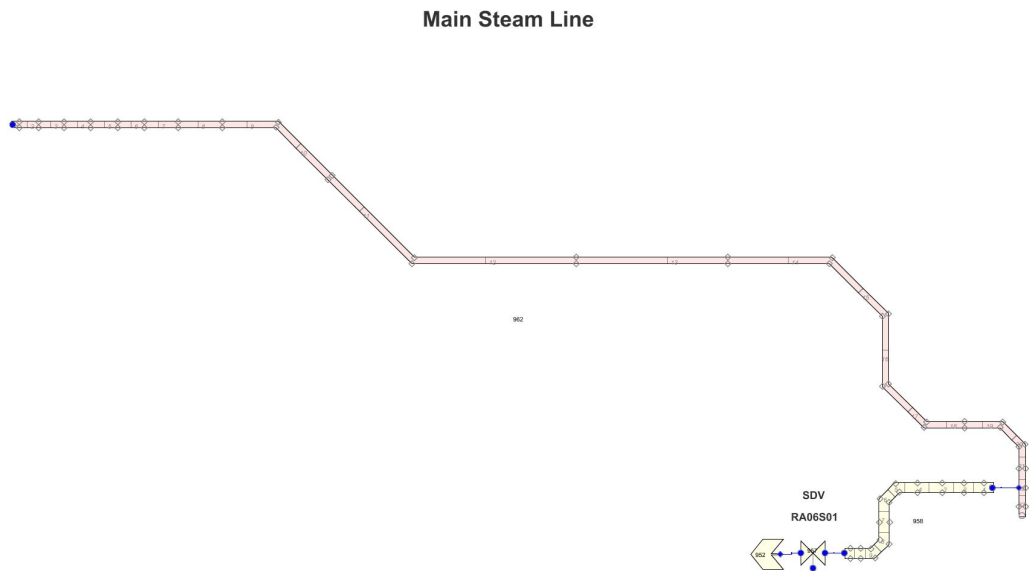
Figure 32 TRACE V5.0 main steam line model

4.3 TRACE V5.0 PSB-VVER Test Facility Model Validation

Third step in the thermal-hydraulic system code assessment process is defined in [2] as:

- Perform assessment calculations. Compare the test data with the results of calculations for the key parameters.

This study follows the concept of OECD/NEA BEMUSE Project, specifically Phase II [13]. In this, the reference case was run in two steps, i.e. the steady state run and the transient run to enable code data evaluation on the steady state level and on the transient level.

4.3.1 Reference Case

Similarly as in Phase II of the BEMUSE project, reference case in PSB-VVER Test-3 post test analysis was run and the test data were compared with the results of the calculation in two steps, on the steady state level, and on the transient level. A 500 second "null transient" code calculation was run to simulate the test specific initial conditions. Code control blocks were set up to force the code to reach predefined primary system coolant mass flows and secondary system steam line pressures. In total 127 measured and calculated parameters characterizing facility initial conditions were compared. In close to 80% of cases, the calculated value at 500 seconds was within the measurement accuracy interval $<\mu-2\sigma; \mu+2\sigma>$, where μ is the measured value of the parameter and 2σ is the measurement accuracy of the parameter as reported in [5]. Table 15 illustrates this steady state data evaluation process in case of the pressurizer model. Please refer to Table 2 and Figure 8 for the measurement channel identification. Please note that pressures (P) are in MPa, coolant temperatures (T) are in °C, and differential pressures (DP) are in kPa.

Table 15 TRACE V5.0 Test-3 reference case steady state data evaluation – PRZ

Experiment		Reference case (steady state)		Measurement accuracy (2σ)	Is cntrlvar value in the interval
Channel ID	Value (μ)	Control block	Value		$<\mu-2\sigma; \mu+2\sigma>$?
YP01P01	15.52	-506	15.52	0.07	TRUE
YP01DP02	-25.91	-508	-23.73	1.3	FALSE
YP01DP03	-37.75	-509	-37.32	1	TRUE
YP01L02	3.05	-597	3.05	0.3	TRUE

The calculated data for the pressurizer pressure (cb_506) match exactly the measured data (YP01P01) and similarly, the calculated data for the pressurizer level (cb_507) match exactly the measured data (YP01L02) due to corresponding steady state calculation controls.

In case of the differential pressure across the lower part of the pressurizer vessel and upper part of the surgeline (YP01DP02) compared with control block 508, the acceptance criterion is not fulfilled, but the result is tolerated due to following reasons. The lower experimental value indicates the presence of colder water in this section. The location of pressurizer heaters and its actions before the initiation of the transient contradicts the presence of colder water in the pressurizer vessel. There was only one measurement of coolant temperature over the surgeline. The model was initialized to reproduce that measurement. Table 16 illustrates the steady state data evaluation process in the case of the reactor pressure vessel model.

Table 16 TRACE V5.0 Test-3 reference case steady state data evaluation – RPV

Experiment		Reference case (steady state)		Measurement accuracy (2σ)	Is cntrlvar value in the interval <μ-2σ; μ+2σ>
Channel ID	Value (μ)	Control block	Value		
YC01T01	285	-2	285.56	4.3	TRUE
YC01T02	282	-3	285.56	3.7	TRUE
YC01T03	292	-4	288.97	3	FALSE
YC01T04b	311	-56	312.12	4.2	TRUE
YC01T05	292	-59	293.84	3	TRUE
YC01P16	15.51	-33	15.53	0.05	TRUE
YC01P17	15.6	-29	15.54	0.06	TRUE
YC01P18	15.58	-9	15.54	0.04	TRUE
YC01DP01	-8.71	-10	-8.63	0.2	TRUE
YC01DP02	-4.02	-12	-3.69	0.2	FALSE
YC01DP03	-25.7	-14	-25.92	0.7	TRUE
YC01DP04	-11.82	-16	-11.15	1	TRUE
YC01DP05	-8.83	-18	-8.94	0.2	TRUE
YC01DP06	8.67	-20	8.47	0.2	TRUE
YC01DP07	-7.38	-22	-7.23	1	TRUE
YC01DP08	-7.9	-24	-7.81	0.2	TRUE
YC01DP09	-4.97	-26	-4.58	0.2	FALSE
YC01DP10	-8.29	-28	-7.88	1	TRUE
YC01DP11	-5.96	-30	-5.47	0.2	FALSE
YC01DP12	-5.83	-32	-5.89	0.2	TRUE
YC01DP13	-11.08	-34	-11.17	0.2	TRUE
YC01DP14	-10.72	-36	-10.38	1.1	TRUE
YC01DP15	-17.67	-38	-17.04	1.1	TRUE
YC01DP16	21.3	-39	17.75	1	FALSE
YC01DP17	-35.98	-42	-31.54	1	FALSE
*DP_CORE	-28.458	-58	-27.50	1	TRUE
*DP_UPUH	-51.127	-60	-49.96	1.1	FALSE
YC01N01	1129	-57	1129.00	15	TRUE
YC01N02	14.9	-6	14.9	0.4	TRUE

Please note that pressures (P) are in MPa, coolant temperatures (T) are in °C, differential pressures (DP) are in kPa, and powers (N) are in kW.

In case of coolant temperature at the core bypass outlet (YC01T03 vs. cb_004), the acceptance criterion is missed by 0.03 K and the case is tolerated. In case of the differential pressure across the upper downcomer (YC01DP02 vs. cb_12), the acceptance criterion is not fulfilled. The case is further evaluated as follows. The sum of two successive differential pressure measurements YC01DP01 and YC01DP02 was compared to the sum of control blocks cb_010 and cb_012. The acceptance criterion is fulfilled for this derived parameter. Moreover, in the verification step steady state data (PSB-VVER Test-5a) evaluation for YC01DP01 and YC01DP02, the TRUE/FALSE results were reversed. In case of the differential pressure over the core section (YC01DP09 vs. cb_026) the acceptance criterion is not fulfilled. The case is tolerated because there is no evidence about the differences in the individual spacer grid design. When the derived parameter comparison technique is applied, i.e. (*DP_CORE vs. cb_058), the acceptance criterion is fulfilled. The "FALSE" case of YC01DP16 is tolerated since if the sum of differential pressures from YC01DP02 to YC01DP13 (18.54 kPa) was compared to cb_039, the acceptance criterion is fulfilled.

Table 17 illustrates the steady state data evaluation process in case of the primary coolant system model. Measured and calculated data of loop No. 1 are compared. The results of reference case steady state data evaluation of remaining loops are similar. The "FALSE" cases are attributed to the fact that thermal-hydraulic characteristics of primary system loops are considered identical in the model.

Table 17 TRACE V5.0 Test-3 reference case steady state data evaluation – PCS

Experiment		Reference case (steady state)		Measurement accuracy (2σ)	Is cntrlvar value in the interval
Channel ID	Value (μ)	Control block	Value		<μ-2σ; μ+2σ>?
YA01P01	15.58	-106	15.54	0.22	TRUE
YA01P03	15.54	-118	15.53	0.23	TRUE
YA01P08	15.57	-121	15.55	0.06	TRUE
YA01P09	15.5	-103	15.52	0.06	TRUE
YA01T02	283	-114	285.64	3	TRUE
YA01T03	310	-108	311.89	3	TRUE
YA01T26	285	-111	285.64	3.7	TRUE
YA01T32	285	-110	285.63	0.5	FALSE
YA01T33	285	-112	285.64	0.5	FALSE
YA01DP01	1.88	-115	1.75	0.2	TRUE
YA01DP02	9.11	-116	9.03	0.2	TRUE
YA01DP03	2.95	-8	3.21	0.1	FALSE
YA01DP04	-22.19	-43	-22.15	0.3	TRUE
YA01DP05	-24.08	-44	-24.51	1.1	TRUE
YA01DP06	-15.3	-45	-15.99	1	TRUE
YA01DP08	4.55	-46	4.51	1	TRUE
YA01DP09	-10.73	-47	-11.06	1	TRUE
YA01DP10	0.41	-48	0.41	0.2	TRUE
YA01DP11	-0.99	-124	-1.08	0.2	TRUE
YA01DP13	-20.38	-49	-20.75	1	TRUE
YA01DP14	-20.42	-50	-20.26	1	TRUE

Table 18 illustrates the steady state data evaluation process in case of the secondary coolant system model.

Table 18 TRACE V5.0 Test-3 reference case steady state data evaluation – SG

Experiment		Reference case (steady state)		Measurement accuracy (2σ)	Is cntrlvar value in the interval <μ-2σ; μ+2σ>?
Channel ID	Value (μ)	Control block	Value		
YB01P01	6.88	-511	6.91	0.05	TRUE
YB02P01	6.91	-521	6.92	0.05	TRUE
YB03P01	6.93	-531	6.92	0.05	TRUE
YB04P01	6.88	-541	6.91	0.05	TRUE

On the transient level, the test data were compared with the results of the calculation using FFTBM [7]. The selection of 22 parameters to be compared closely follows earlier studies [13] and [15]. For each parameter, the FFTBM algorithm is run in time window 0 – 2590 s (whole transient) to get average amplitudes (AA) and weighted frequencies (WF). These results are further combined using corresponding weighting factors to obtain total average amplitude (AA_{tot}) and total weighted frequency (WF_{tot}). In [7], the authors discuss the accuracy of code predictions as follows:

- $AA_{tot} \leq 0.3$ characterize very good code predictions
- $0.3 \leq AA_{tot} \leq 0.5$ characterize good code predictions
- The acceptability factor K is then defined for total average amplitude K = 0.4, and for primary system pressure K = 0.1. The acceptable code predictions are those with $AA_{tot} \leq 0.4$, and $AA_{PSP} \leq 0.1$.

The results of FFTBM application on the reference case are summarized in Table 19. Since $AA_{tot} < 0.4$ and $AA_1 = AA_2 = 0.1$, the reference case code predictions are acceptable.

Table 19 Test-3 TRACE V5.0 reference case FFTBM results

N	Parameter	ID Exp	ID Cal	AA
1	Upper plenum pressure	YC01P16	cb_033	0.080
2	Pressurizer pressure	YP01P01	cb_506	0.060
3	Accumulator #2 pressure	TH02P01	pn-620A04	0.103
4	Accumulator #4 pressure	TH04P01	cb_300	0.090
5	Steam generator #1 secondary side pressure	YB01P01	cb_511	0.390
6	Steam generator #3 secondary side pressure	YB03P01	cb_531	0.384
7	Core inlet coolant temperature	YC01T02	cb_003	0.155
8	Core outlet coolant temperature	YC01T04b	cb_056	0.499
9	Integrated break flow	MBr	cb_725	0.229
10	Primary coolant mass	M1k	cb_580	0.251
11	Accumulator #2 level	TH02L01	cb_204	0.100
12	Accumulator #4 level	TH04L01	cb_200	0.088
13	Differential pressure across downcomer	YC01DP03	cb_014	0.824
14	Differential pressure across downcomer	YC01DP04	cb_016	0.952
15	Differential pressure across the downcomer outlet and core simulator inlet	YC01DP06	cb_020	0.899
16	Differential pressure across the core	DP_CORE	cb_058	0.765
17	Differential pressure across the upper plenum	DP_UPUH	cb_060	0.370
18	Differential pressure across the upper plenum outlet and downcomer inlet	YC01DP16	cb_039	0.895
19	Peak cladding temperature	YC01T11	cb_pct	0.451
20	Cladding temperature – core bottom	YC01T113	cb_bot	0.163
21	Cladding temperature – core center	YC01T55	cb_mid	0.539
22	Cladding temperature – core top	YC01T39	cb_top	0.322
	Total average amplitude - **AA$_{tot}$**	-	-	0.306

Appendix C contains the figures with graphical comparisons of measured and TRACE calculated results.

Figure C.1 compares the data for integrated break mass flows. In the experiment, this parameter was not measured directly, but a specific algorithm for measured data evaluation was applied. In agreement with experimental data evaluation, the code predicts first vaporization at break at 108 s. After that, experimental data evaluation shows the break flow stagnation for approximately 50 s. In the reference case calculation with Cd = 0.85, no attempt to reproduce this phenomenon was applied. Approximately from 160 s until the end of the transient, the difference between the results slightly increases. The experimental data evaluation does not account for break mass flow increase following the LPIS injection.

Figure C.2 and Figure C.3 show good agreement between measured and calculated primary system pressures. Consequently, the timing of the accumulator injection is well predicted in the model (see Figures C.4 – C.7).

Figure C.8 shows the comparison of the primary system coolant mass between that evaluated in experiment and TRACE results. The experimental data is the product of the specific algorithm using data measured directly. According to the experimenters the accuracy of this evaluation is ± 50 kg. As shown in Table 19, parameter No. 10, the average amplitude is 0.251 which characterizes very good code prediction.

Figures C.9 – C.12 show the comparison of the secondary system pressure (at the steam generator steam dome) between measured and TRACE results. Approximately from 180 s in the transient the secondary system pressure exceeds the primary system pressure. The heat transfer across the steam generator tube bundle is modelled in TRACE, however, in the reference case; the heat losses from steam line pipes to environment were not simulated. As shown in Table 19, parameters No. 5 and No. 6, the average amplitudes are just below the acceptance limit (K = 0.4) for good code predictions. The heat loss model from secondary system pipe walls to the environment is considered for further refining the reference case results before the uncertainty and sensitivity study.

Figure C.13 shows the comparison of the core simulator inlet coolant temperature between measured and TRACE results. The measured data follows the saturation temperature. During the period of the accumulator injection, the TRACE data shows that subcooled liquid reached the core simulator inlet.

Figure C.14 compares core simulator outlet coolant temperatures. The measured data show three periods of steam superheat during the final FRSB dryout. TRACE data reproduce the phenomenon qualitatively well. Quantitatively, as shown in Table 19, parameter No. 8, the average amplitude is 0.499 just on the edge (0.5) of good code prediction characteristics. Due to the weighting factors applied when calculating AAtot, this parameter is by far the largest contributor (0.047) to AAtot = 0.306.

Figures C.15 – C.17 show the comparison of differential pressures across the downcomer and lower plenum simulators between measured and TRACE results. Qualitatively, the code predictions agree well with the measurements except cb_016 compared to YC01DP04 on Figure C.16, where the calculated liquid loss after 2200 s is more significant.

Figures C.18 – C.20 show the comparison of differential pressures across other parts of the reactor pressure vessel simulator between measured and TRACE results. Qualitatively, the code predictions agree with the measurements. Quantitatively, good code prediction is reached only for cb_060 compared to sum of YC01DP11 to YC01DP15, as shown I Table 19, parameter

No. 17, which contributes 0.006 to AAtot. The individual contribution of other selected differential pressure parameters to AAtot varies from 0.012 to 0.014.

In case of SB LOCA events, the transient is affected by the loop seal clearing processes. If at least one loop seal remains cleared, then coolant level depression in the core region is limited. Figures C.21 – C.28 compare the differential pressures in loop seal descending and ascending legs for all the loops. After the accumulator injection is terminated, the loop seal No. 4 remains clear. Please note that loop No. 4 is the broken loop.

Finally, the measured and calculated cladding temperatures are compared on Figures C.29 – C.32. Similarly to approach adopted in [13] and [15], the representative measurements are selected for the bottom, middle, and top third of the FRSB. In addition, the measurement channel data with maximum cladding temperature recorded during the transient (YC01T11) is compared to the corresponding TRACE data. TRACE predicts only temporary and limited heatup during the final heatup period observed in experiment. Two axial level calculated data are compared to YC01T113 thermocouple readings, which show no FRSB heatup at that elevation. Only the final heatup was recorded by thermocouples located close to the middle of FRSB. The readings of YC01T55 thermocouple measurements are representative and compared to each of four azimuthal sectors calculated data for the given axial position. TRACE predicts the start of the final heatup later and the prediction of its termination agrees well with the measurement. Azimuthal sector No. 4 (adjacent to the broken loop) is slightly favoured for cooling. The second and third (final) heatup were recorded by the thermocouples located close to the center of the top third of FRSB. The readings of YC01T39 thermocouple measurements are representative and compared to each of four azimuthal sectors calculated data for the given axial position. TRACE predicts the second heatup to begin earlier and to be of minimal and shortly lasted deviation from the saturation temperature. TRACE predicts the final heatup to begin later. The code prediction of its termination agrees well with the measurement. Measured and calculated peak cladding temperatures are shown in Figure C.32. Measured data document all three periods of cladding heatup at the top of the FRSB. First measured heatup was brief in time and of very small overheat with respect to saturation temperature. This heatup is not predicted by the code. During the experiment, the second dryout begun at about 400 s. With correct timing, but lower in magnitude, the corresponding FRSB cladding heatup is predicted by the code. During the experiment, the third dryout begun at about 2060 s. Delayed by 80 s, and lower in magnitude, the corresponding FRSB cladding heatup at that elevation is predicted by the code. During the experiment, the third dryout was terminated by the LPIS injection. The timing of this event is well predicted by the code.

4.3.2 Preliminary sensitivity study

This section is titled "preliminary" sensitivity study in order to distinguish between activities being carried out before and after the uncertainty study. Before the uncertainty study is started, preliminary sensitivity study may be carried out, e.g. [13] with the aim to determine the code response to the variation of values of input parameters which may be considered in a later uncertainty study.

If a full scale preliminary sensitivity study were performed within the project reported here, the selection of code input parameters would have corresponded closely to the case reported in [13]. In this project the preliminary sensitivity study is limited to one uncertain parameter, namely the discharge coefficient in the critical flow model. As shown in comment to Figure C.1, the reference case Cd = 0.85. In the sensitivity run with Cd = 1.0, the code response, in

particular the prediction of peak cladding temperature, is evaluated. The transient was analyzed to 2500 s, and the key results are compared in Figure C.33. The final dryout started earlier in the sensitivity calculation and its timing closely matched the experimental data. Calculated peak cladding temperature is expected to be overpredicted by approximately 50 K the measured value since cladding temperature in azimuthal sector #4 has already reached its maximum and taking into account the delay in the timing of peak cladding temperatures in other azimuthal sectors as in Figure C.32.

4.4 Conclusions on TRACE V5.0 Code Assessment

The independent code assessment reported here is based on TRACE V5.0 PSB-VVER thermal-hydraulic model validation against small break LOCA test data. The experiment denoted as Test-3 [5] was carried out within the frame of OECD/NEA PSB Project. The conclusions are drawn to each of four major steps considered:

- PSB-VVER model conversion
- PSB-VVER model verification
- PSB-VVER model validation
- Preliminary sensitivity study

SNAP [8] was successfully applied for R5/M33 PSB-VVER model conversion to TRACE V5.0 PSB-VVER model. In addition SNAP Model Editor was successfully applied in TRACE V5.0 PSB-VVER model verification step for gradual abandonment of RELAP5/MOD3.3 inherited 1D component modelling technique toward TRACE 3D component modelling technique. The number of TRACE V5.0 PSB-VVER model versions (~45) developed during the model verification step may appear high. However, the "one change at the time" technique which had been intentionally preferred by new TRACE code user finally paid off. In the validation step only 4 TRACE V5.0 PSB-VVER model versions were needed for refining the initial and boundary conditions of the test selected.

In both the model verification and the model validation steps, the model was shown to be qualified on the steady state level. In close to 80% of the ~120 parameters compared, the acceptance criterion was fulfilled. Other cases were tolerated primarily due to the modelling approach that was followed, i.e. no consideration of differences in the primary loop hydraulic characteristics which may be test dependent.

In the verification step, the model was shown to reproduce main phenomena of the large break LOCA test qualitatively and quantitatively well. However, according the FFTBM criteria applied it was not possible to conclude that the model was qualified on the transient level. In this case the total average amplitude (AA_{tot} = 0.41) that exceeded the acceptability factor (K = 0.4). The main challenge to the TRACE V5.0 PSB-VVER model in reproducing large break LOCA test data more accurately was identified in modelling upper plenum ECCS injection related phenomena. Less accurate predictions of differential pressures across the upper plenum and core simulators lead to the lesser accuracy of cladding temperatures during the transient.

In the validation step, the model was shown to be qualified on the transient level. The FFTBM applied acceptance criteria were fulfilled with conclusion of good code predictions.

Preliminary sensitivity study shown that model is capable of reproducing key safety parameter (peak cladding temperature) when considering the uncertainty of critical discharge coefficient.

TRACE V5.0 PSB-VVER thermal-hydraulic model was validated for small break LOCA analyses against the experimental data from Test-3. This independent validation case may contribute to the TRACE V5.0 code assessment.

5. REFERENCES

1.   MELIKHOV, O. I., et al. "Report about PSB-VVER Description (including measurement system)", OECD PSB-VVER Project PSB-03, Elektrogorsk, 2003.

2.   TRACE V5.0 Assessment Manual, Main Report, USNRC Division of Risk Assessment and Special Projects, March 2010.

3.   BEMUSE Phase VI Report, Status report on the area, classification of the methods, conclusions and recommendations; NEA/CSNI/R(2011)4, March 2011.

4.   ELKIN, I. V., et al. "Experimental Data Report Test 5a (Version 1)", OECD PSB-VVER Project PSB-31, Elektrogorsk, 2008.

5.   MELIKHOV, O. I., et al. "Post-Test Full Experimental Data Report (Test-3)", OECD PSB-VVER Project PSB-18, Elektrogorsk, 2004.

6.   D' Auria, F., Review of methods of Calculation, Assumptions and Acceptance Criteria for the Analyses, IAEA Regional Workshop on Evaluation and Licensing of NPP Modifications, Jožef Stefan Institute, Ljubljana, 21-25 June, 1999.

7.   Prošek, A., D' Auria, F., Mavko, B., Review of quantitative accuracy assessments with fast Fourier transform based Method (FFTBM), Technical Note, Nucl. Eng. Des., 217, 179-206, 2002.

8.   Symbolic Nuclear Analysis Package, Version 2.0.7, August 15, 2011
        © 2002-2011 Applied Programming Technology, Inc.

9.   RELAP5/MOD3.3 Code Manual, Volume III: DEVELOPMENTAL ASSESSMENT PROBLEMS, Information Systems Laboratories, NUREG/CR-5535/Rev 1-Vol III, December 2001.

10.   Douglas L. Reeder: "LOFT System and Test Description (5.5 FT Nuclear Core)", NUREG/CR-0247, TREE-1208, July 1978.

11.   Paul D. Bayless, Janice M. Divine: "Experiment Data Report for LOFT Large Break Loss-of-Coolant Experiment L2-5", NUREG/CR-2826, INEL, August 1982.

12.   "CSNI Integral Test Facility Validation Matrix for the Assessment of Thermal-Hydraulic Codes for LWR LOCA and Transients", Committee on the Safety of Nuclear Installations, OECD Nuclear Energy Agency, NEA/CSNI/R(96)17 (also referenced as: OCDE/GD(97)12, July 1996, France.

13.   BEMUSE Phase II Report, Re-analysis of the ISP-13 Exercise, Post Test Analysis of the LOFT L2-5 Test Calculation; NEA/CSNI/R(2006)2, May 2006.

14.   Validation Matrix for the Assessment of Thermal-Hydraulic Codes for VVER LOCA and Transients, A Report by the OECD Support Group on the VVER Thermal-Hydraulic Code Validation Matrix; NEA/CSNI/R(2001)4, June 2001.

15.   Del Nevo, A., et al. Benchmark on OECD NEA PSB-VVER Project Test 5a: LB-LOCA Transient in PSB-VVER Facility, DIMNP NT 638(08) Rev. 0, Pisa, November 2008.

16. "BEMUSE Phase III Report, Uncertainty and Sensitivity Analysis of the LOFT L2-5 Test", Nuclear Energy Agency, Committee on the Safety of Nuclear Installations, NEA/CSNI/R(2007)4,
Coordinators: A. de Crécy, P. Bazin (CEA),
Authors (Organizations): P. Bazin, A. de Crécy (CEA, France), H. Glaeser, T. Skorek (GRS, Germany), J. Joucla, P. Probst (IRSN, France), B. Chung (KAERI, South Korea), M. Kyncl, R. Pernica (NRI-1, Czech Republic), J. Macek, R. Meca (NRI-2, Czech Republic), R. Macian (Switzerland), F. D'Auria, A. Petruzzi (UNIPI, Italy), M. Perez, F. Reventos (UPC, Spain), K. Fujioka (JNES, Japan).

17. A. de Crécy et al. "Uncertainty and sensitivity analysis of the LOFT L2-5 test: Results of the BEMUSE programme". Nuclear Engineering and Design 238 (2008), 3561-3578

18. M. Perez et al., Uncertainty and sensitivity analysis of a LBLOCA in a PWR Nuclear Power Plant: Results of the Phase V of the BEMUSE programme. Nuclear Engineering and Design 241 (2011) 4206– 4222.

19. "RELAP5/MOD3.3 Code Manual", Volume II: Appendix A Input Requirements, Information Systems Laboratories, Inc., NUREG/CR-5535/Rev P4-Vol II App A, October 2010.

20. "RELAP5/MOD3.3 Code Manual", Volume I – Volume VIII, Information Systems Laboratories, Inc,. NUREG/CR-5535/Rev P4, October 2010.

21. Bemuse Phase IV Report, "Simulation of a LB-LOCA in ZION Nuclear Power Plant – Appendices A to D", Nuclear Energy Agency, Committee on the Safety of Nuclear Installations, NEA/CSNI/R(2008)6/vol2, November 2008.

22. Sachs L., "Applied Statistics", Springer-Verlag, New York, 1982.

23. StatSoft, Inc. (2006). Electronic Statistics Textbook. Tulsa, OK: StatSoft. WEB: http://www.statsoft.com/textbook/stathome.html

24. TRACE V5.0 Assessment Manual, Appendix C: Integral Effects Tests, USNRC Division of Risk Assessment and Special Projects, March 2010.

25. Annunziato, A., Quick Look Report on LOBI-MOD2 Test BL-34 (LOBI/BETHSY Counterpart Test), J.R.C., LQC 91-60.

APPENDIX A

List of Figures

Fig. A.1: PSB-VVER Test-5a Integrated Break Mass Flow
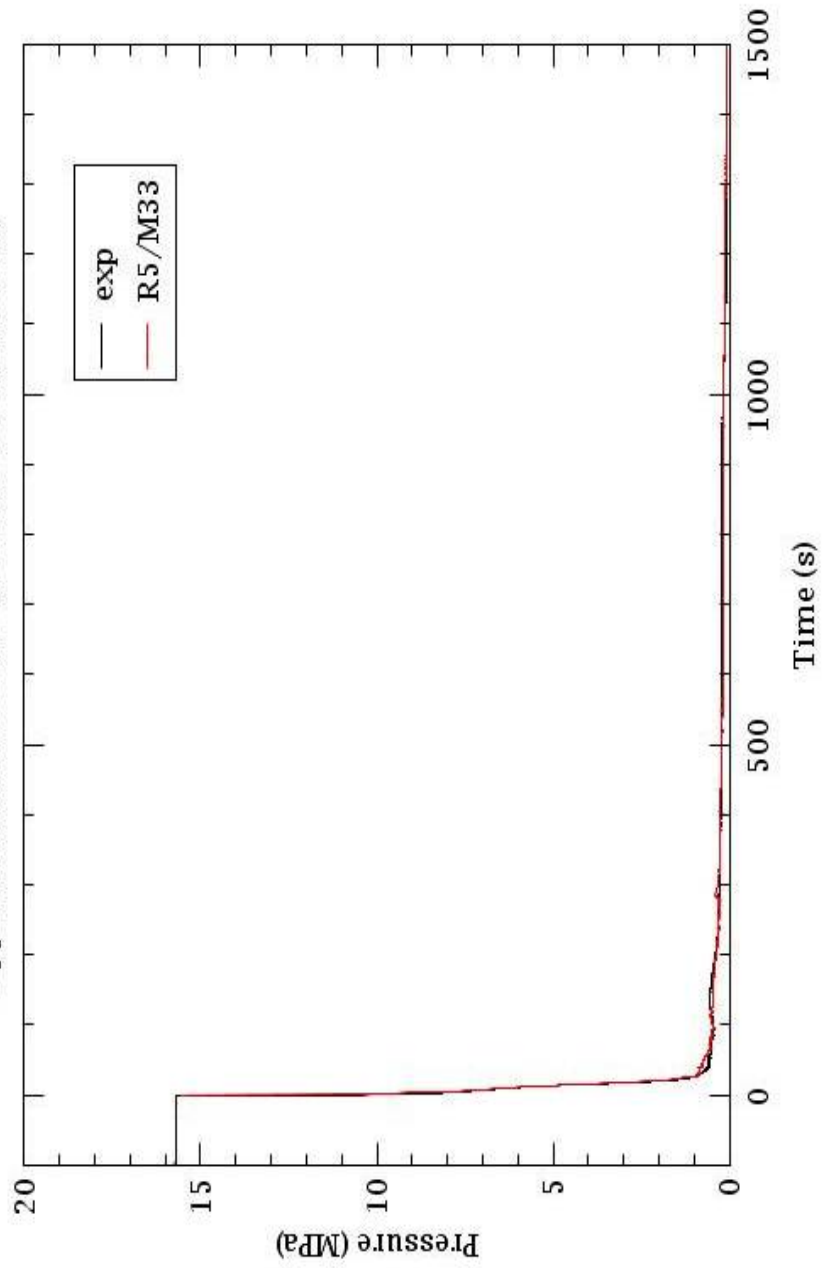
Fig. A.2: PSB-VVER Test-5a Upper Plenum Pressure
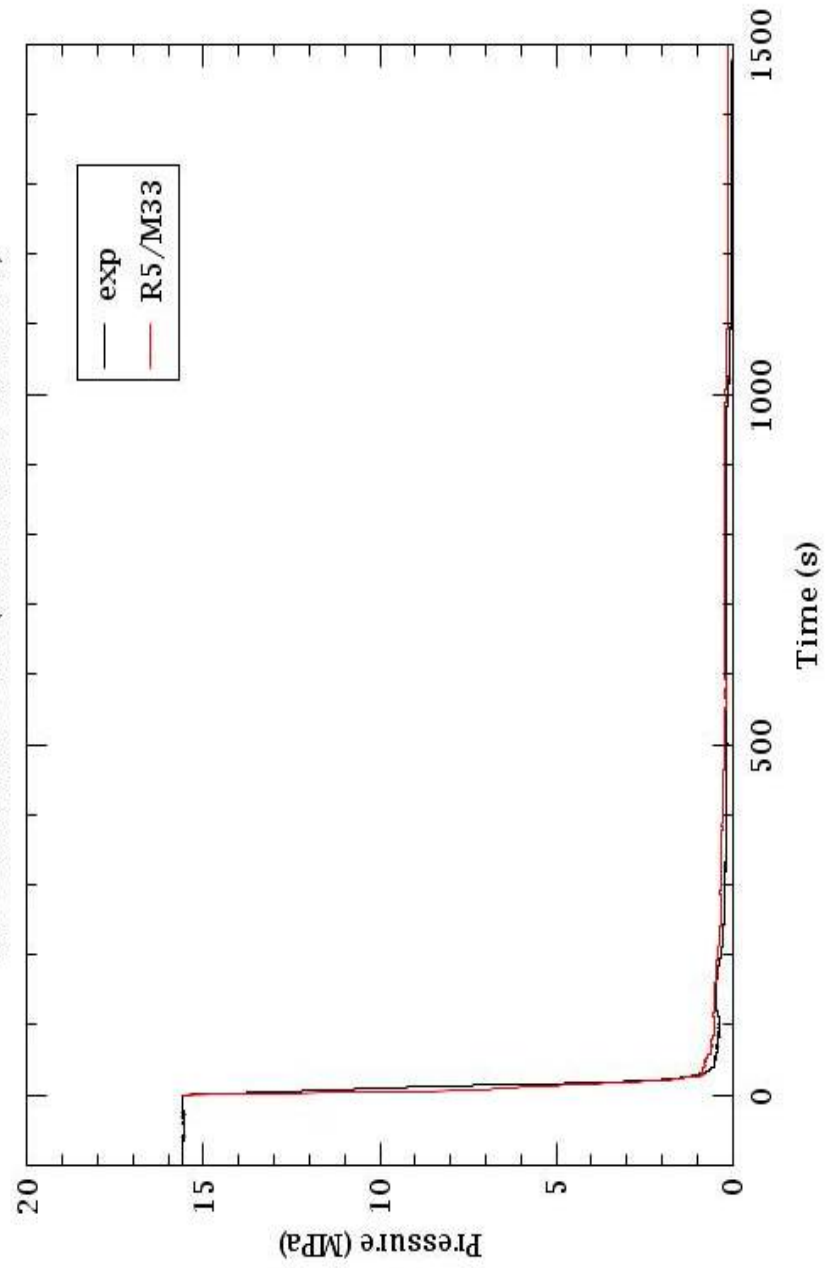
Fig. A.3: PSB-VVER Test-5a Pressurizer Pressure
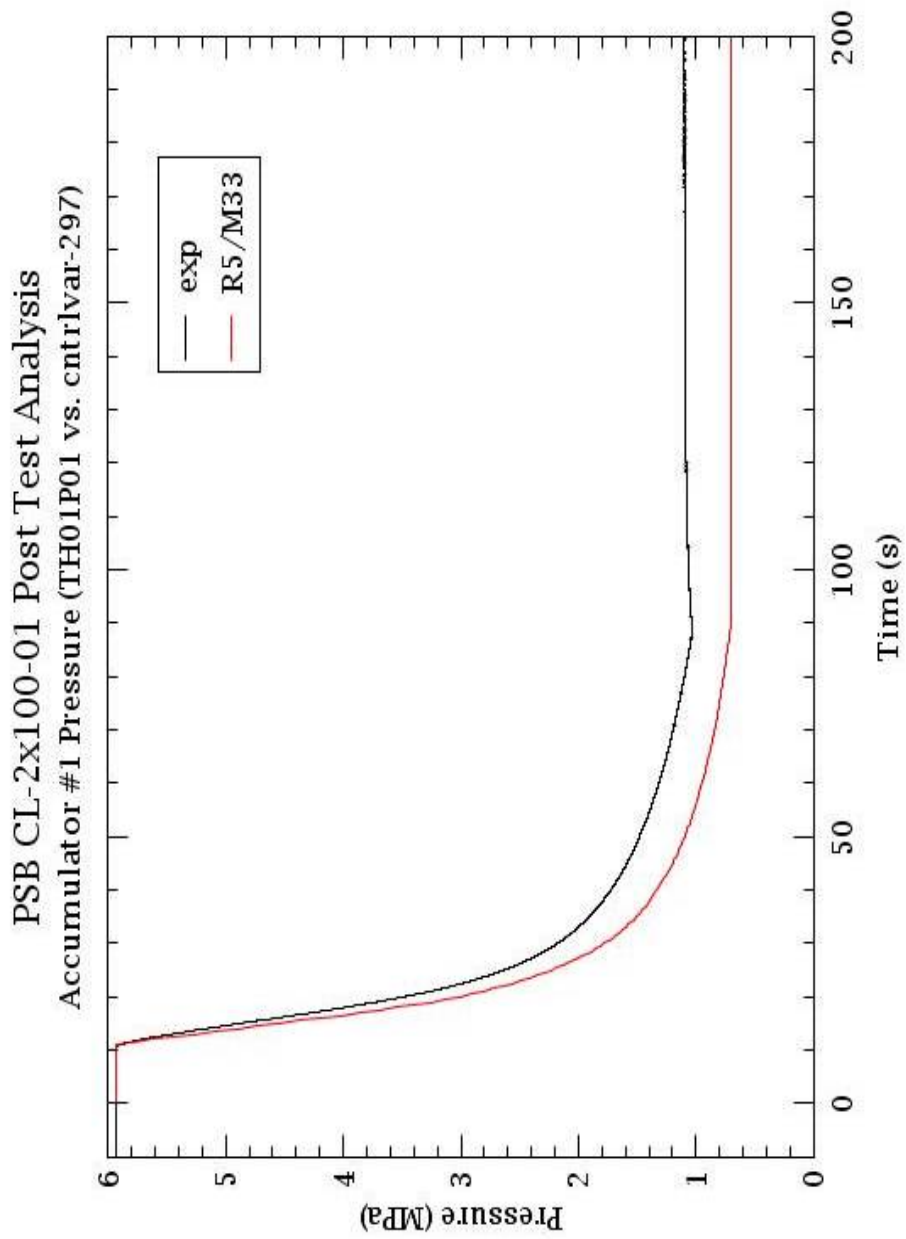
Fig. A.4: PSB-VVER Test-5a Accumulator #1 Pressure
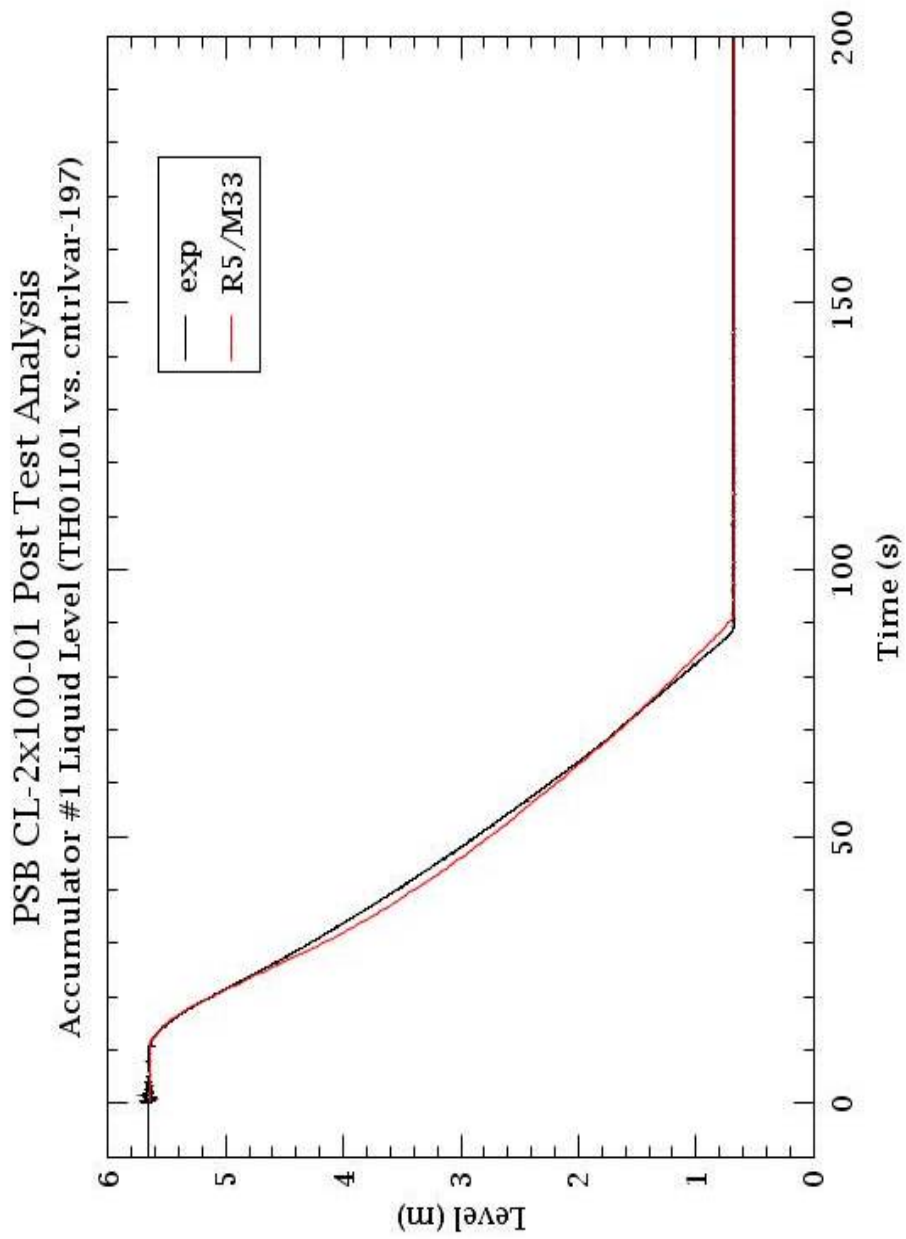
Fig. A.5: PSB-VVER Test-5a Accumulator #1 Level
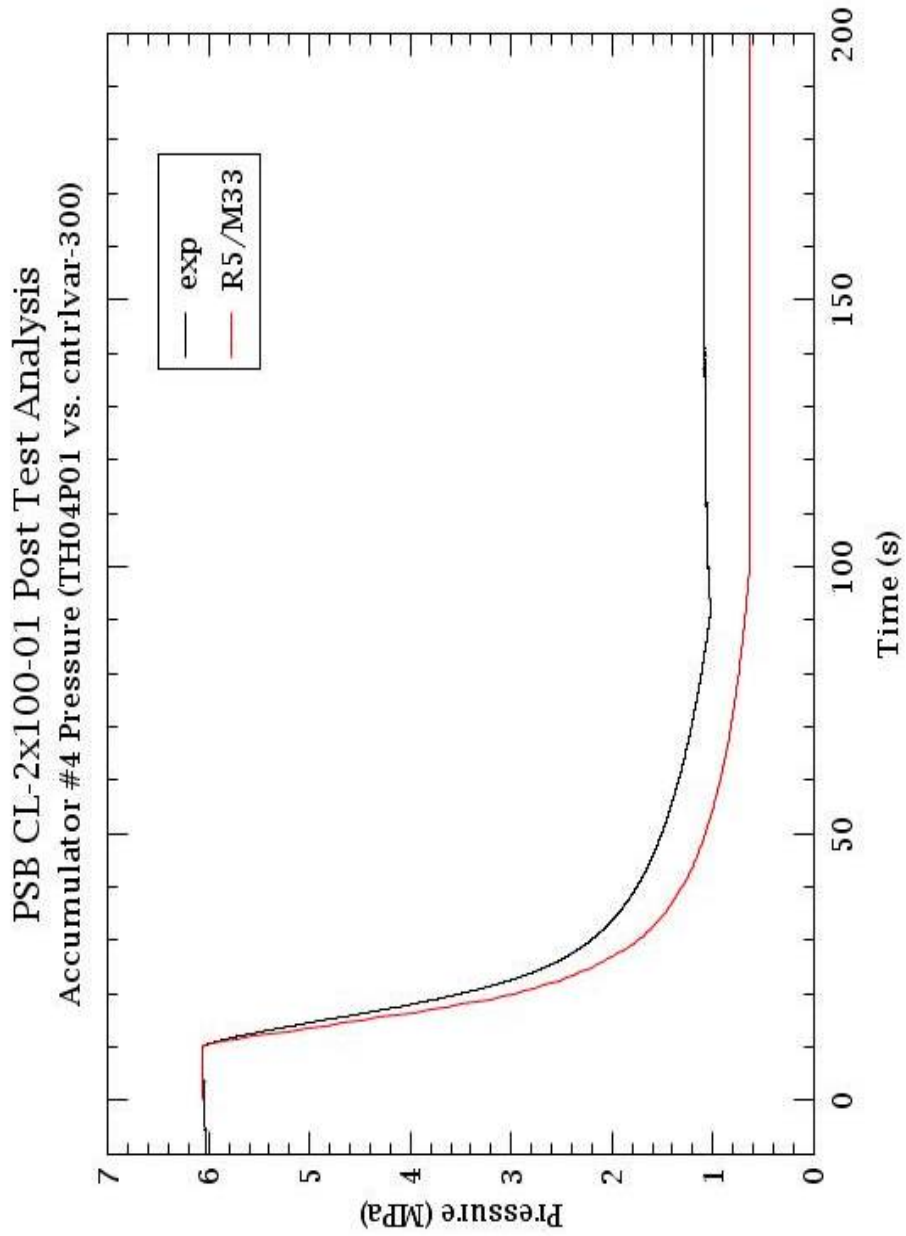
Fig. A.6: PSB-VVER Test-5a Accumulator #4 Pressure
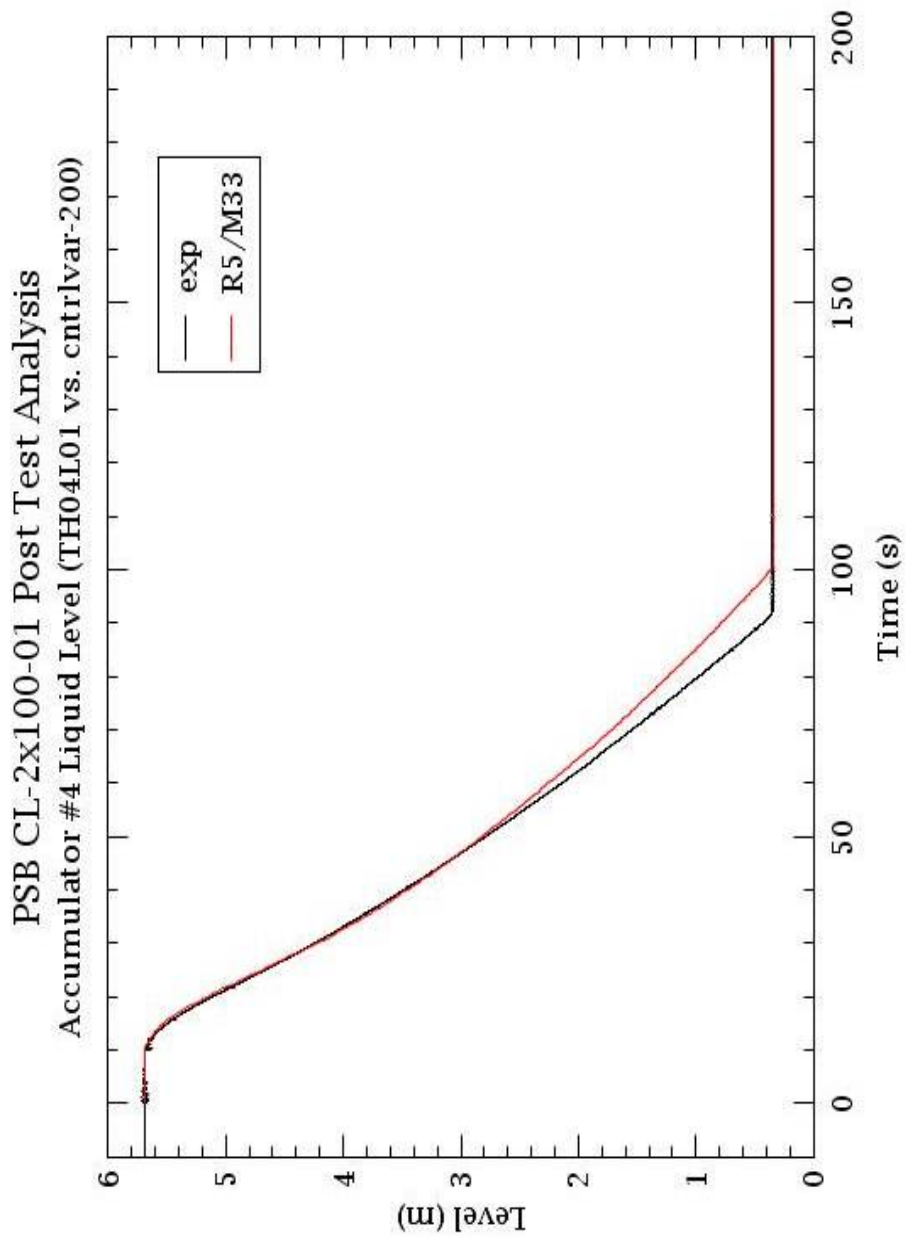
Fig. A.7: PSB-VVER Test-5a Accumulator #4 Level
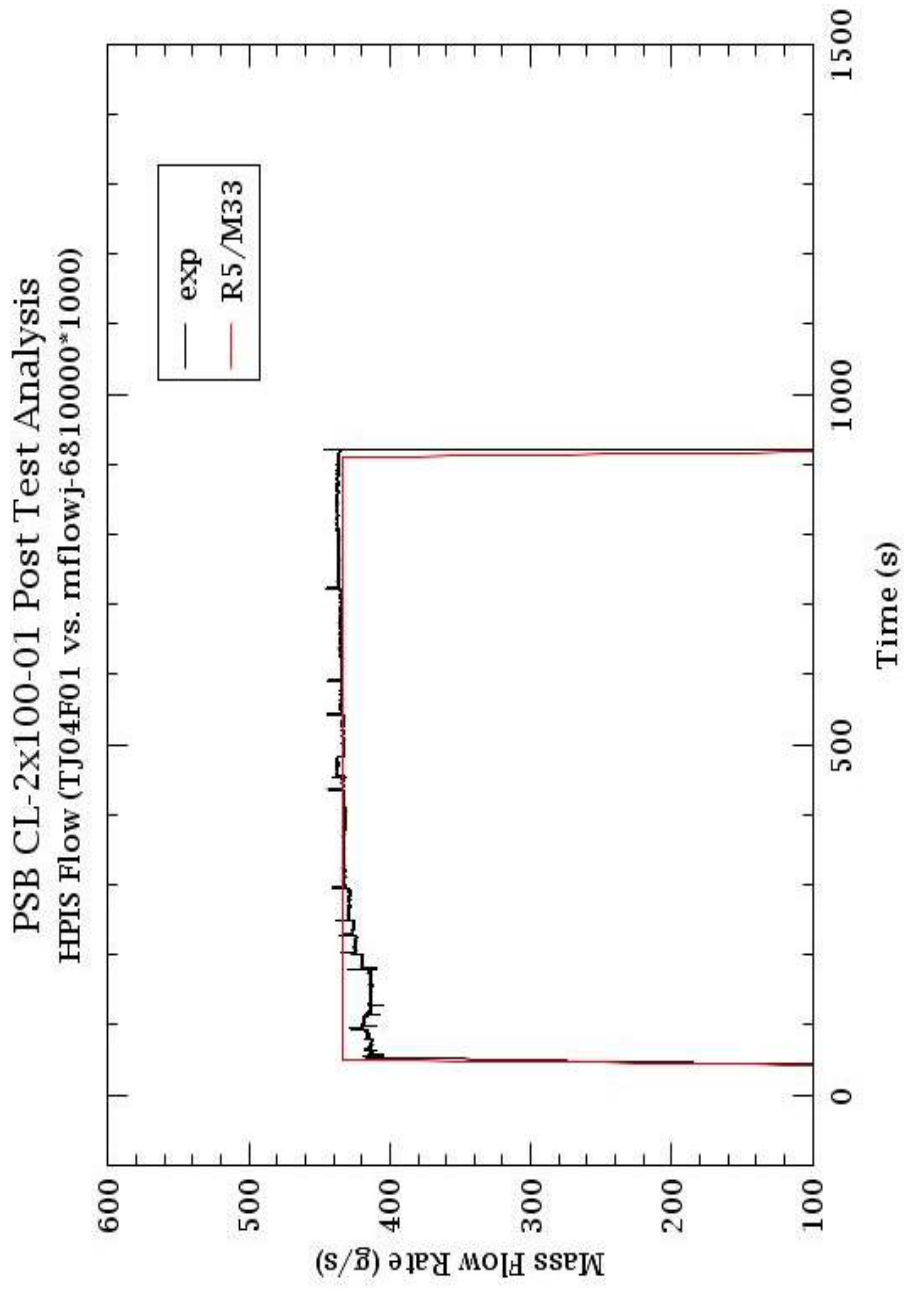
Fig. A.8: PSB-VVER Test-5a HPIS Mass Flow
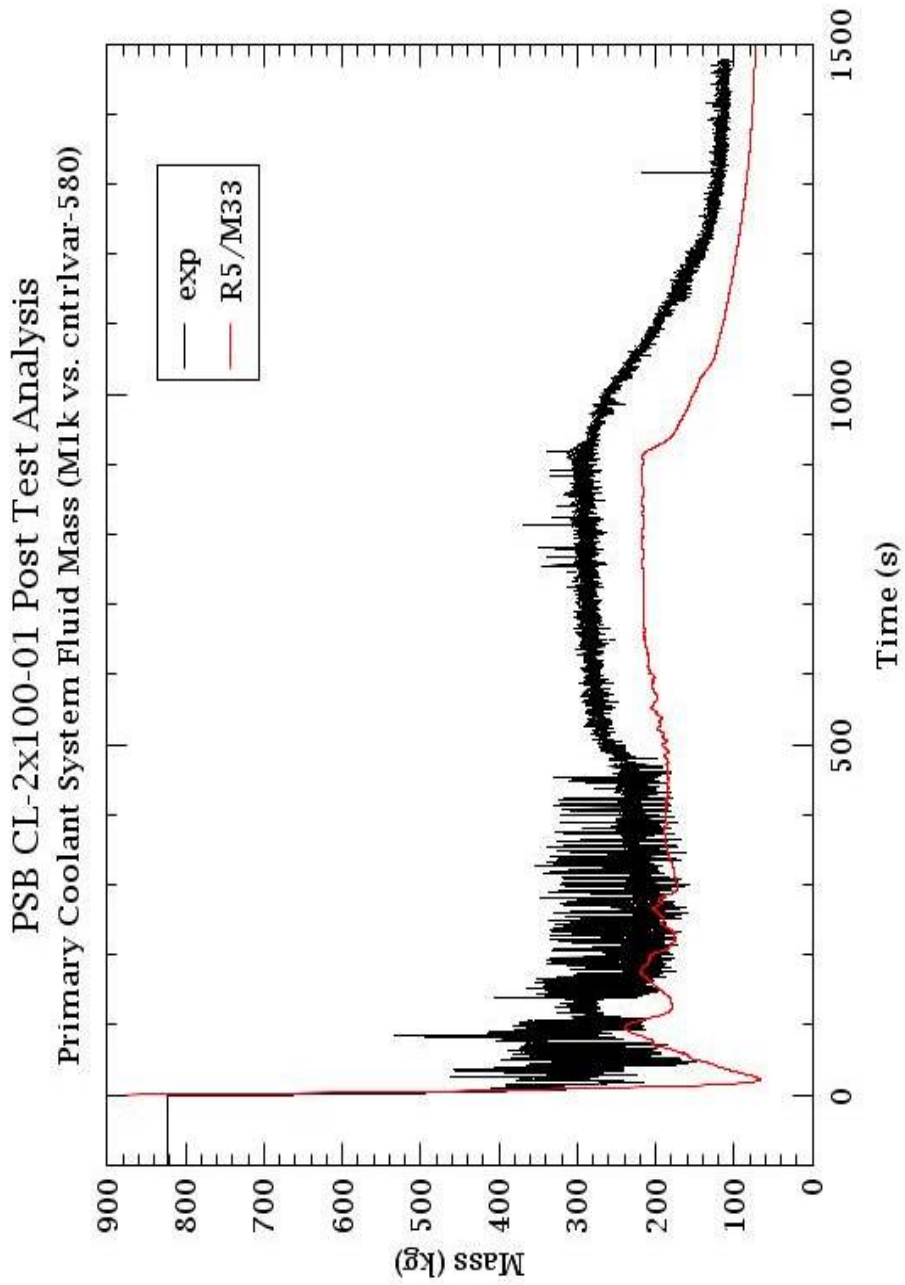
Fig. A.9: PSB-VVER Test-5a Primary Coolant Mass
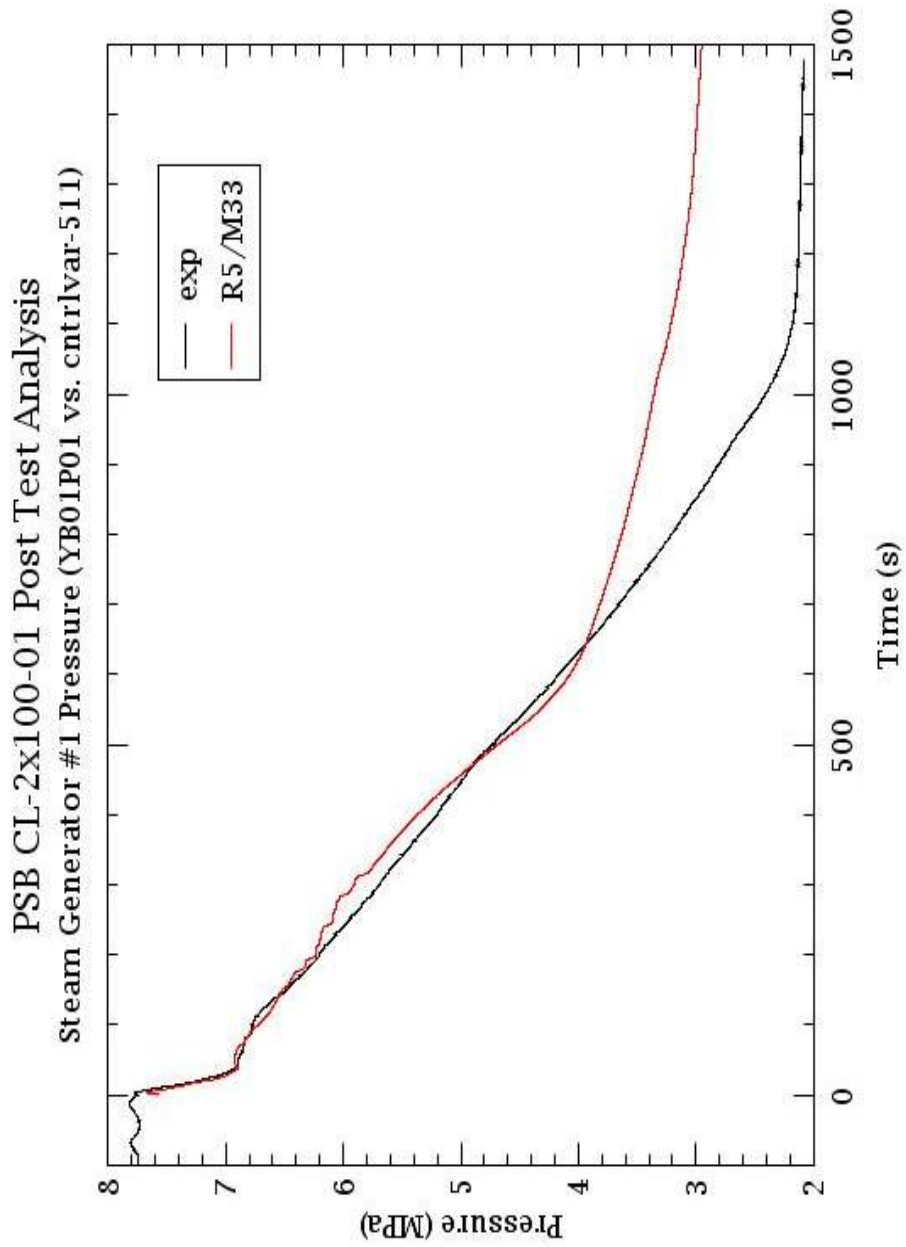
Fig. A.10: PSB-VVER Test-5a Steam Generator #1 Pressure
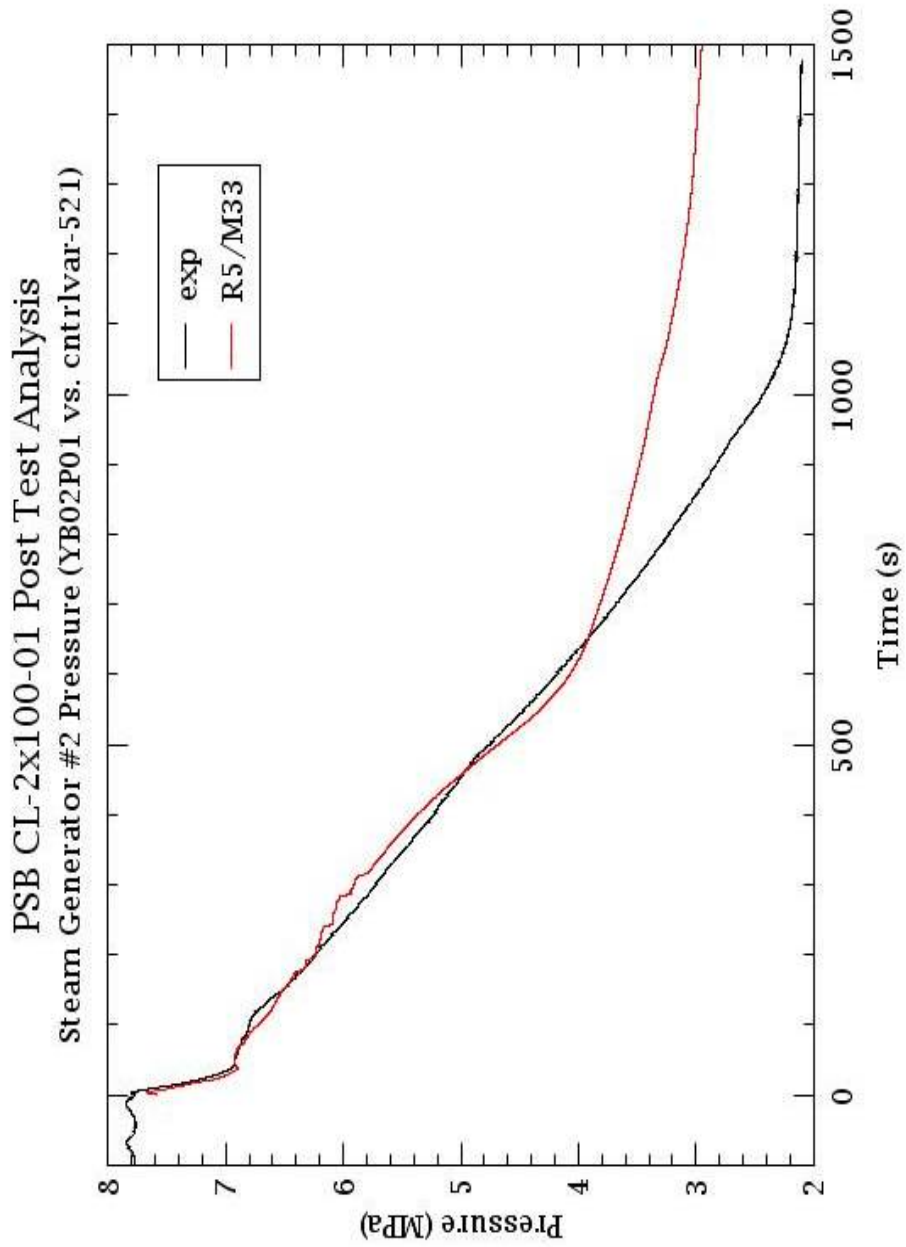
Fig. A.11: PSB-VVER Test-5a Steam Generator #2 Pressure
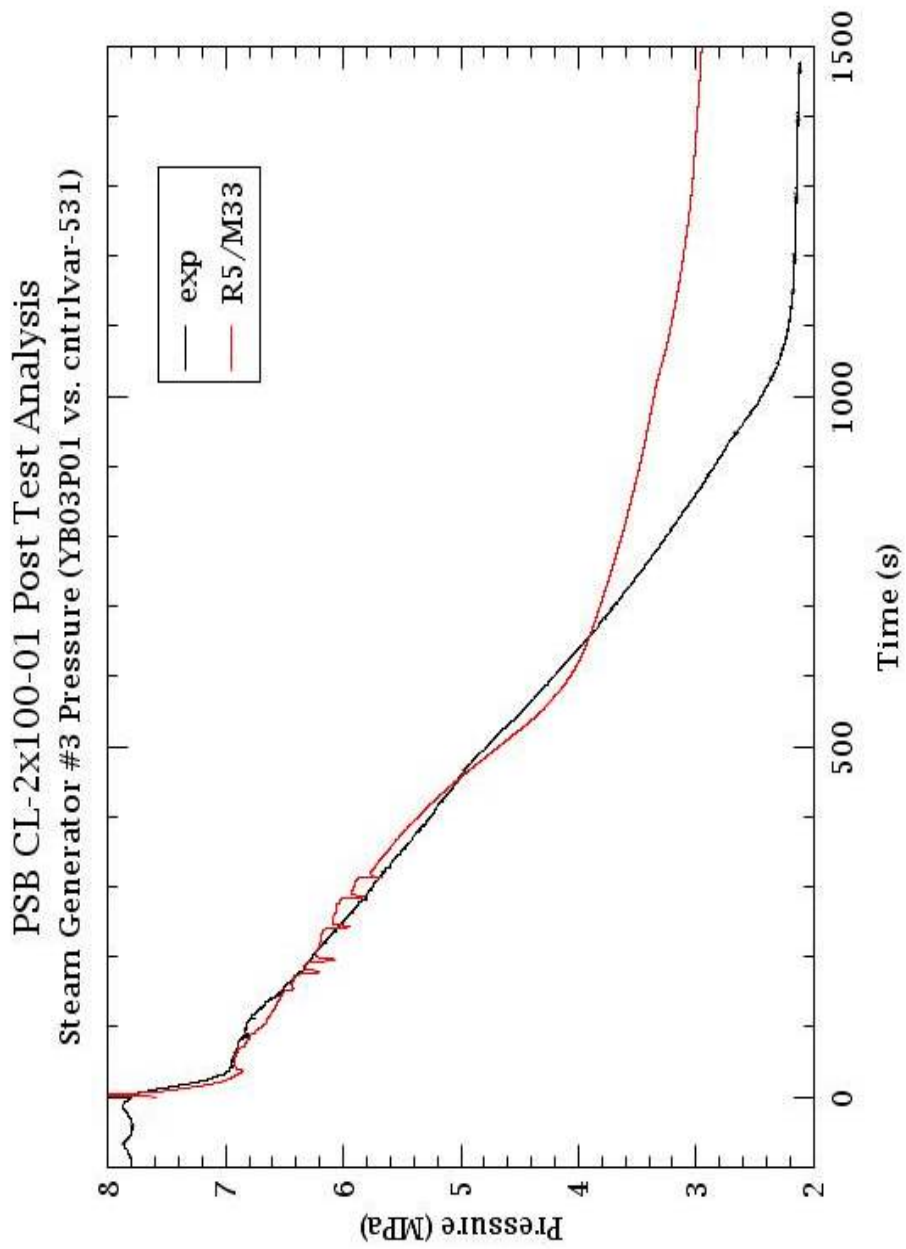
Fig. A.12: PSB-VVER Test-5a Steam Generator #3 Pressure
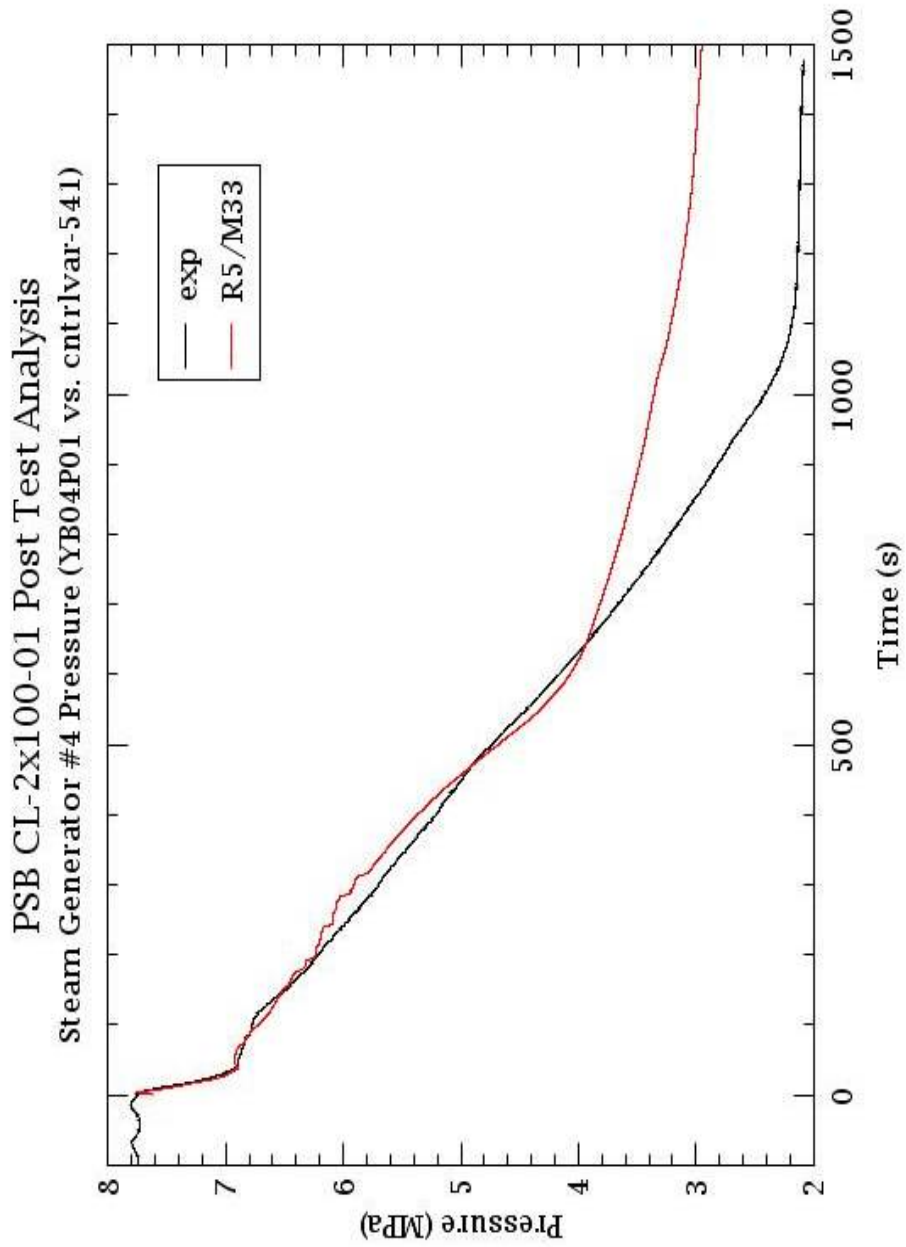
Fig. A.13: PSB-VVER Test-5a Steam Generator #4 Pressure
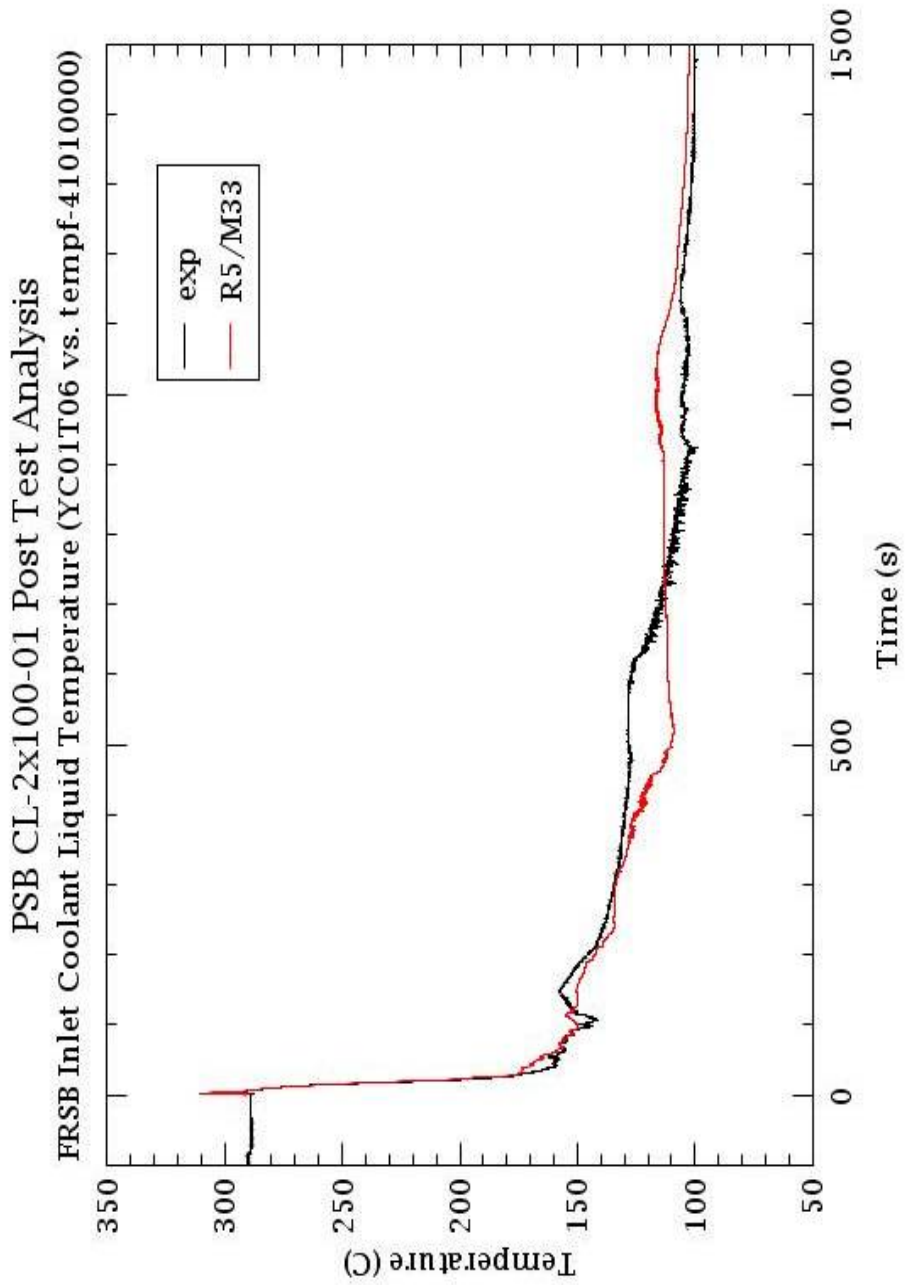
Fig. A.14: PSB-VVER Test-5a Core Simulator Inlet Liquid Temperature
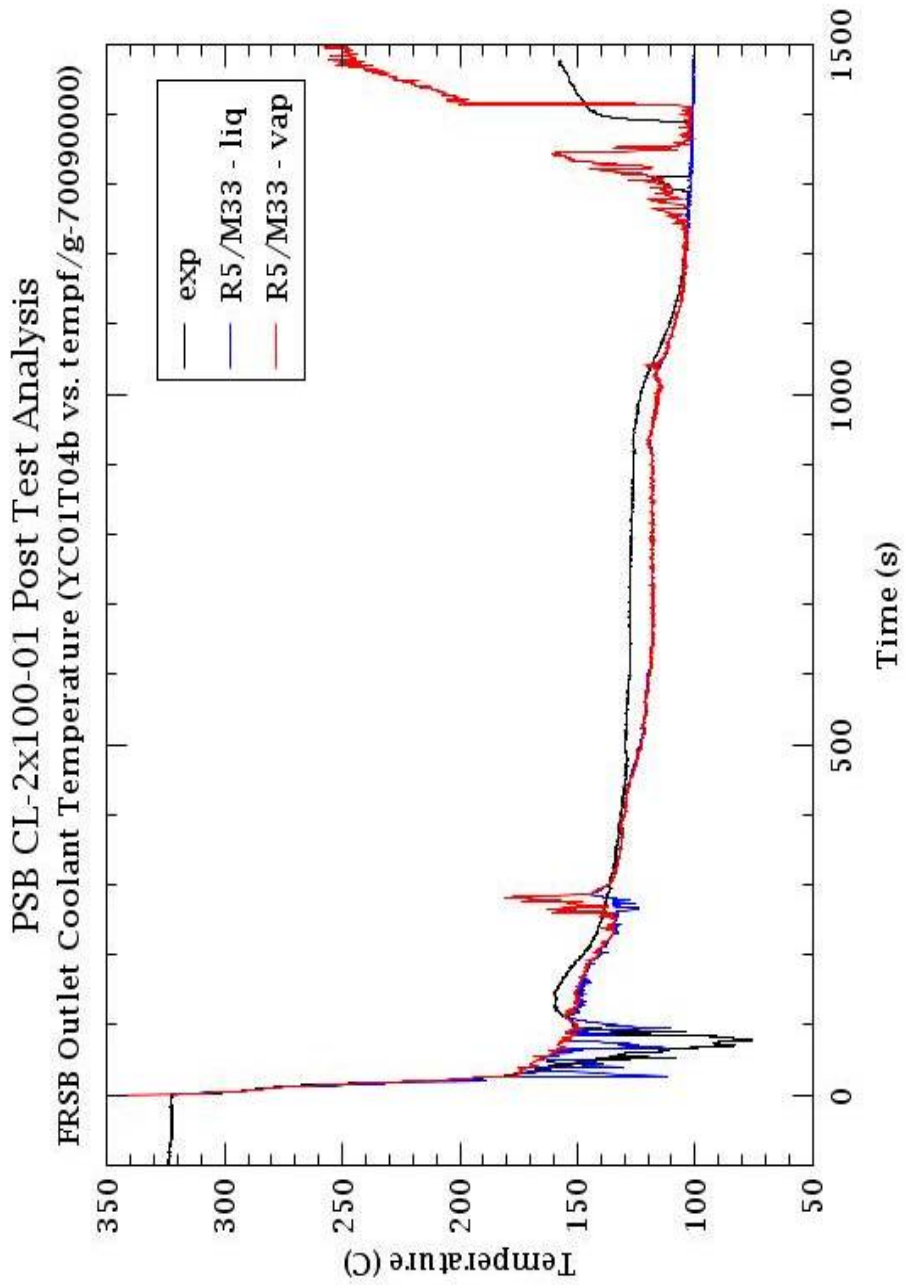
Fig. A.15: PSB-VVER Test-5a Core Simulator Outlet Coolant Temperature
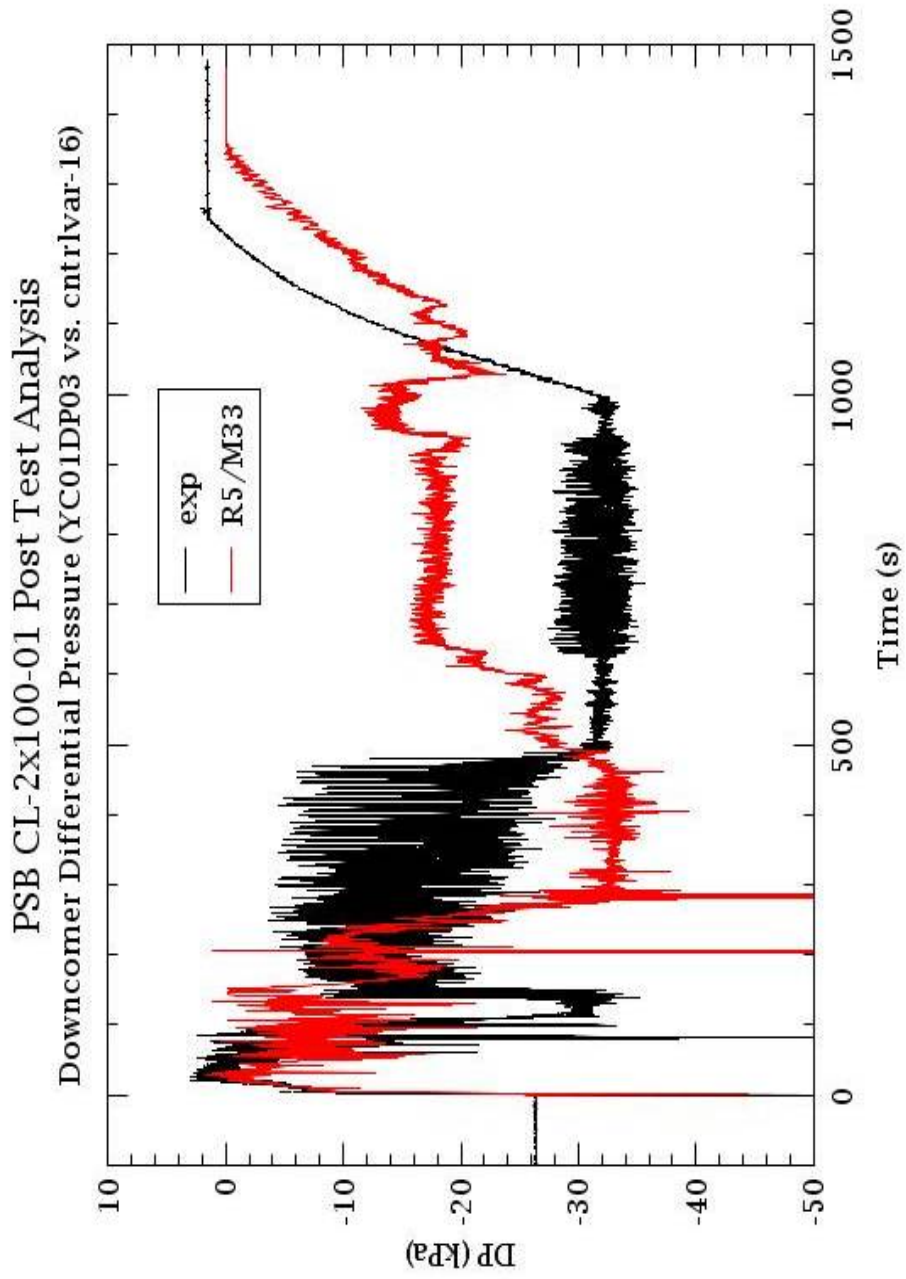
Fig. A.16: PSB-VVER Test-5a Downcomer Simulator (6310 – 2790 mm) Differential Pressure
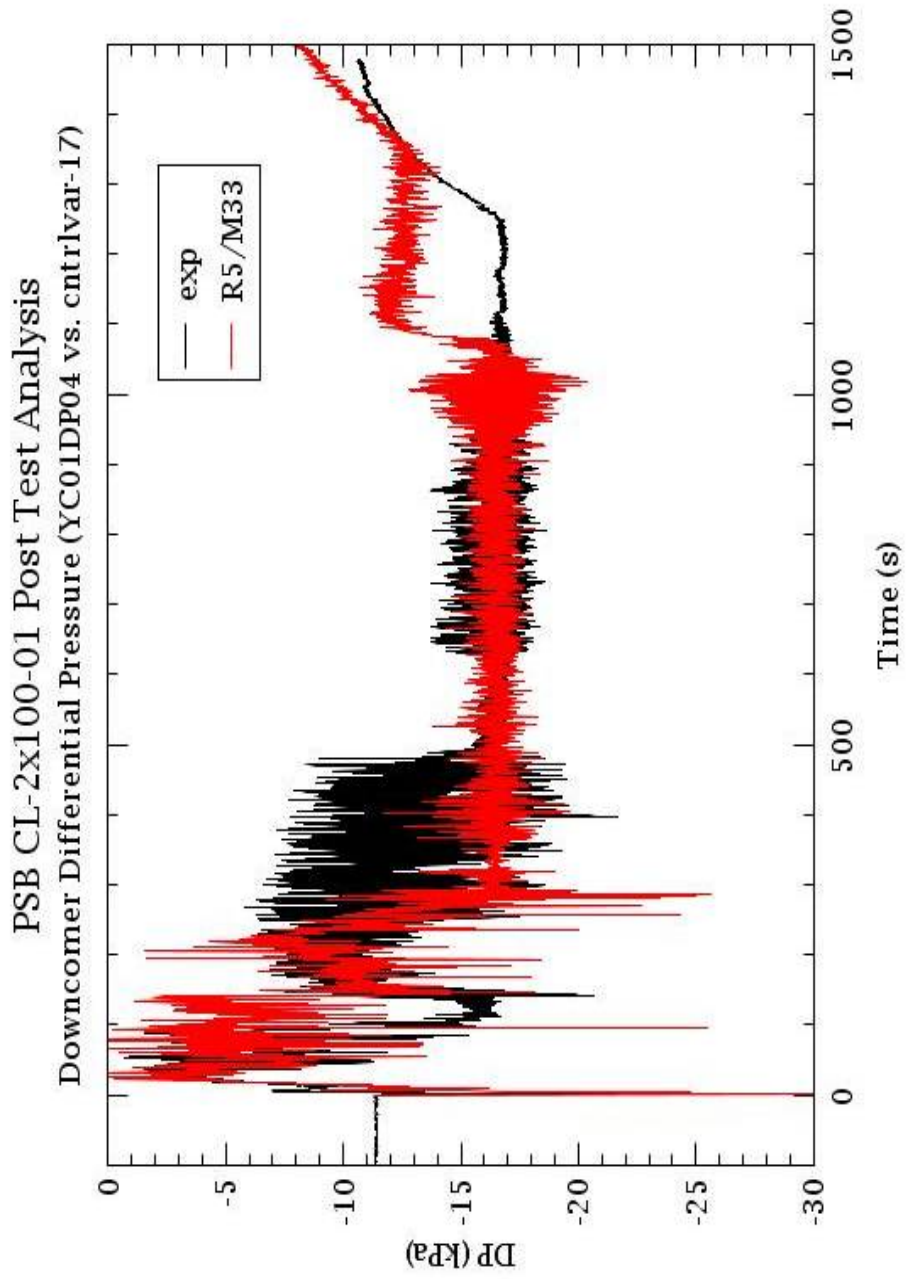
Fig. A.17: PSB-VVER Test-5a Downcomer Simulator (2790 – 1010 mm) Differential Pressure
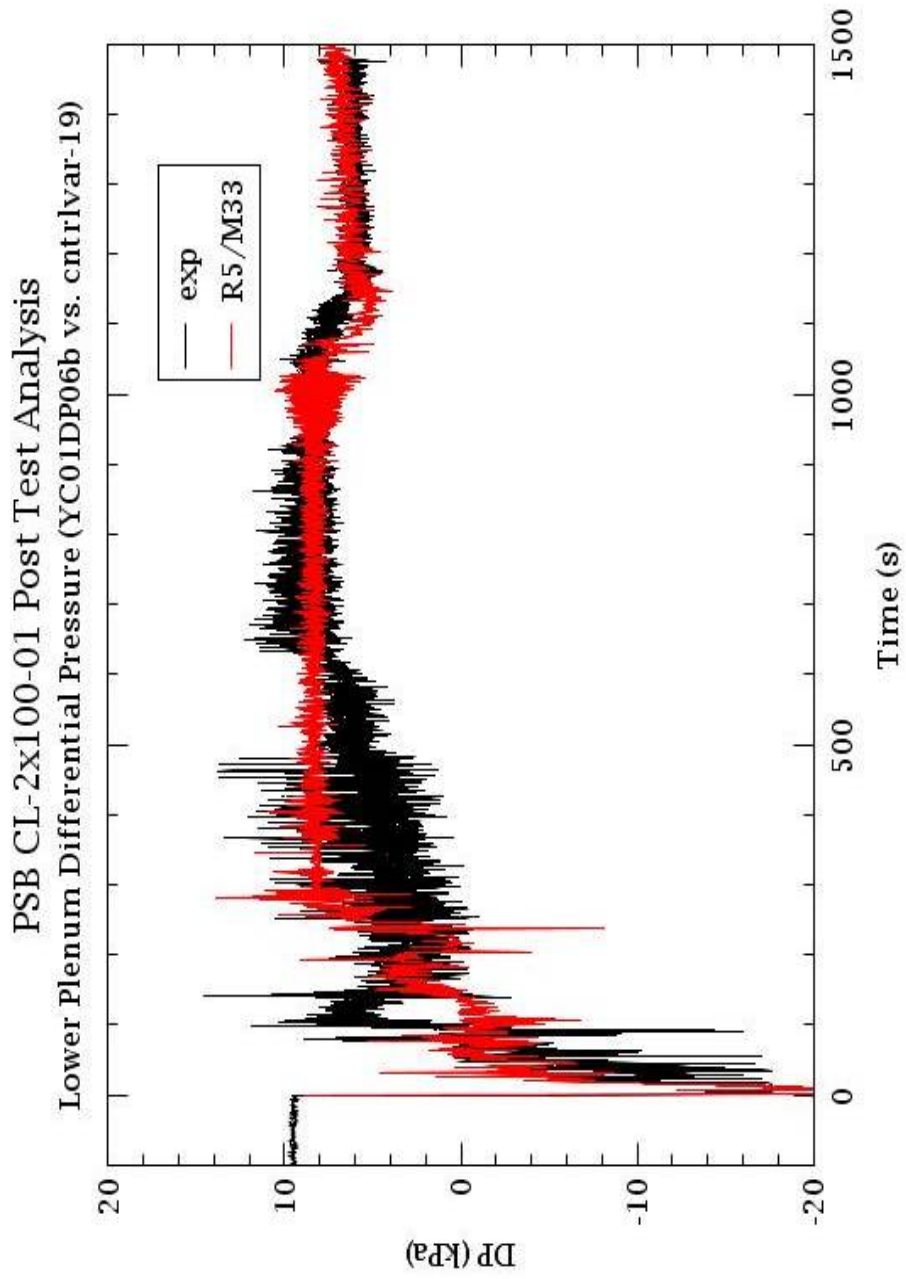
Fig. A.18: PSB-VVER Test-5a Lower Plenum Simulator (1010 – 1915 mm) Differential Pressure
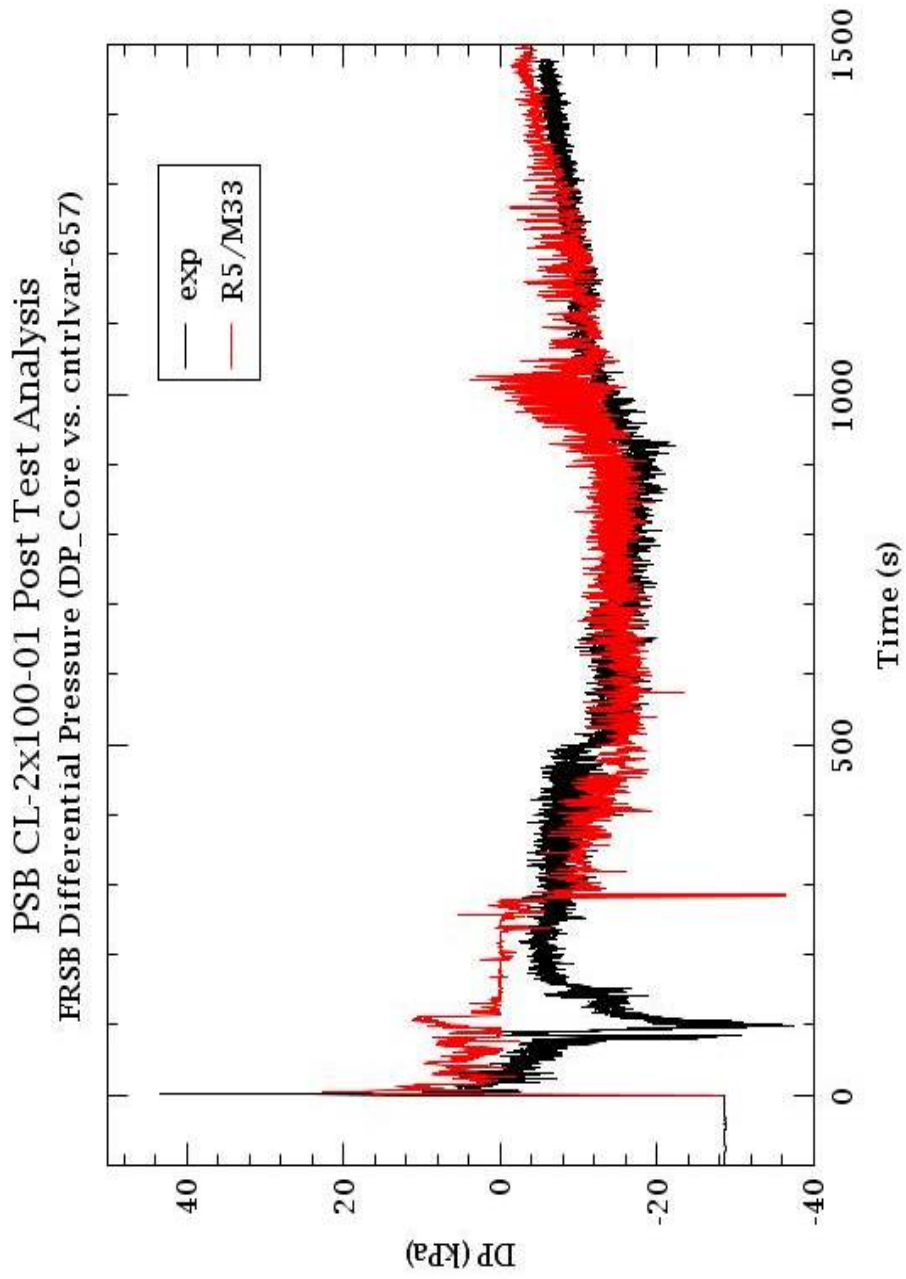
Fig. A.19: PSB-VVER Test-5a Core Simulator (5440 – 1915 mm) Differential Pressure
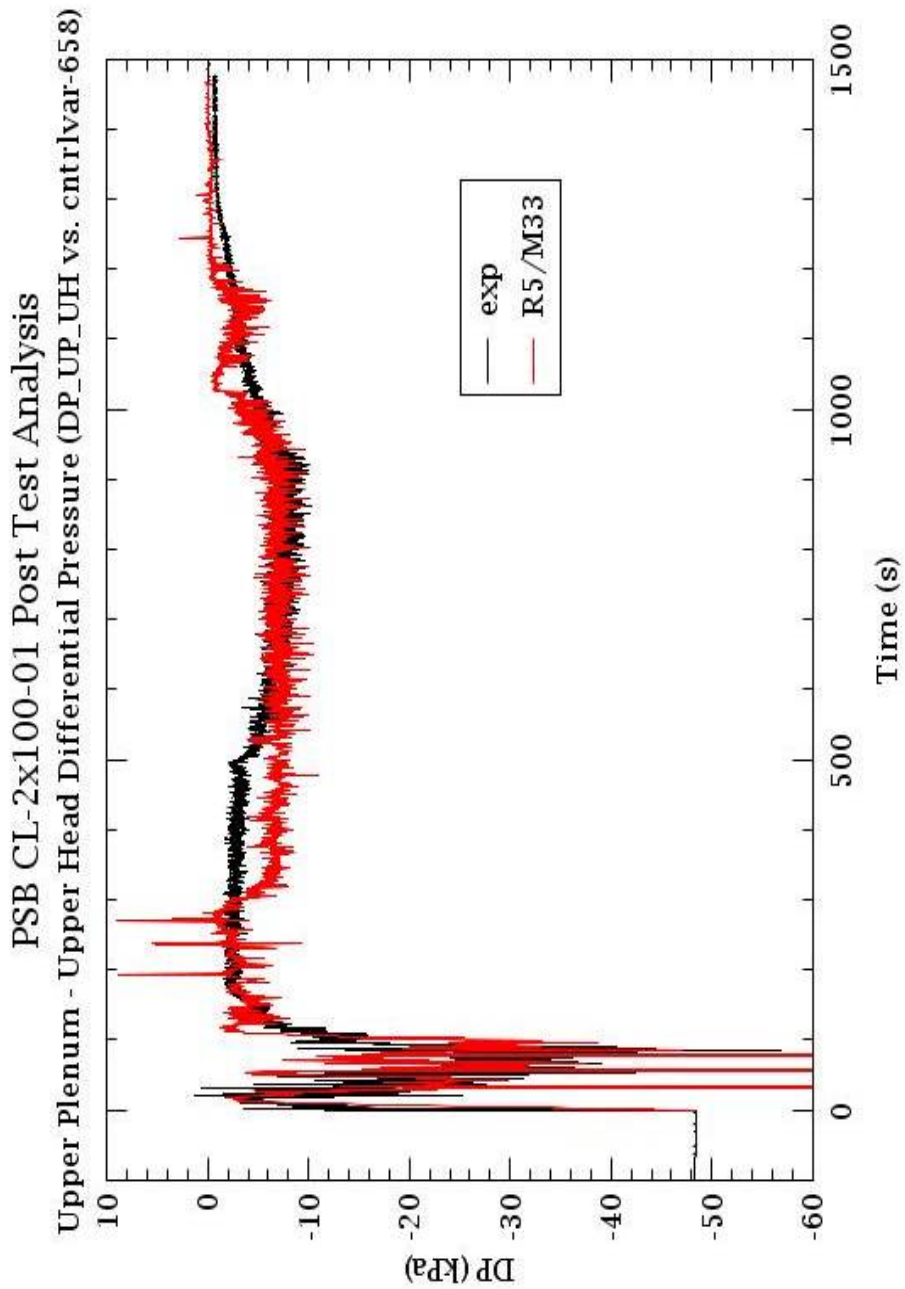
Fig. A.20: PSB-VVER Test-5a Upper Plenum & Upper Head Simulator (12525 – 5440 mm) Differential Pressure
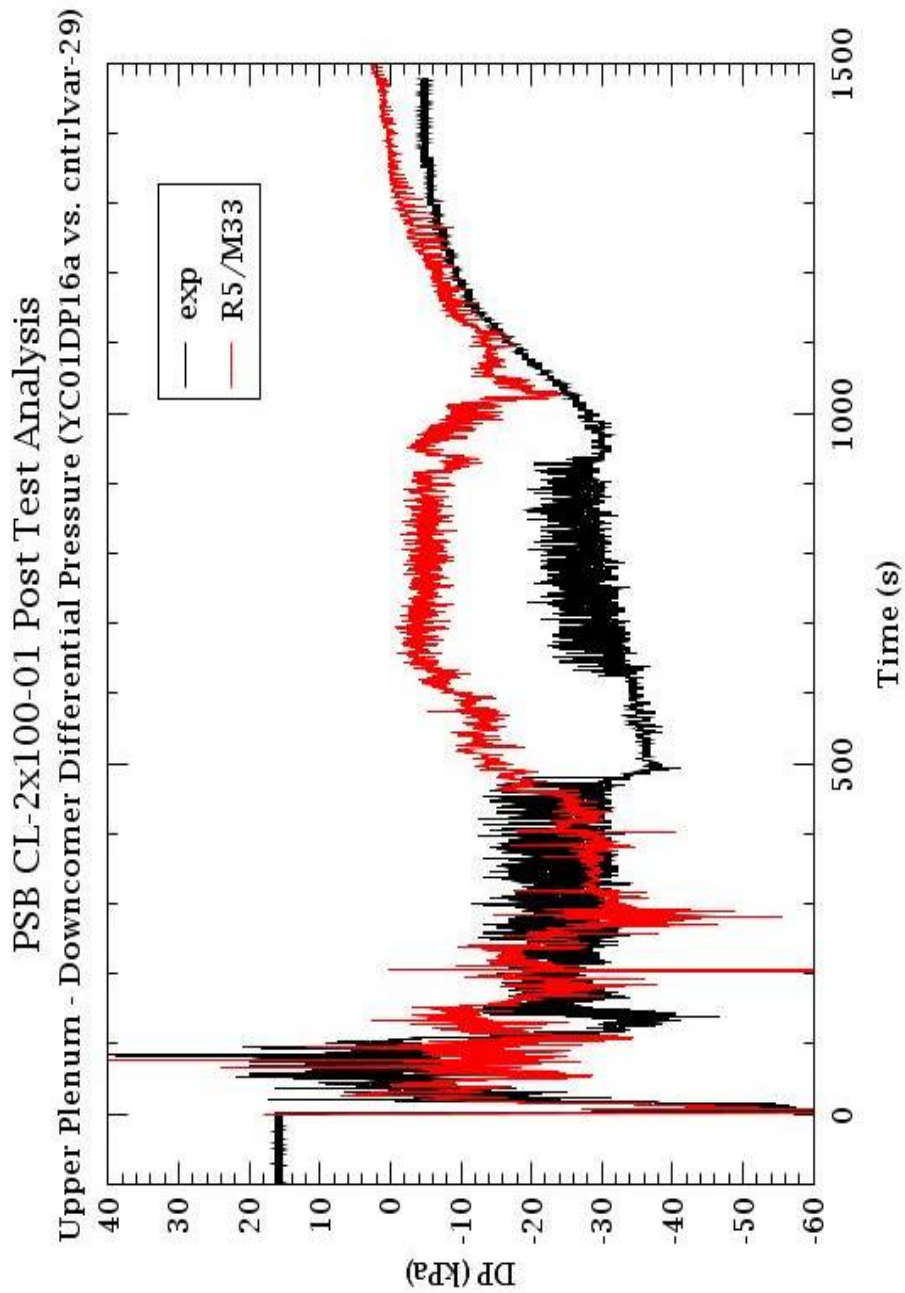
Fig. A.21: PSB-VVER Test-5a Downcomer Simulator to Upper Plenum Simulator (6870 – 8650 mm) Differential Pressure
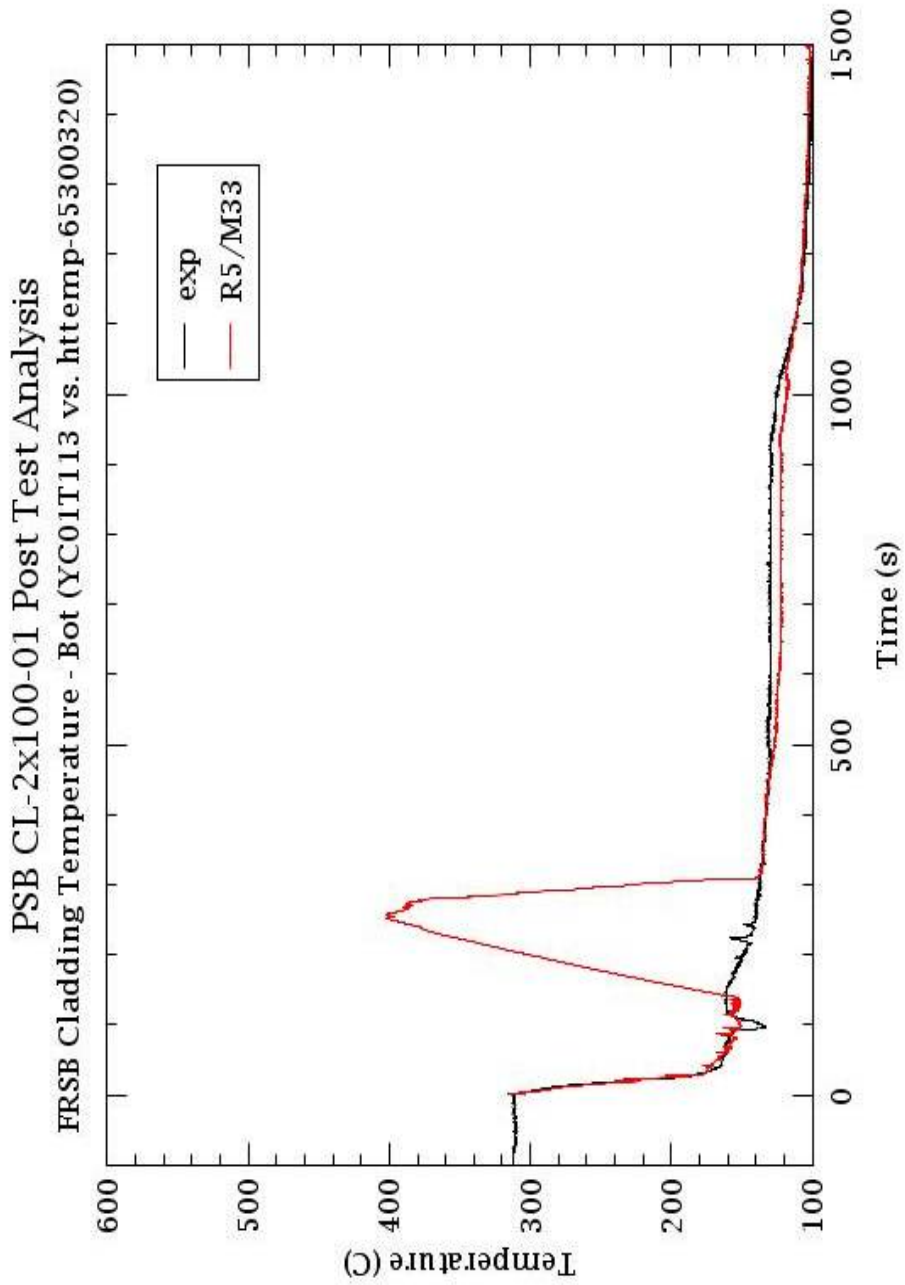
Fig. A.22: PSB-VVER Test-5a FRSB Bottom Third Cladding Temperature
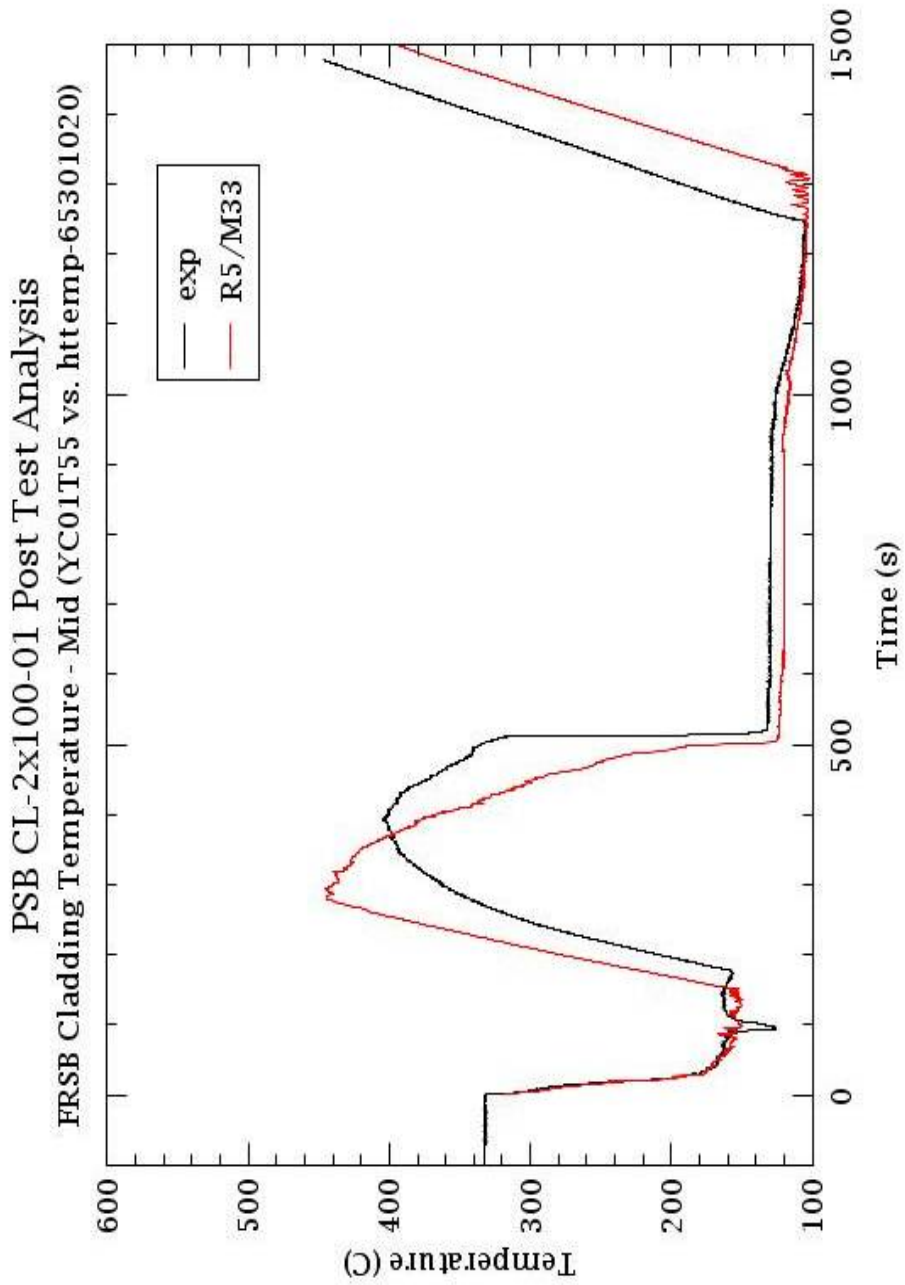
Fig. A.23: PSB-VVER Test-5a FRSB Middle Third Cladding Temperature
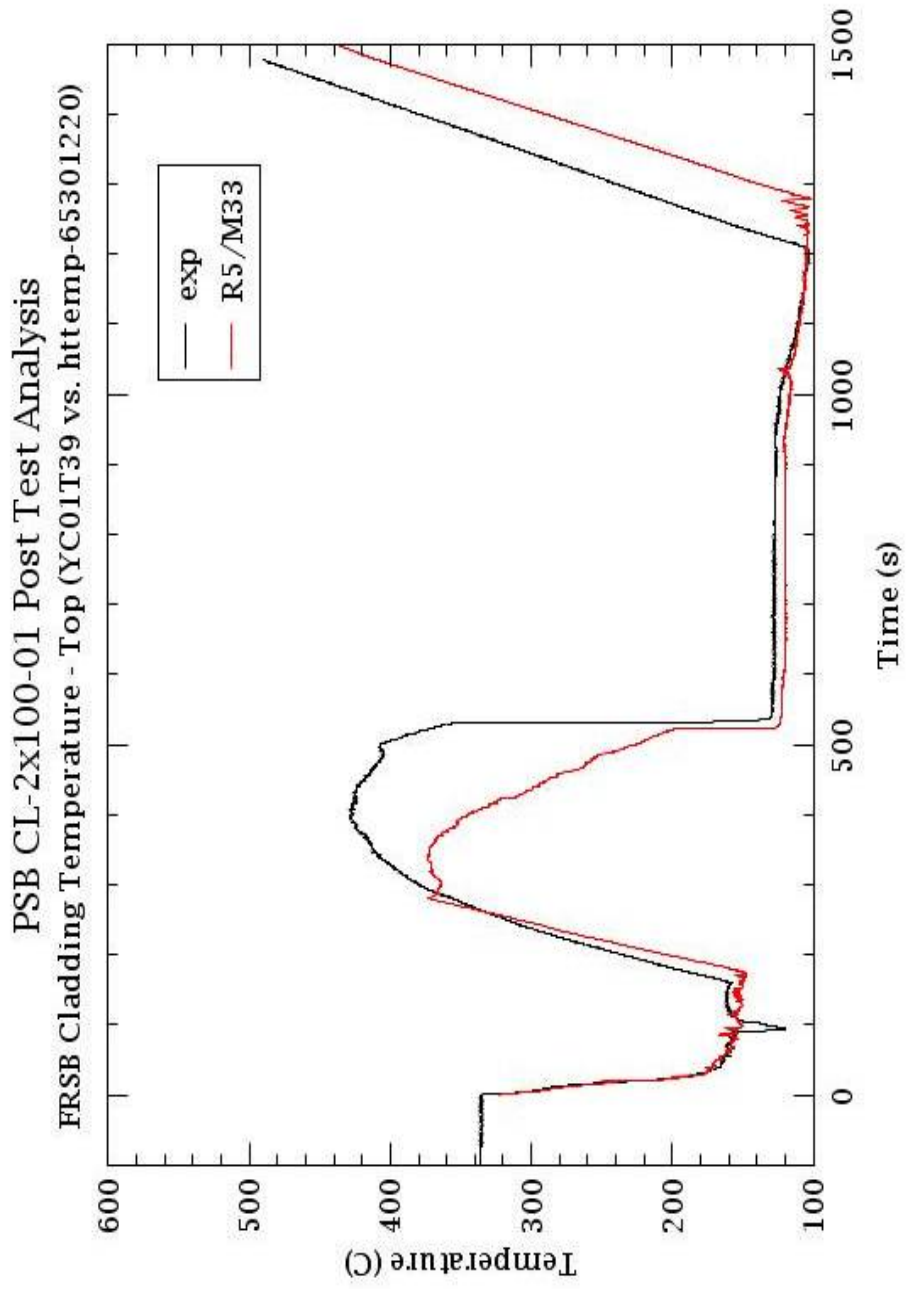
Fig. A.24: PSB-VVER Test-5a FRSB Top Third Cladding Temperature
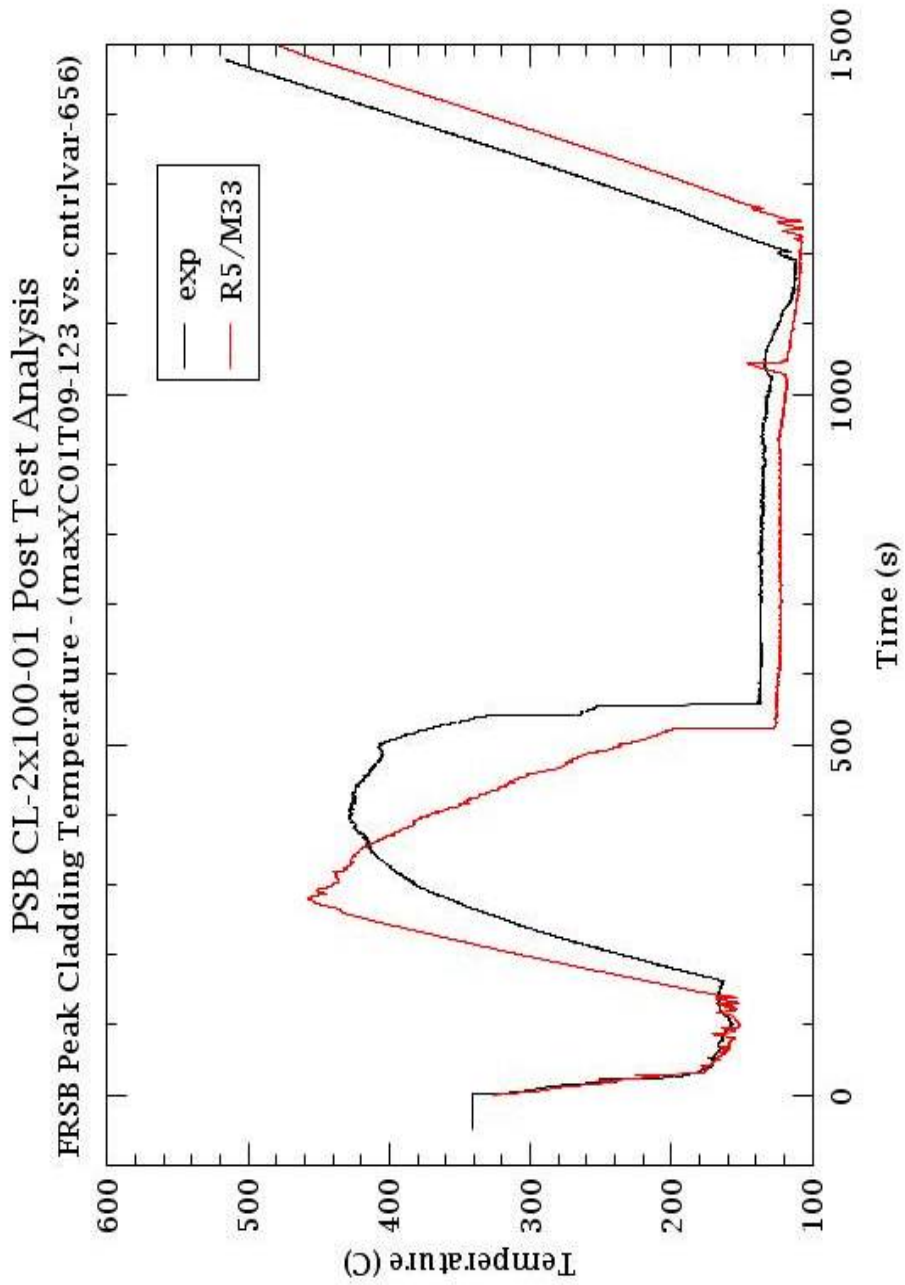
Fig. A.25: PSB-VVER Test-5a FRSB Peak Cladding Temperature

APPENDIX B

List of Figures

115

Fig. B.1 PSB-VVER Test-5a measured data: pressures in upper plenum (UPP), pressurizer (PRZ), accumulator (ACC), steam generator (SG), core power(N) and primary circuit mass (PCM).

Fig. B.2. PSB-VVER Test-5a measured data: maximum cladding temperature (maxT), primary coolant mass (PCM) and integrated break flow (IBF).
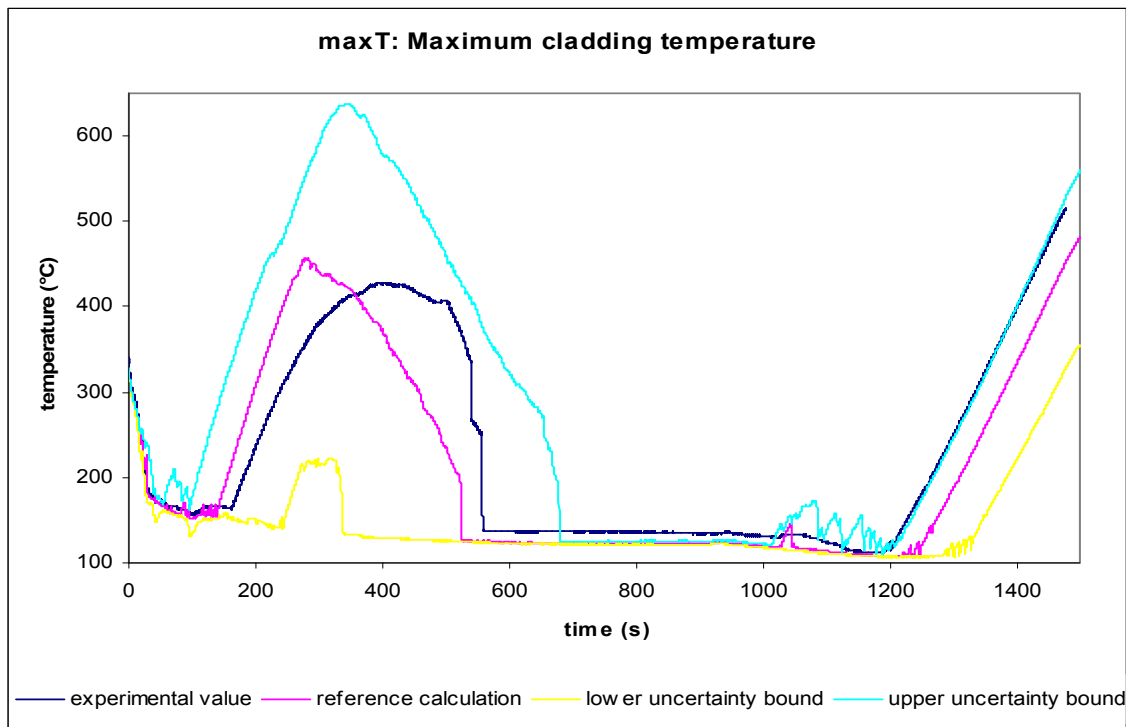
Fig. B.3. Uncertainty analysis for the maximum cladding temperature (maxT).

117
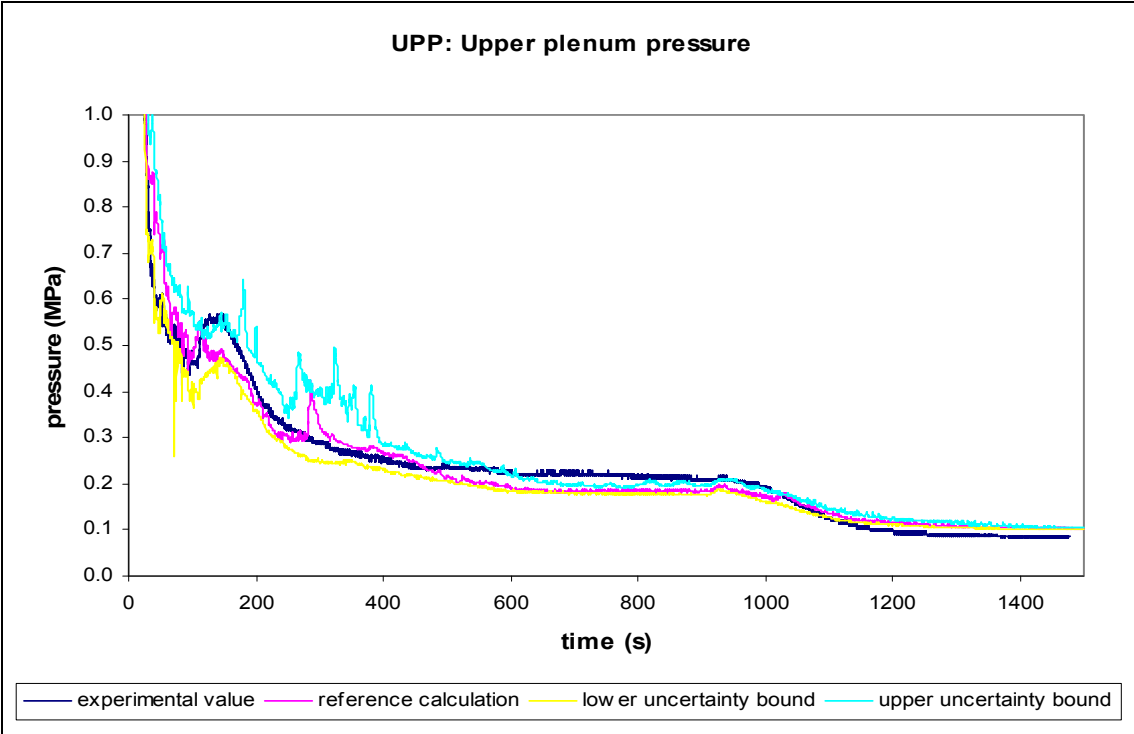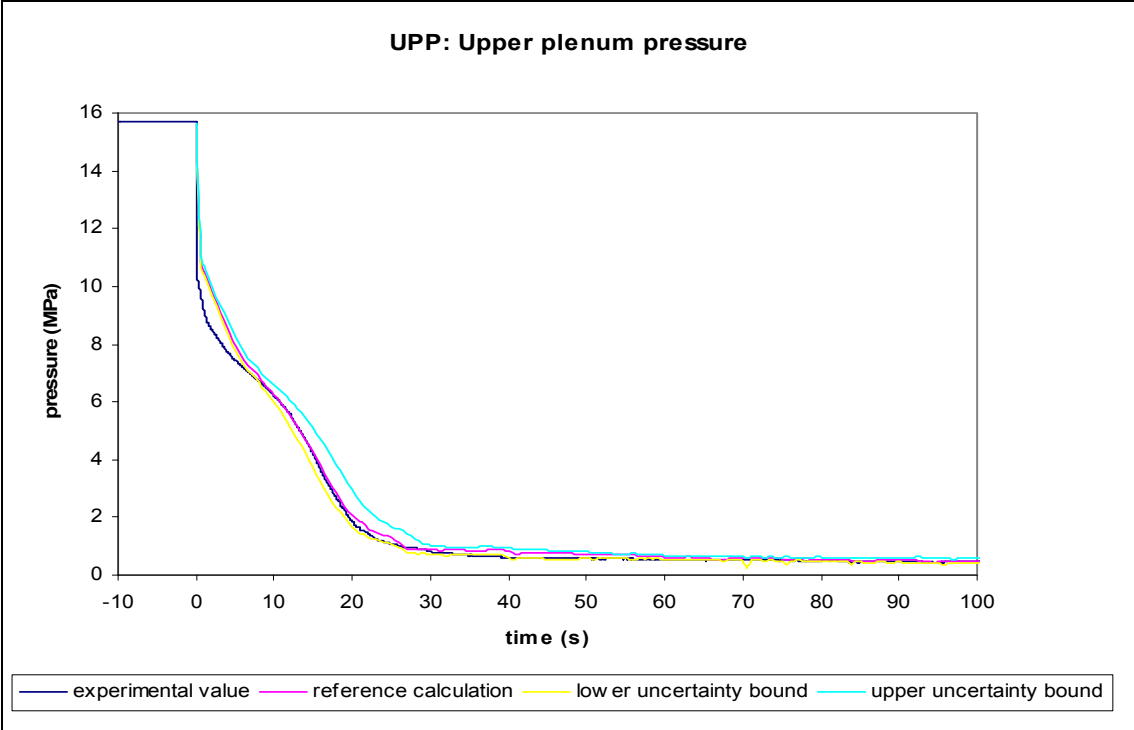
Fig. B.4. Uncertainty analysis for the upper plenum pressure (UPP).
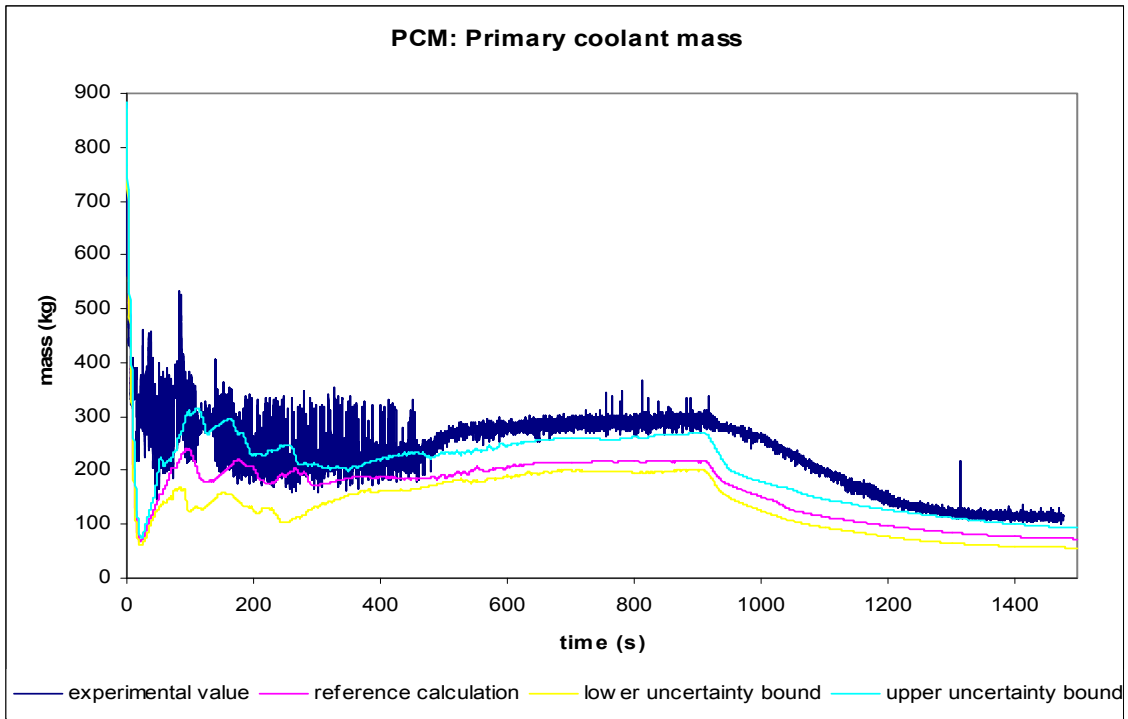
Fig. B.5. Uncertainty analysis for the primary coolant mass (PCM).
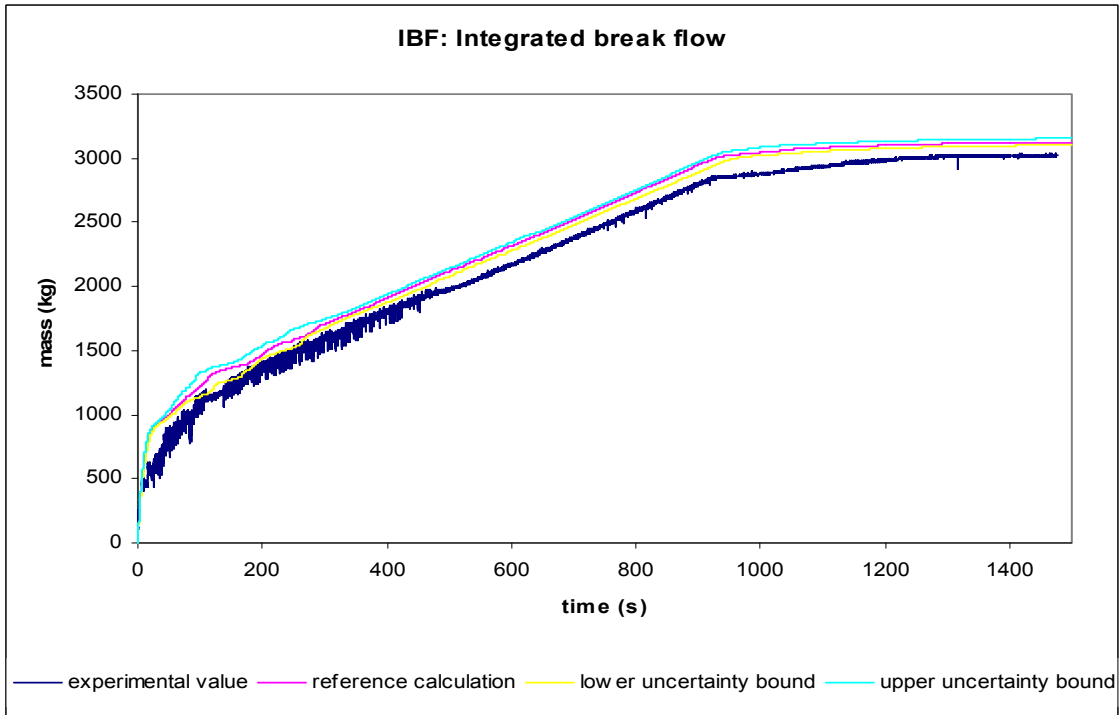
Fig. B.6. Uncertainty analysis for theintegrated break flow (IBF).
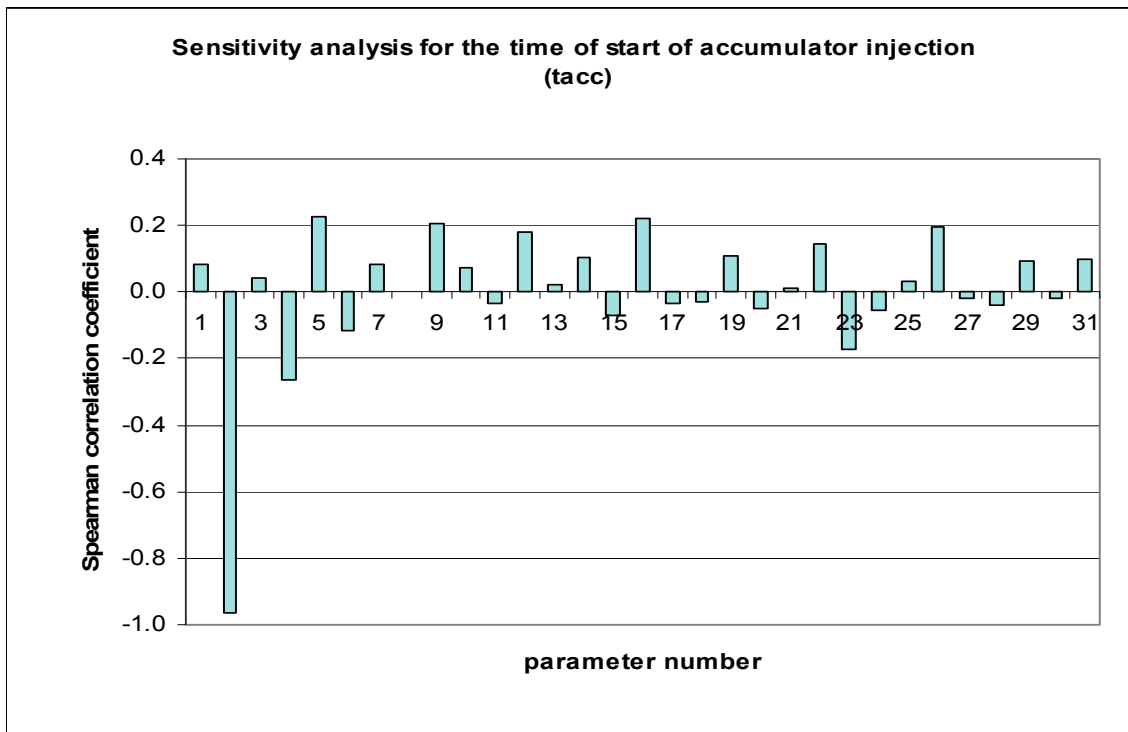
Fig. B.7. Influence on the accumulator injection time (t$_{acc}$) per uncertain input parameter.
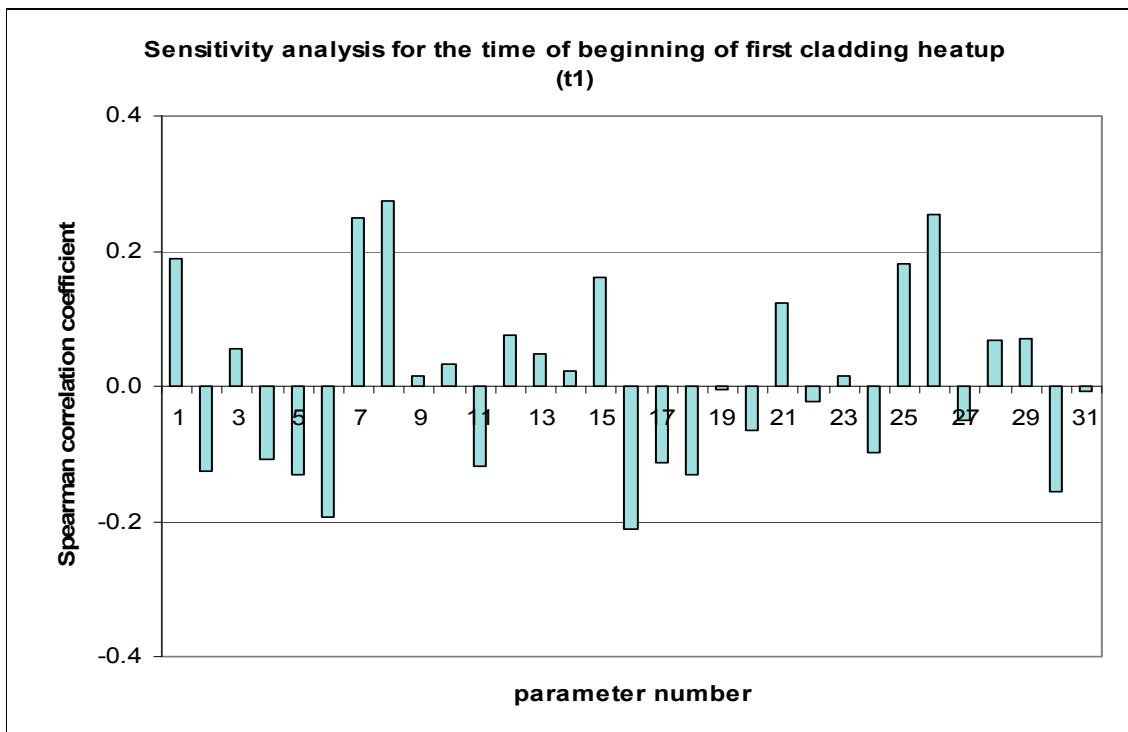
Fig. B.8. Influence on the cladding first overheating time (t$_1$) per uncertain input parameter.
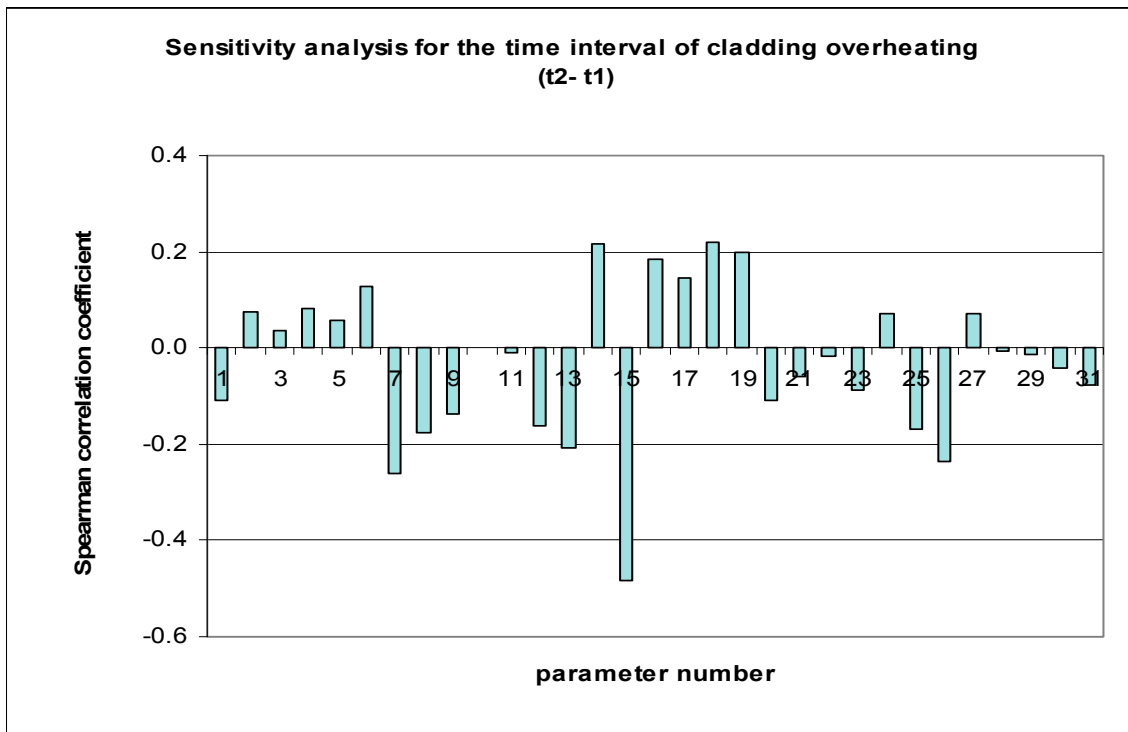
Fig. B.9. Influence on the cladding first overheating time interval (t_2 - t_1) per uncertain input parameter.
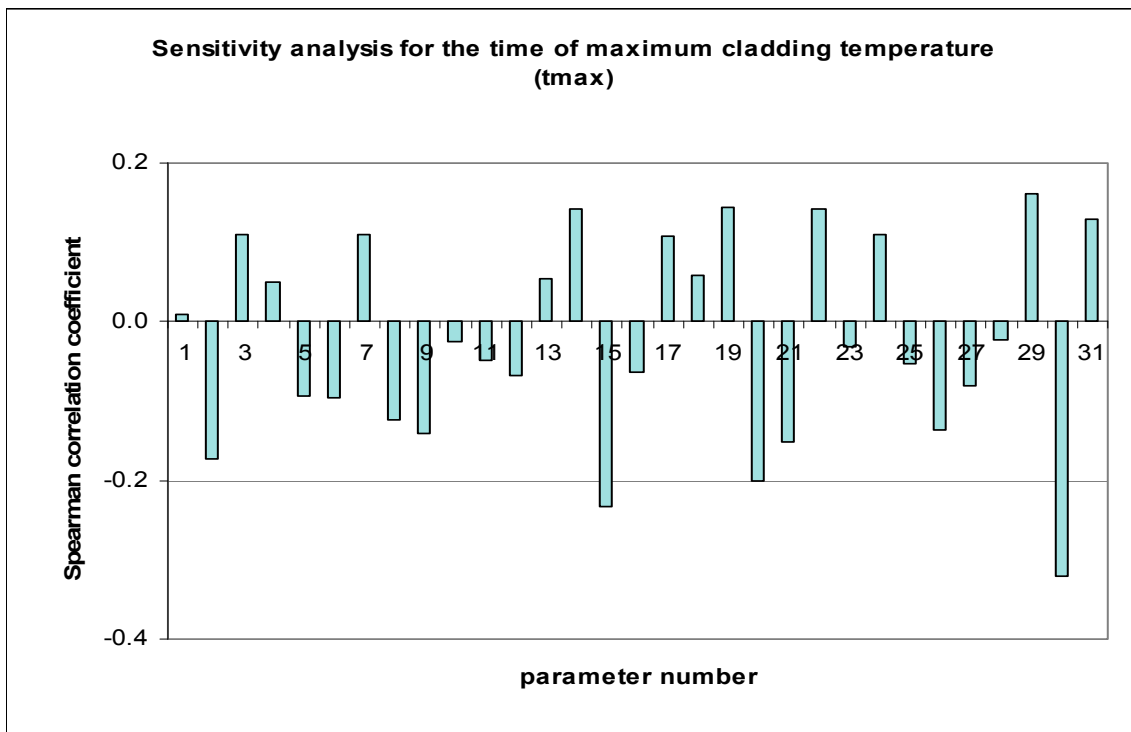
Fig. B.10. Influence on the maximum peak cladding temperature time (t_{max}) per uncertain input parameter.
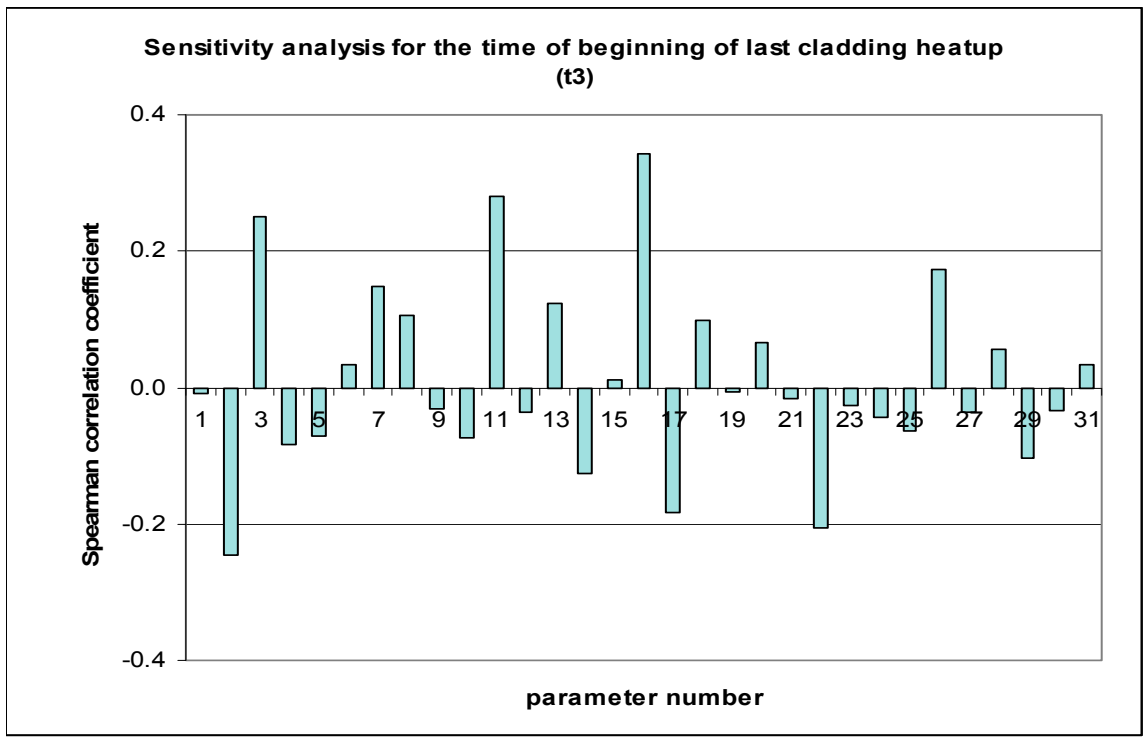
Fig. B.11. Influence on the complete core quenching time (t₃) per uncertain input parameter.
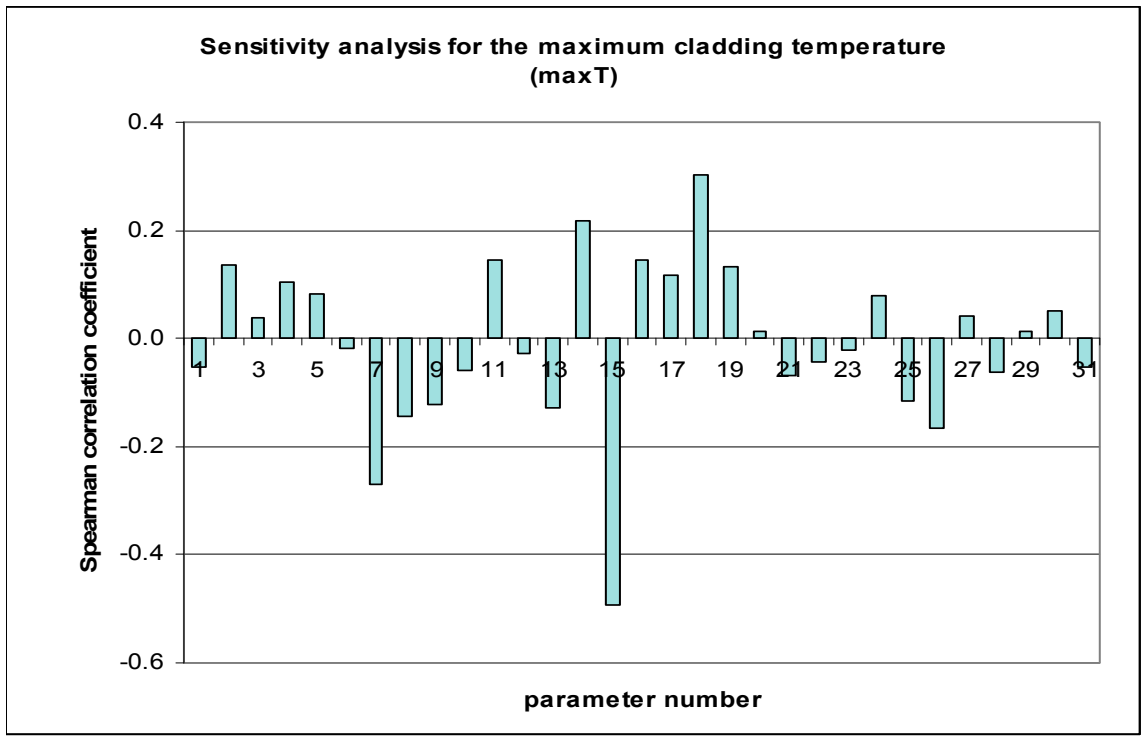
Fig. B.12. Influence on the maximum peak cladding temperature maxT per uncertain input parameter.
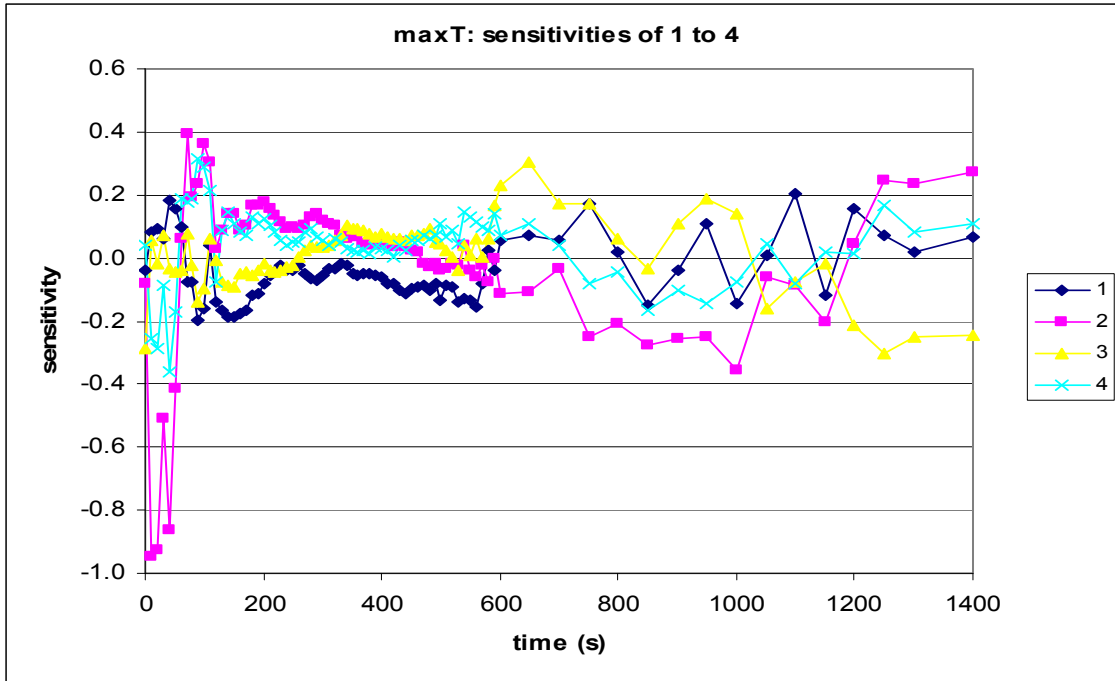
Fig. B.13. Sensitivity results for the maximum peak cladding temperature (maxT) for the parameters 1 to 4: Spearman's correlation coefficients.
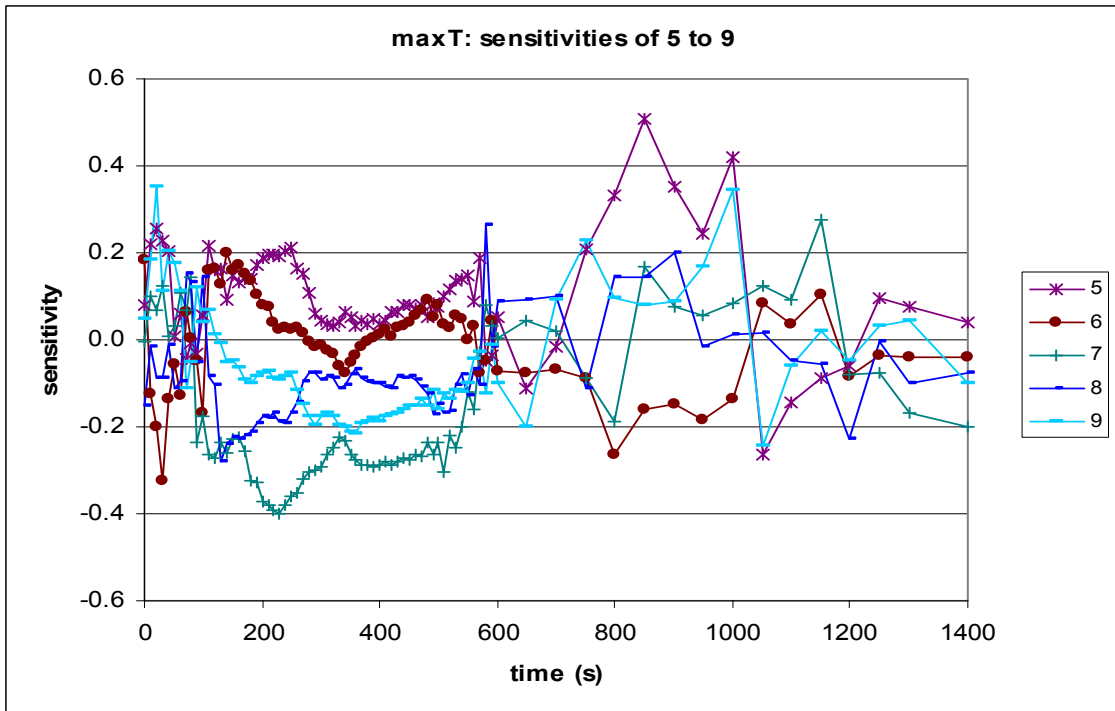
Fig. B.14. Sensitivity results for the maximum peak cladding temperature (maxT) for the parameters 5 to 9: Spearman's correlation coefficients.
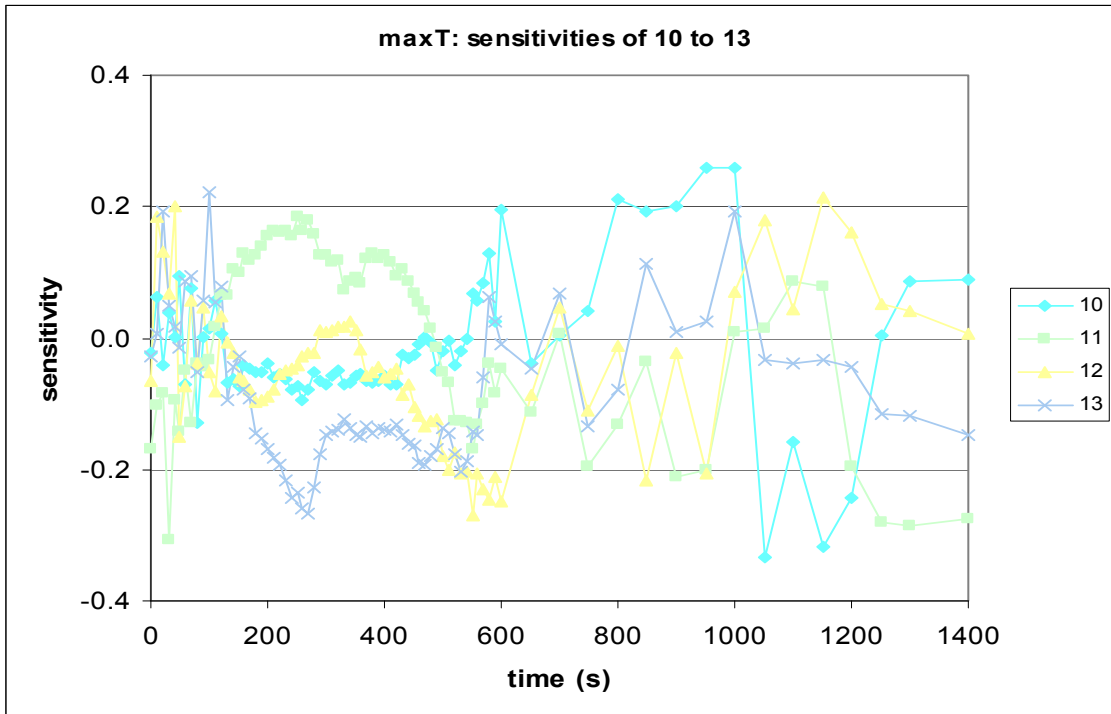
Fig. B.15. Sensitivity results for the maximum peak cladding temperature (maxT) for the parameters 10 to 13: Spearman's correlation coefficients.
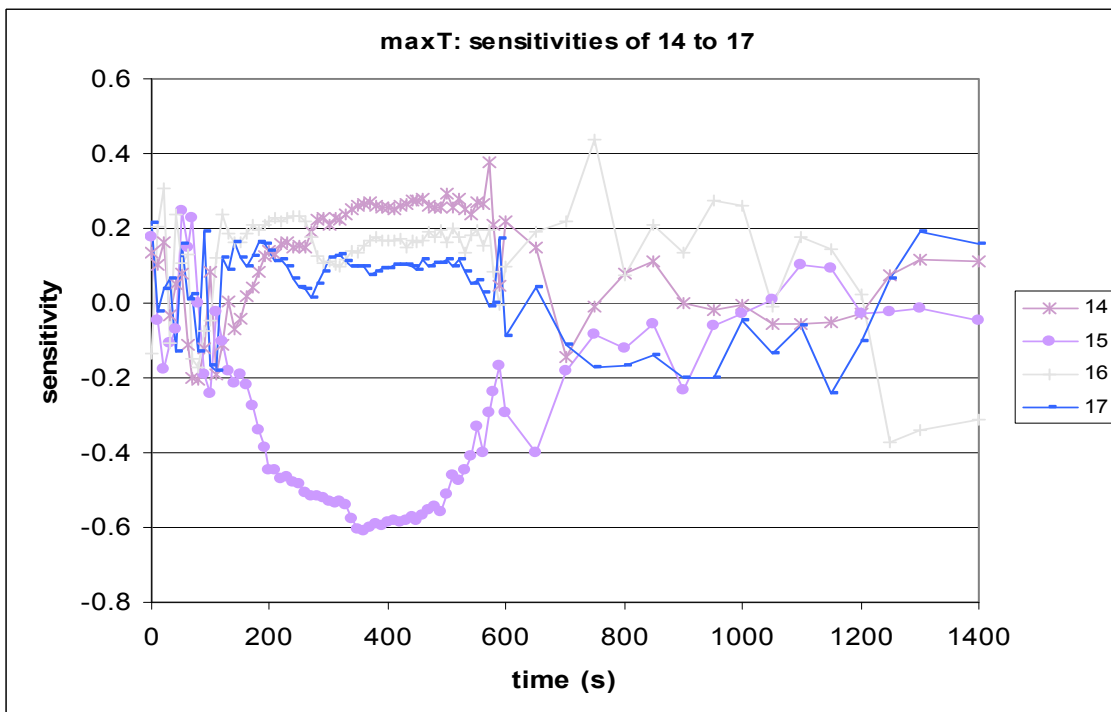
Fig. B.16. Sensitivity results for the maximum peak cladding temperature (maxT) for the parameters 14 to 17: Spearman's correlation coefficients.
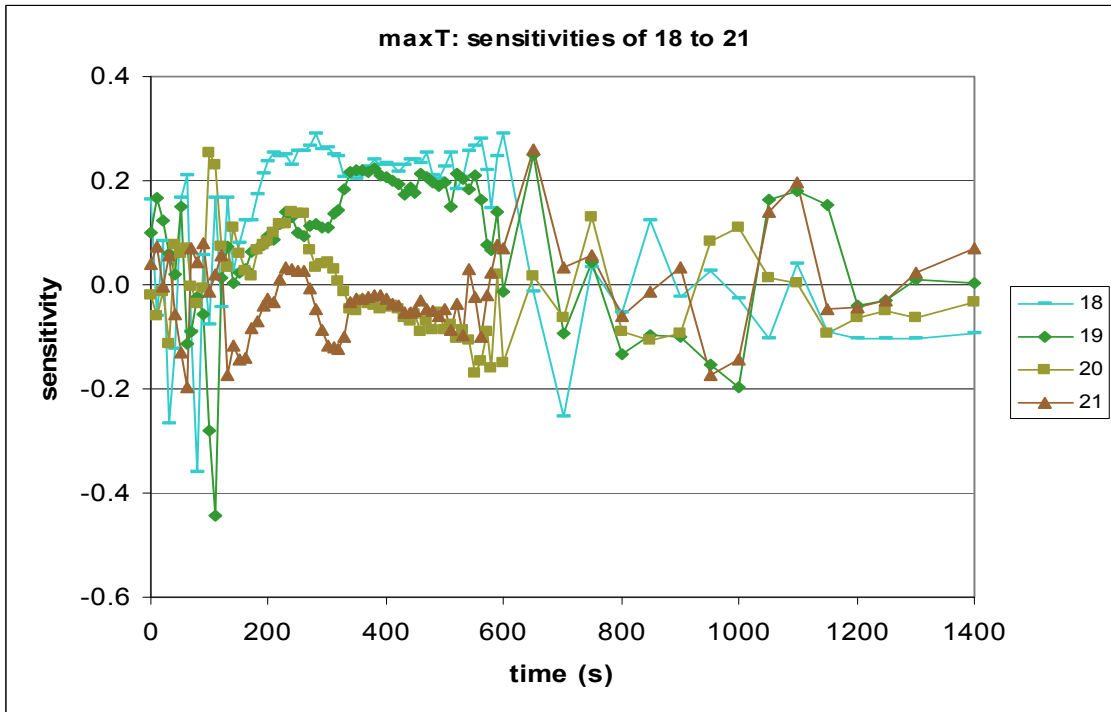
Fig. B.17. Sensitivity results for the maximum peak cladding temperature (maxT) for the parameters 18 to 21: Spearman's correlation coefficients.
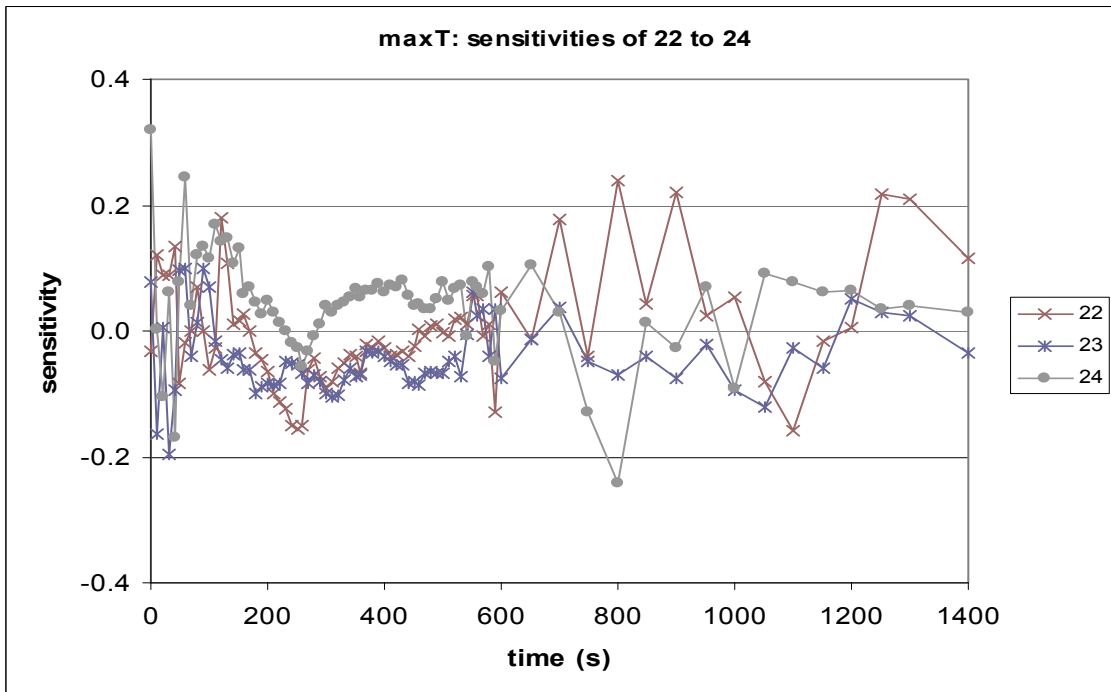
Fig. B.18. Sensitivity results for the maximum peak cladding temperature (maxT) for the parameters 22 to 24: Spearman's correlation coefficients.

125
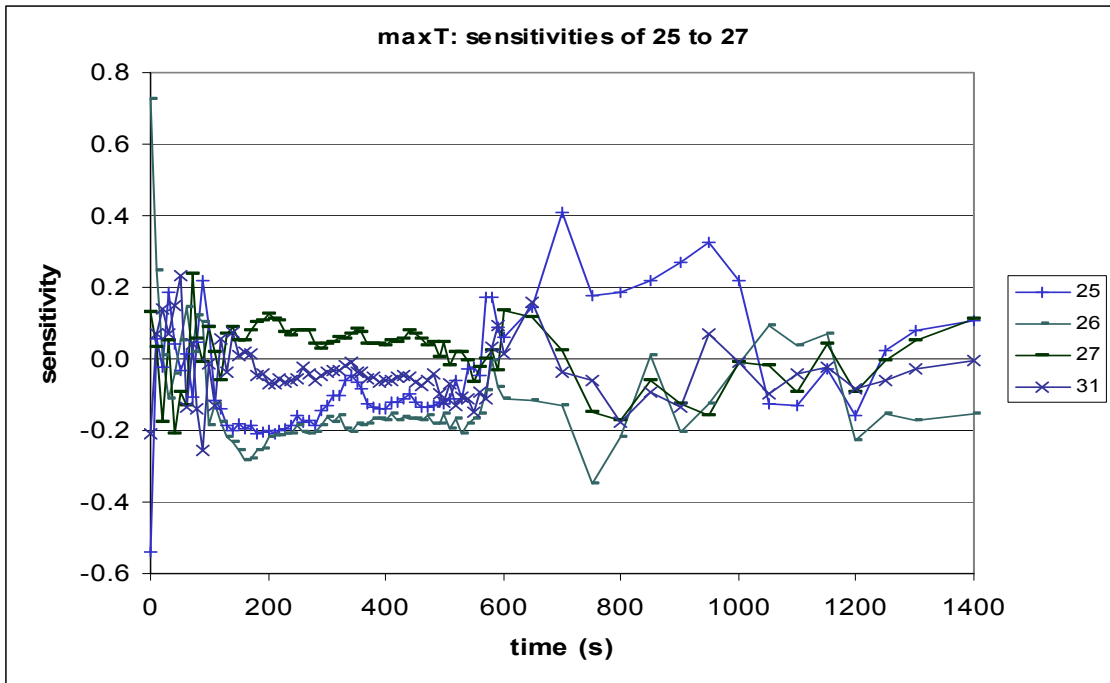
Fig. B.19. Sensitivity results for the maximum peak cladding temperature (maxT) for the parameters 25 to 27: Spearman's correlation coefficients.
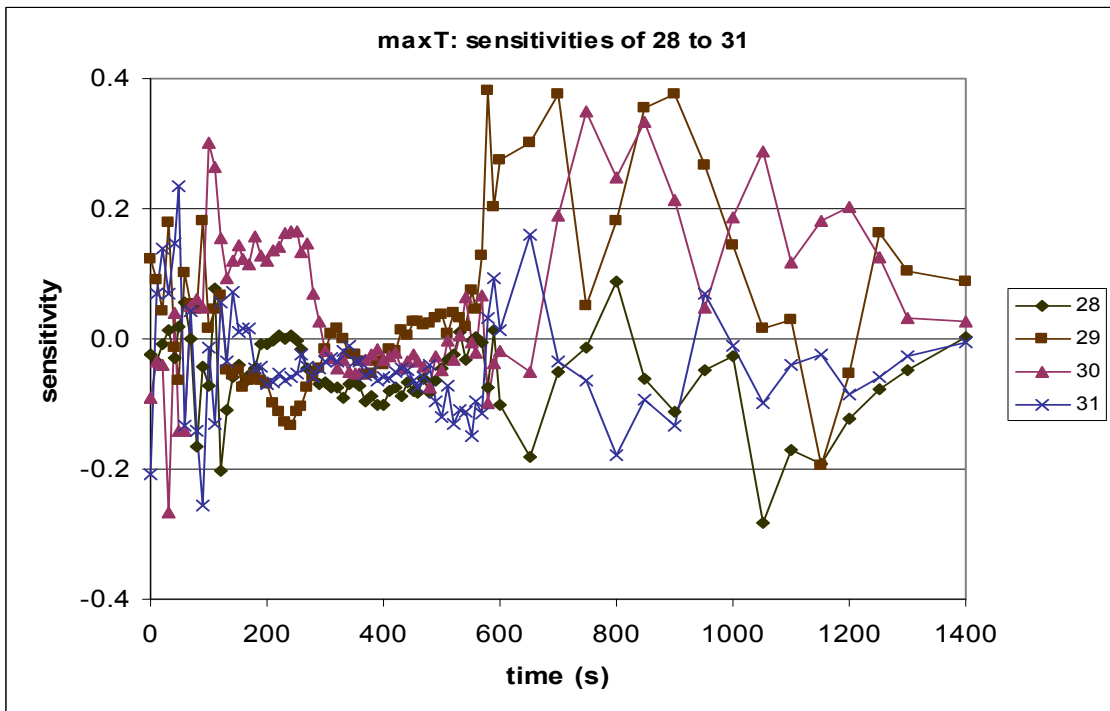
Fig. B.20. Sensitivity results for the maximum peak cladding temperature (maxT) for the parameters 28 to 31: Spearman's correlation coefficients.
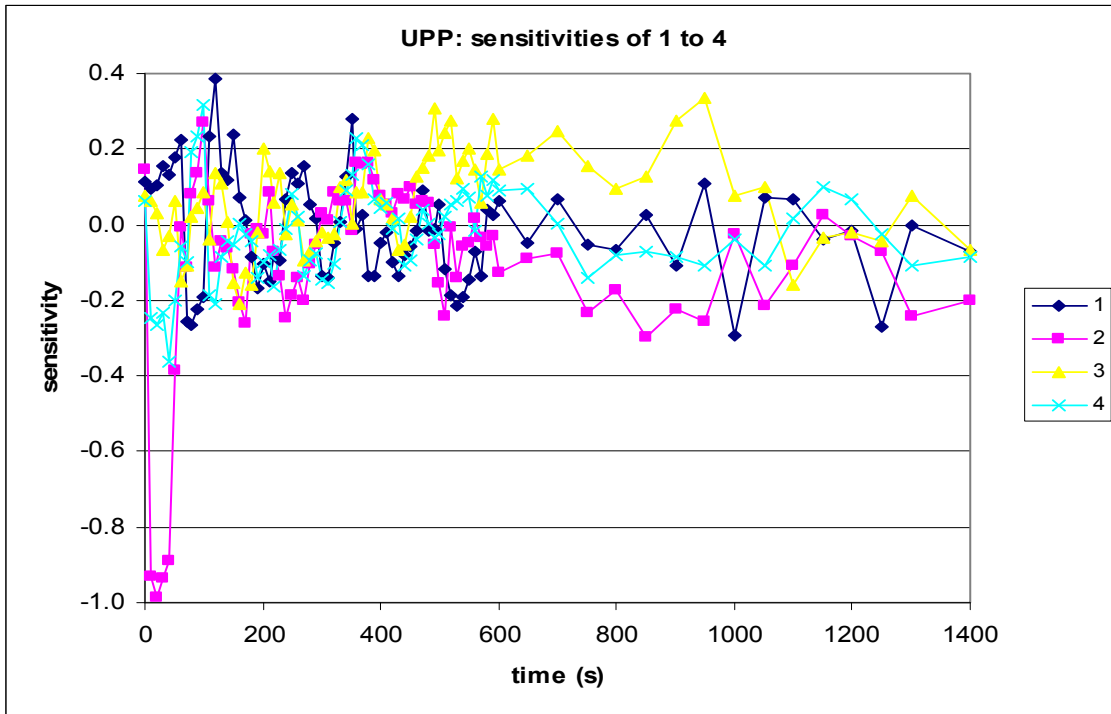
Fig. B.21. Sensitivity results for the upper plenum pressure (UPP) for the parameters 1 to 4: Spearman's correlation coefficients.
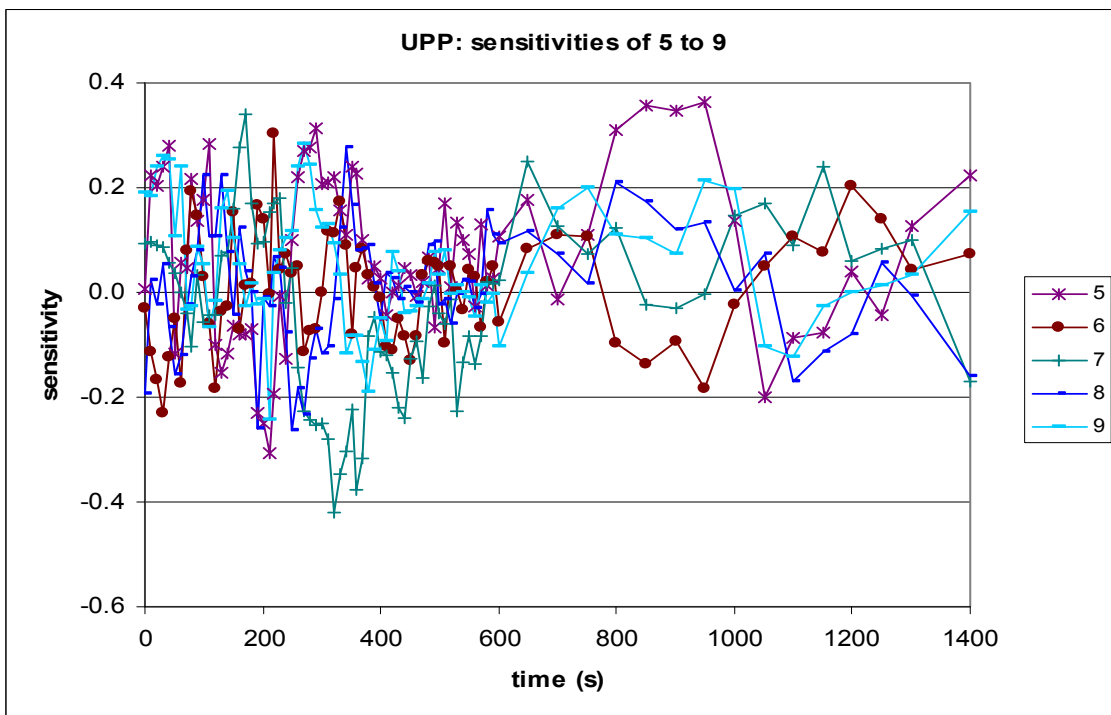
Fig. B.22. Sensitivity results for the upper plenum pressure (UPP) for the parameters 5 to 9: Spearman's correlation coefficients.
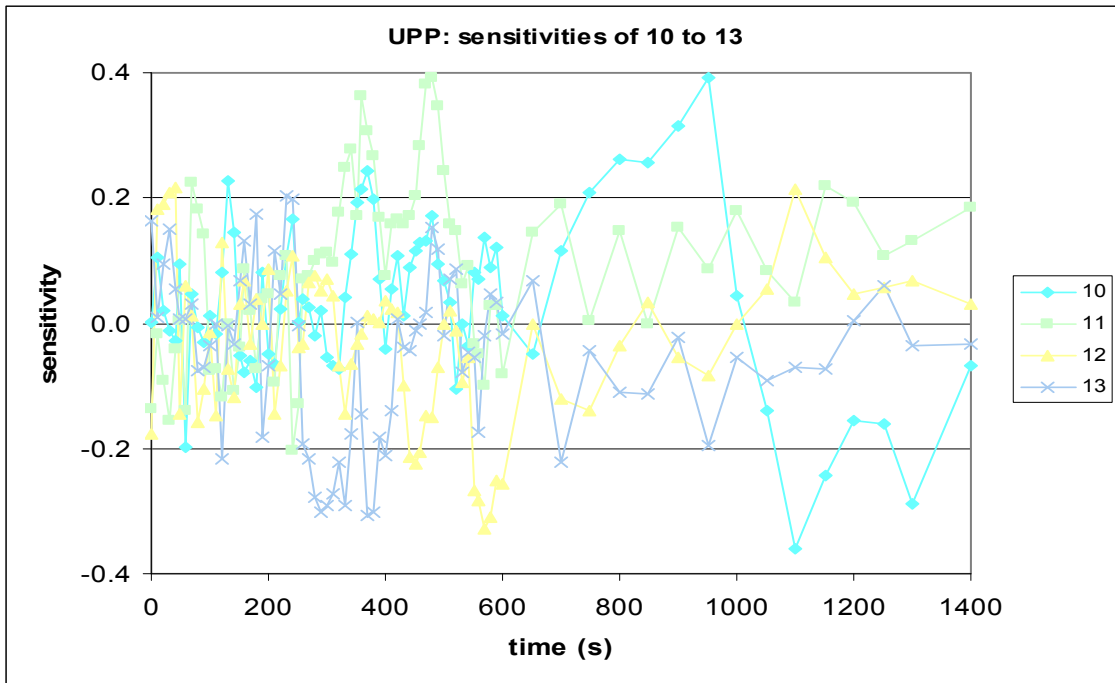
Fig. B.23. Sensitivity results for the upper plenum pressure (UPP) for the parameters 10 to 13: Spearman's correlation coefficients.
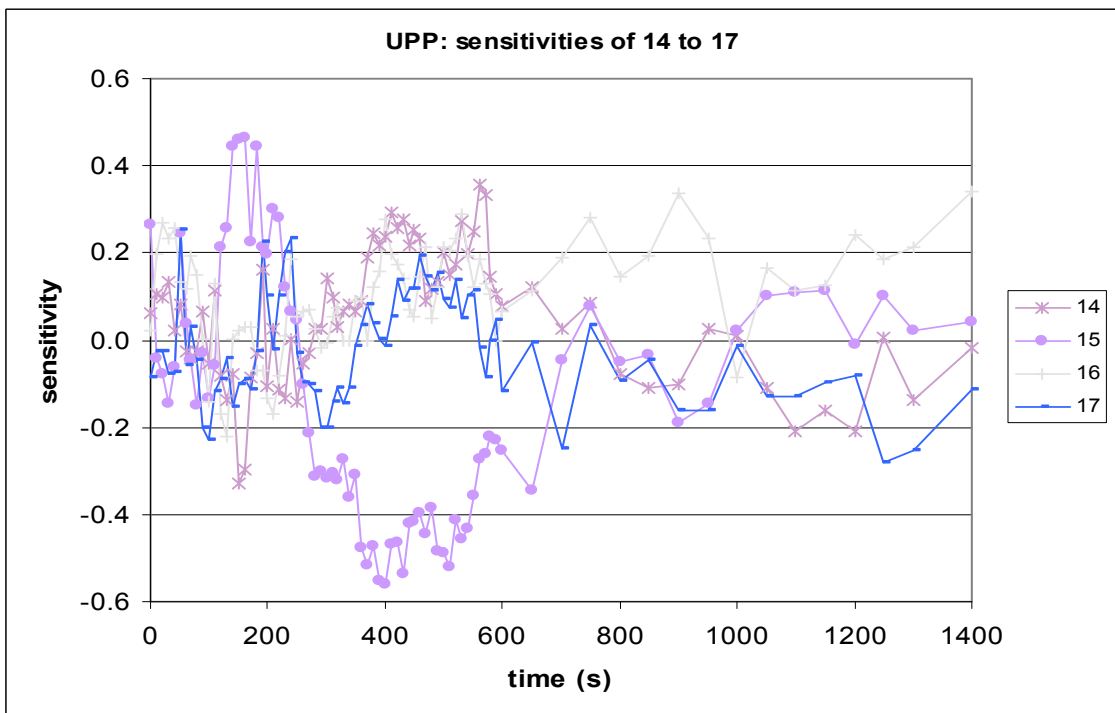
Fig. B.24. Sensitivity results for the upper plenum pressure (UPP) for the parameters 14 to 17: Spearman's correlation coefficients.
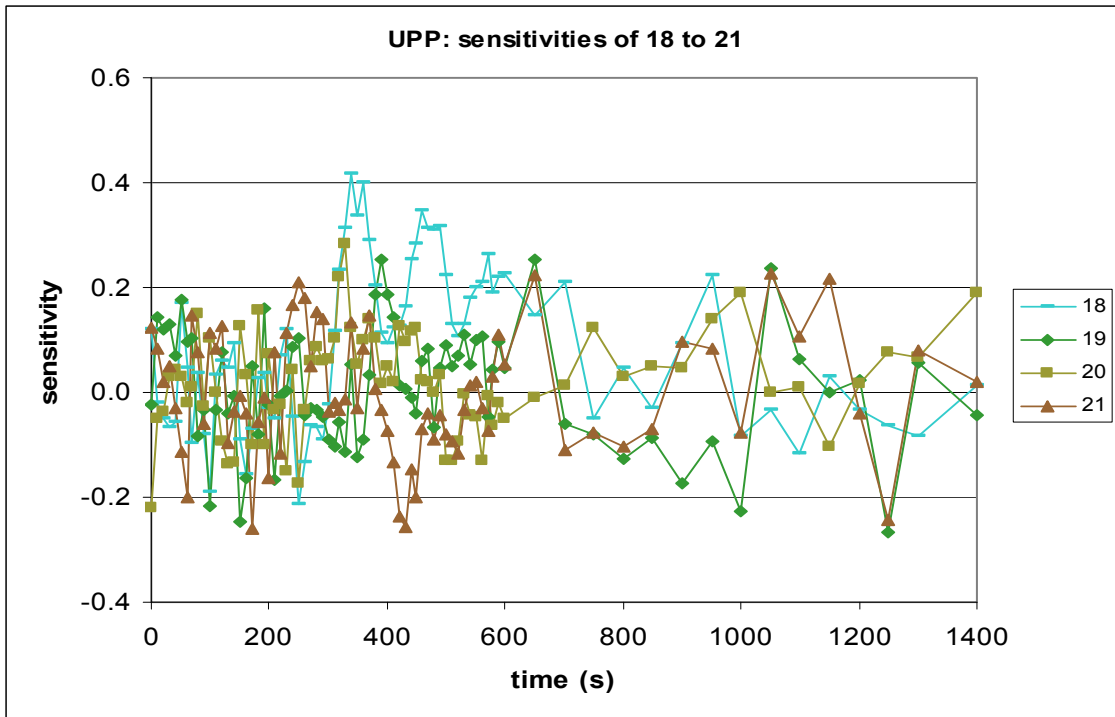
Fig. B.25. Sensitivity results for the upper plenum pressure (UPP) for the parameters 18 to 21: Spearman's correlation coefficients.
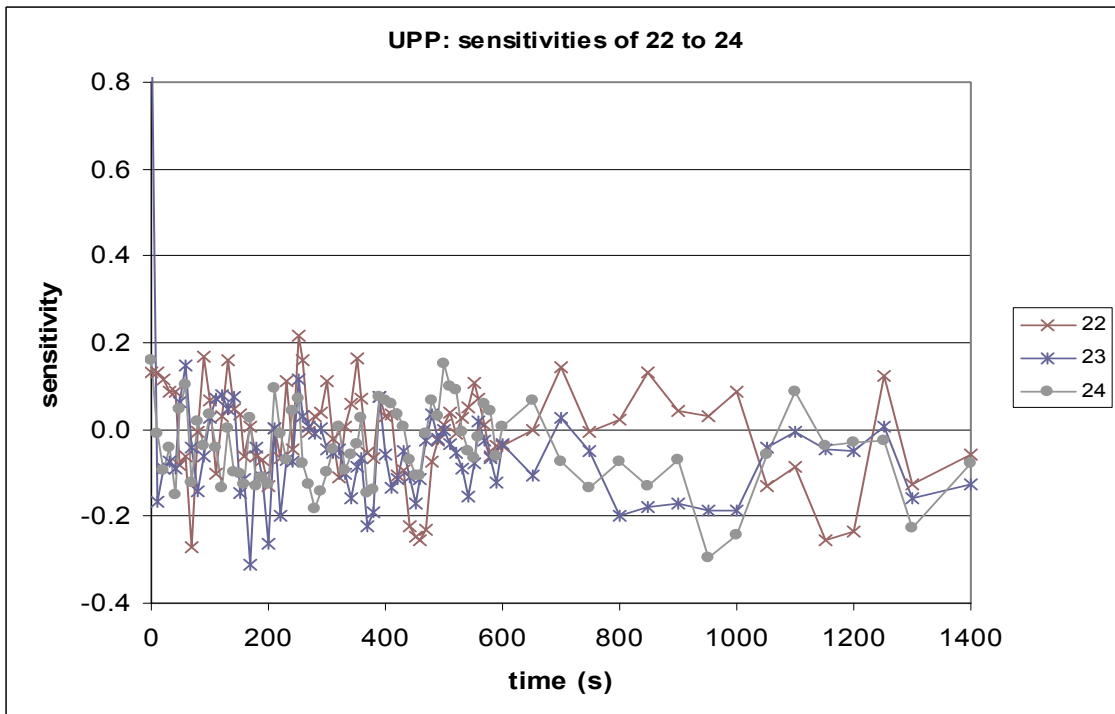
Fig. B.26. Sensitivity results for the upper plenum pressure (UPP) for the parameters 22 to 24: Spearman's correlation coefficients.

129
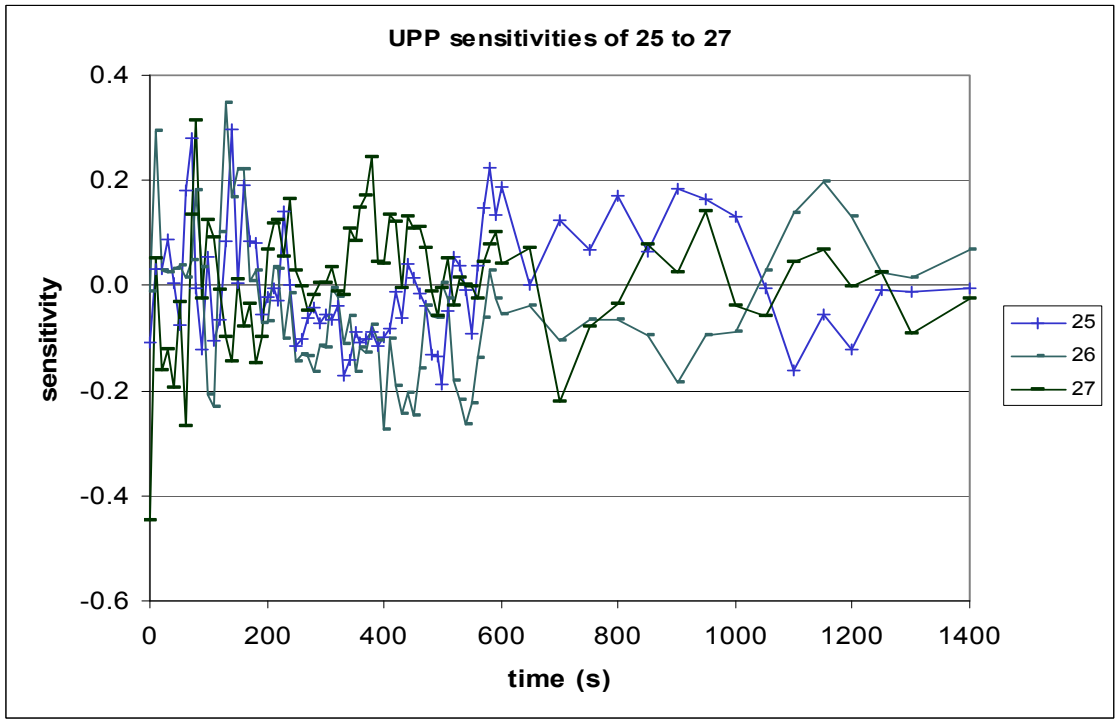
Fig. B.27. Sensitivity results for the upper plenum pressure (UPP) for the parameters 25 to 27: Spearman's correlation coefficients.
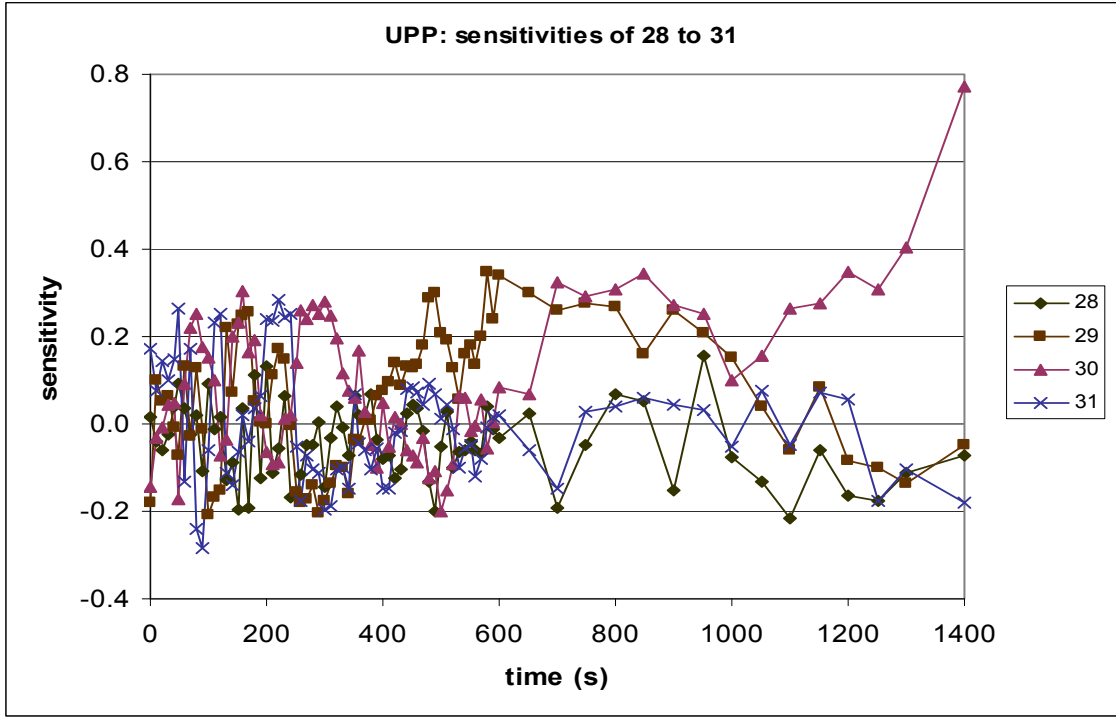
Fig. B.28. Sensitivity results for the upper plenum pressure (UPP) for the parameters 28 to 31: Spearman's correlation coefficients.
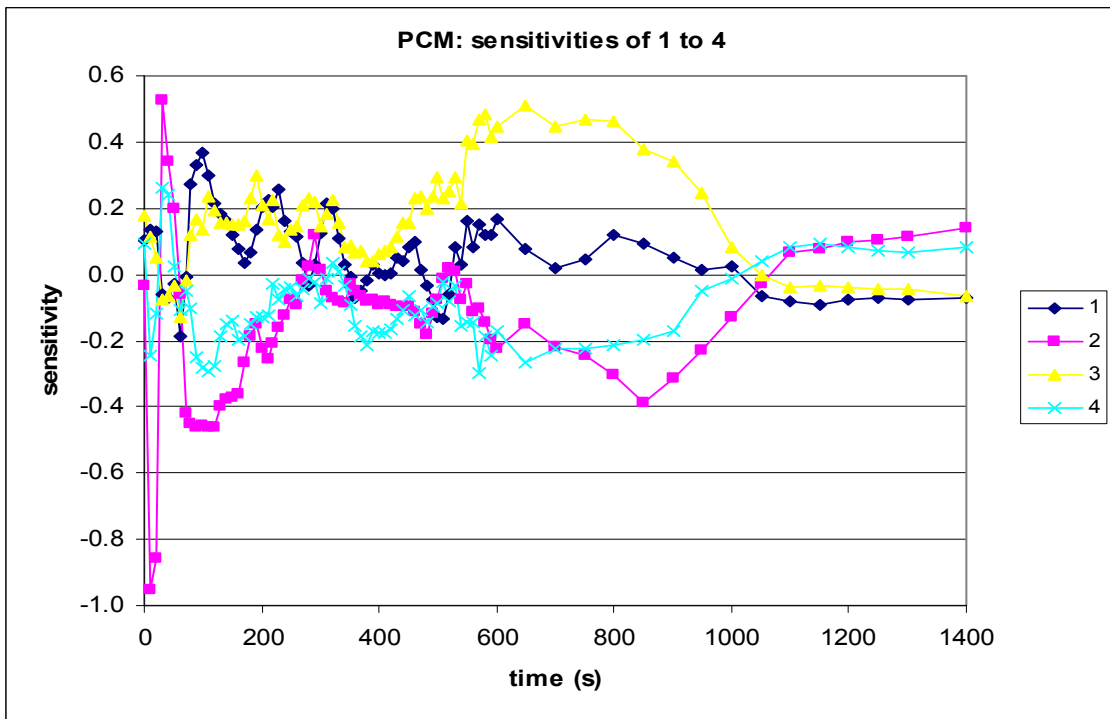
Fig. B.29. Sensitivity results for the primary coolant mass (PCM) for the parameters 1 to 4: Spearman's correlation coefficients.
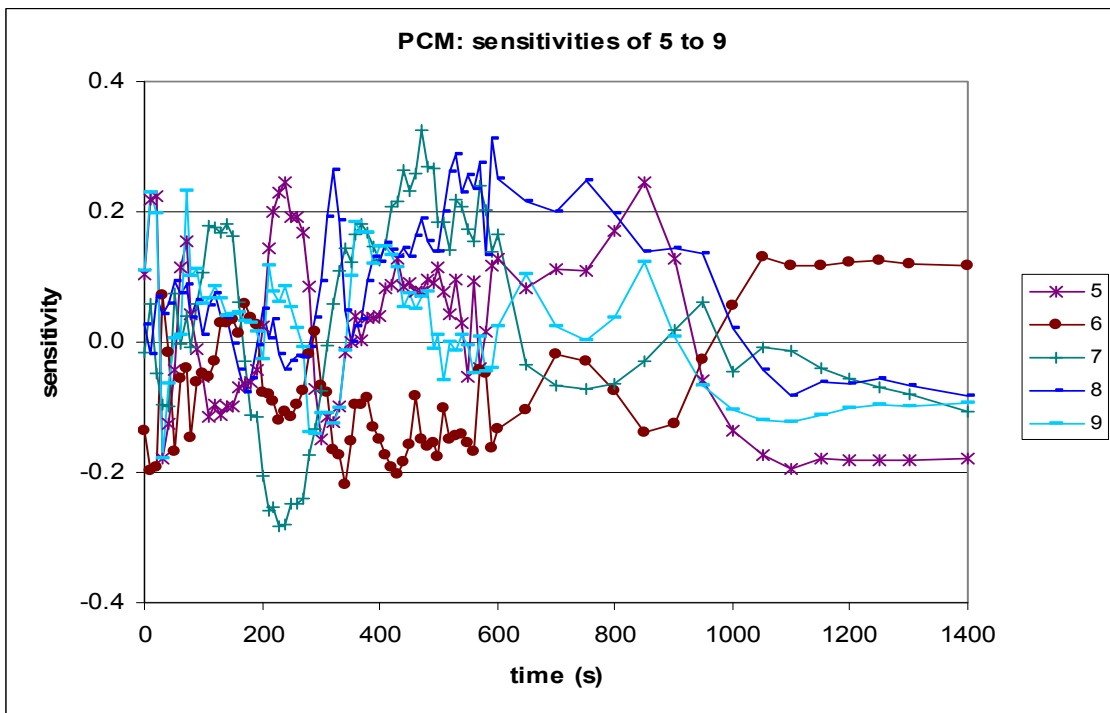
Fig. B.30. Sensitivity results for the primary coolant mass (PCM) for the parameters 5 to 9: Spearman's correlation coefficients.
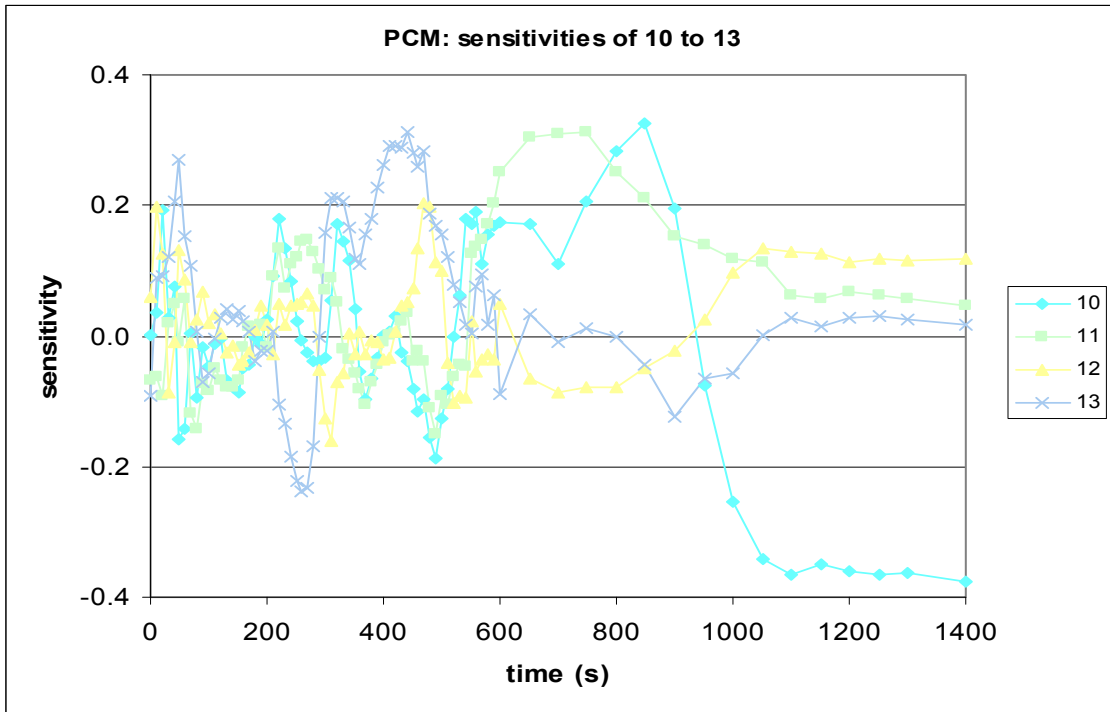
Fig. B.31. Sensitivity results for the primary coolant mass (PCM) for the parameters 10 to 13: Spearman's correlation coefficients.
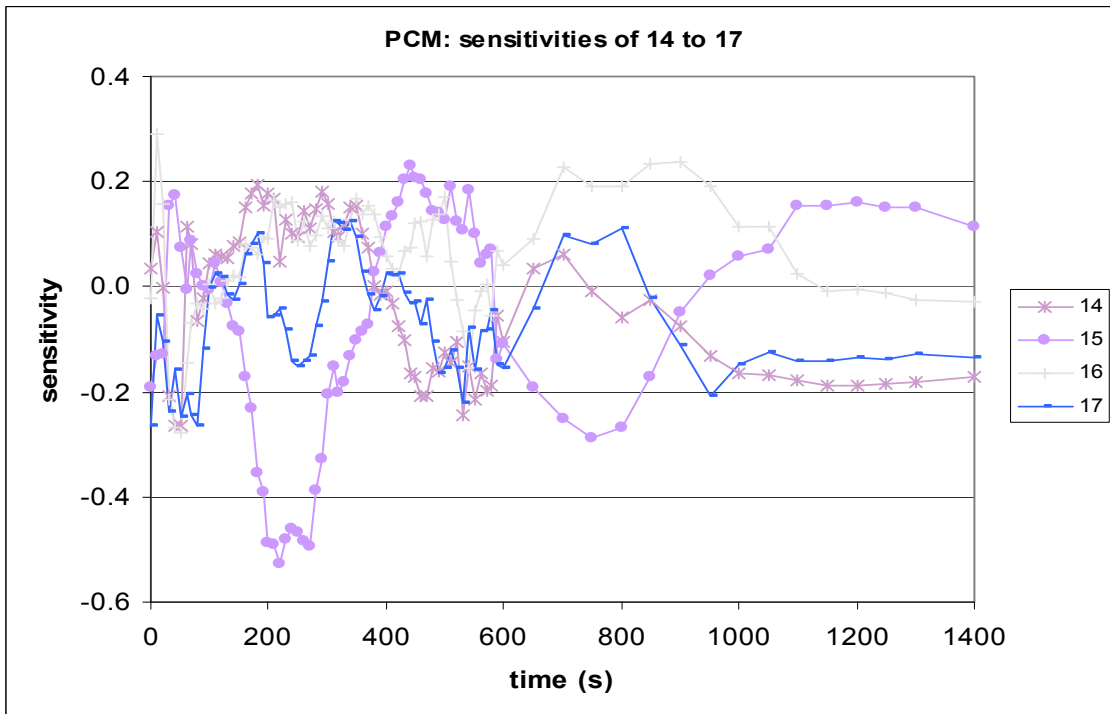
Fig. B.32. Sensitivity results for the primary coolant mass (PCM) for the parameters 14 to 17: Spearman's correlation coefficients.
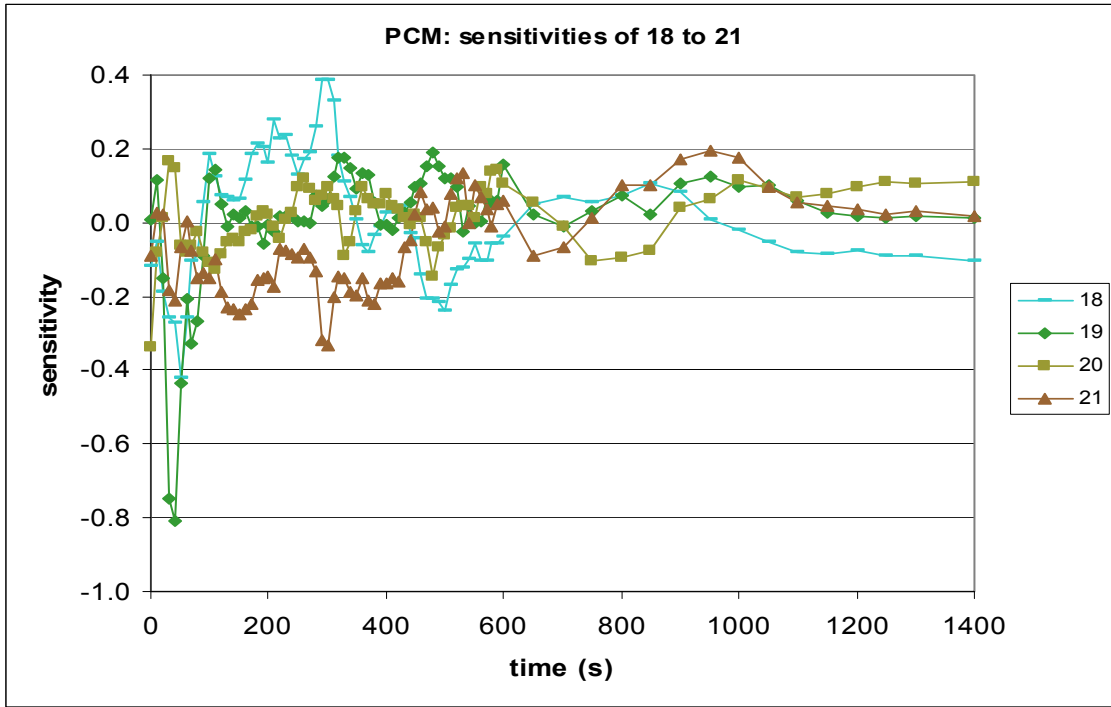
Fig. B.33. Sensitivity results for the primary coolant mass (PCM) for the parameters 18 to 21: Spearman's correlation coefficients.
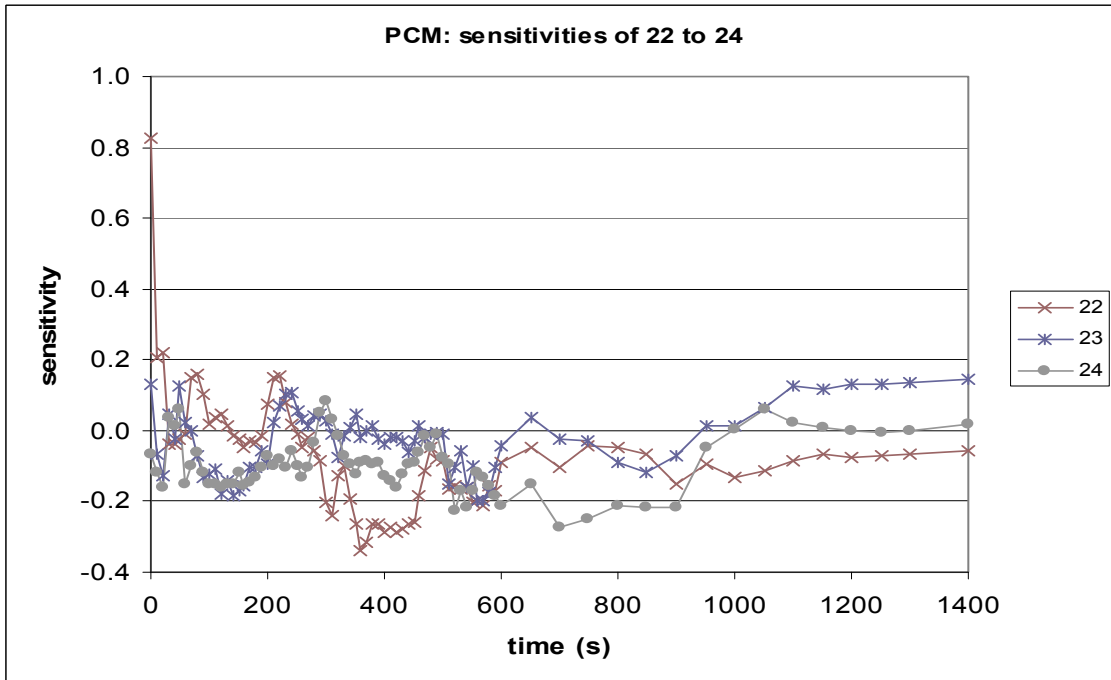
Fig. B.34. Sensitivity results for the primary coolant mass (PCM) for the parameters 22 to 24: Spearman's correlation coefficients.
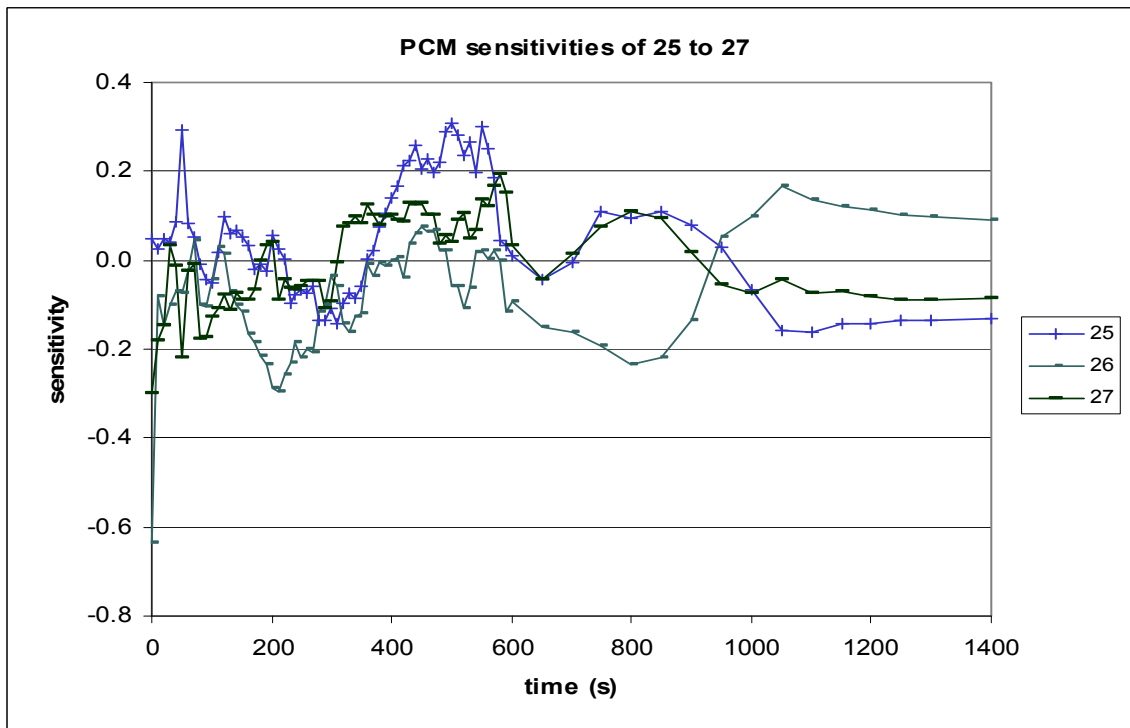
Fig. B.35. Sensitivity results for the primary coolant mass (PCM) for the parameters 25 to 27: Spearman's correlation coefficients.
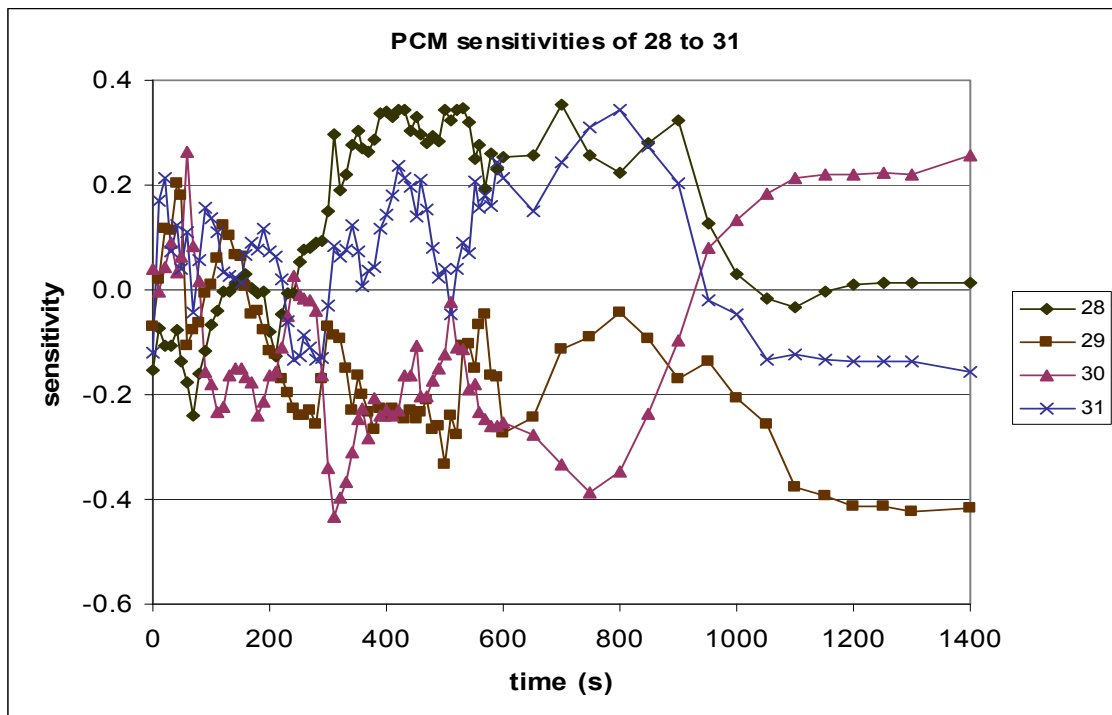
Fig. B.36. Sensitivity results for the primary coolant mass (PCM) for the parameters 28 to 31: Spearman's correlation coefficients.

134
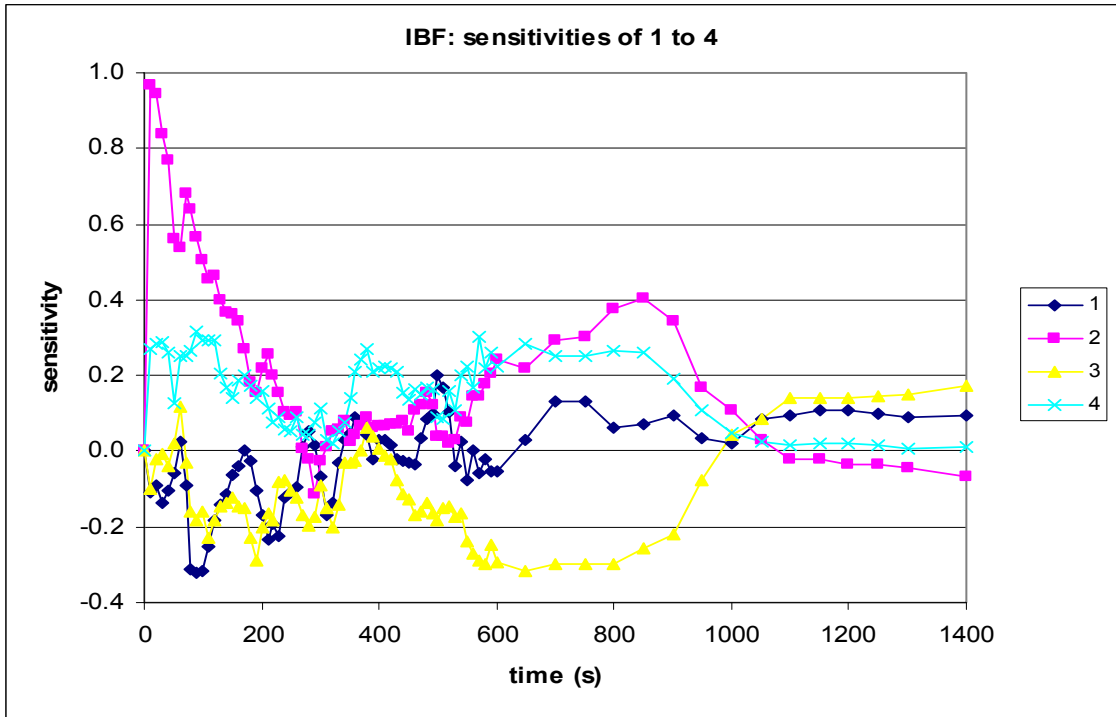
Fig. B.37. Sensitivity results for the integrated break flow (IBF) for the parameters 1 to 4: Spearman's correlation coefficients.
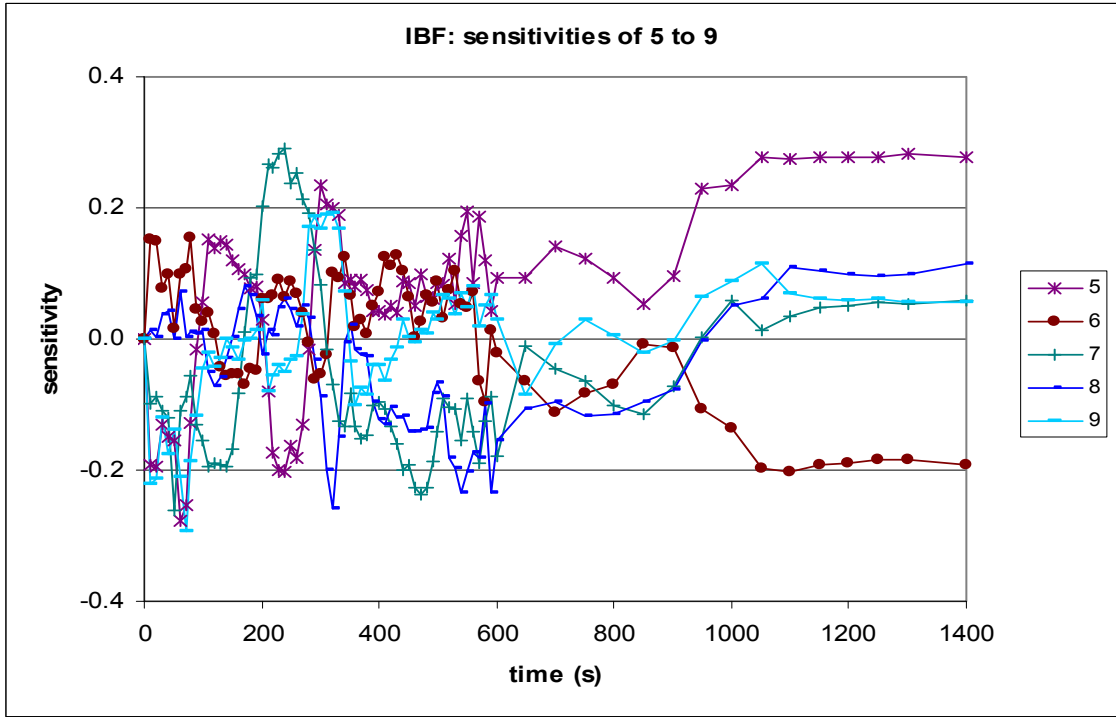
Fig. B.38. Sensitivity results for the integrated break flow (IBF) for the parameters 5 to 9: Spearman's correlation coefficients.

135
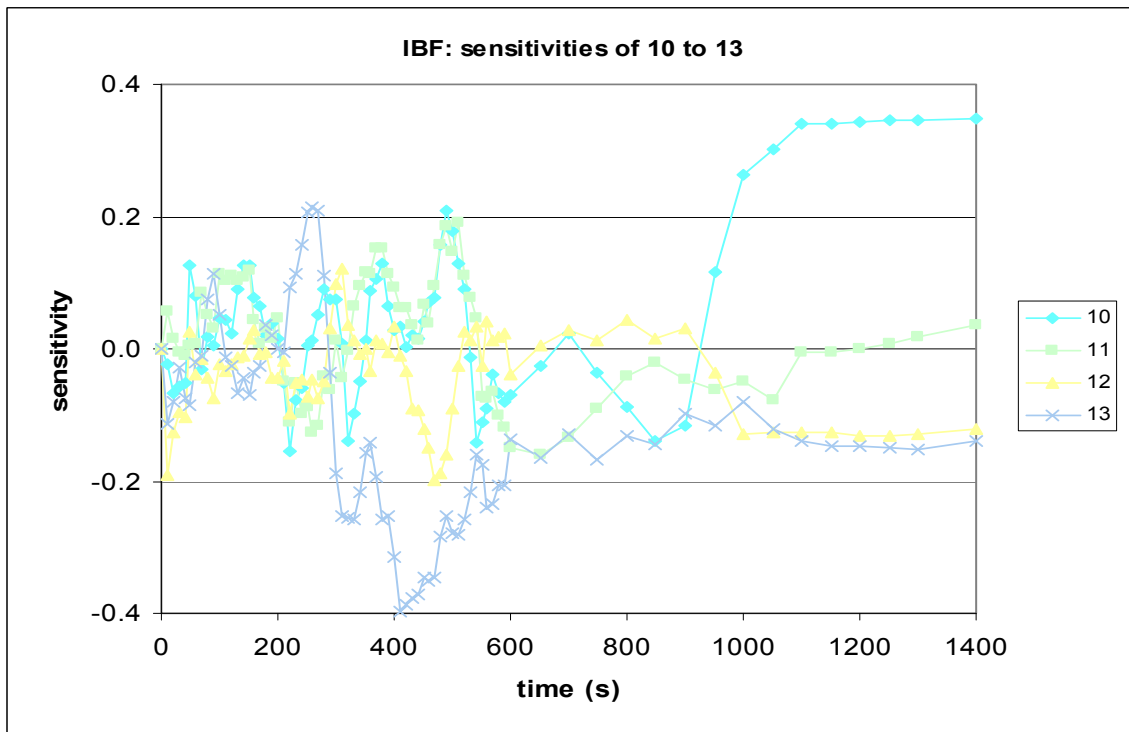
Fig. B.39. Sensitivity results for the integrated break flow (IBF) for the parameters 10 to 13: Spearman's correlation coefficients.
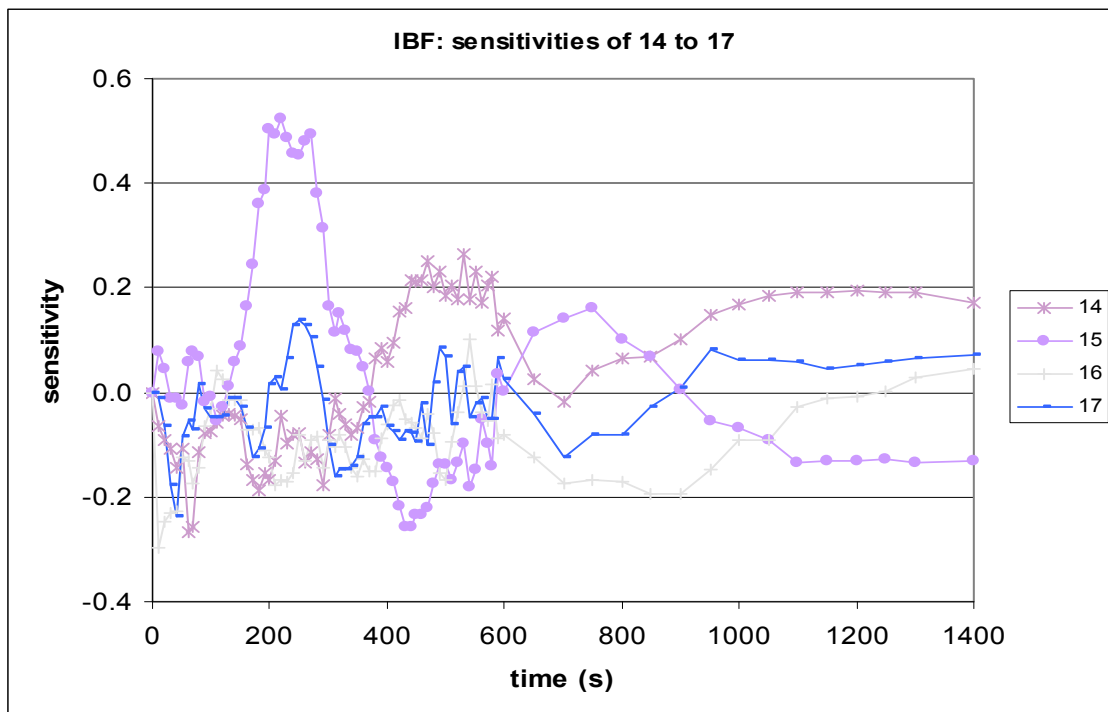
Fig. B.40. Sensitivity results for the integrated break flow (IBF) for the parameters 14 to 17: Spearman's correlation coefficients.

136
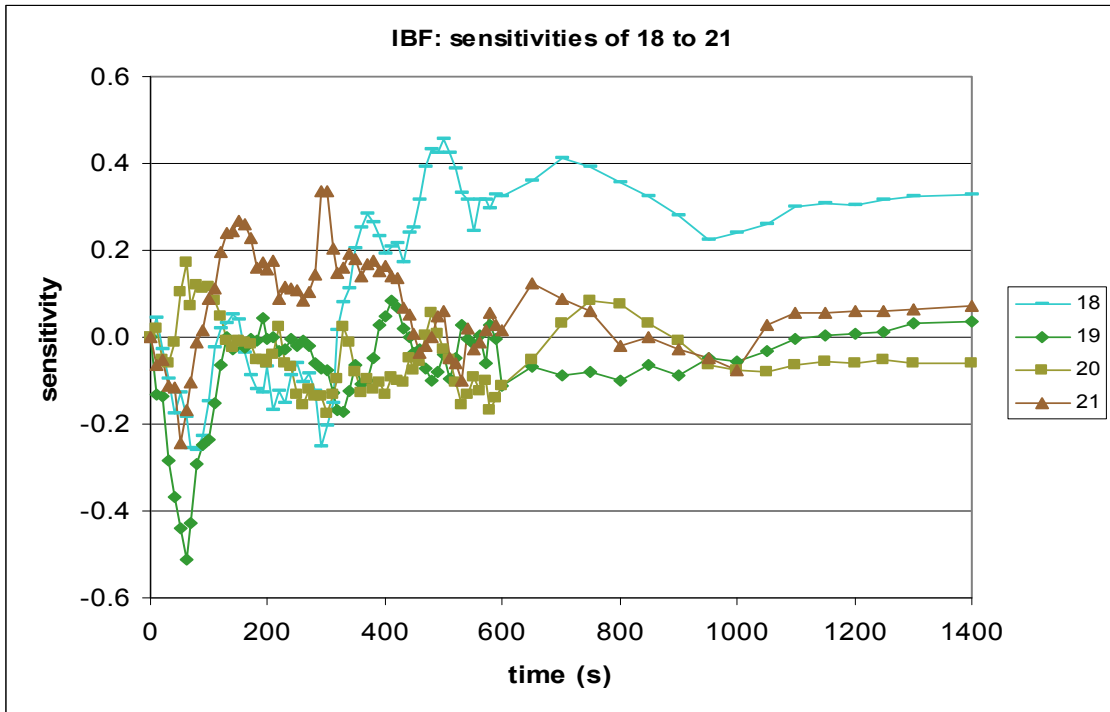
Fig. B.41. Sensitivity results for the integrated break flow (IBF) for the parameters 18 to 21: Spearman's correlation coefficients.
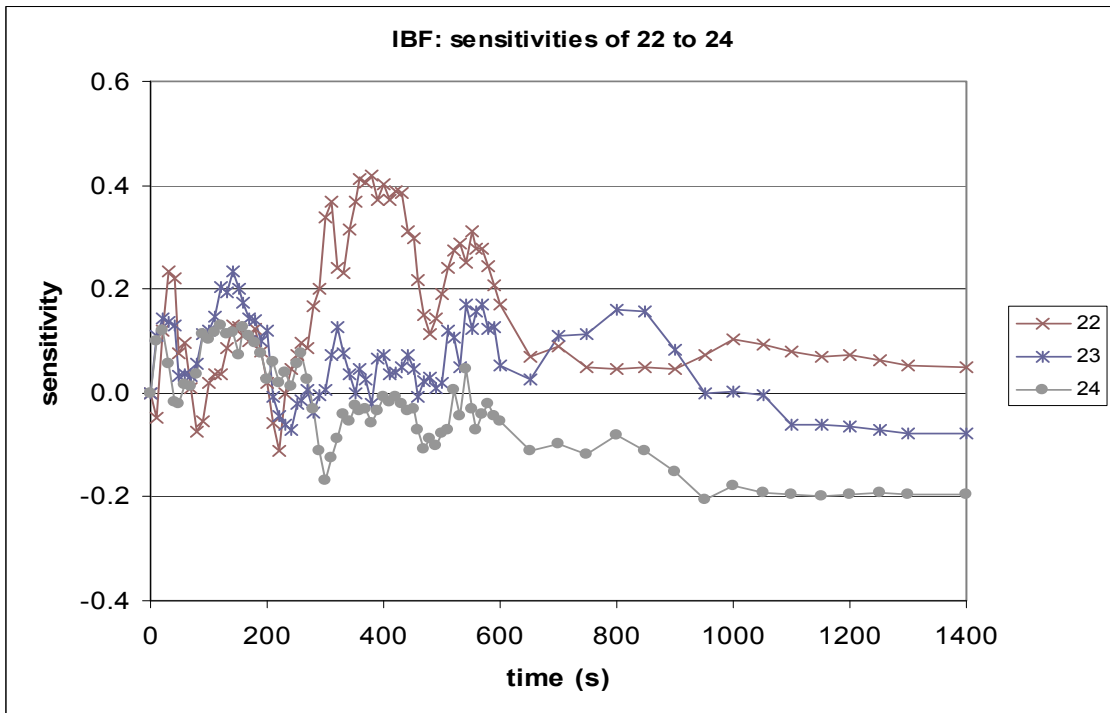
Fig. B.42. Sensitivity results for the integrated break flow (IBF) for the parameters 22 to 24: Spearman's correlation coefficients.

137
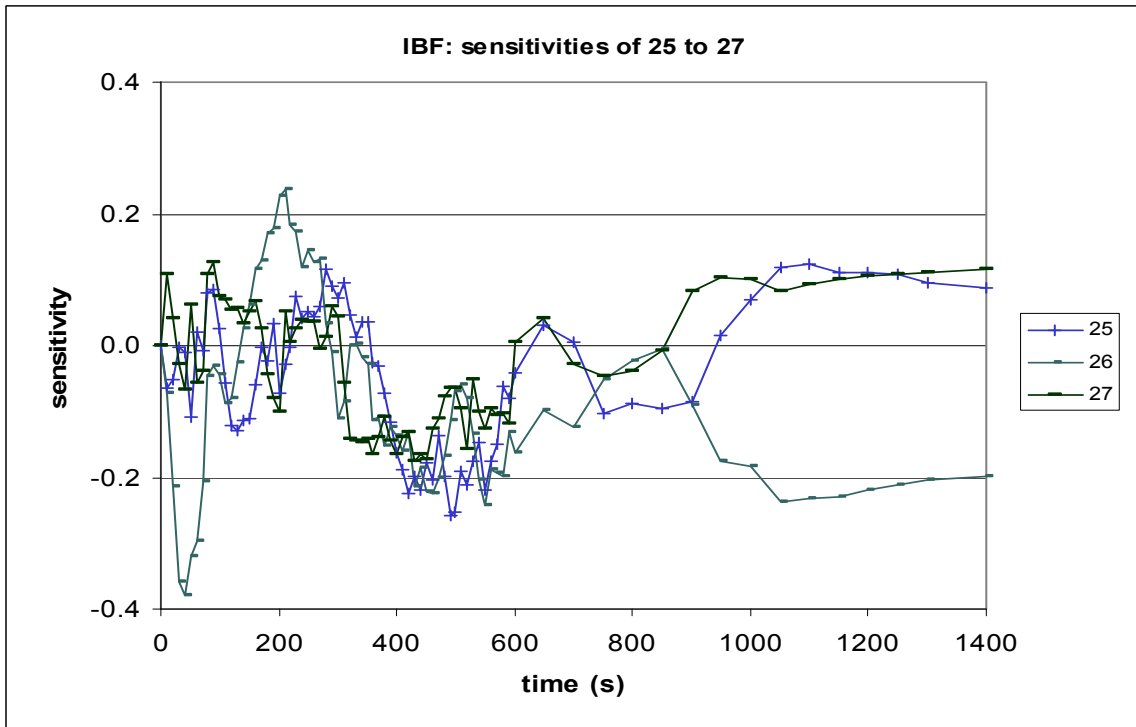
Fig. B.43. Sensitivity results for the integrated break flow (IBF) for the parameters 25 to 27: Spearman's correlation coefficients.
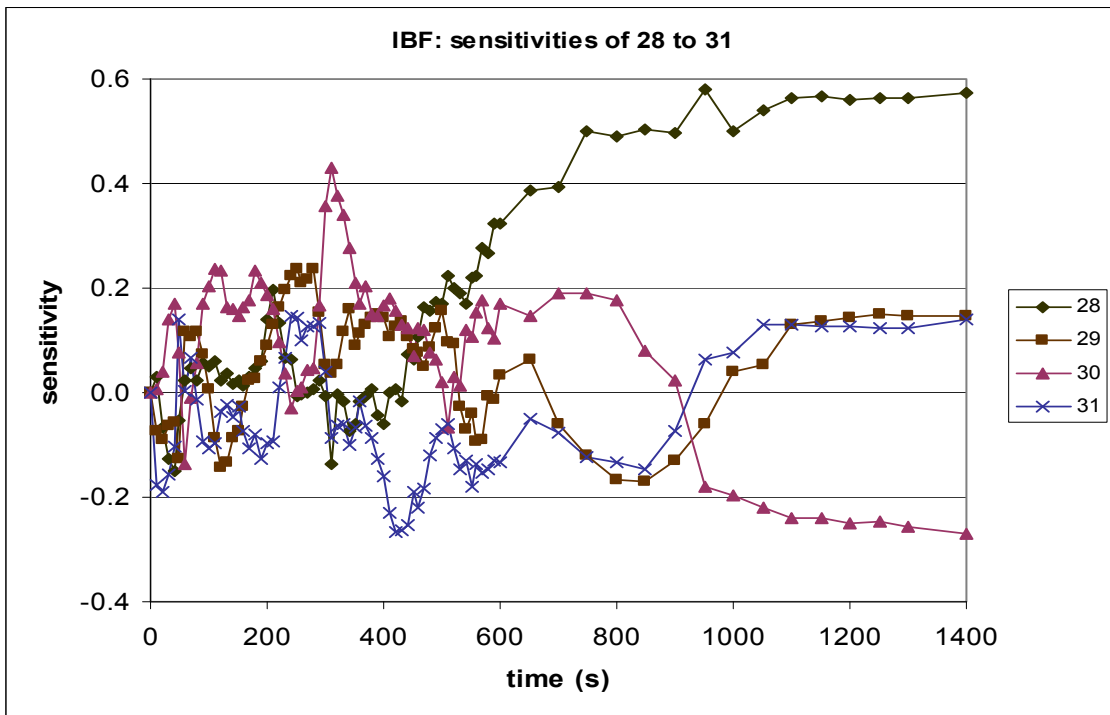
Fig. B.44. Sensitivity results for the integrated break flow (IBF) for the parameters 28 to 31: Spearman's correlation coefficients.
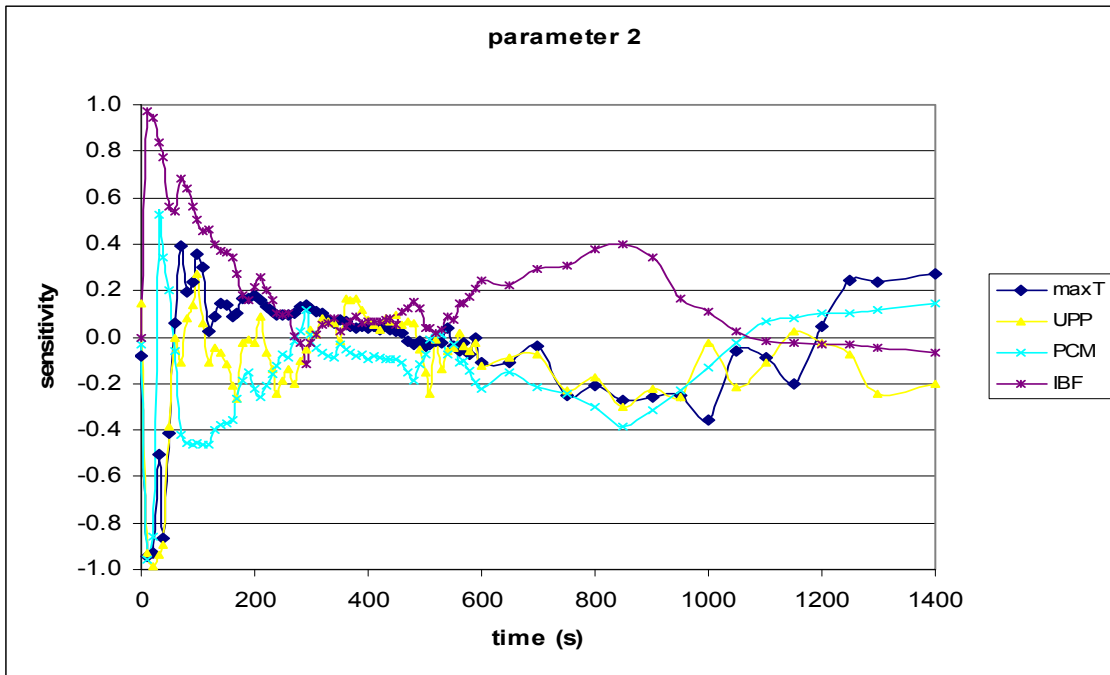
Fig. B.45. Sensitivity code results (maxT, UPP, PCM and IBF) for the break discharge coefficient (parameter 2):
Spearman's correlation coefficients.
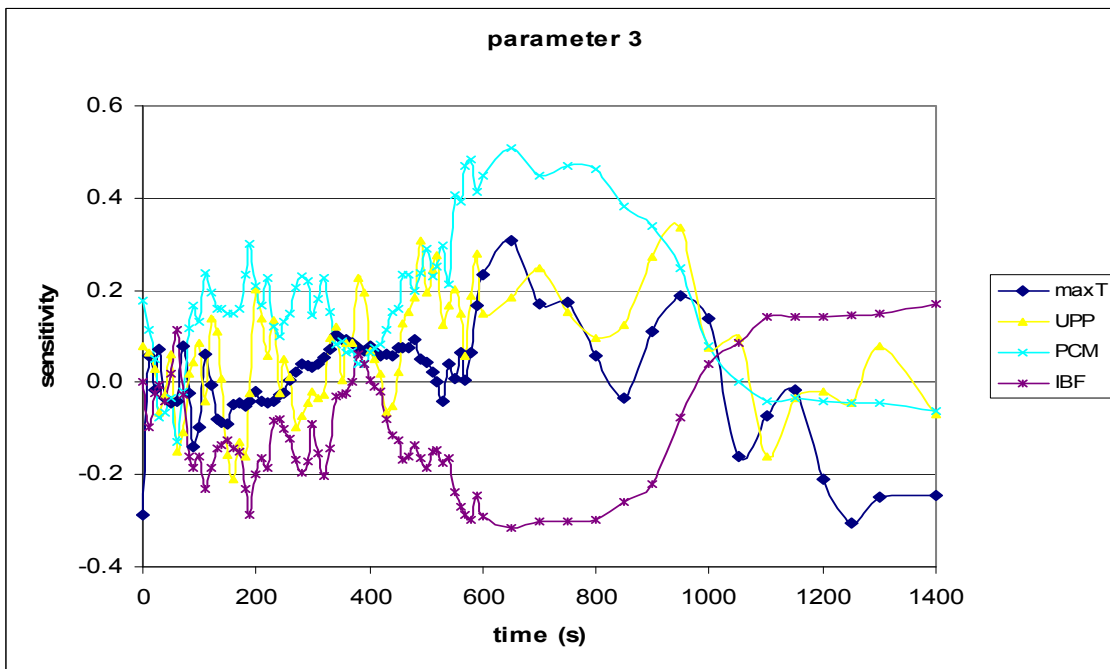
Fig. B.46. Sensitivity code results (maxT, UPP, PCM and IBF) for the thermal nonequilibrium constant (parameter 3):
Spearman's correlation coefficients.
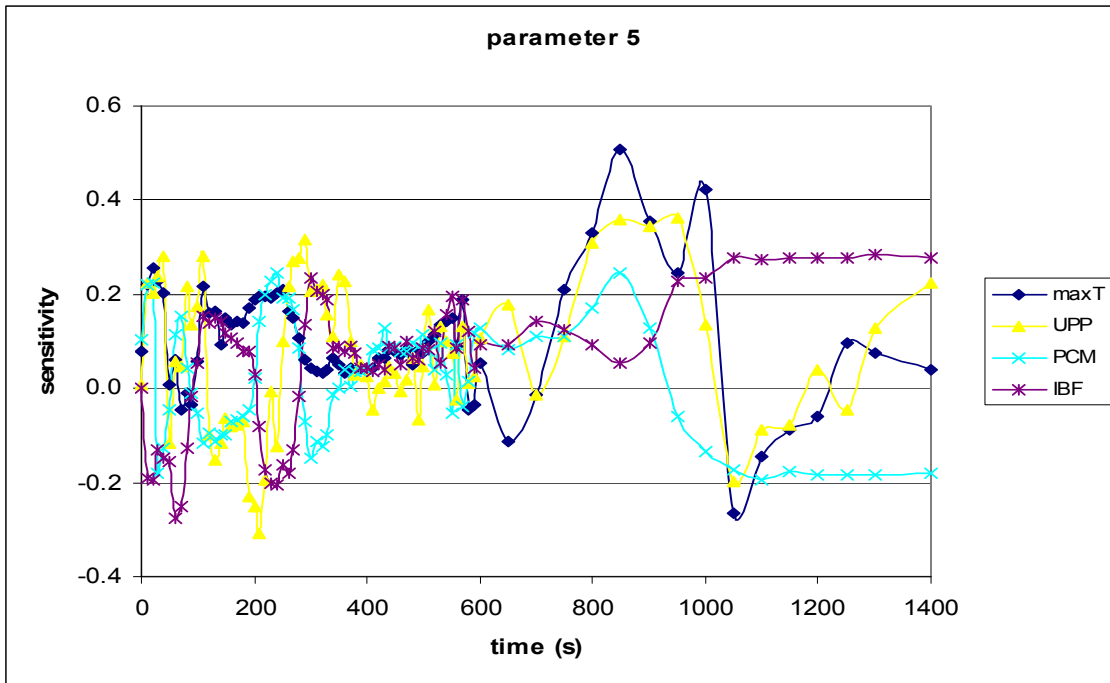
Fig. B.47. Sensitivity code results (maxT, UPP, PCM and IBF) for the initial core power (parameter 5):
Spearman's correlation coefficients.
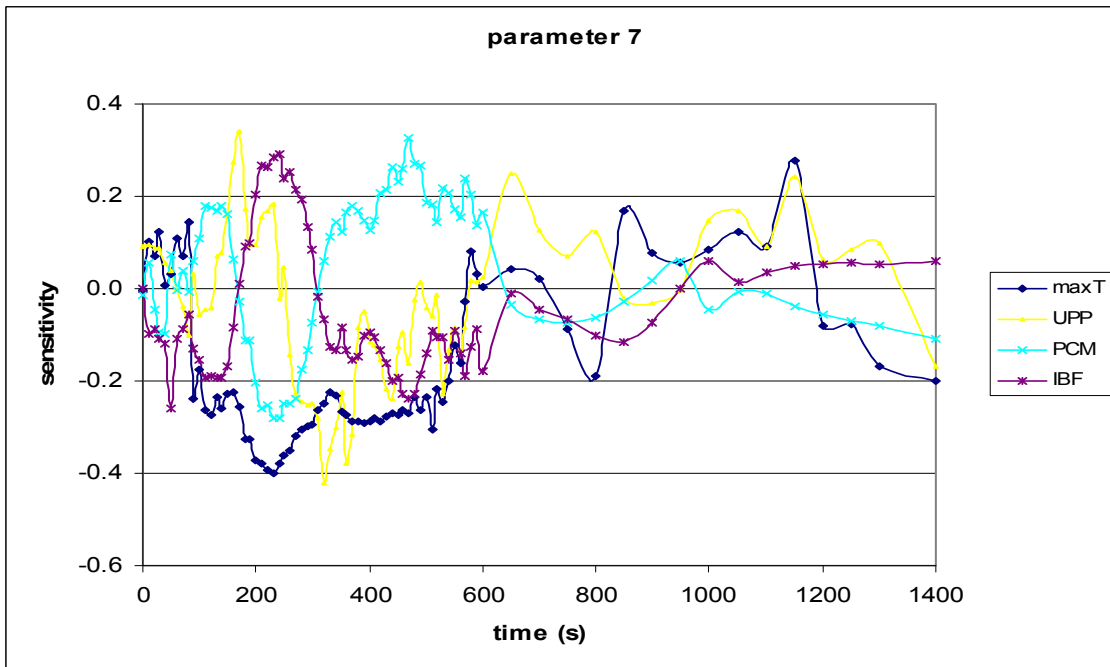
Fig. B.48. Sensitivity code results (maxT, UPP, PCM and IBF) for the cladding specific heat capacity (parameter 7):
Spearman's correlation coefficients.
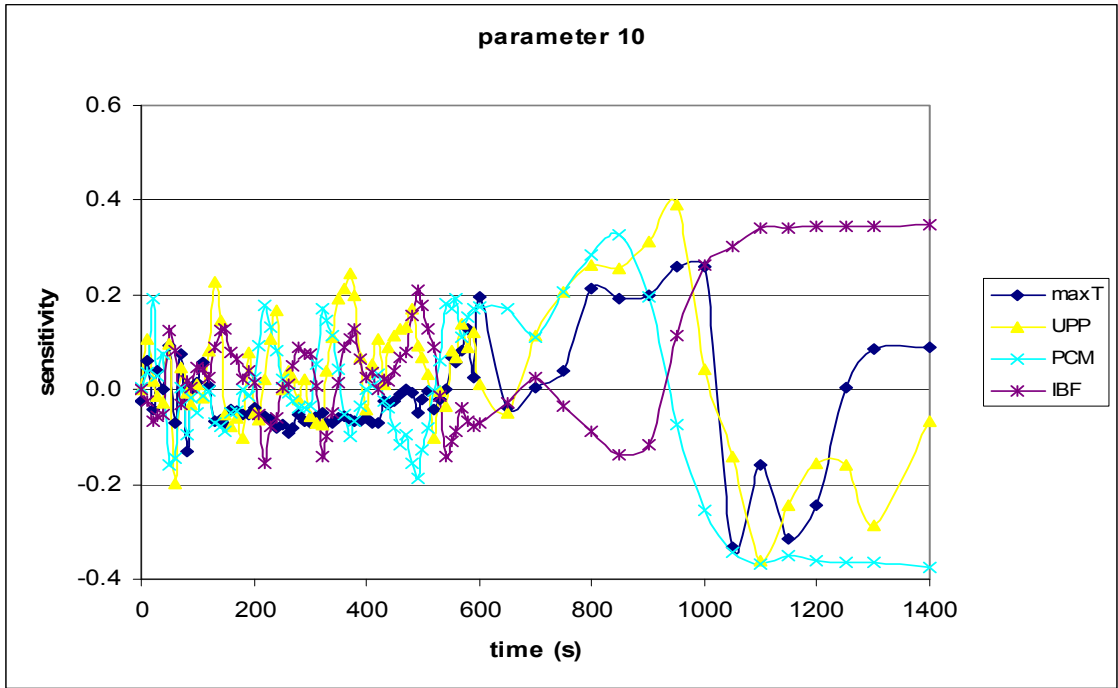
Fig. B.49. Sensitivity code results (maxT, UPP, PCM and IBF) for the 2-phase degradation input of the pump (parameter 10): Spearman's correlation coefficients.
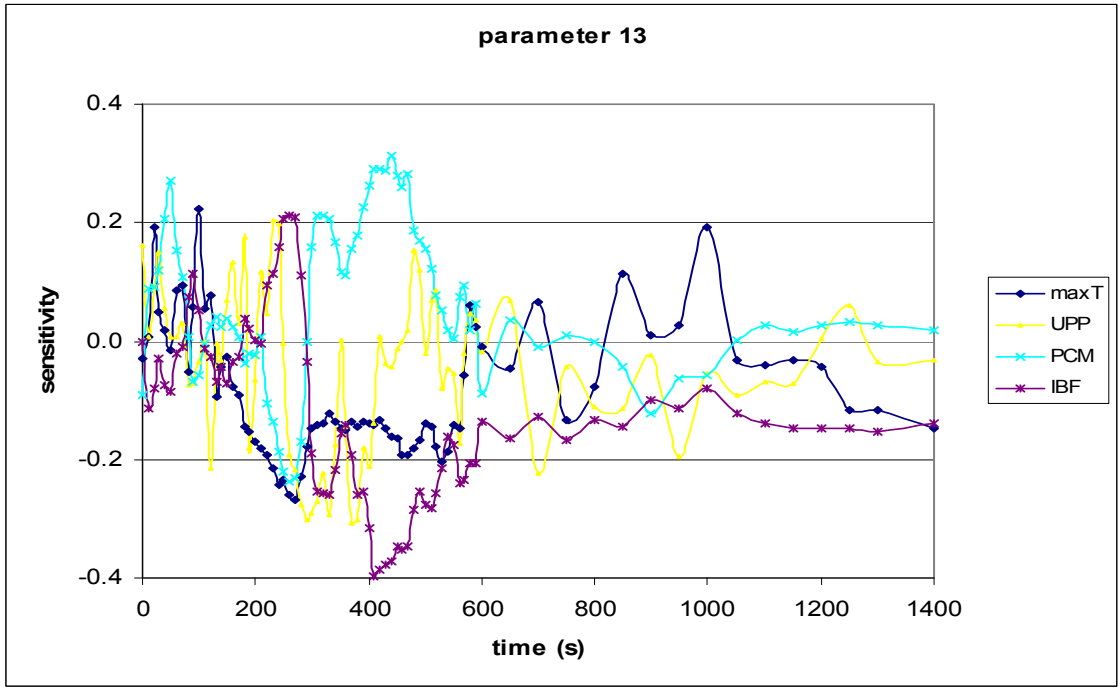
Fig. B.50. Sensitivity code results (maxT, UPP, PCM and IBF) for the heat transfer coefficient on outside surfaces of piping (parameter 13): Spearman's correlation coefficients.
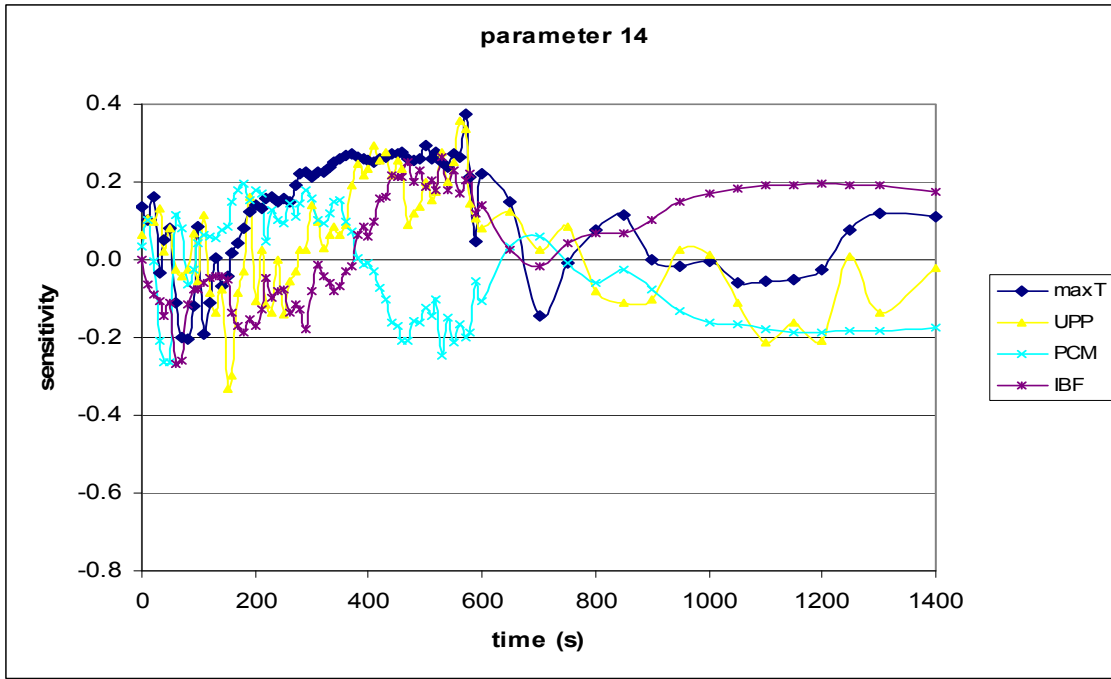
Fig. B.51. Sensitivity code results (maxT, UPP, PCM and IBF) for the CCFL upper core plate; c of Wallis correlation (parameter 14): Spearman's correlation coefficients.
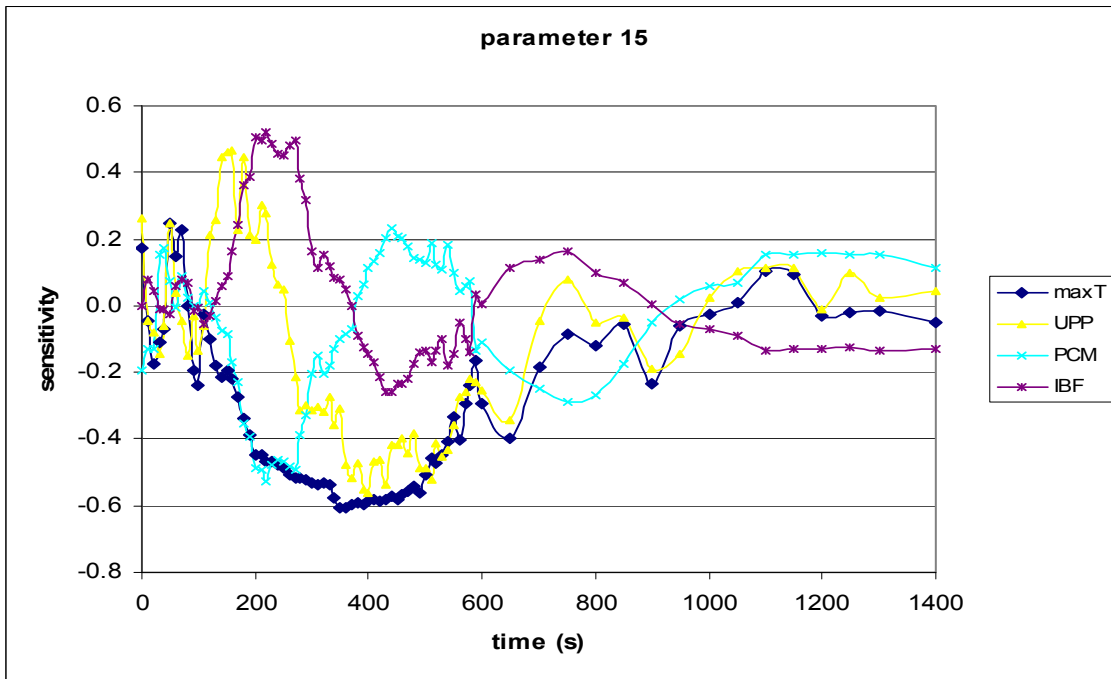
Fig. B.52. Sensitivity code results (maxT, UPP, PCM and IBF) for the CCFL upper plenum; c of Kutateladze correlation (parameter 15): Spearman's correlation coefficients.
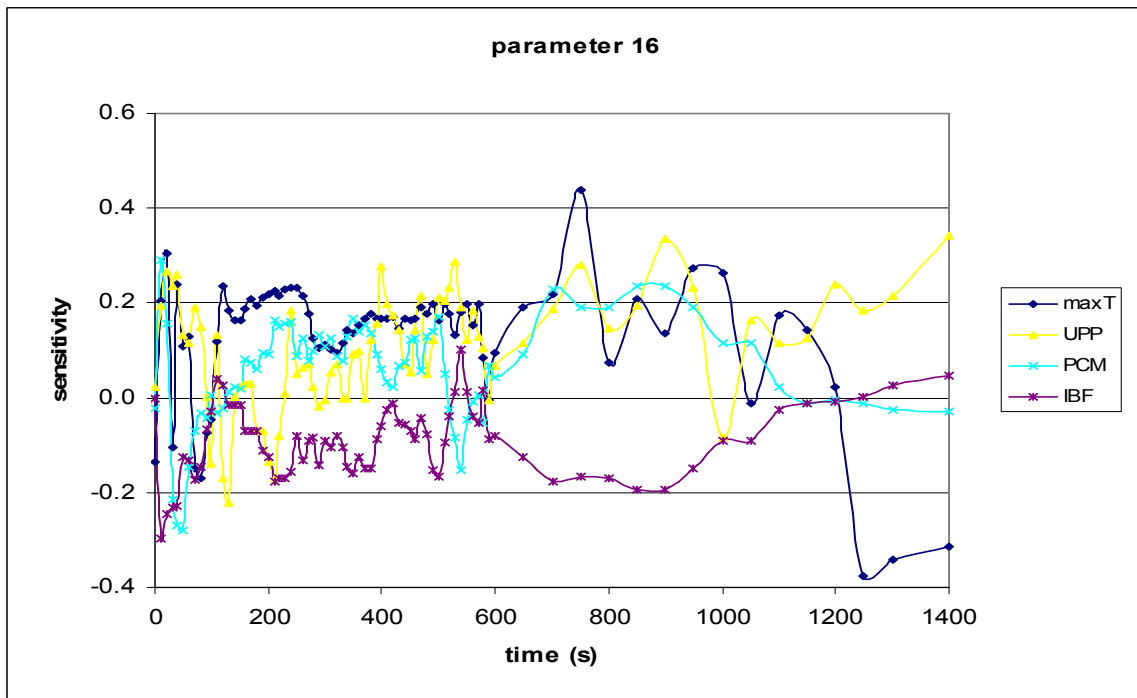
Fig. B.53. Sensitivity code results (maxT, UPP, PCM and IBF) for the CCFL steam generator tubes inlet; c of Kutateladze correlation (parameter 16): Spearman's correlation coefficients.
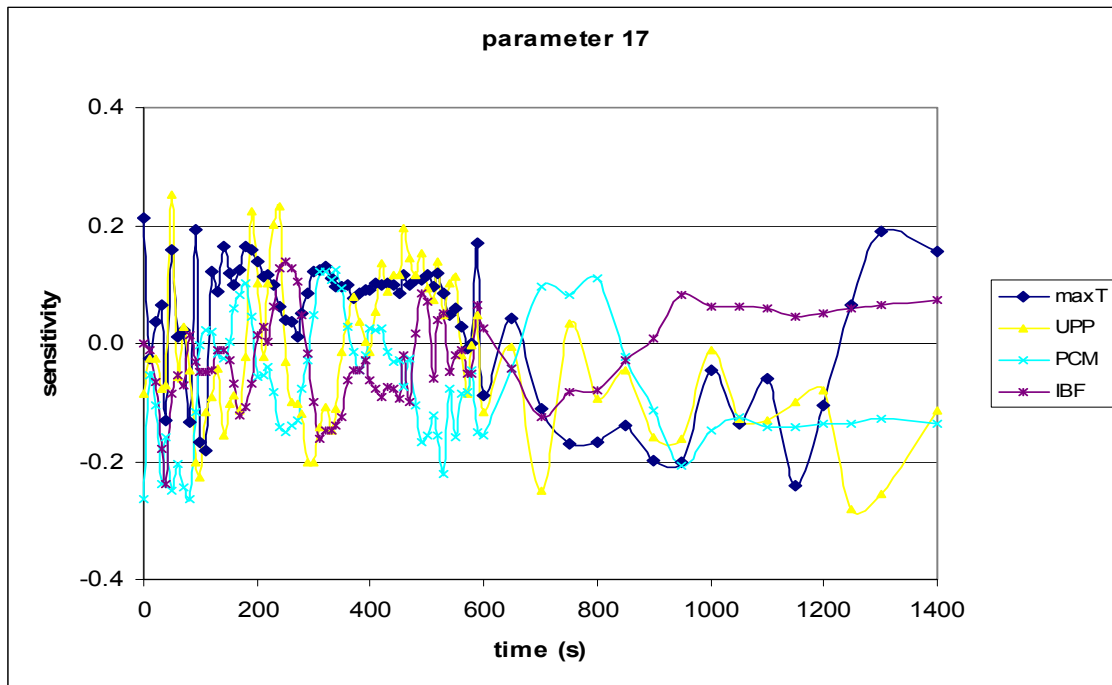
Fig. B.54. Sensitivity code results (maxT, UPP, PCM and IBF) for the CCFL downcomer; c of Wallis correlation (parameter 17): Spearman's correlation coefficients.
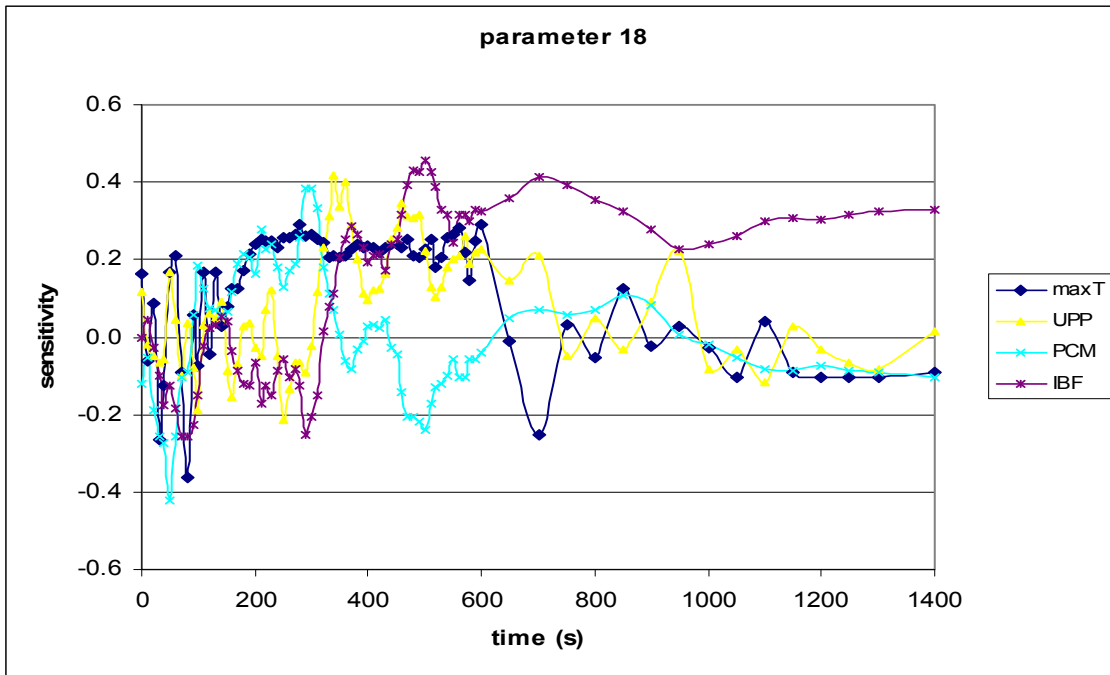
Fig. B.55. Sensitivity code results (maxT, UPP, PCM and IBF) for the accumulator initial liquid level (parameter 18):
Spearman's correlation coefficients.
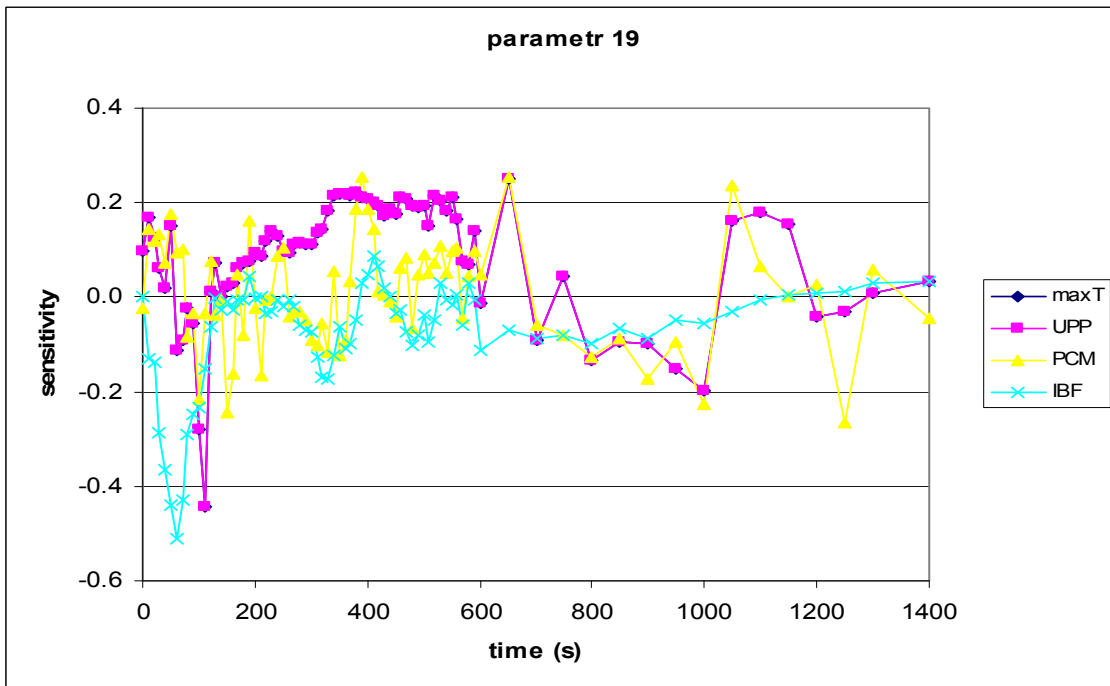
Fig. B.56. Sensitivity code results (maxT, UPP, PCM and IBF) for the friction form loss in the accumulator line (parameter 19):
Spearman's correlation coefficients.
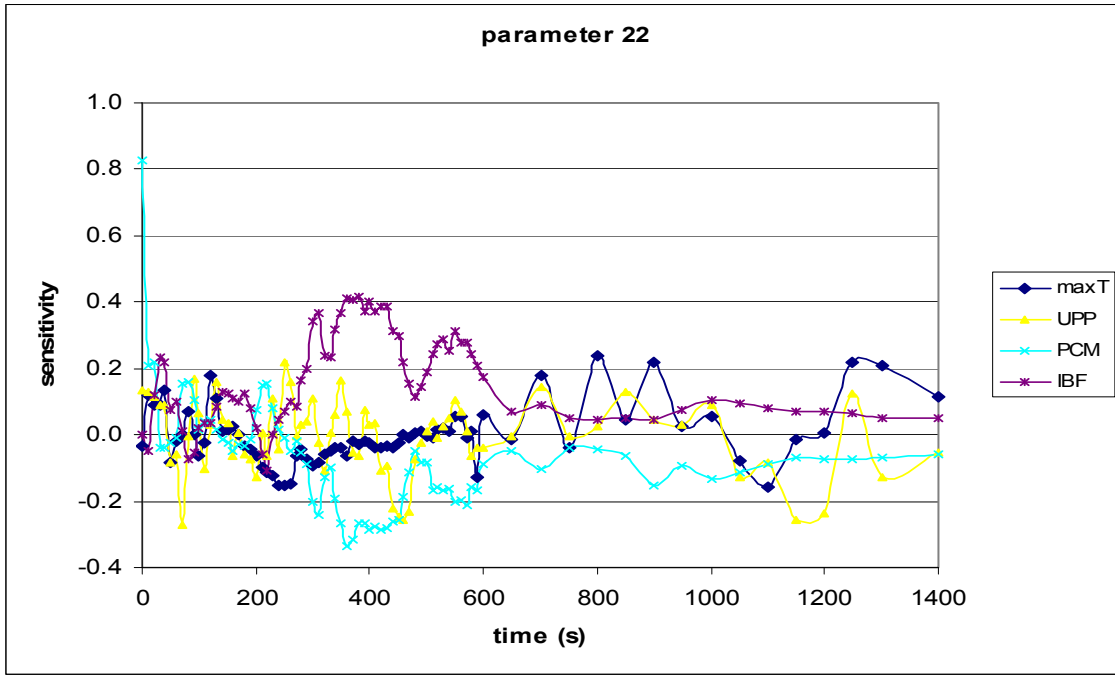
Fig. B.57. Sensitivity code results (maxT, UPP, PCM and IBF) for the pressurizer initial level (parameter 22):
Spearman's correlation coefficients.
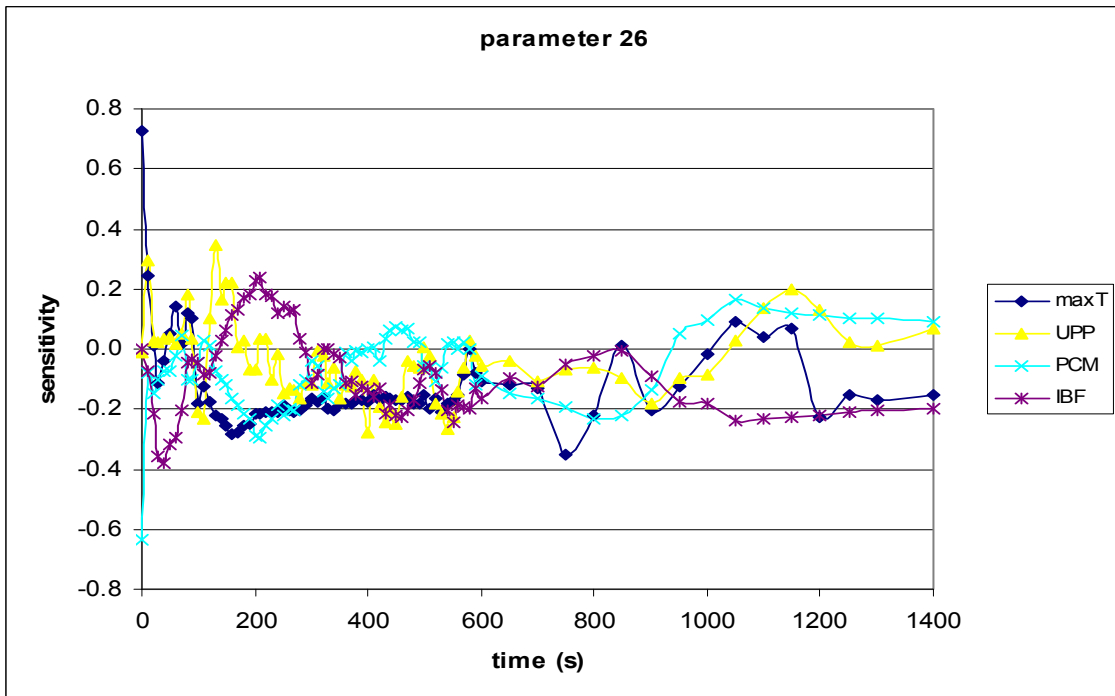
Fig. B.58. Sensitivity code results (maxT, UPP, PCM and IBF) for the initial pressure on steam generator secondary side (parameter 26):
Spearman's correlation coefficients.

145
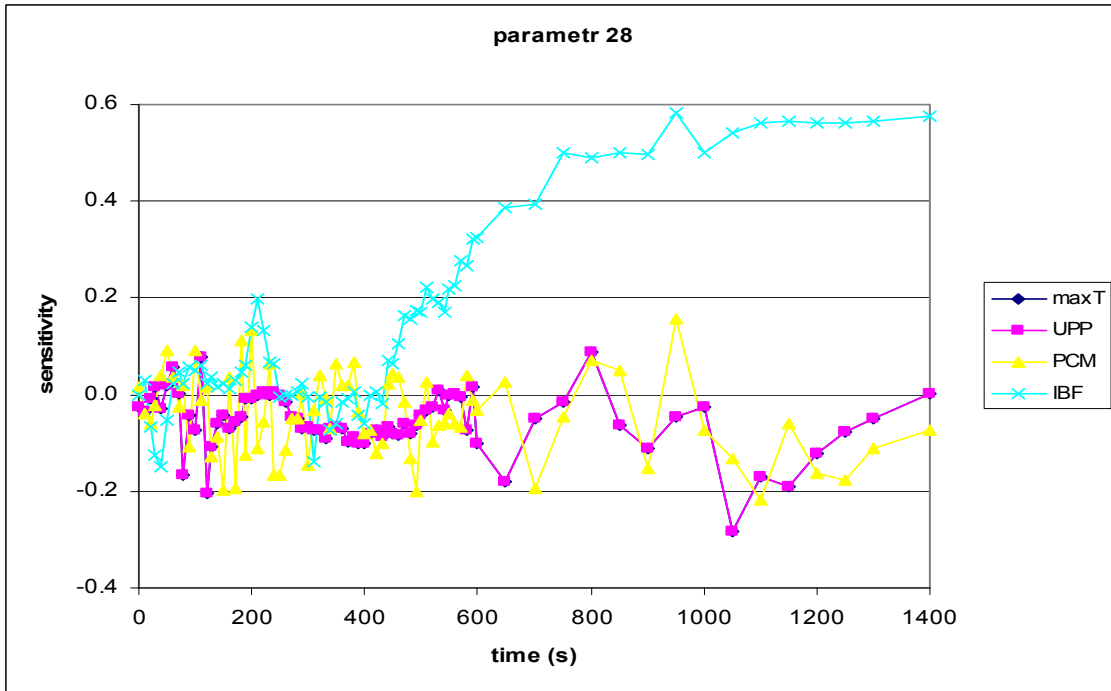
Fig. B.59. Sensitivity code results (maxT, UPP, PCM and IBF) for the liquid injection flow variation (HPSI/LPSI) (parameter 28): Spearman's correlation coefficients.
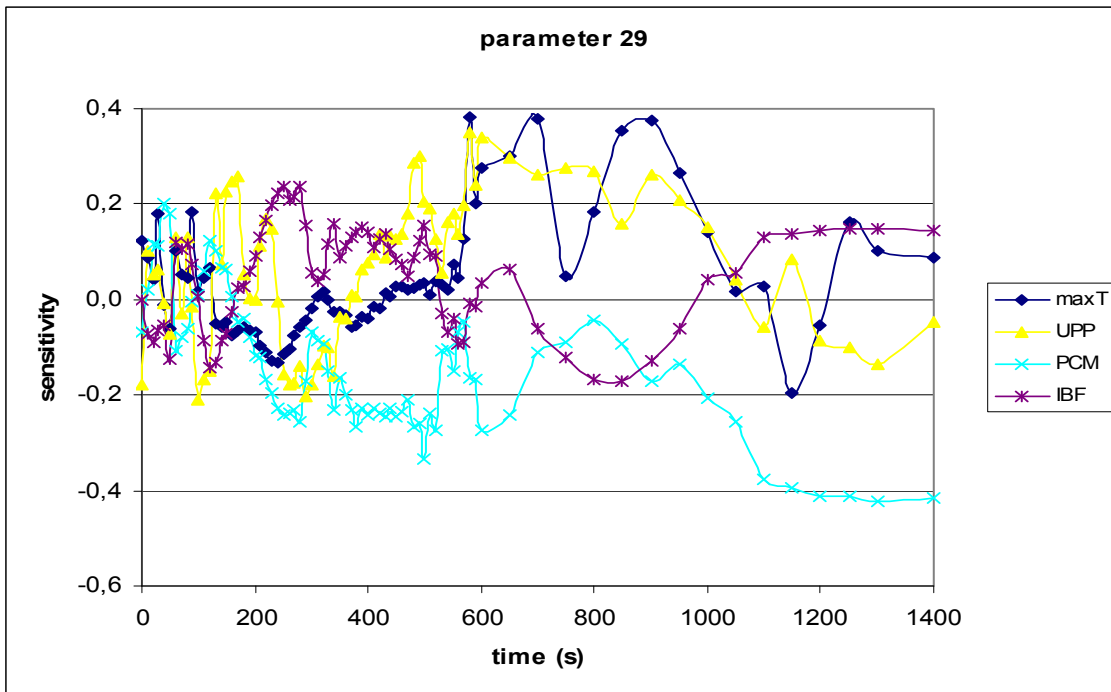
Fig. B.60. Sensitivity code results (maxT, UPP, PCM and IBF) for the liquid injections temperature (parameter 29): Spearman's correlation coefficients.
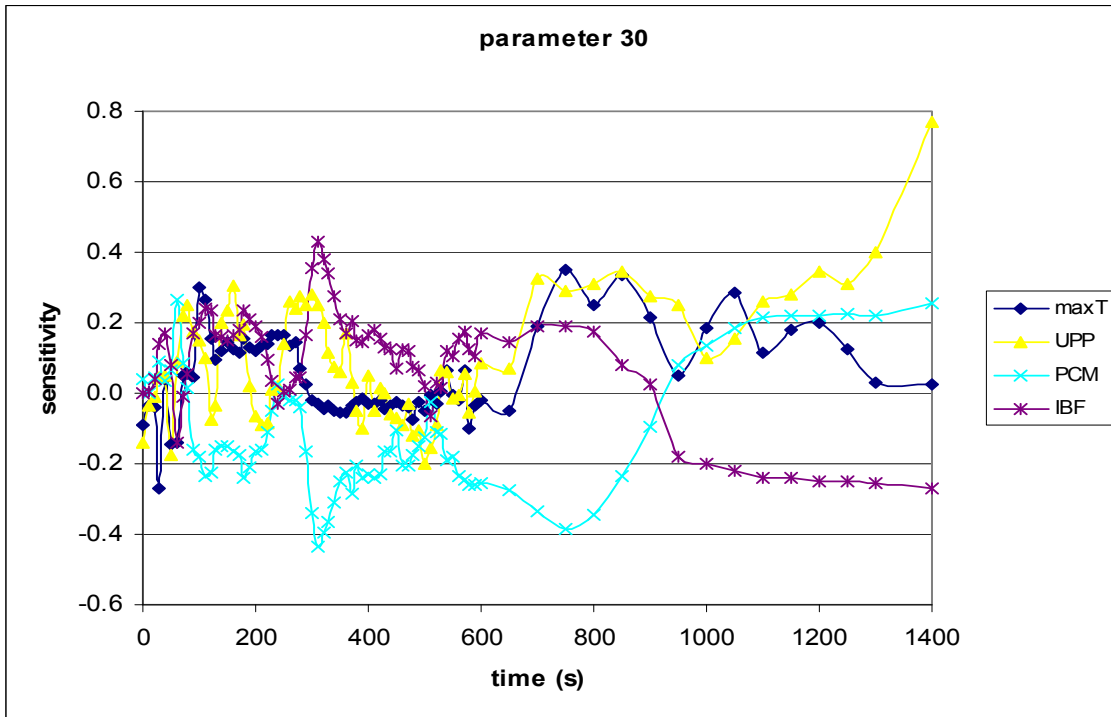
Fig. B.61. Sensitivity code results (maxT, UPP, PCM and IBF) for the cold leg discharge pressure (parameter 30):
Spearman's correlation coefficients.

147

APPENDIX C

List of Figures

Fig. C.1: PSB-VVER Test-3 Integrated Break Flow

Fig. C.2: PSB-VVER Test-3 Upper Plenum Pressure

Fig. C.3: PSB-VVER Test-3 Pressurizer Pressure

Fig. C.4: PSB-VVER Test-3 Accumulator #2 Pressure

Fig. C.5: PSB-VVER Test-3 Accumulator #2 Level

Fig. C.6: PSB-VVER Test-3 Accumulator #4 Pressure

Fig. C.7: PSB-VVER Test-3 Accumulator #4 Level
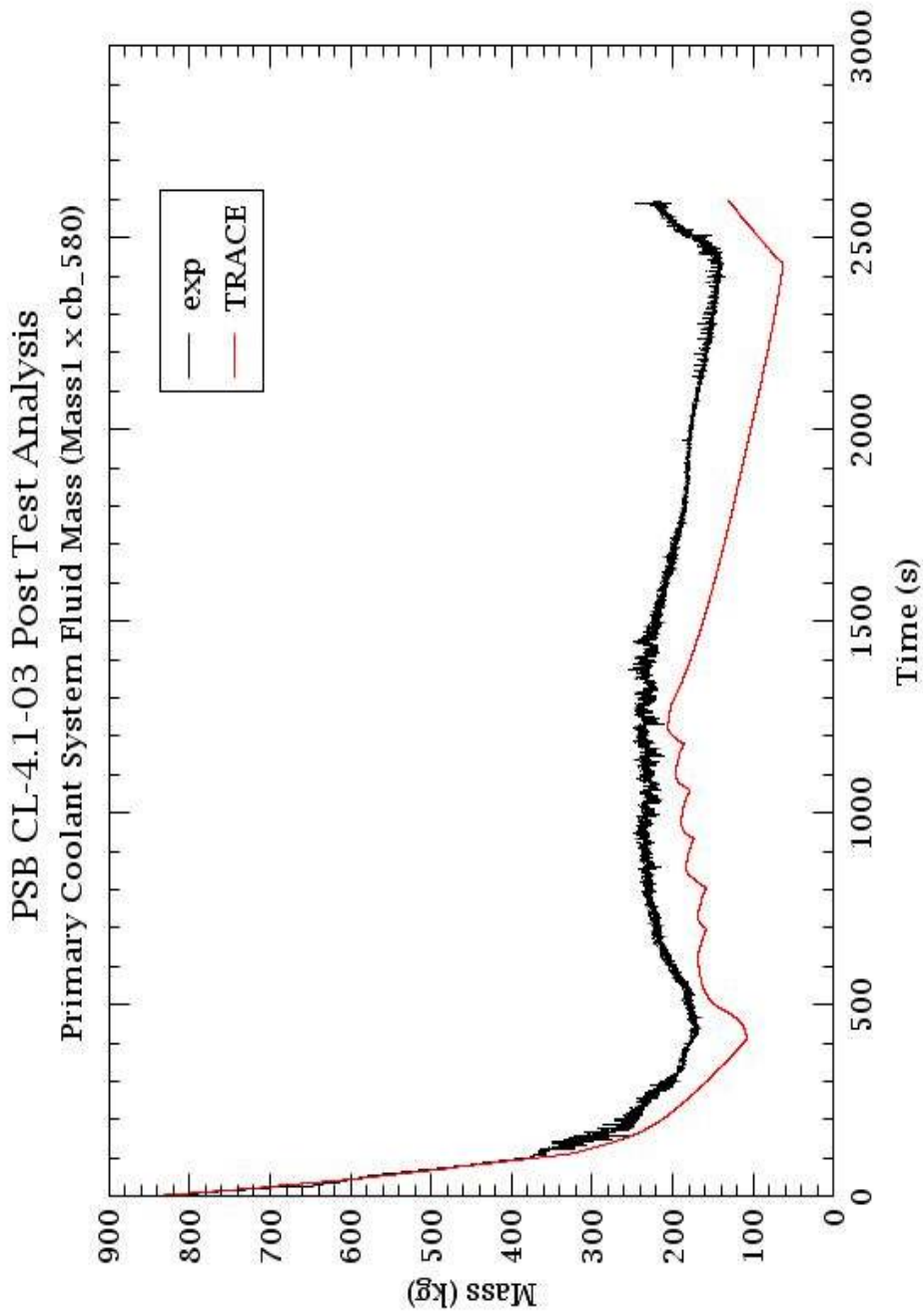
Fig. C.8: PSB-VVER Test-3 Primary Coolant Mass
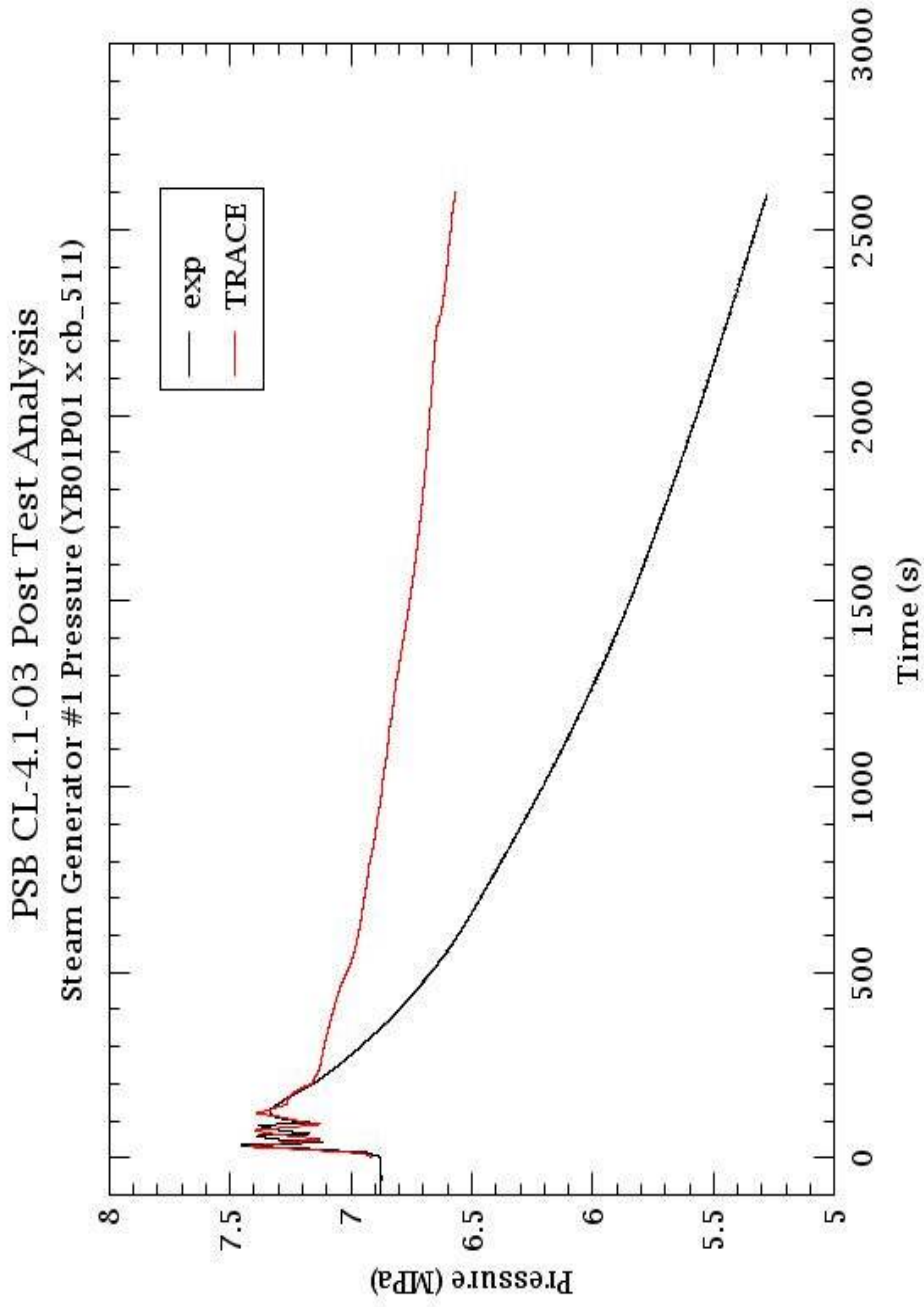
Fig. C.9: PSB-VVER Test-3 Steam Generator #1 Pressure
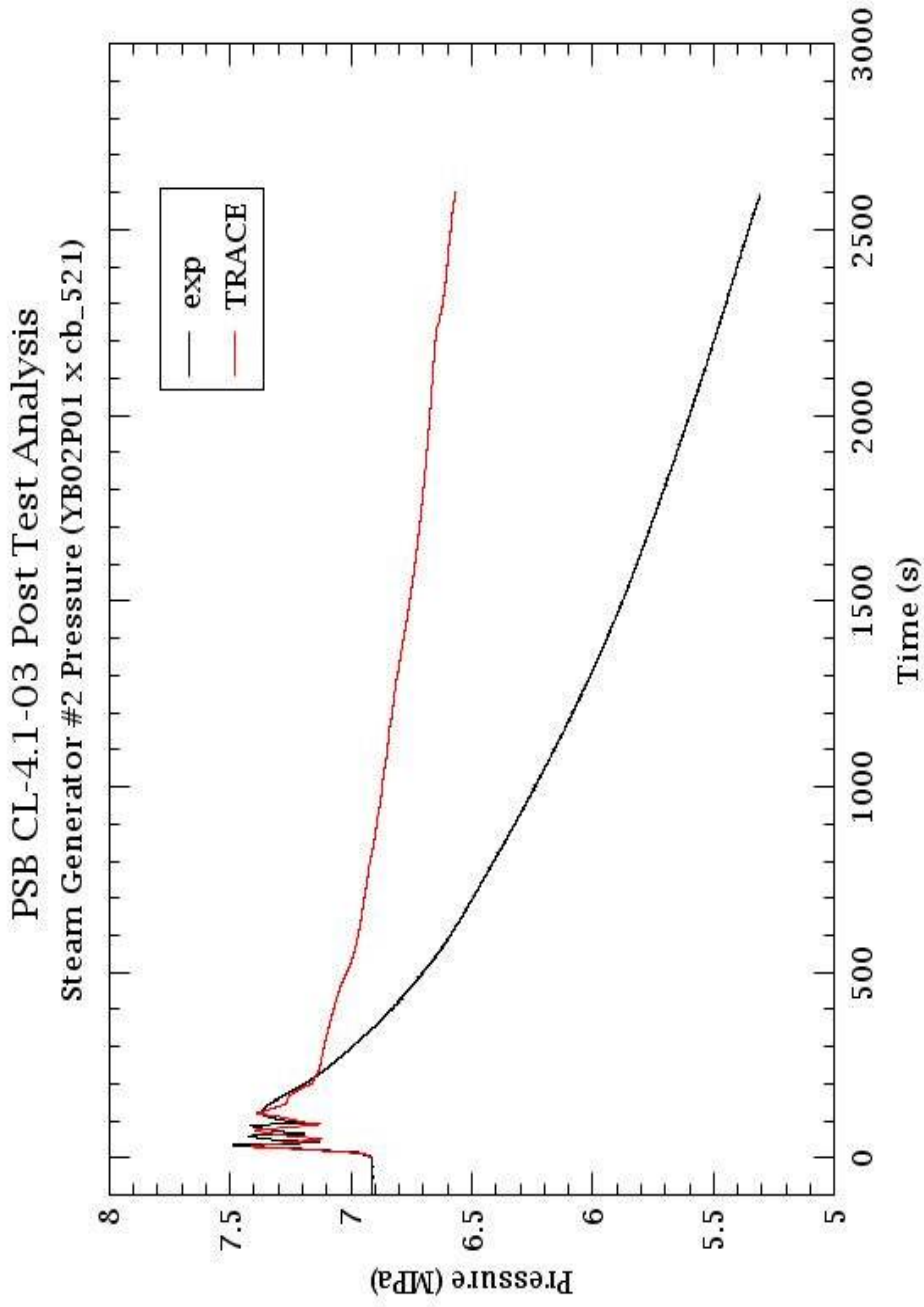
Fig. C.10: PSB-VVER Test-3 Steam Generator #2 Pressure
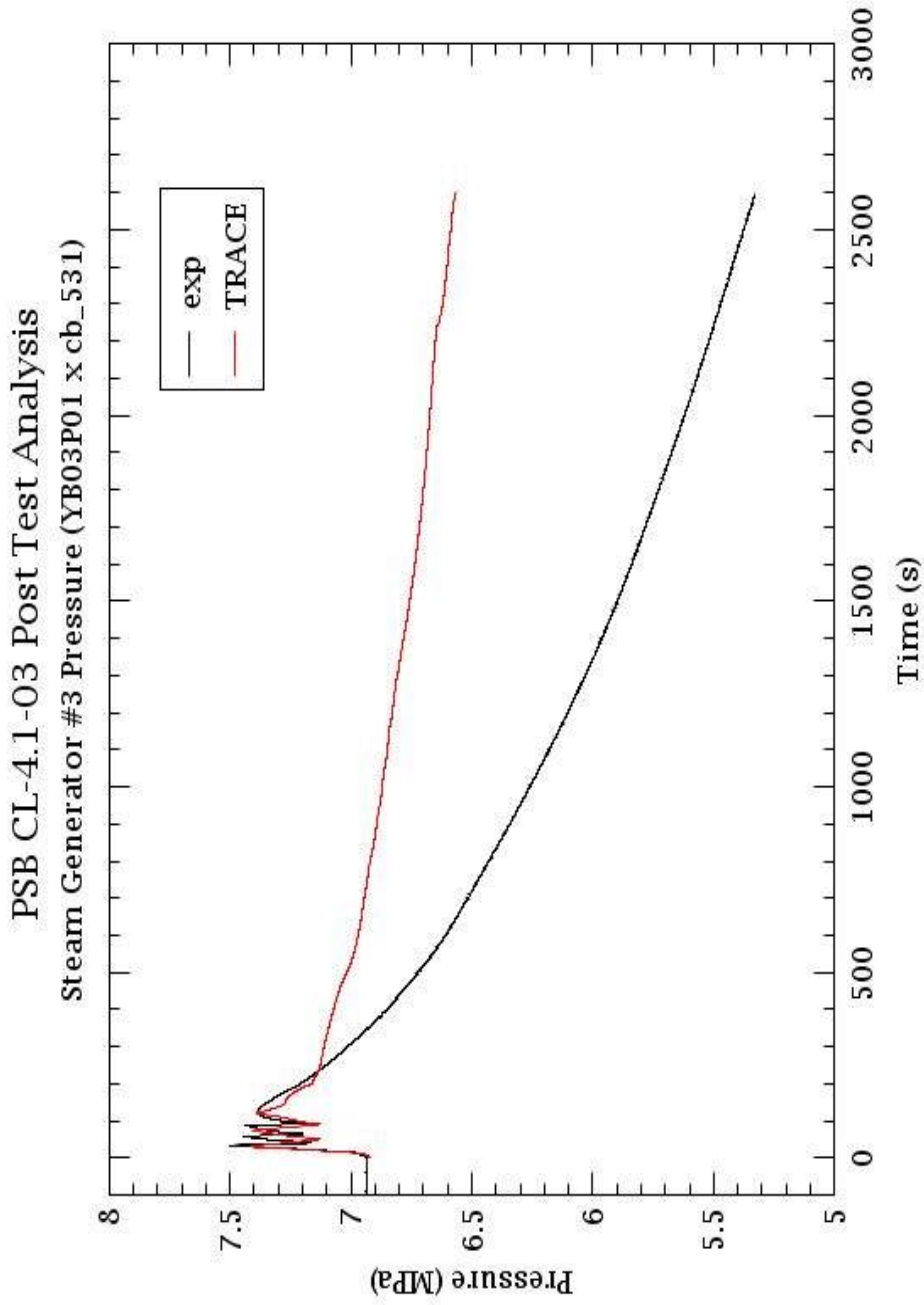
Fig. C.11: PSB-VVER Test-3 Steam Generator #3 Pressure
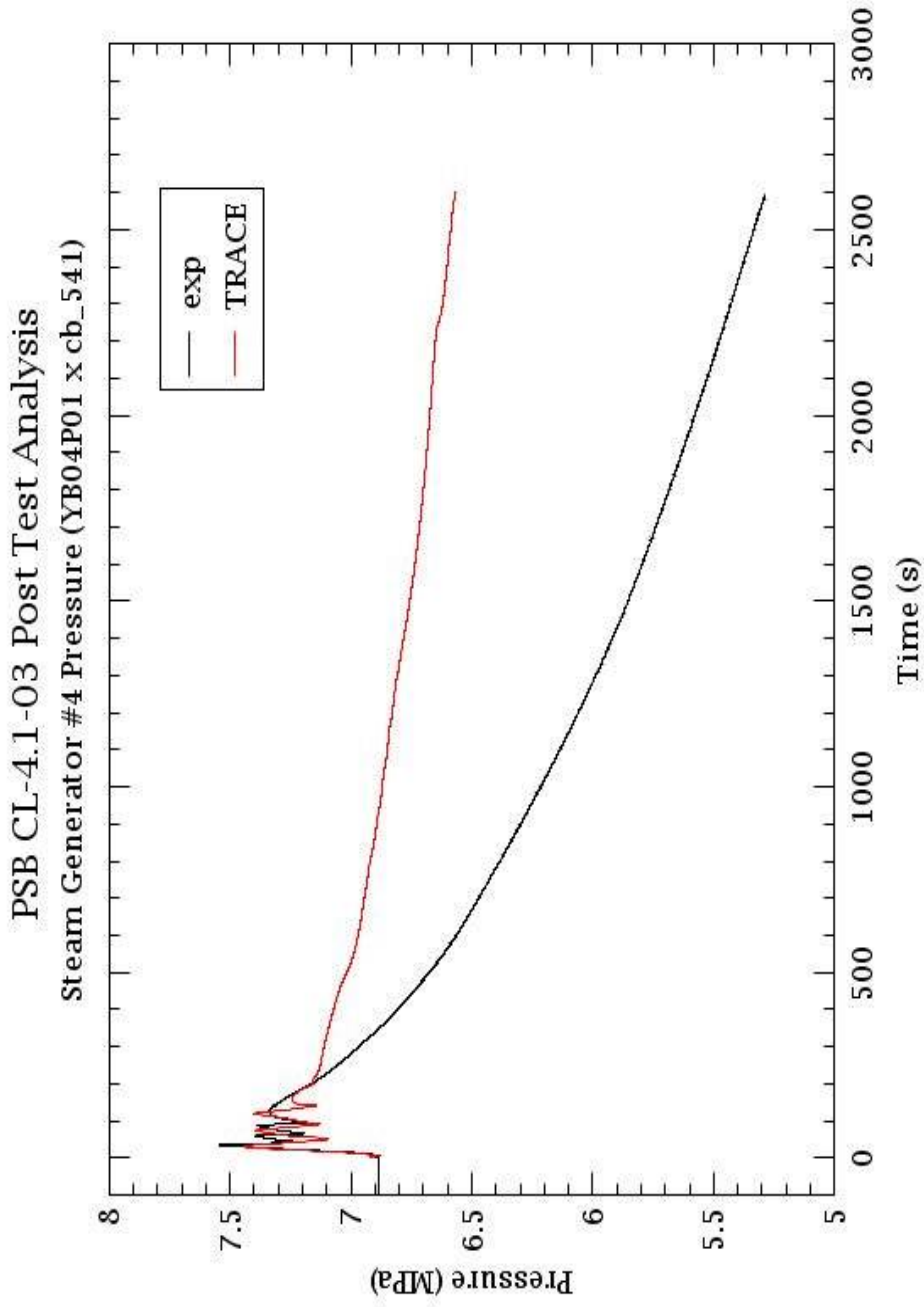
Fig. C.12: PSB-VVER Test-3 Steam Generator #4 Pressure
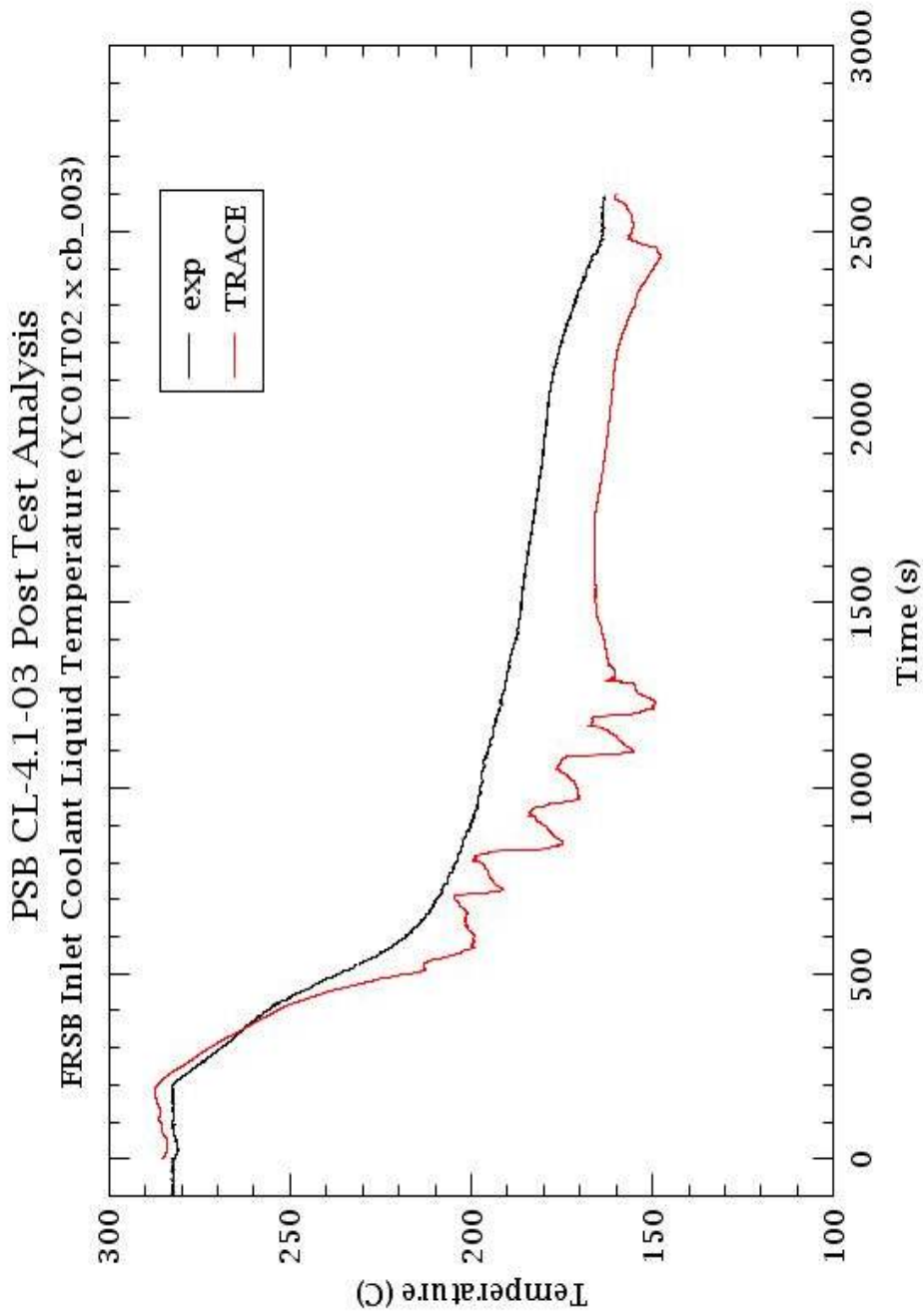
Fig. C.13: PSB-VVER Test-3 Core Simulator Inlet Coolant Temperature
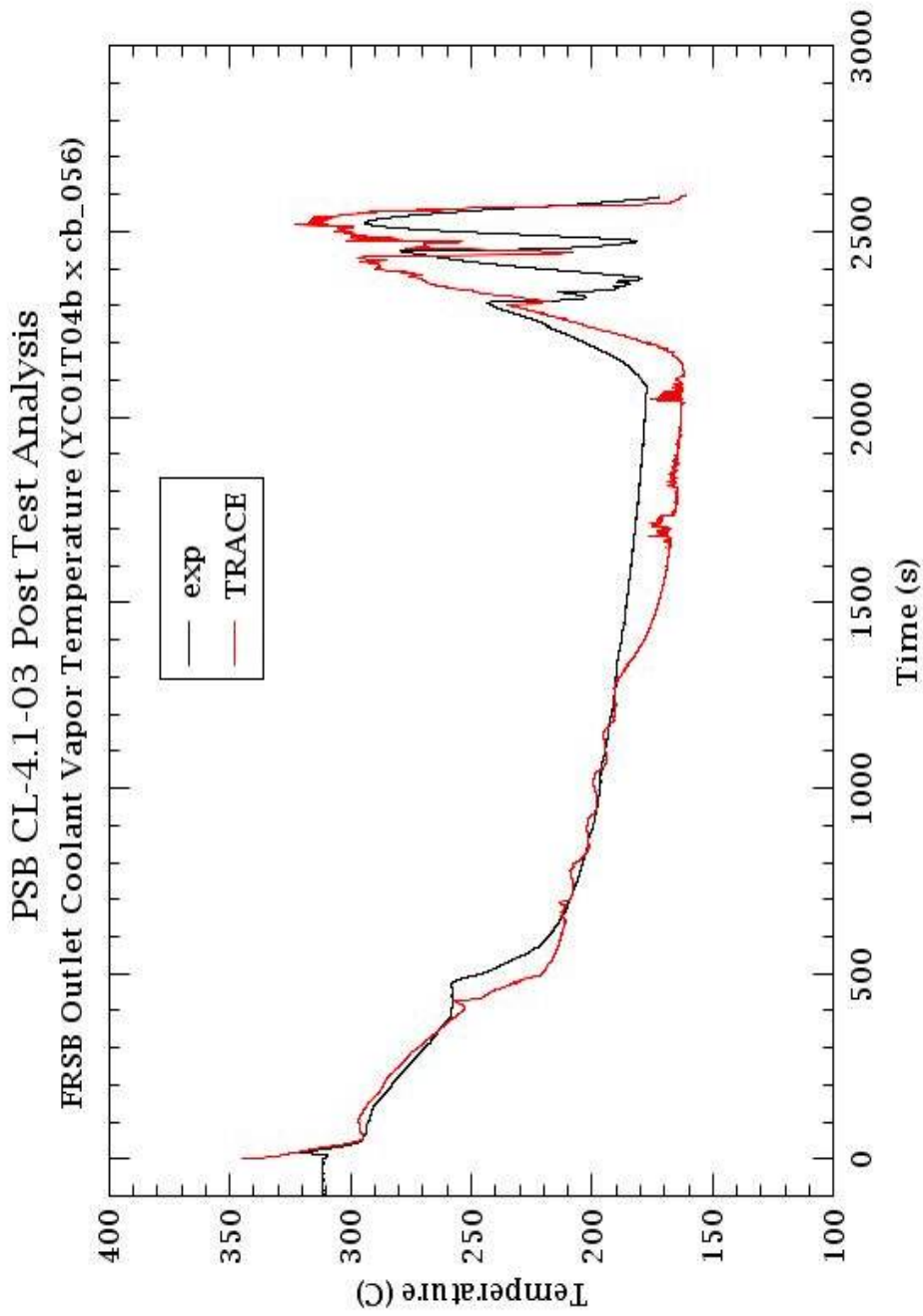
Fig. C.14: PSB-VVER Test-3 Core Simulator Outlet Coolant Temperature
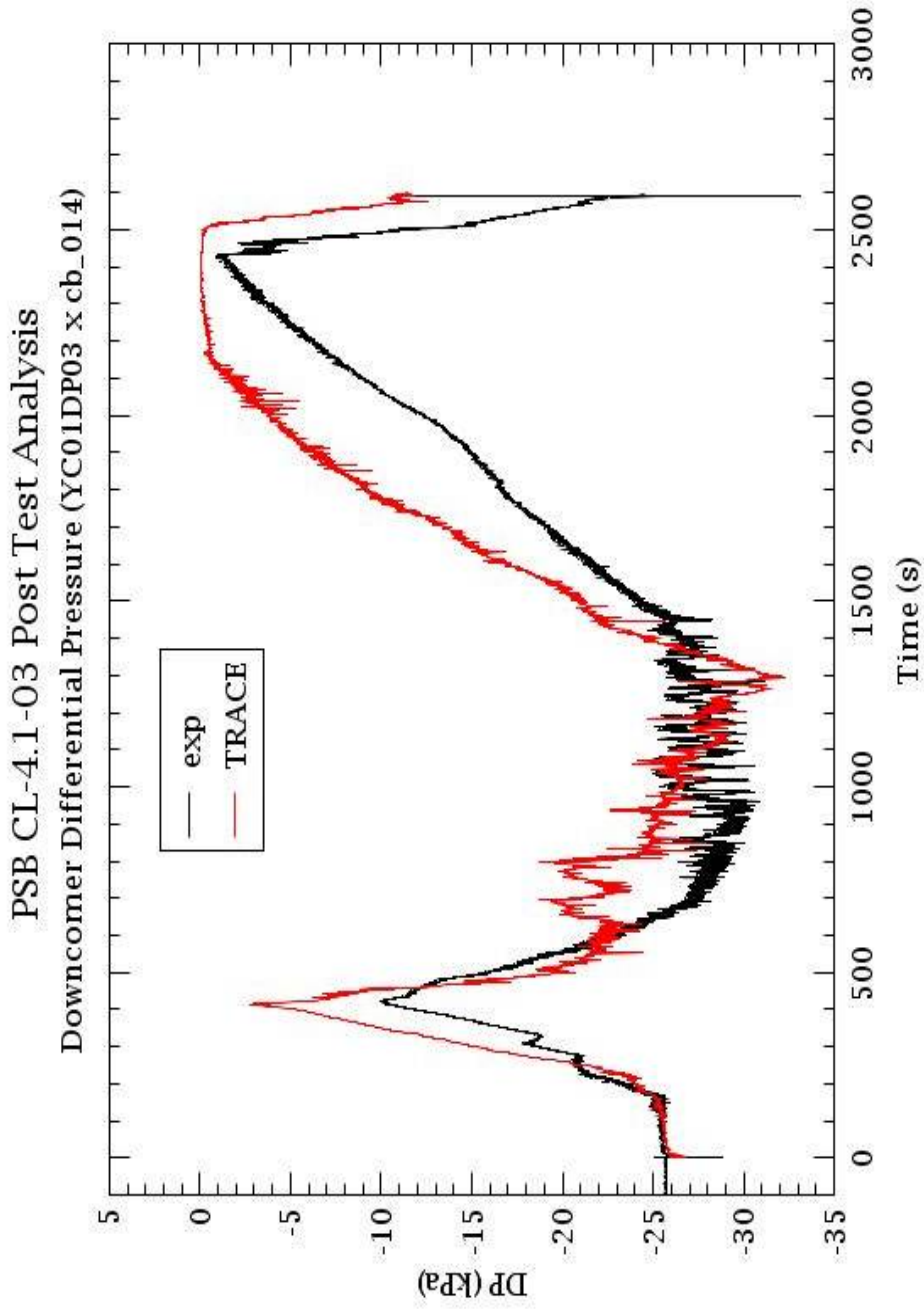
Fig. C.15: PSB-VVER Test-3 Downcomer Simulator (6310 – 2790 mm) Differential Pressure
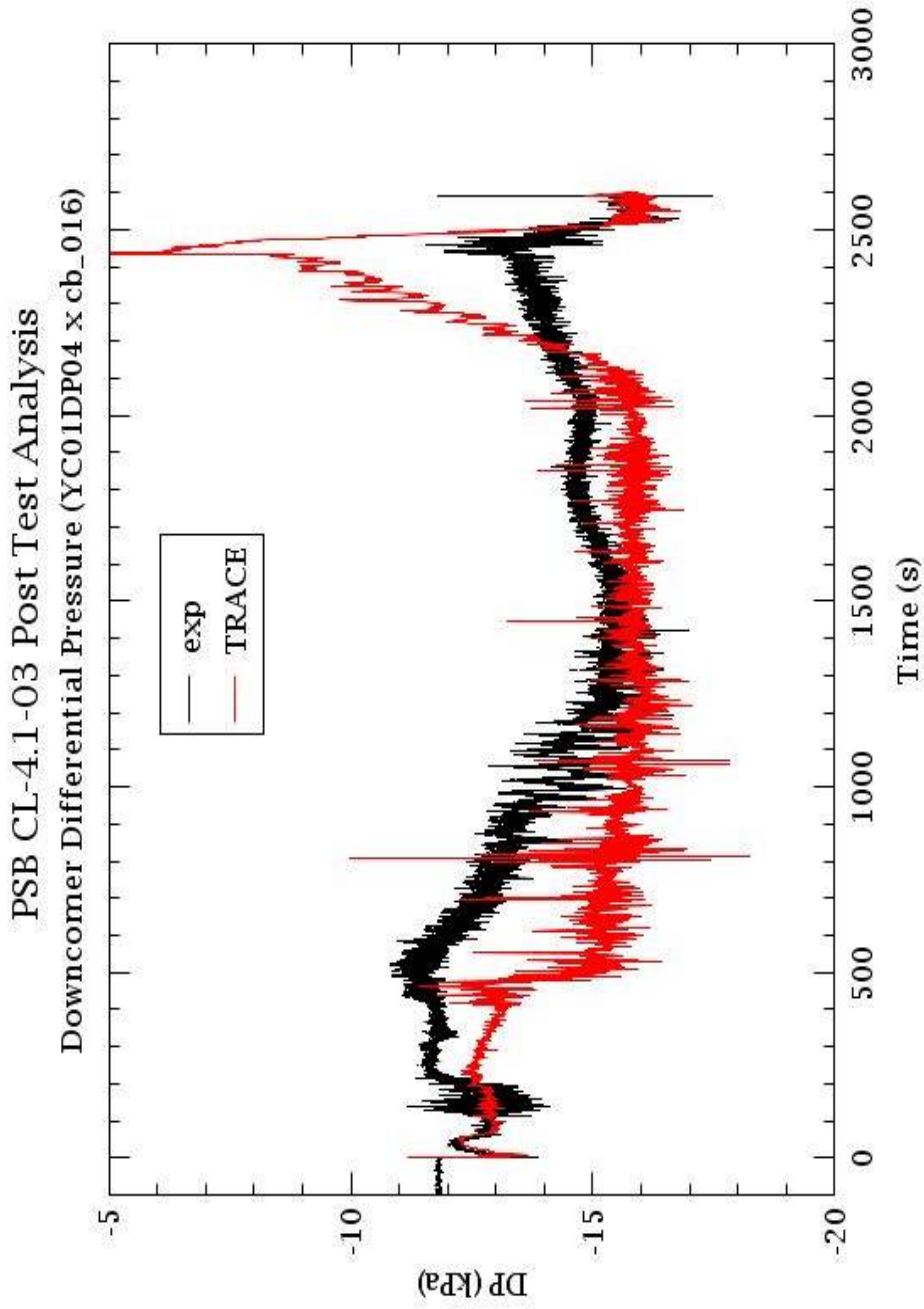
Fig. C.16: PSB-VVER Test-3 Downcomer Simulator (2790 – 1010 mm) Differential Pressure
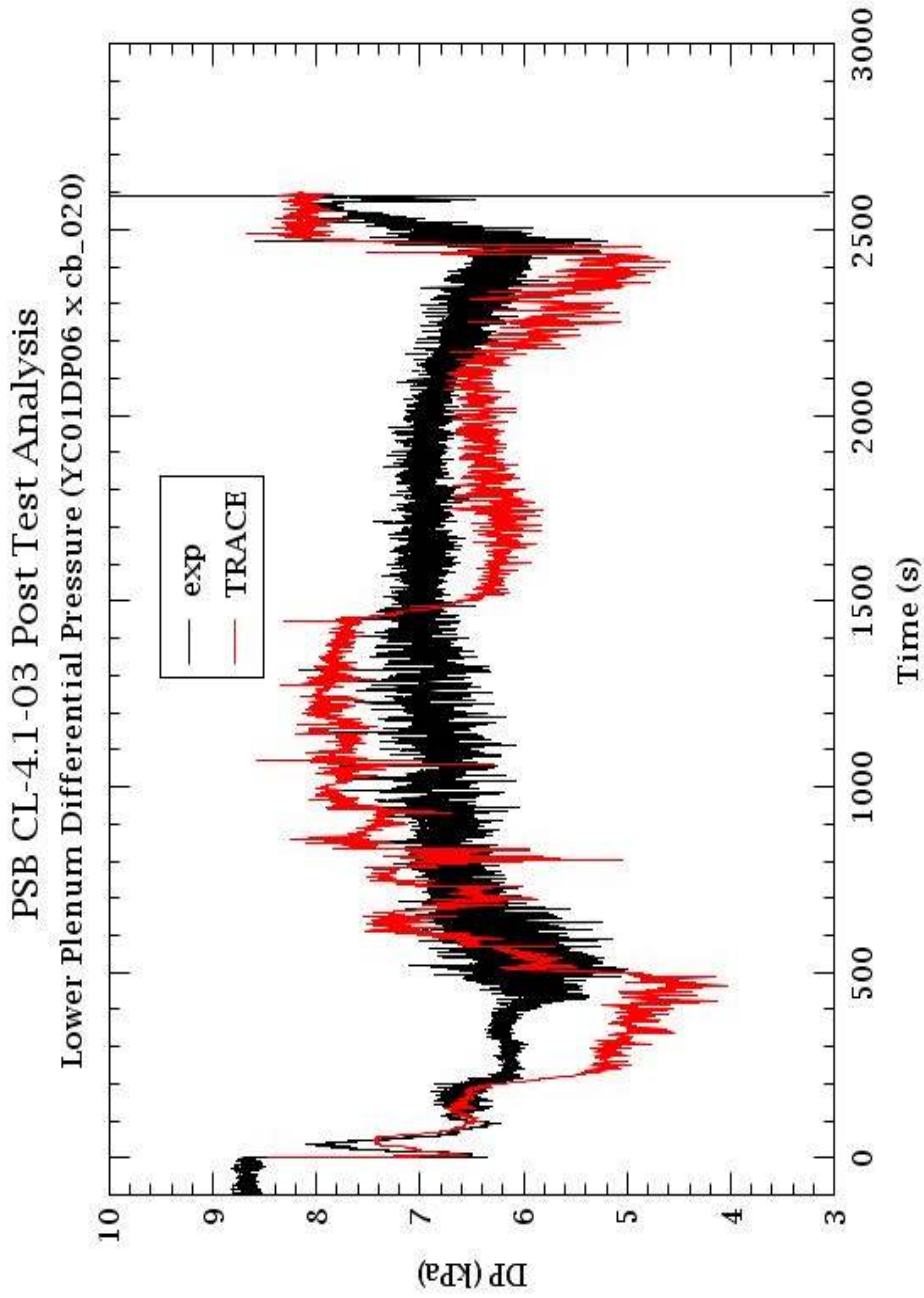
Fig. C.17: PSB-VVER Test-3 Lower Plenum Simulator (1010 – 1915 mm) Differential Pressure
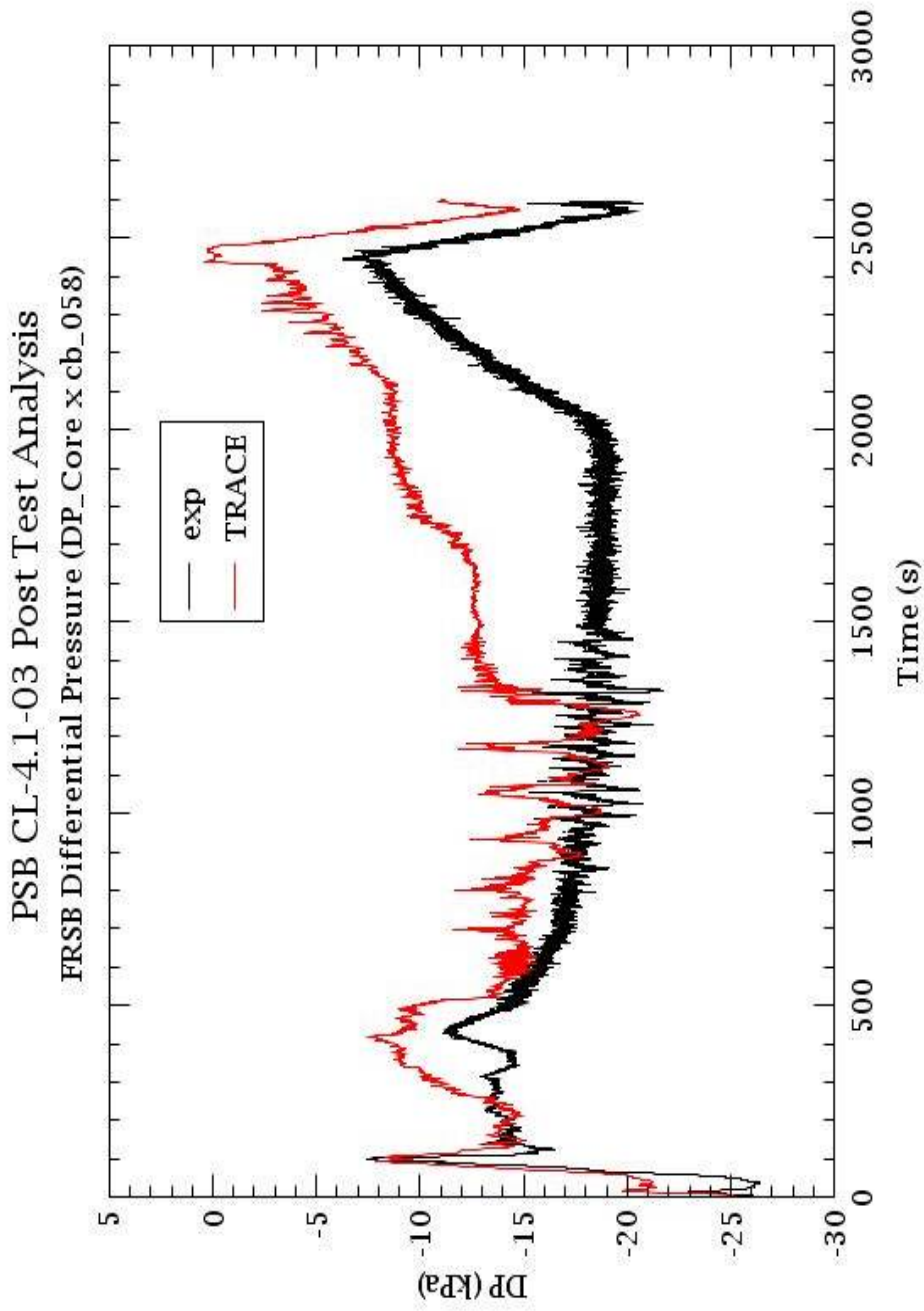
Fig. C.18: PSB-VVER Test-3 Core Simulator (5440 – 1915 mm) Differential Pressure
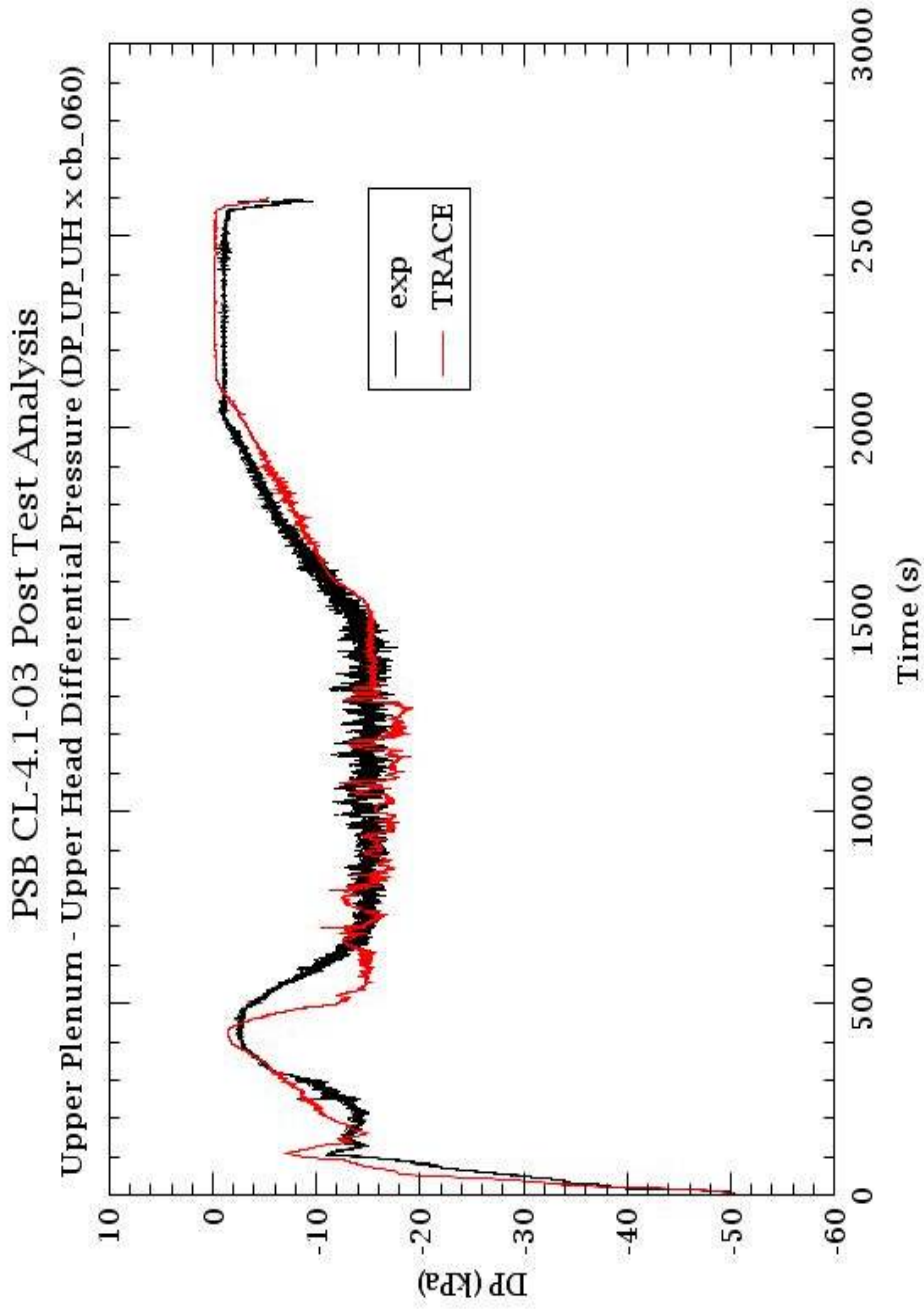
Fig. C.19: PSB-VVER Test-3 Upper Plenum & Upper Head Simulator (12525 – 5440 mm) Differential Pressure
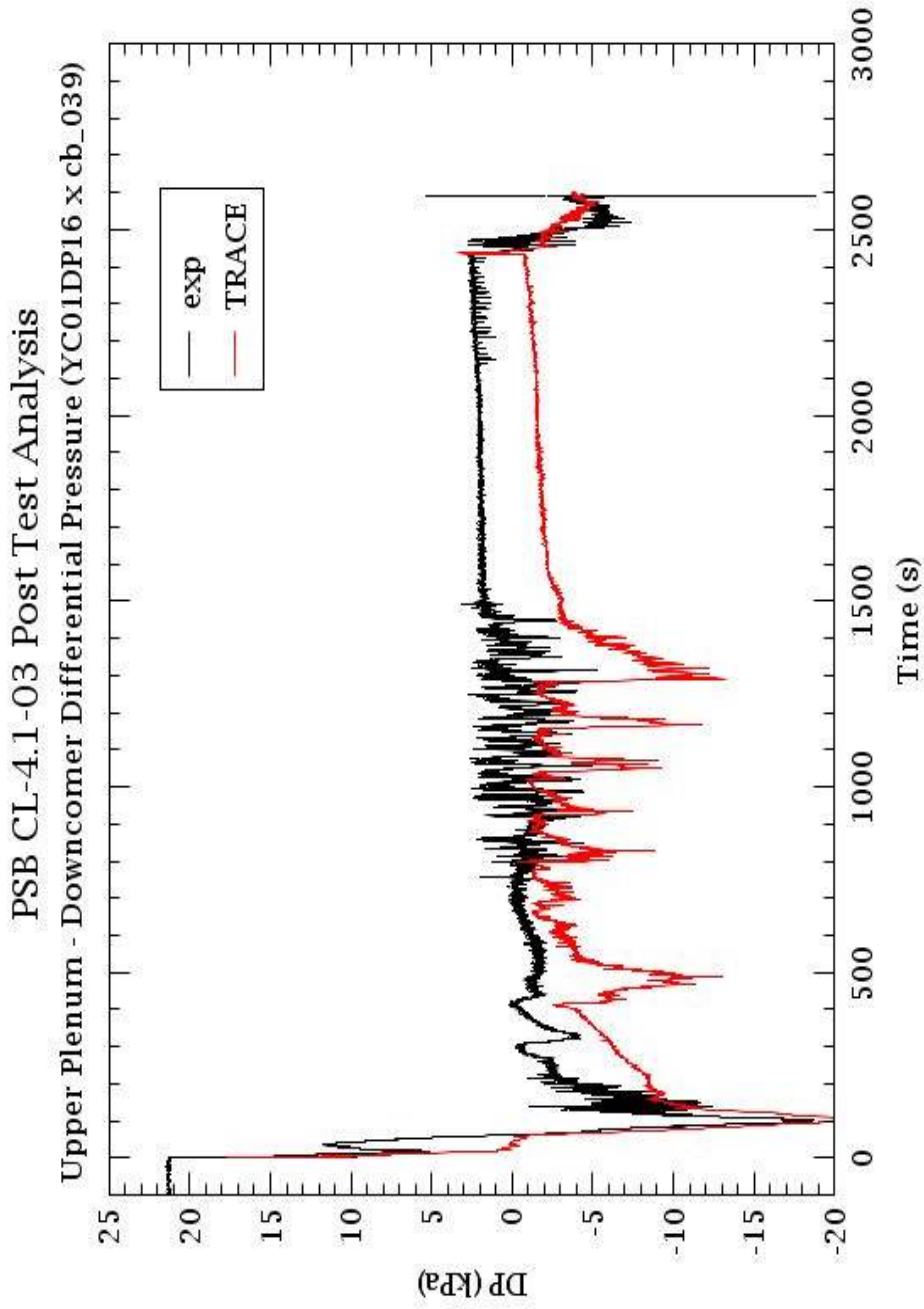
Fig. C.20: PSB-VVER Test-3 Downcomer Simulator to Upper Plenum Simulator (6870 – 8650 mm) Differential Pressure
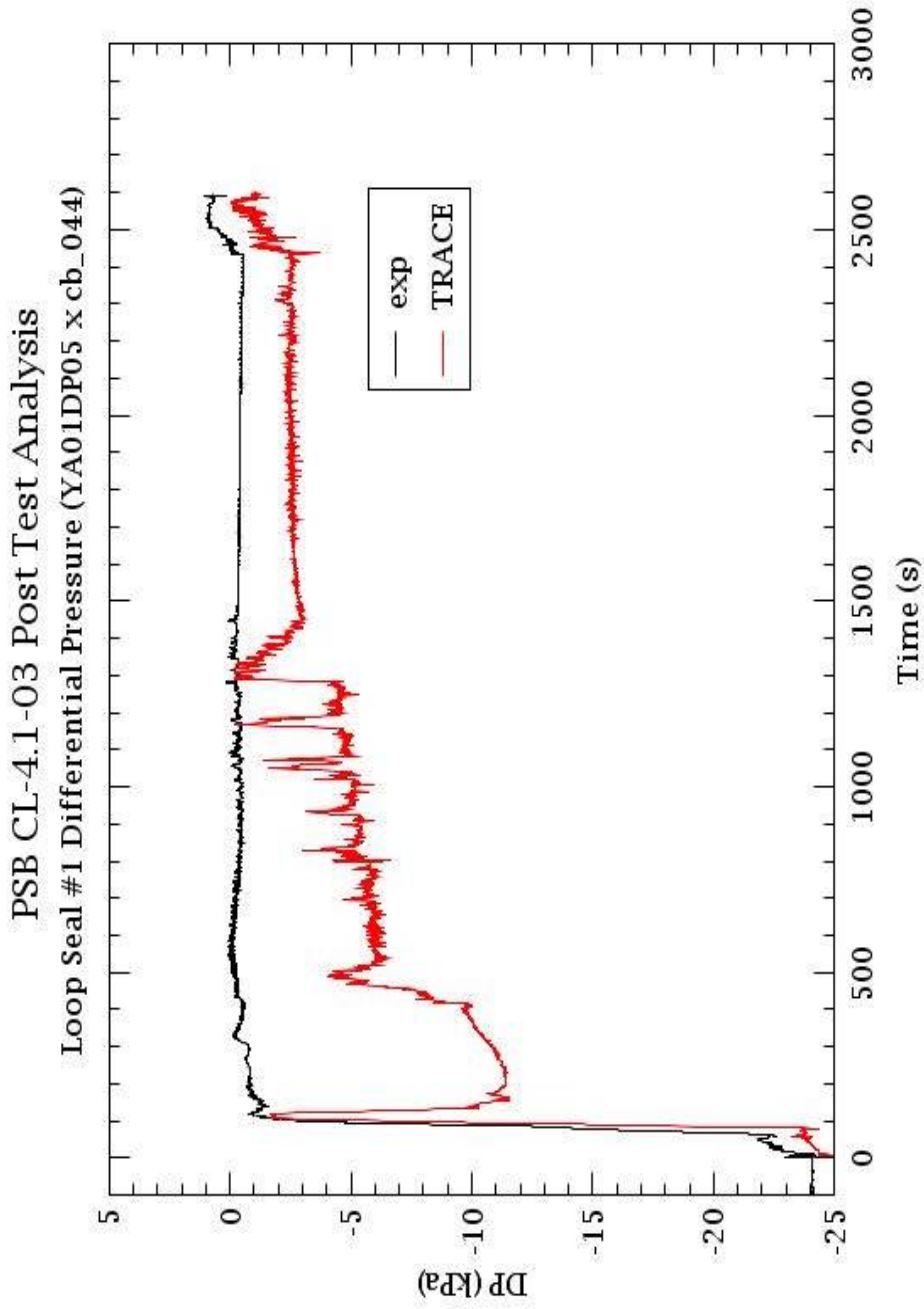
Fig. C.21: PSB-VVER Test-3 Loop Seal #1 Descending Leg (7150 – 3810 mm) Differential Pressure
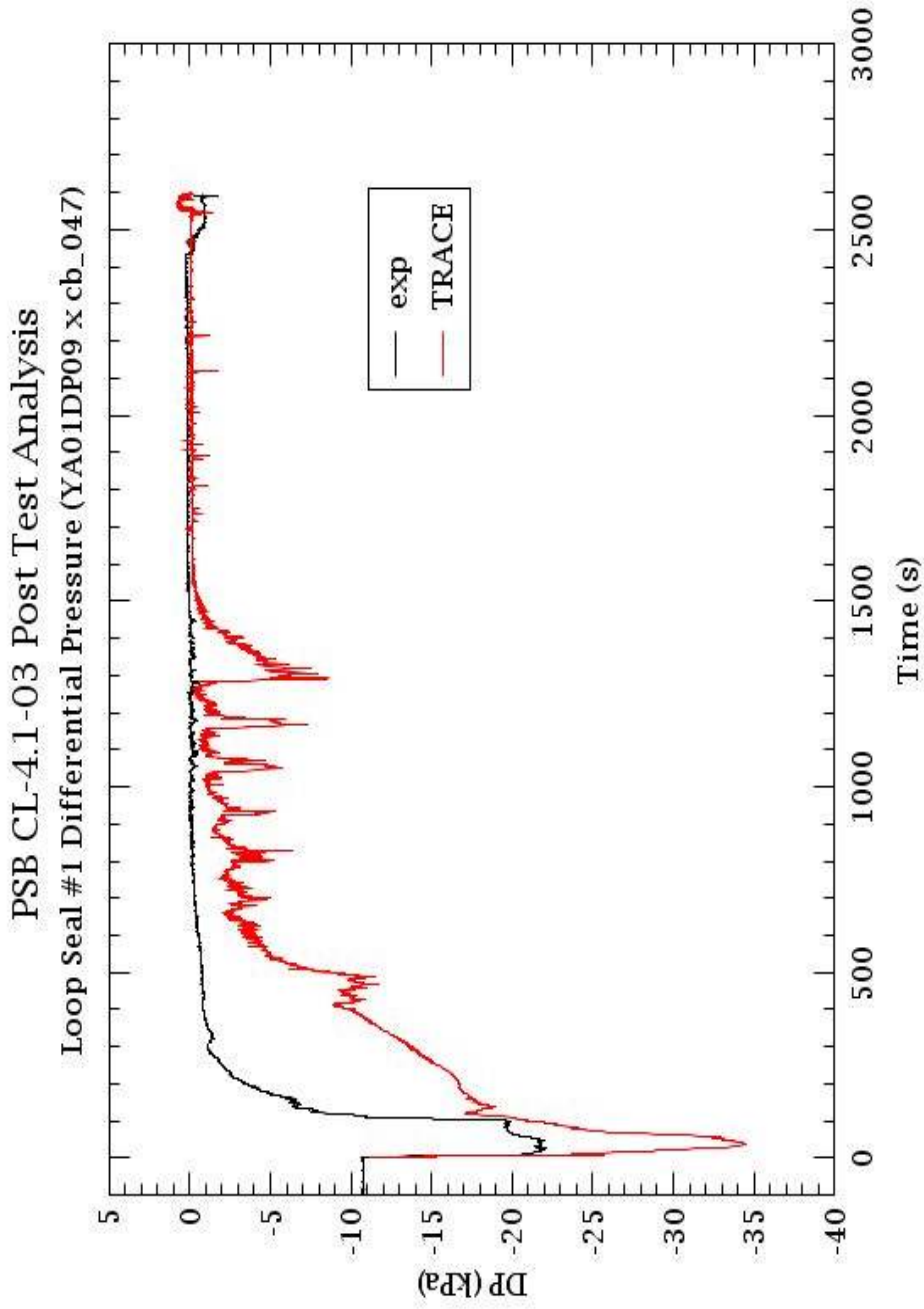
Fig. C.22: PSB-VVER Test-3 Loop Seal #1 Ascending Leg (7065 – 4370 mm) Differential Pressure
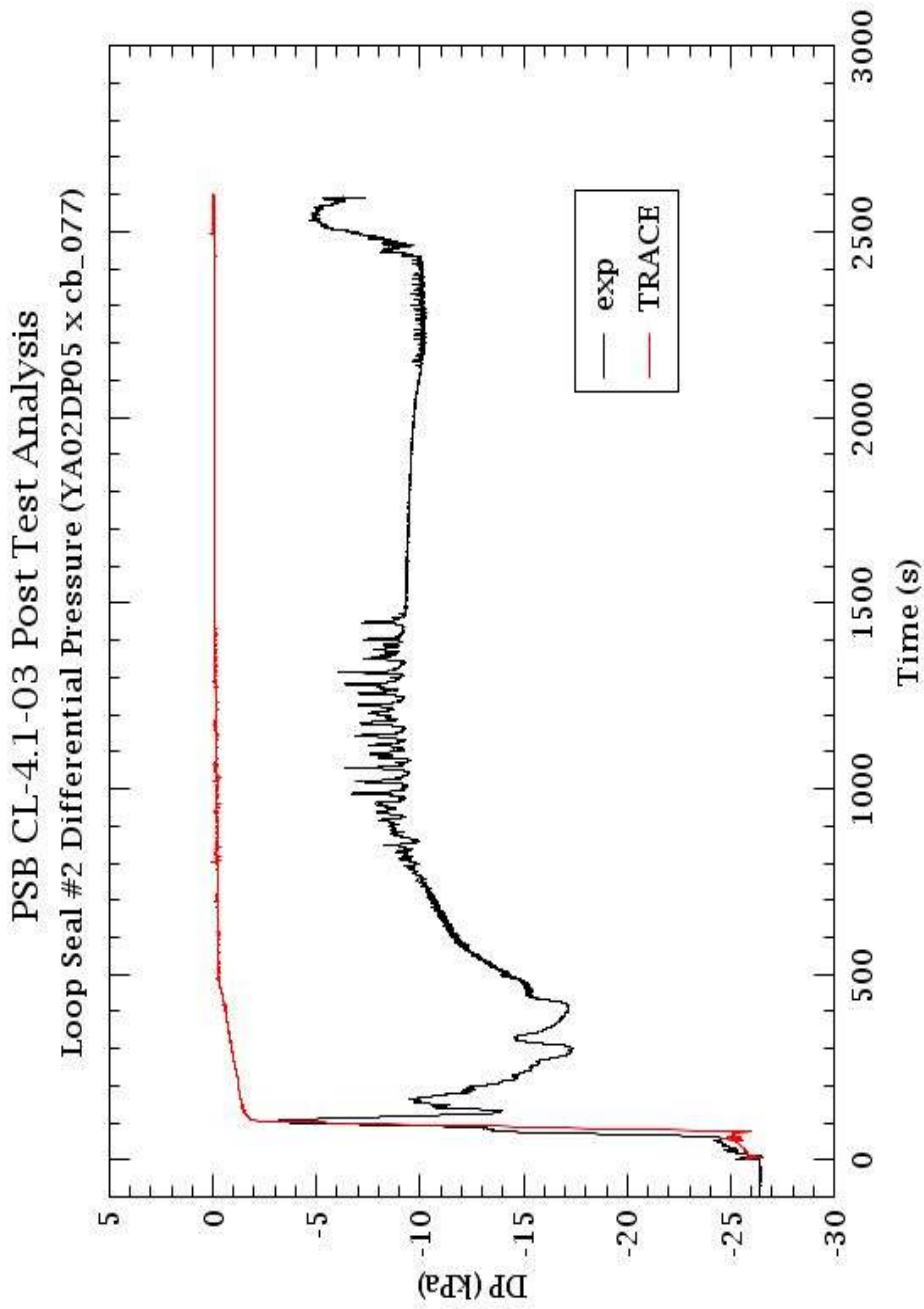
Fig. C.23: PSB-VVER Test-3 Loop Seal #2 Descending Leg (7345 – 3795 mm) Differential Pressure
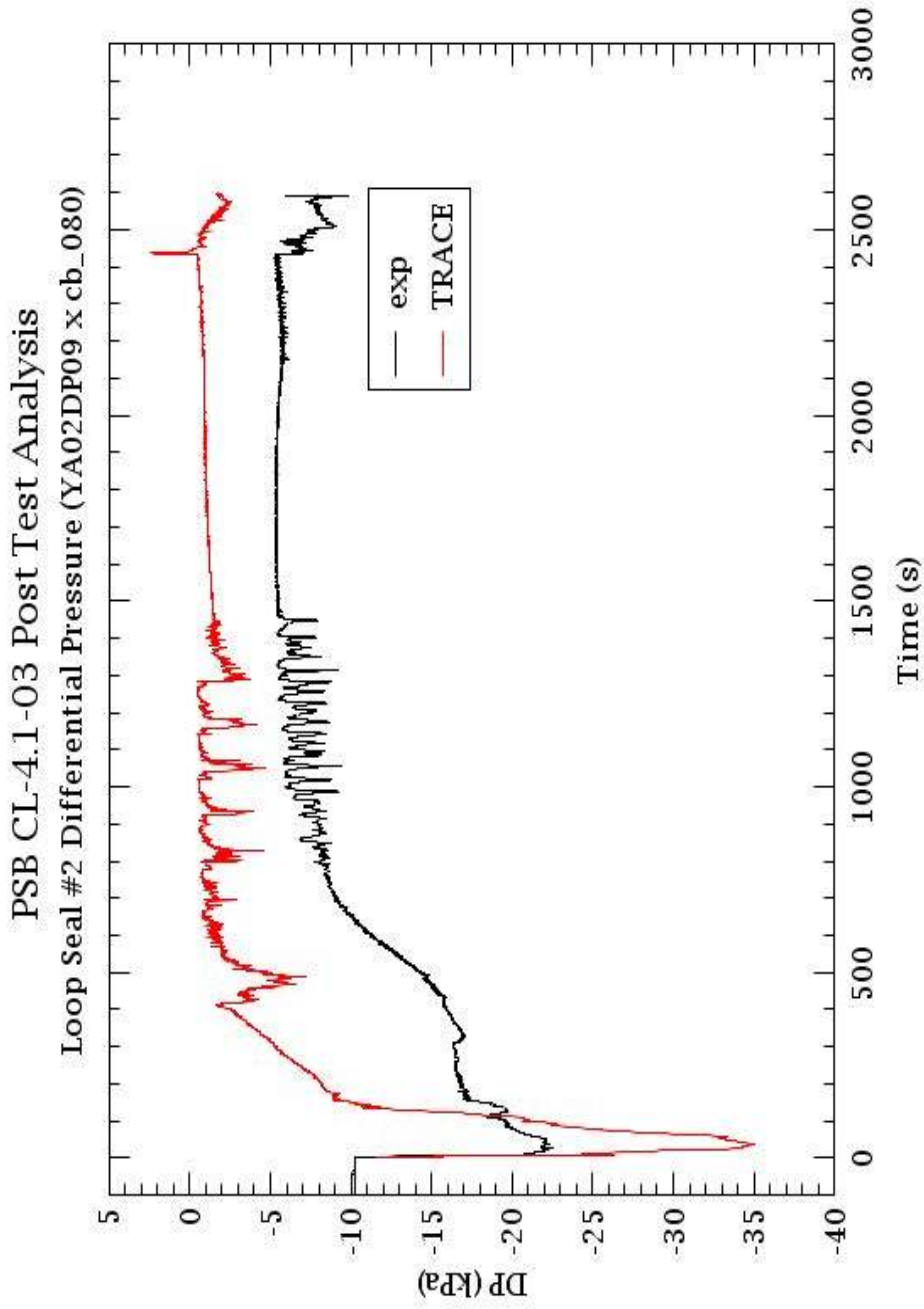
Fig. C.24: PSB-VVER Test-3 Loop Seal #2 Ascending Leg (7065 – 4315 mm) Differential Pressure

174
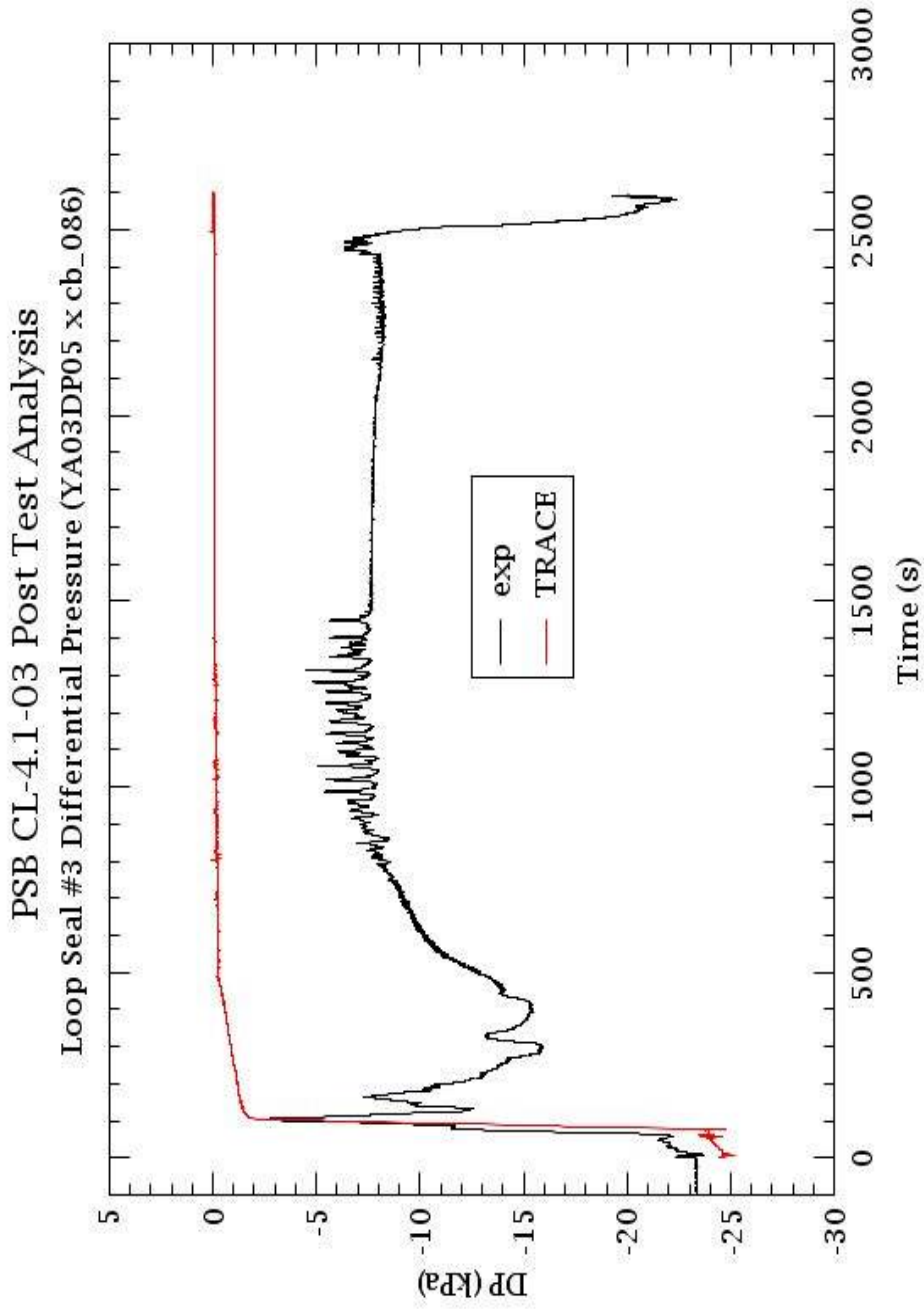
Fig. C.25: PSB-VVER Test-3 Loop Seal #3 Descending Leg (7155 – 3780 mm) Differential Pressure
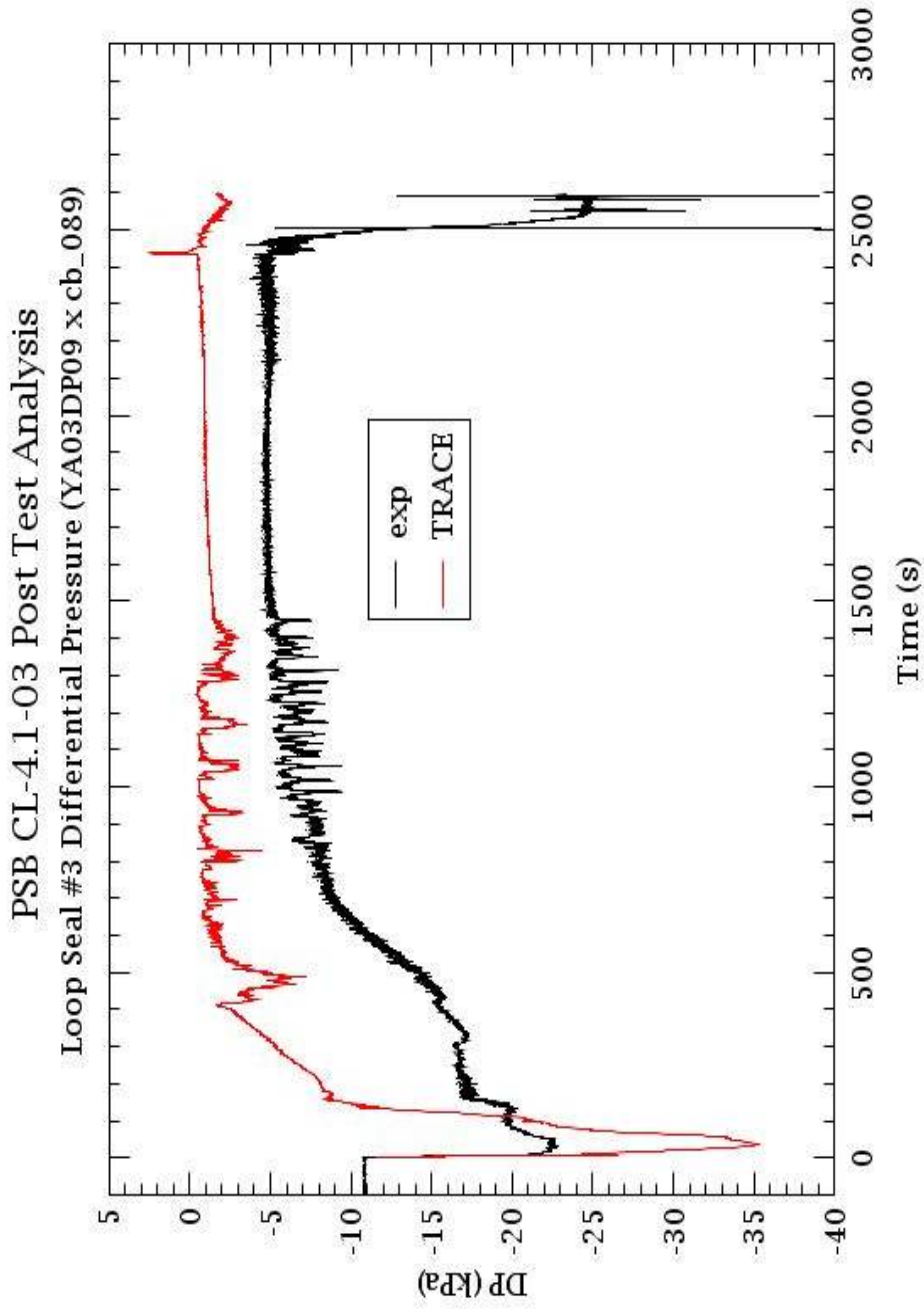
Fig. C.26: PSB-VVER Test-3 Loop Seal #3 Ascending Leg (7065 – 4300 mm) Differential Pressure
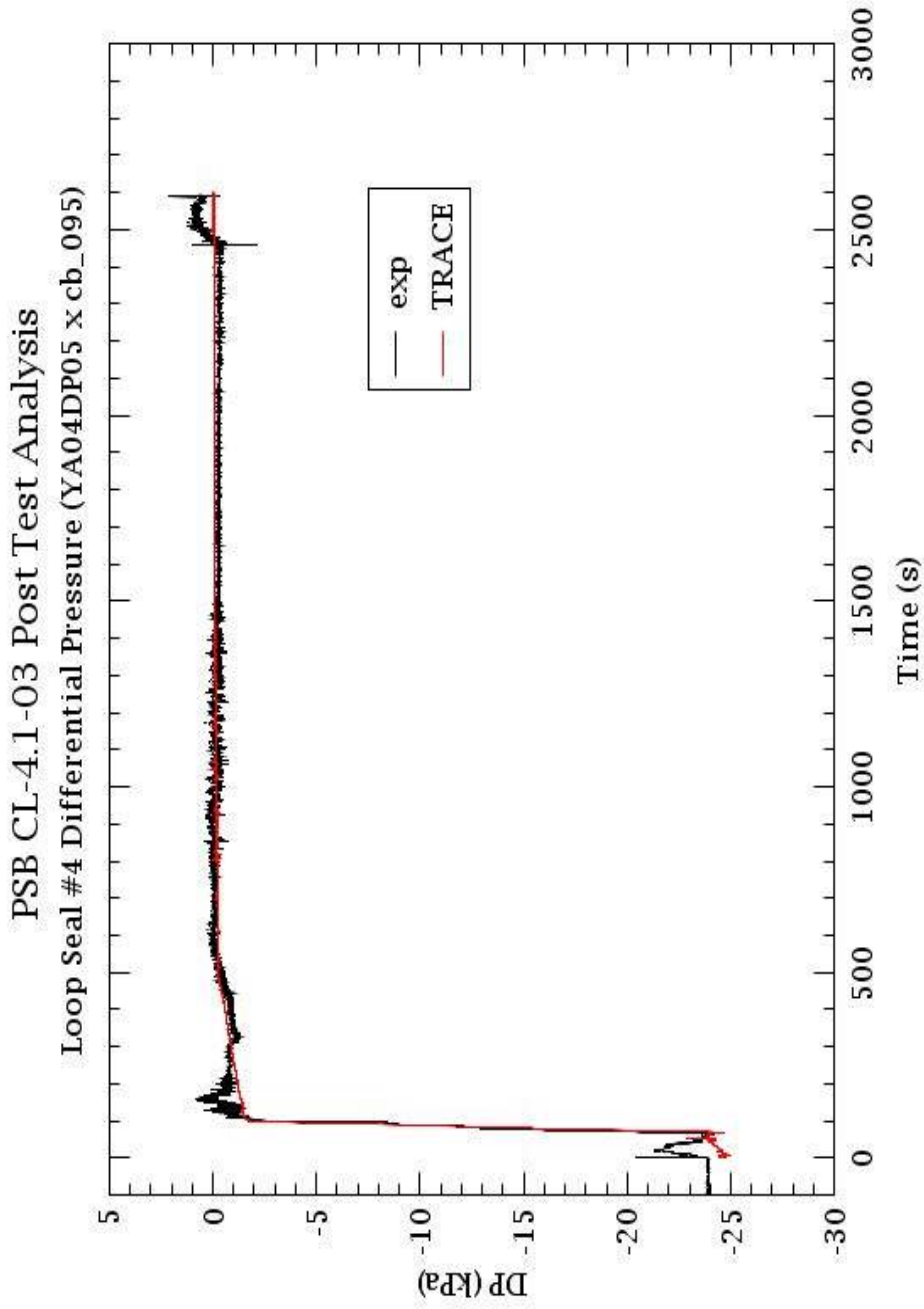
Fig. C.27: PSB-VVER Test-3 Loop Seal #4 Descending Leg (7170 – 3800 mm) Differential Pressure
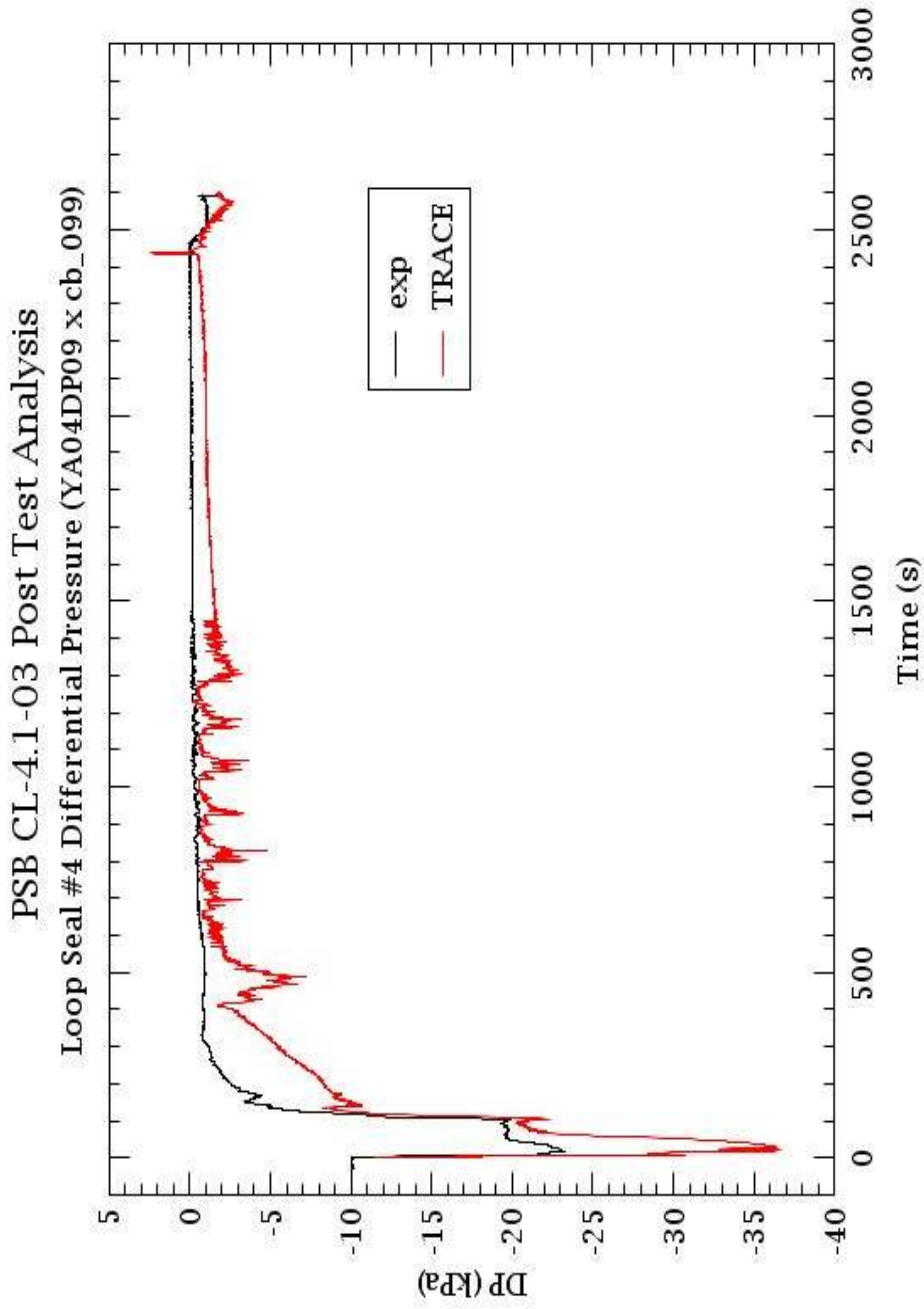
Fig. C.28: PSB-VVER Test-3 Loop Seal #4 Ascending Leg (7065 – 4350 mm) Differential Pressure
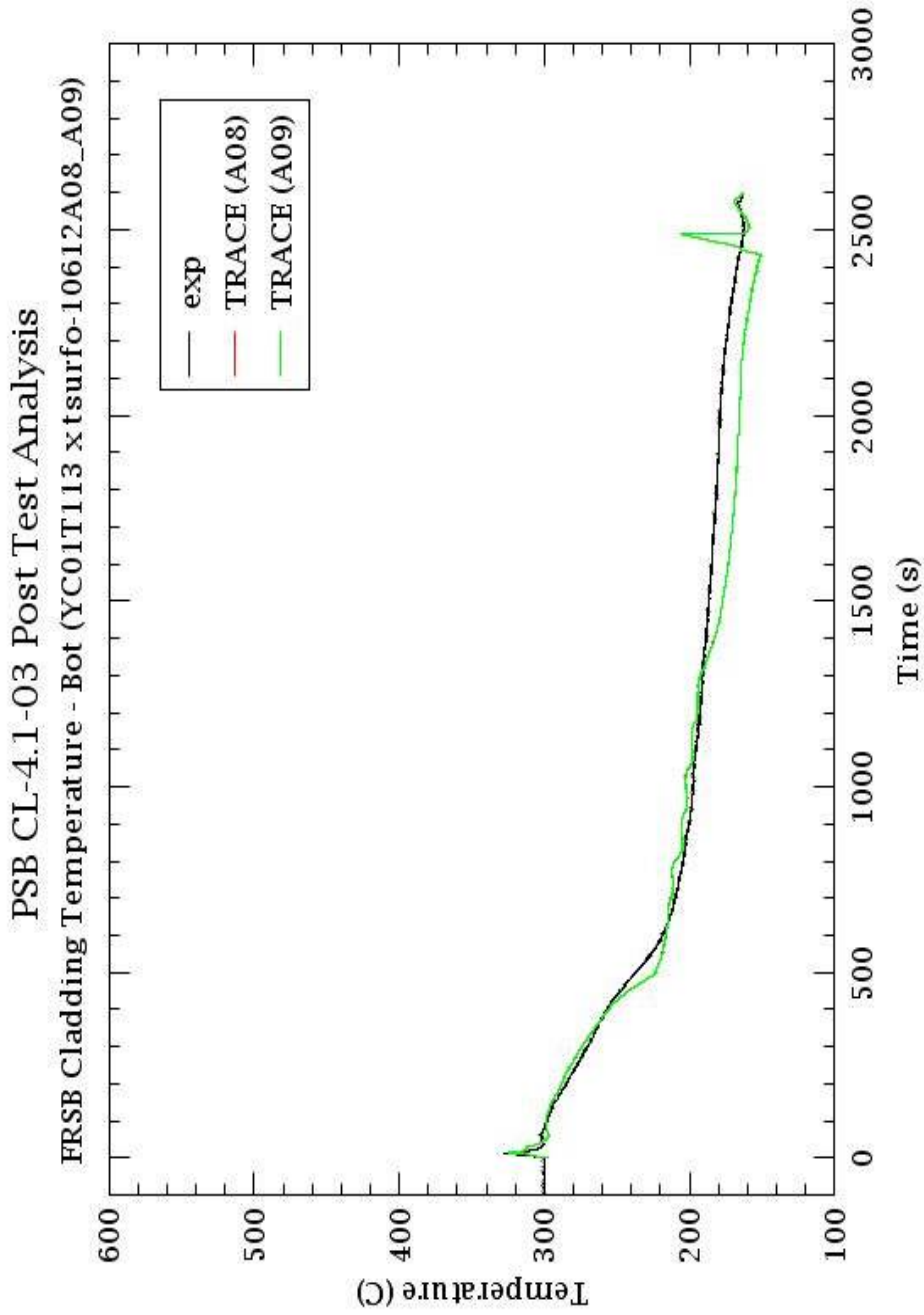
Fig. C.29: PSB-VVER Test-3 FRSB Bottom Third Cladding Temperature
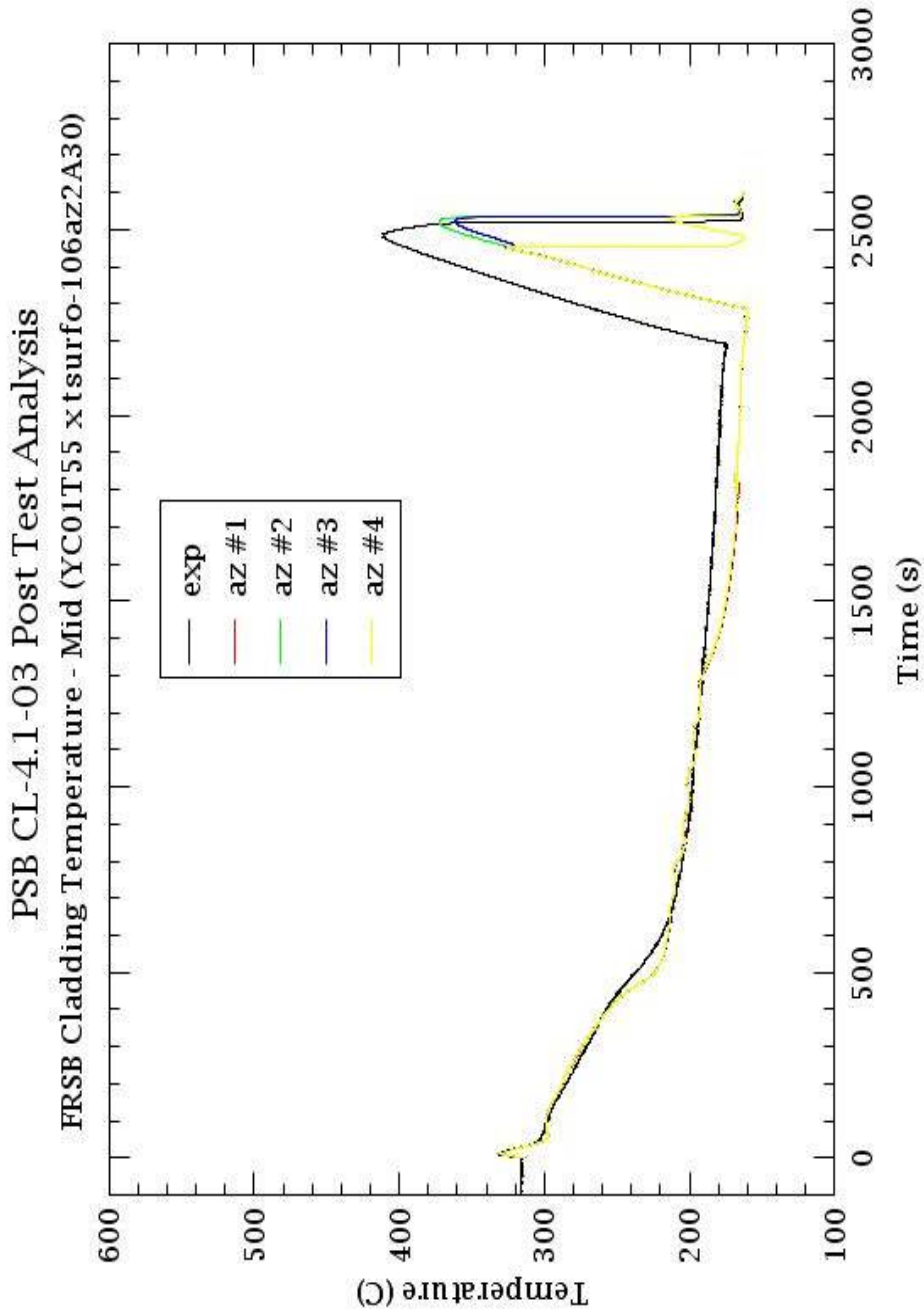
Fig. C.30: PSB-VVER Test-3 FRSB Middle Third Cladding Temperature
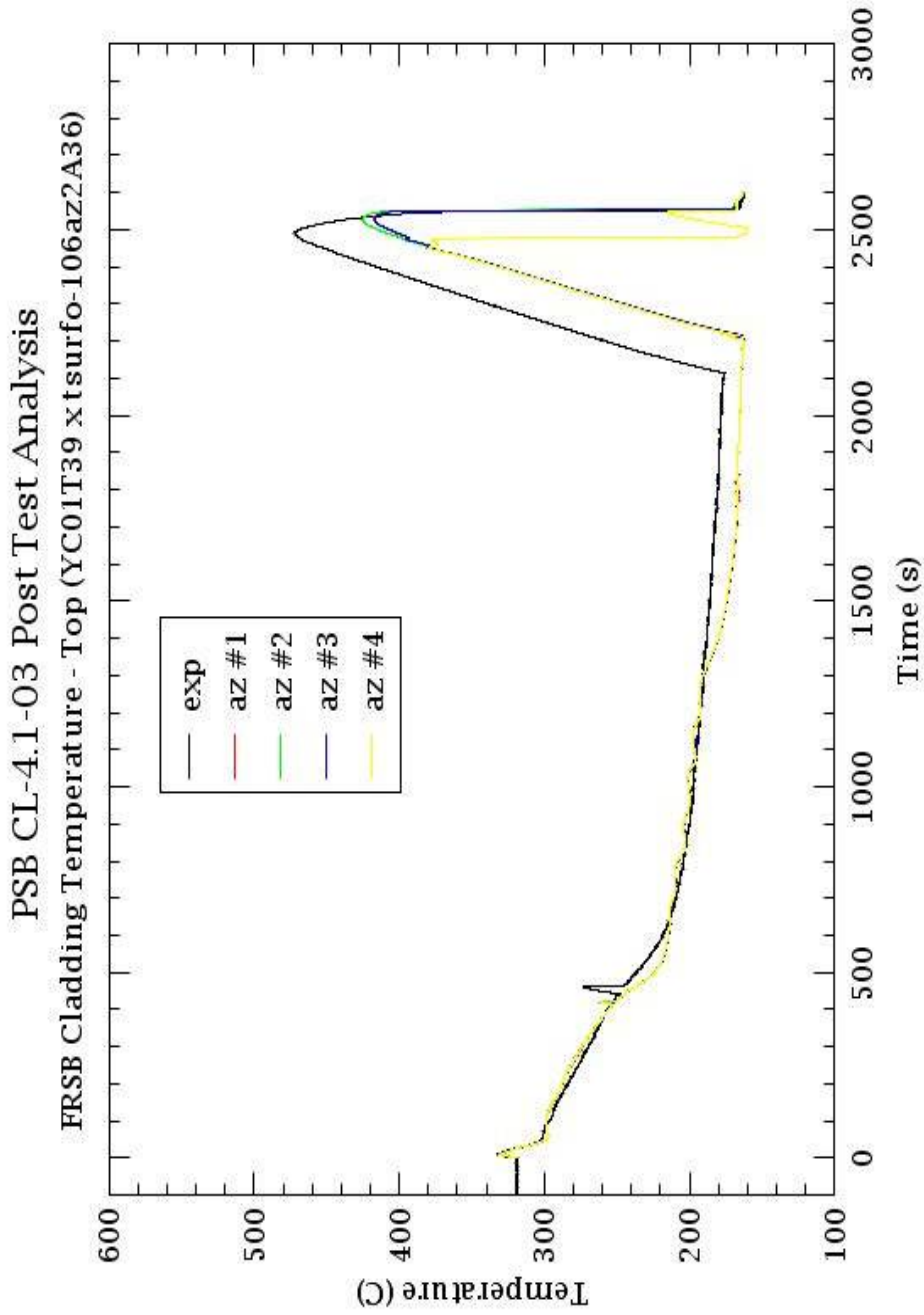
Fig. C.31: PSB-VVER Test-3 FRSB Top Third Cladding Temperature
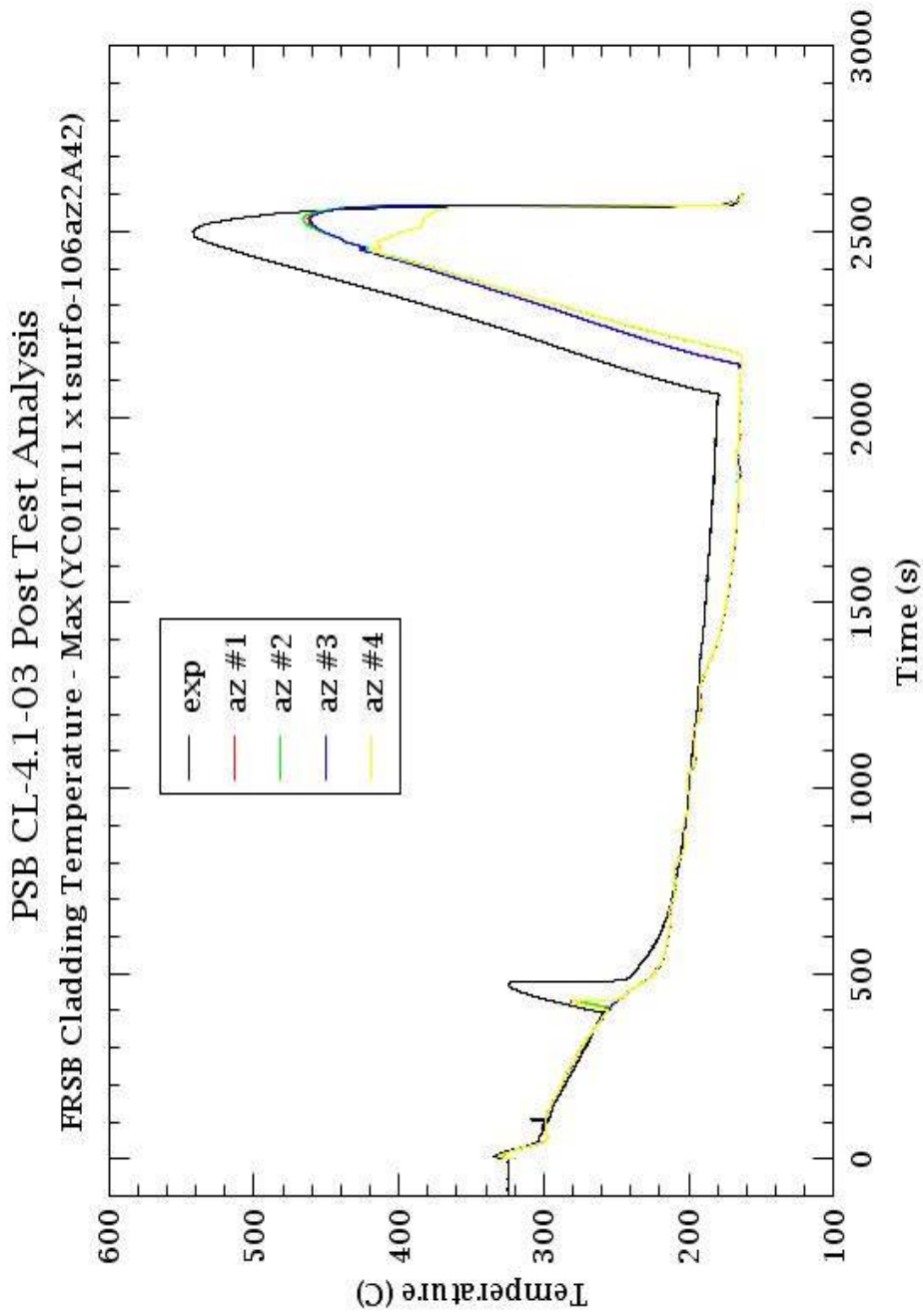
Fig. C.32: PSB-VVER Test-3 FRSB Peak Cladding Temperature
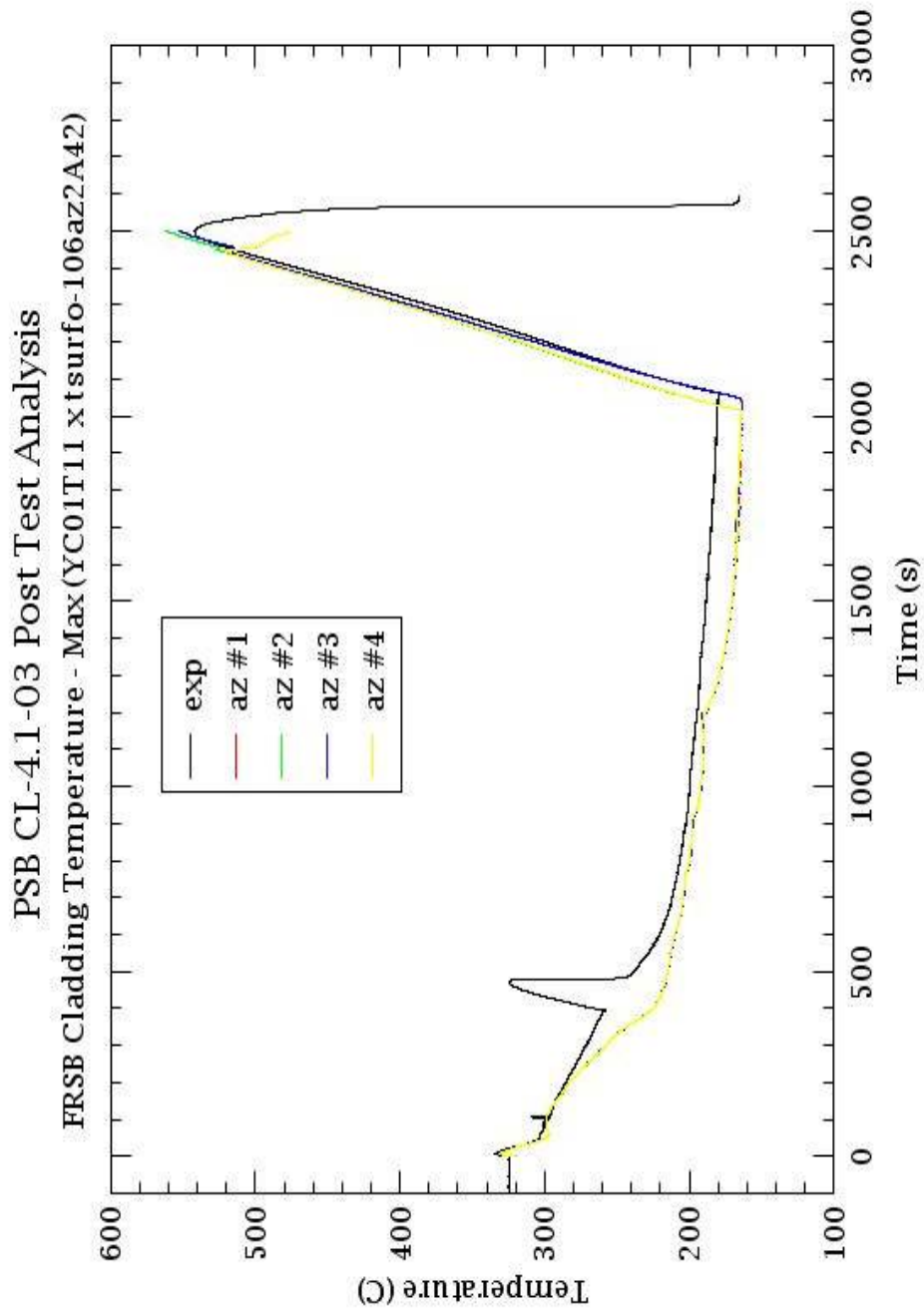
Fig. C.33: PSB-VVER Test-3 FRSB Peak Cladding Temperature – Sensitivity to Critical Discharge Coefficient

2. TITLE AND SUBTITLE

Assessment of RELAP5/MOD3.3 and TRACE V5.0 Computer Codes against LOCA Test Data from PSB-VVER Test Facility

5. AUTHOR(S)

M. Kynčl, R. Pernica

6. TYPE OF REPORT

Technical

7. PERIOD COVERED *(Inclusive Dates)*

8. PERFORMING ORGANIZATION - NAME AND ADDRESS *(If NRC, provide Division, Office or Region, U.S. Nuclear Regulatory Commission, and mailing address; if contractor, provide name and mailing address.)*

Research Centre Řež, TSO
Hlavní 130
250 68 Husinec-Řež, Czech Republic

10. SUPPLEMENTARY NOTES

A. Calvo, NRC Project Manager

11. ABSTRACT *(200 words or less)*

This report documents the USNRC system thermal-hydraulic codes assessment performed at Research Centre Rez. RELAP5/MOD3.3 and TRACE V5.0 computer codes were assessed against the experimental data from two LOCA tests carried out at PSB-VVER test facility built and operated at Electrogorsk Research and Engineering Center on NPPs Safety in Russia. Experimental data and all necessary information for developing the facility database and facility model notebook were available through the OECD/NEA/CSNI/WGAMA PSB Project.

In the RELAP5/MOD3.3 case, in addition to the best estimate post test analysis of LB LOCA experiment denoted as CL-2x100-01 by EREC and as Test-5a as part of the OECD PSB project, the uncertainty and sensitivity analysis was performed, and the results are presented here. Double ended cold leg guillotine break with initial power scaled further down to 15% was simulated in Test-5a.

In the TRACE V5.0 case, the best estimate post test analysis of SB LOCA experiment denoted as CL-4.1-03 by EREC and as Test-3 as part of the OECD PSB project was carried out, and the results are presented here. A 4.1% cold leg break was simulated in Test-3. The test scenario applied was very close to the scenario realized in LOBI test BL-34.

12. KEY WORDS/DESCRIPTORS *(List words or phrases that will assist researchers in locating the report.)*

CAMP (Code Applications and Maintenance Program)
SNAP (Symbolic Nuclear Analysis Program)
Research Centre Řež, TSO
PSB-VVER test facility
OECD PSB project
RELAP5/MOD3.3
Electrogorsk Research and Engineering Center
OECD/NEA/CSNI/WGAMA PSB Project

13. AVAILABILITY STATEMENT

unlimited

14. SECURITY CLASSIFICATION

(This Page)
unclassified

(This Report)
unclassified

15. NUMBER OF PAGES

16. PRICE

NUREG/IA-0435

Assessment of RELAP5/MOD3.3 and TRACE V5.0 Computer Codes
Against LOCA Test Data from PSB-VVER Test Facility

December 2013